University Library



A gateway to Melbourne's research publications

Minerva Access is the Institutional Repository of The University of Melbourne

Author/s:
Shamsaei Zafarghandi, Narges

Title:
Investigating fundamental radical reactivity in ionic liquids

Date:
2020

Persistent Link:
https://hdl.handle.net/11343/241951

Terms and Conditions:
Terms and Conditions: Copyright in works deposited in Minerva Access is retained by the copyright owner. The work may not be altered without permission from the copyright owner. Readers may only download, print and save electronic copies of whole works for their own personal non-commercial use. Any use that exceeds these limits requires permission from the copyright owner. Attribution is essential when quoting or paraphrasing from these works.

Investigating fundamental radical reactivity in ionic liquids

Narges Shamsaei Zafarghandi

Submitted in total fulfilment of the requirements of the degree of Doctor of Philosophy

April 2020

School of Chemistry

The University of Melbourne

Produced on archival quality paper

Dedicated to my lovely husband

Mohammad Hashtari

,

My dear sons

Ilia and Yasin

And

My supportive parents and siblings

Abstract

Despite significant advances over the past few decades, most free radical reactions are traditionally carried out in organic solvents that are often toxic, flammable, and difficult to recycle. It is therefore timely to explore whether and how free radical chemistry can be moved away from "conventional" solvents into ionic liquids. Ionic liquids are green alternatives to traditional organic solvents, being recyclable, non-volatile, non-flammable and air resistance. Ionic liquids are composed entirely of ions, and they can be designed for specific applications by the variation of either the anions, cations or by modification on the substituents on the anion and cation. Therefore, a wide variety of ILs structure is available for various requirements. For example, the physical properties of the ILs including density, viscosity, melting point, hydrophobicity and solubility of the ILs can be tuned.

While chemistry involving ionic liquids has dramatically increased in the last decade, their impact upon chemical kinetics is still unclear. Further, very little traditional radical chemistry has been performed in ionic liquids, and it is essential to understand how critical rate constants for hydrogen atom transfer and radical rearrangements are impacted by these alternative solvents. Although ionic liquids are often considered as 'green solvents', it is their ionic nature in particular that may influence reactivity and selectivity of radical reactions.

In this work the first kinetic parameters for the intramolecular homolytic cyclisation of a series of alkyl and alkoxyl radicals, intramolecular homolytic substitution at selenium and intermolecular homolytic addition at double bond in the [EMIm][NTf_2], an imidazolium-based ionic liquid, as well as in organic solvents such as benzene, *n*-hexane or *t*-butylbenzene have been reported. Through the combination of laser flash photolysis and competition kinetic studies we obtained the absolute rate coefficient for the hydrogen abstraction from *t*-BuSH by primary alkyl radicals in [EMIm][NTf_2] of $k_H = (4.1 \pm 0.1) \times 10^7$ M^{-1} s^{-1}, which is about five times higher than k_H in conventional organic solvents. Competition kinetic studies were used to determine k_C for a number of 5-*exo* radical cyclisations and an intramolecular homolytic substitution on Se, which are up to one order of magnitude higher in the ionic liquid than in organic solvents.

Generally, the rate of the 5-*exo* cyclisation at room temperature is up to 50% more facile in the ionic liquid, depending on the nature of the radical, without any impact on the stereochemical outcome. The faster cyclisations observed for all studied radicals in [EMIm][NTf_2] is ascribable to the favourable activation entropies for all radicals that are suggestive of less-organised transition states for the 5-*exo* cyclisation, compared to the corresponding reactions in conventional organic solvents.

Lowering the viscosity of ionic liquid by performing the reaction at elevated temperatures led to a significant acceleration in the cyclisation rate. No interfering reaction involving the ionic liquid constituents were observed and all products can be quantitatively extracted from the ionic liquid phase, which can be reused without purification. On the whole, our results highlight the potential of ionic liquids as alternatives to conventional organic solvents for radical cyclisations, intramolecular homolytic substitutions with neutral radicals and intermolecular radical addition to the alkene.

Declaration

This is to certify that:

i. The thesis comprises only my original work towards the PhD except there indicated in the Preface,
ii. Due acknowledgement has been made in the text to all other material used,
iii. The thesis is less than 100,000 words in length, exclusive of tables, figures, bibliographies and appendices.

Narges Shamsaei Zafarghandi

April 2020

Preface

In accordance with the regulations of the University of Melbourne, I acknowledge that some of the work presented in this thesis was collaborative.

Chapter 2

Laser flash photolysis (LFP) was performed by Josses Nathanael, School of chemistry, The University of Melbourne.

Density functional theory (DFT) calculation was performed by Prof. Uta Wille, School of chemistry, The University of Melbourne.

The remainder of this thesis comprises only my original work. Overall, I assess my contribution to be greater than 95%.

Acknowledgments

First, I would like to extend my gratitude to my first supervisor Prof. Carl H. Schiesser, who guided and encouraged me through my PhD. Thank you for allowing me to work on such a rewarding project and for all the wonderful opportunities you have provided throughout this journey.

I would also like to thank my second supervisor Assoc. Prof. Uta Wille for helping me to continue my PhD. Thank you for being hugely supportive when I got completely obstructed. You open a new aspect in my research that enabled me to continue that after finishing my PhD.

A huge thank you as well to the members of my advisory panel, Prof. Jonathan White and Prof. Craig Hutton for their guidance and very helpful suggestions regarding problematic reactions at our yearly meetings. My appreciation goes to past and present members of the Schiesser and Wille groups, who made the laboratory an enjoyable environment to work in and in many different ways made possible the conclusion of this work. However, special thanks go to Joses Nathanael for Doing Laser Flash Photolysis part of my project. To the other Chemistry groups in Bio21, especially the Craig, Rizzacasa and Williams Groups, thank you for allowing me to utilize equipment, borrow chemicals and share in valuable discussions and expertise.

Thank you to Dr. Hamish Grant for his assistance with NMR spectroscopy and Dr. Athanasios Zavras for the high-resolution MS as well as all the general and technical staff in the School of Chemistry at the University of Melbourne.

This work was financially supported by an Australian Postgraduate Award and the ARC Centre of Excellence for Free Radical Chemistry and Biotechnology. Numerous overseas conference and research trips were funded by the ARC Centre of Excellence for Free Radical Chemistry.

I am greatly indebted to my family, who have provided me with continuous support and encouragement throughout my life and finally, my sincerest gratitude goes to my husband Mohammad Hashtari for his boundless support and encouragement.

Abbreviations

A°	angstrom
AR	analytical reagent
aq.	aqueous
atm.	atmosphere
AIBN	azobisisobutyronitrile
BDE	bond dissociation energy
°C	degree Celsius
calc.	calculated
δ	delta
DFT	density function theory
d	doublet (NMR)
dd	doublet of doublets (NMR)
DMF	N, N-dimethylformamid
DMSO	dimethyl sulfoxide
dt	doublet of triplets (NMR)
eq.	equivalent/s
Et	ethyl
Et$^{\bullet}$	ethyl radical
GC	gas chromatography
g	gram/s
HRMS	high resolution mass spectrometry
h	hour/s
Hz	hertz (NMR)
in vacuo	under vacuum

in situ	in solution
^{i}Pr	isopropyl
J	coupling constant (NMR)
l	litre
LDA	lithium diisopropylamide
Lit.	literature
LFP	laser flash photolysis
µ	micro
m	multiplet (NMR)
M	concentration in moles per litre
Me	methyl
min	minute/s
MHz	megahertz (NMR)
mol	mole/s
MS	mass spectrometry
m/z	mass to charge ratio
nm	nanometer
ns	nanosecond
NMR	nuclear magnetic resonance
ppm	parts per million (NMR)
Pet. Spirits	petroleum spirits
Ph	phenyl
psi	Pounds per square inch
q	quartet (NMR)
R	gas constant
ref.	reference

RT	room temperature
s	singlet (NMR)
Sat.	saturated
t	tertiary
T	temperature
TS	transition state
THF	tetrahydrofuran
TLC	thin-layer chromatography
TFA	trifluoroacetic acid
UV	ultraviolet
W	watt

Table of contents

ABSTRACT ..... **IV**

DECLARATION ..... **VI**

PREFACE ..... **VII**

ACKNOWLEDGMENTS ..... **VIII**

ABBREVIATIONS ..... **IX**

TABLE OF CONTENTS ..... **XIII**

LIST OF FIGURES ..... **XVI**

LIST OF TABLES ..... **XVIII**

1 INTRODUCTION **1**

1.1 Ionic liquids **1**
1.1.1 History and applications 1
1.1.2 Physicochemical properties 1
1.1.3 ILs and green chemistry 5
1.1.4 ILs as convenient solvents for synthetic chemistry 6

1.2 Free radicals in organic chemistry **11**
1.2.1 General aspects of free radicals 11
1.2.2 Polar effects on radical additions to double bonds 12
1.2.3 Intramolecular radical addition to double bonds (radical cyclisations) 13
1.2.4 Direct and indirect competition kinetic techniques 13
1.2.5 Well-studied radical clocks 17
1.2.6 Stereochemistry of the 5-*exo* cyclisation of substituted 5-hexenyl radicals 21
1.2.7 Alkoxy radical cyclisation 25
1.2.8 Intramolecular homolytic substitutions 27
1.2.9 Intermolecular addition to alkene 28
1.2.10 Solvent effects on radical reactions 29

1.3 Free radical reactions in ionic liquids **31**
1.3.1 1-Ethyl-3-methylimidazolium bis(trifluoromethylsulfonyl)imide ([EMIm][NTf_2]) as a medium for radical reactions 32

1.4 Aim and methodology of this thesis **34**

1.5 References **37**

2 5-*EXO* CYCLISATION OF PRIMARY ALKYL RADICALS **51**

2.1 Exploring the compatibility of [EMIm][NTf_2] in radical reactions **52**

2.2 Synthesis of the radical precursors 43 and reference compounds **53**

2.3 Extraction procedure **58**

2.4 Kinetic experiments **61**

2.4.1 Determination of the absolute rate constant, k_C, in [EMIm][NTf_2] using the direct method 61
2.4.2 Competition kinetic studies 64

2.5 Recyclability 83

2.6 Summary 84

2.7 References 85

3 CYCLISATION OF SECONDARY 5-HEXENYL RADICALS 89

3.1 Synthesis of the radical precursors 62a-d and reference compounds 90

3.2 Kinetic experiments 91
3.2.1 Cyclisation of 1-methyl-5-hexenyl radical (63a) 92
3.2.2 Cyclisation of the 1-ethyl-5-hexenyl radical (63b) 98
3.2.3 Cyclisation of 1-isopropyl-5-hexenyl radical (63c) 103
3.2.4 Cyclisation of 1-*t*-butyl-5-hexenyl radical (63d) 107

3.3 Tandem radical cyclisations 115
3.3.1 Synthesis of the radical precursor 70 115
3.3.2 Product assignment 116

3.4 Summary 121

3.5 References 123

4 MISCELLANEOUS REACTIONS: INTRAMOLECULAR HOMOLYTIC SUBSTITUTIONS, 5-*EXO* ALKOXY RADICAL CYCLISATIONS AND INTERMOLECULAR HOMOLYTIC ADDITION TO ALKENES 126

4.1 Intramolecular homolytic substitution 126
4.1.1 Synthesis of the PTOC ester 77 and pentamethylene selenide (79) as reference compound 127

4.2 Alkoxy radical cyclisations 130

4.3 Intermolecular addition of alkyl radicals to alkenes 136
4.3.1 Intermolecular addition of 3-phenylpropyl radical (90) to methylacrylate (MA) 138
4.3.2 Intermolecular addition of 3-phenylpropyl radical (90) to methyl methacrylate (MMA) 144

4.4 Summary 148

4.5 References 149

5 CONCLUSION AND PERSPECTIVE 151

5.1 Conclusion 151

5.2 Future directions 152

6 EXPERIMENTAL 154

6.1 General materials, equipment and methods 154

6.2 Synthesis library 155
6.2.1 Synthesis of the acids 47a-d and 66a-d 155

6.2.2 Synthesis of the PTOC esters (43a-d) and (62a-d)..... 159
6.2.3 Synthesis of the radical precursor 70 and 77 161
6.2.4 Synthesis of the radical precursor (81a-b) 163

6.3 Synthesis of the reference compounds 164

6.4 Competition kinetic experiments..... 167

6.5 References..... 169

APPENDIX..... 171

List of Figures

Chapter 1

Figure 1.1. Common IL cations and anions. R = alkyl substituent. 2
Figure 1.2. Arrhenius plots of dynamic viscosity (η) of ILs: [EMIm][$EtSO_4$], O; [EMIm][NTf_2], □; [EMIm][$N(CN)_2$], Δ; [OMA][NTf_2]. 3
Figure 1.3. Examples of hydrophobic and hydrophilic ILs. 5
Figure 1.4. Examples of toxic and non-toxic and biodegradable ILs. 6
Figure 1.5. *In situ* formation of phosphine-imidazolylidene palladium complex 13. ... 9
Figure 1.6. Coordination of the carbonyl oxygen to the phosphorus atom in trioctylethylphosphonium tosylate. 10
Figure 1.7. Frontier molecular orbitals in electrophilic and nucleophilic radicals. 12
Figure 1.8. Nitroxyl radical coupling reactions. 16
Figure 1.9. The PTOC-thiol method chain sequence in a competition kinetic experiment. 17
Figure 1.10. Reaction coordinate for the competing cyclisation pathways of 5-hexenyl radical (25). 20
Figure 1.11. Orbital overlap in the transition state (TS) of the 5-*exo* cyclisation of the hept-6-en-2-yl radical (32). 22
Figure 1.12. Structures of Monensin A and Calcimycin. 25
Figure 1.13. TS model for stereoselective alkoxy radical cyclisation. 26
Figure 1.14. Interaction between nitroxide radical and imidazolium based ionic liquid. 32
Figure 1.15. Structure of [EMIm][NTf_2], the IL used in this thesis. 33
Figure 2.1. Products of 5-hexenyl radical (25a) cyclisation. 59
Figure 2.2. Products of radical 25c cyclisation. 60
Figure 2.3. Time-resolved spectrum of transients produced by photolysis of PTOC ester 43b obtained 60 ns after irradiation with 355 nm light in acetonitrile (red line) and [EMIm][NTf_2] (blue line). Experiments performed by Dr J. Nathanael. 62
Figure 2.4. Time-dependent formation of (diphenylmethylene)cyclopentyl radical 26b at 310 nm in [EMIm][NTf_2] ([PTOC] = 0.23 mM). Experiments performed by Dr J. Nathanael. 64
Figure 2.5. Dependence of [26b-H]/[25b-H] on *t*-BuSH concentration at 24 ± 1 °C for the cyclisation of the 6,6-diphenyl-5-hexenyl radical (25b). 67
Figure 2.6. Dependence of [26a-H]/[25a-H] on *t*-BuSH concentration at 24 ± 1 °C for the cyclisation of the 5-hexenyl radical (25a). 71
Figure 2.7. A plot of ln (k_C/k_H)) *vs*.1/T for the cyclisation of the 5-hexenyl radical (25a) and reduction through hydrogen abstraction from *t*-BuSH in [EMIm][NTf_2]. (R = 8.314 J K^{-1} mol^{-1}) 73
Figure 2.8. Structures and chemical shifts of compound 43a, 43c and 43d. 74
Figure 2.9. Dependence of [26c-H]/[25c-H] on *t*-BuSH concentration at 24±1 °C for the cyclisation of the 5-hexenyl 25c radical and reduction through hydrogen abstraction from *t*-BuSH. 76
Figure 2.10. (ln (k_C/k_H)) *vs*.1/T for the ring closure of the 5-hexenyl radical 25c and reduction through hydrogen abstraction from *t*-BuSH. (R = 8.314 J K^{-1} mol^{-1}).. 79
Figure 2.11. Dependence of [26d-H]/[25d-H] on *t*-BuSH concentration at 24 ± 1 °C for the cyclisation of the 5-hexenyl radical 25d. 82

Figure 3.1. Dependence of [64a-H]/[63a-H] on *t*-BuSH concentration at 24 ± 1 °C for the cyclisation of the 5-hexenyl radical 63a and reduction through hydrogen abstraction from *t*-BuSH. 94
Figure 3.2. (ln (k_C/k_H)) *vs*.1/T for the 5-*exo* ring closure of the 5-hexenyl radical 63a and reduction through hydrogen abstraction from *t*-BuSH in [EMIm][NTf_2] and *t*-BuPh (R = 8.314 kJ mol^{-1}). 96
Figure 3.3. Temperature dependence of the 5-*exo* cyclisation of 63a ([*cis*/*trans*-64a-H]) *vs*. the direct reduction by *t*-BuSH in *t*-BuPh (■) and [EMIm][NTf_2] (●); with [*t*-BuSH]/[62a] = 10 (left axis). Viscosity data for [EMIm][NTf_2] (○) are taken from ref. [19] (right axis). 97
Figure 3.4. Dependence of [64b-H]/[63b-H] on *t*-BuSH concentration at 24 ± 1 °C for the cyclisation of the 1-ethyl-5-hexenyl radical (63b). 100
Figure 3.5. Structures of *cis*-64a-H and *cis*-64b-H. 100
Figure 3.6. (ln (k_C/k_H)) *vs*.1/T for the ring closure of the 5-hexenyl radical 63b in [EMIm][NTf_2] and *t*-BuPh (R = 8.314 kJ mol^{-1}). 102
Figure 3.7. Dependence of [64c-H]/[63c-H] on *t*-BuSH concentration at 24 ± 1 °C for the cyclisation of the 5-hexenyl radical 63c and reduction through hydrogen abstraction from *t*-BuSH. 104
Figure 3.8. (ln (k_C/k_H)) *vs*.1/T for the ring closure of the 5-hexenyl radical 63c in [EMIm][NTf_2] and *t*-BuPh (R = 8.314 kJ mol^{-1}). 106
Figure 3.9. Cyclisation of the 1-*t*-butyl-5-hexenyl radical (63d). 107
Figure 3.10. The 5-*exo* cyclisation of substrates 68 and 69. 108
Figure 3.11. Dependence of [64d-H]/[63d-H] on *t*-BuSH concentration at 24 ± 1 °C for the cyclisation of the 1-*t*-butyl-5-hexenyl radical 63d. 110
Figure 3.12. Transition structure for the ring closure of radical 63d. 111
Figure 3.13. a: (ln (k_C/k_H)) *vs*.1/T and b: (ln (k_{cis}/k_{trans})) *vs*.1/T for the ring closure of the 5-hexenyl radical 63d in [EMIm][NTf_2] and *t*-BuPh (R = 8.314 kJ mol^{-1}). 113
Figure 3.14. DEPT ^{13}C NMR spectra of the reaction mixture resulting from cyclisation of 1-propargyl-5-hexenyl radical (71) in C_6D_6 at 90 ^oC. 119
Figure 3.15. ^{13}C NMR(500 MHz, C_6D_6) of the reaction mixture resulting from cyclisation of 1-propargyl-5-hexenyl radical (71). 120
Figure 4.1. (ln (k_C/k_H)) *vs*.1/T for the homolytic substitution of radical 78 in [EMIm][NTf_2] and benzene. (R = 8.314 J K^{-1} mol^{-1}) 129
Figure 4.2. (ln (k_C/k_H)) *vs*.1/T for the ring closure of the alkoxy radical 82b in [EMIm][NTf_2] and *t*-BuPh (R = 8.314 kJ mol^{-1}). 134
Figure 4.3. Dependence of [Add]/[90-H] on [MA]/[*t*-BuSH] at 24 ± 1°C for the addition of radical 90 to MA. [Add] = [91a-H] + [92a-H]. 142
Figure 4.4. (ln (k_{add}/k_H)) *vs*.1/T for the addition of radical 90 to MA in [EMIm][NTf_2]. 143
Figure 4.5. Dependence of [Add]/[90-H] on [MMA]/[*t*-BuSH] at 24 ± 1 °C for the addition of radical 90 to MMA. 145
Figure 4.6. (ln (k_{add}/k_{Red})) *vs*.1/T for the addition of radical 90 to MMA in [EMIm][NTf_2] and benzene (R = 8.314 kJ mol^{-1}). 147

List of Tables

Chapter 1

Table 1.1. *Cis*/*trans* stereoselectivity for the 5-*exo* cyclisation of substituted 5-hexenyl radicals in different solvents. 31

Chapter 2

Table 2.1. The ratio of GC peak areas of methylcyclopentane (26a-H) and 1-hexene (25a-H) in *t*-BuPh and after extraction from [EMIm][NTf_2]. 60
Table 2.2. The ratio of GC peak areas of compounds 26c-H and 25c-H in *t*-BuPh and after extraction from [EMIm][NTf_2]. 60
Table 2.3. GC results of the competition kinetic experiments for the 5-*exo* cyclisation of the 6,6-diphenyl-5-hexenyl radical (25b) at 24 ± 1 °C. 66
Table 2.4. Kinetic data for the 5-*exo* cyclisation of the 6,6-diphenyl 5-hexenyl radical 25b. 68
Table 2.5. GC results of the competition kinetic experiments for the 5-*exo* cyclisation of the 5-hexenyl radical (25a) at 24 ± 1 °C in *t*-BuPh and [EMIm][NTf_2]. 70
Table 2.6. GC results of the competition kinetic experiments for the 5-*exo* cyclisation of the 5-hexenyl radical 25a at different temperatures in [EMIm][NTf_2]. 72
Table 2.7. Kinetic rate data for the 5-*exo* cyclisation of the 5-hexenyl radical (25a). 73
Table 2.8. GC results of the competition kinetic experiments for the 5-*exo* cyclisation of the 5-hexenyl radical 25c at 24 ± 1 °C. 76
Table 2.9. GC results of the competition kinetic experiments for the 5-*exo* cyclisation of the 5-hexenyl radical 25c at different temperature. 78
Table 2.10. Kinetic rate data for the 5-*exo* cyclisation of the 3,3-diester-5-hexenyl radical. 79
Table 2.11. GC results of the competition kinetic experiments for the 5-*exo* cyclisation of the 5-hexenyl radical 25d at 24 ± 1 °C. 81
Table 2.12. Kinetic rate data for the 5-*exo* cyclisation of the 2,2-diester-5-hexenyl radical 25d. 83

Chapter 3

Table 3.1. GC results of the competition kinetic experiments for the 5-*exo* cyclisation of the 1-methyl-5-hexenyl radical (63a) at 24 ± 1 °C. 93
Table 3.2. GC results of the competition kinetic experiments for the 5-*exo* cyclisation of the 1-methyl-5-hexenyl radical (63a) at different temperatures. 95
Table 3.3. Kinetic data for the 5-*exo* cyclisation of the 5-hexenyl radical 63a. 98
Table 3.4. Results of the competition kinetic experiments for the 5-*exo* cyclisation of the 1-ethyl-5-hexenyl radical (63b) at 24 ± 1 °C. 99
Table 3.5. GC results of the competition kinetic experiments for the 5-*exo* cyclisation of the 1-ethyl-5-hexenyl radical (63b) at different temperatures. 101
Table 3.6. Kinetic rate data for the 5-*exo* cyclisation of the 5-hexenyl radical 63b. 103

Table 3.7. GC results of the competition kinetic experiments for the 5-*exo* cyclisation of the 1-isopropyl-5-hexenyl radical (63c) at 24 ± 1 °C. 104
Table 3.8. GC results of the competition kinetic experiments for the 5-*exo* cyclisation of the 1-isopropyl-5-hexenyl radical (63c) at different temperatures. 105
Table 3.9. Kinetic rate data for the 5-*exo* cyclisation of the 1-isopropyl-5-hexenyl radical (63c). 106
Table 3.10. *Cis*/*trans* ratio for the 5-*exo* cyclisation of the substrates 68, 69 and 63d in different solvents. 108
Table 3.11. GC results of the competition kinetic experiments for the 5-*exo* cyclisation of the 1-*t*-butyl-5-hexenyl radical (63d) at 24 ± 1 °C. 110
Table 3.12. GC results of the competition kinetic experiments for the 5-*exo* cyclisation of the 1-*t*-butyl-5-hexenyl radical (63d) at different temperatures. 112
Table 3.13. Kinetic data for the ring closure of 5-hexenyl radical 63d. 114

Chapter 4

Table 4.1. GC results of the competition experiments for the intramolecular homolytic substitution of the radical 78 at different temperatures. 129
Table 4.2. Kinetic data for the homolytic substitution of the radical 78 in benzene and in [EMIm][NTf_2]. 130
Table 4.3. GC results of the competition kinetic experiments for the 5-*exo* cyclisation of the alkoxyl radical 82b at different temperatures. 134
Table 4.4. Kinetic data for the 5-e*xo* cyclisation of the alkoxy radical 82b. 136
Table 4.5. GC results of the competition experiments for intermolecular addition of radical 90 to MA at 24 ± 1 °C. 141
Table 4.6. GC results of the competition experiments for the intermolecular addition of radical 90 to MA at different temperatures in [EMIm][NTf_2]. 143
Table 4.7. Results of the competition experiments for the intermolecular addition of radical 90 to MMA at 23 °C. 145
Table 4.8. Results of the competition experiments for the intermolecular addition of radical 90 to MMA at different temperatures. 146
Table 4.9. Kinetic rate data for the addition of radical 90 to alkenes. 148
Table 6.1. Temperature program used for the analysis of the radical reactions studied in this work. 168

1 Introduction

1.1 Ionic liquids

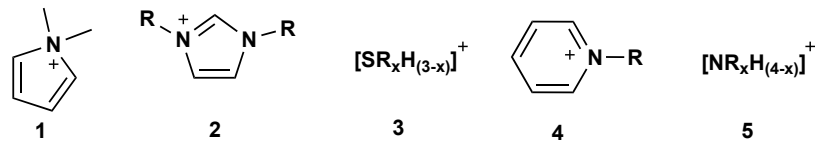
1.1.1 History and applications

Ionic liquids (commonly abbreviated as IL) consist of oppositely charged ions, where a combination of van der Waals, hydrogen bonding and coulombic interactions causes most ILs to be liquid at ambient temperature (so-called "Room Temperature ILs", or RTILs), with melting points below 100°C.[1] ILs were first mentioned in the late 19th century, with Sir William Ramsay describing the product of citric acid and picoline as an "uncrystallisable syrup" in 1876.[2] However, the first intentionally synthesised IL, ethylammonium nitrate (Et_3NH^+ NO_3^-), is generally attributed to Paul Walden (1914), without knowing that it would eventually become an important area of science.[3] The recent popularity of ILs is manifested by the number of publications on these solvents, which have increased from only a few in the early 2000s to more than 40000 in the second half of 2019 Research into ILs occurs in diverse fields including biotechnology,[4] batteries,[5] material processing,[6] fuel cells,[7] sensors,[8] solvents,[9] electrochemical applications,[10-11] environmental science and solar cells.[12]

1.1.2 Physicochemical properties

The advantage of ILs, compared to conventional organic solvents, are their properties as non-flammable and non-volatile solvents with high water and air resistance, which makes them highly desirable media for many applications.[13] While it is true to say that some ILs are moister and air stable, chloroaluminate, chloride and sulphate anions produce hydrophilic ILs.[14] ILs consist of cations, such as [*N*,*N*-dialkyl pyrrolidinium]$^+$ (**1**), [1,3-dialkyl imidazolium]$^+$ (**2**), [trialkyl sulfonium]$^+$ (**3**), [*N*-alkyl pyridinium]$^+$ (**4**) or [tetra-alkyl ammonium]$^+$ (**5**), combined with various inorganic or organic anions, such as tosylate (**6**), alkyl sulfonate (**7**), tetrafluoroborate (**8**) and bis(trifluoromethyl sulfonyl)imide (**9**) , which are shown in Figure 1.1.

Common cations:



Common anions:

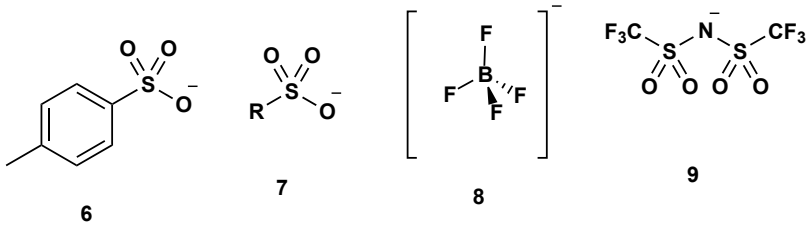


Figure 1.1. Common IL cations and anions. R = alkyl substituent.

ILs can be designed for specific applications by variation of either the anions, cations or by modification of the substituents on the ions.[15, 16] Therefore, a wide variety of IL structures with different physical properties, such as density, viscosity, melting point, hydrophobicity and solubility, are (commercially) available. For example, imidazolium-based ILs were first reported by Wikes in 1982 and developed for use as battery electrolytes.[17] The following are the main features of ILs:

I. Composed of large organic cations and anions with asymmetric and complex shapes that prevent the ions being held together in a crystalline structure; melting and freezing points are reduced so that ILs are liquid at ambient temperature.[18]
II. Strong electrostatic interactions between ions reduce the volatility of these solvents.[19] Despite very low vapour pressure, ILs can be distilled under ultrahigh vacuum to produce very pure solvents for analytical purposes.[20]
III. ILs are electrolytes which do not require co-solvents, so they are in the liquid phase across a wide range of temperatures.[21-22]

IV. Mixing different ILs,[23-24] or diluting them with organic solvents[25] enables modification of the physical properties of the solvent to obtain functionality for specific purposes.[26]

V. ILs are recyclable and re-usable.[27-29]

VI. ILs could enable chemical transformations that are not possible in conventional solvents, for example when nonpolar and polar compounds need to be dissolved simultaneously.[30]

Given the above points, knowledge about the physicochemical properties, and the relationship between property and structure of ILs allows to take advantage of different ILs for specific applications.[31-33] It should be noted, however, that the physicochemical properties of the ILs can be affected by impurities, either from absorbing atmospheric moisture or during IL preparation, which hamper the accurate understanding of the property-structure relationship.[34-36] Fröba, Kremer and Leipertz made important contributions to determining the physical properties, including refractive index, density, surface tension and viscosity of various ILs as a function of temperature.[37] Figure 1.2 represents the dynamic viscosity of four different ILs including [EMIm][$EtSO_4$] (1-ethyl-3-methyl imidazolium ethyl sulfate), [EMIm][NTf_2], [EMIm][$N(CN)_2$] (1-ethyl-3-methyl imidazolium dicyanimide) and [OMA][NTf_2] (trioctyl methyl ammonium bis(trifluoromethyl sulfonyl)imide) as a function of temperature at atmospheric pressure measured using surface light scattering (SLS).[38] The graph clearly shows the drop in IL viscosity with increasing temperature.

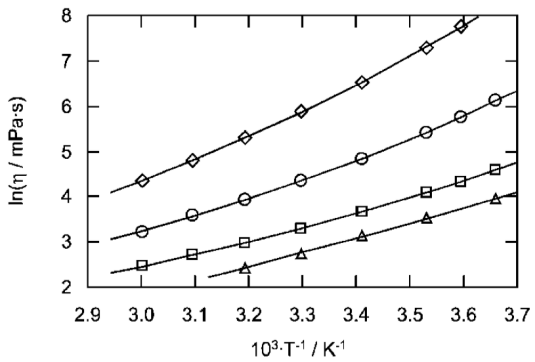


Figure 1.2. Arrhenius plots of dynamic viscosity (η) of ILs: [EMIm][$EtSO_4$], O; [EMIm][NTf_2], □; [EMIm][$N(CN)_2$], Δ; [OMA][NTf_2], ◇. This graph is taken from ref. [34].

To the best of our knowledge there is no data indicating that this behaviour of ILs could possibly change the outcome of any reactions, which could be interesting topics of study.

ILs as reaction media for free radical polymerisations have also been reported.[9, 39-41] The advantages of ILs over conventional organic solvents for polymerisation processes is not just related to the low volatility or non-flammability of the solvent, but as a medium for polymerisation from which polymers with higher molar mass are obtained. High viscosity of ILs in comparison with organic solvents,[42] caused higher degree of polymerisation due to diffusion-controlled termination, which leads to generate less volatile thermolysis fragments and produce polymers with lower thermal degradation.[41]

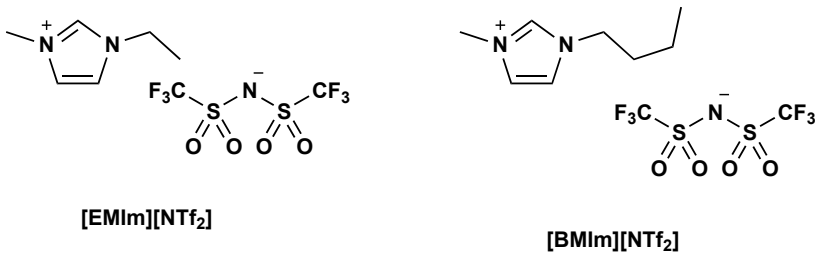
Apart from radical polymerisations, which can be carried out on industrial scales, and have been successfully performed in ILs,[9] studies of the behaviour of free radicals in ILs in other synthetic radical processes are sparse, as evident from the relatively few publications available on this topic.

In addition to room temperature ILs (RTILs),[26] many other types of ILs are available today, for example polymerized ILs (PILs) with polymeric structure consisting of IL monomers,[42] task specific ILs (TSILs), which are designed for specific purposes, granting a dual use of solvent and catalyst or reagent for particular tasks,[44] and supported IL membranes (SILM), which consist of pores that are filled with an IL and can be used for selective separation of organic compounds or mixtures of gases.[45] Thus, the use of ILs as "designable" solvents has seen increasing use in organic reactions, and also as media for radical polymerisations. In addition, the application of ILs in drug delivery systems has been reported.[46]

The applications of ILs mostly make use of their physical properties including solubility, miscibility and viscosity. For example, ILs can be either hydrophobic such as [EMIm][NTf_2] (1-ethyl-3-methylimidazolium bis(trifluoromethyl sulfonyl)imide) and [BMIm][NTf_2] (1-butyl-3-methylimidazolium bis(trifluoromethyl sulfonyl)imide) or hydrophilic such as [EMIm]Cl (1-ethyl-3-methylimidazolium chloride) and [EMIm][$EtSO_4$] (1-ethyl-3-methylimidazolium ethyl sulphate) (Figure 1.3).[14] Water miscibility of an IL mostly determined by the choice of anions. Hydrophilic anions

such as chloride and sulphate produce hydrophilic ILs. In comparison, hydrophobic anions including NTf_2^- and PF_6^- produce ILs that are not miscible with water. A hydrophobic IL can be used as a non-soluble polar solvent to make a two-phase system with water.

Hydrophobic ILs



Hydrophilic ILs

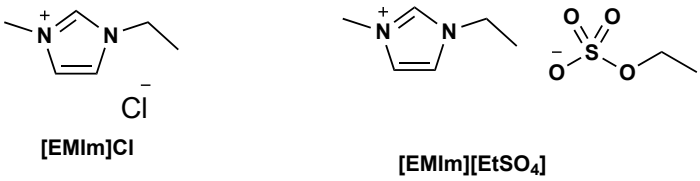
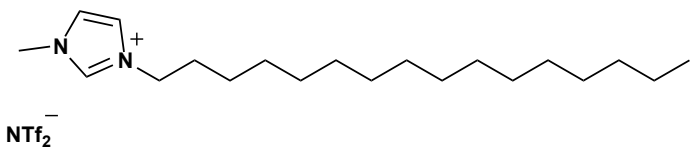


Figure 1.3. Examples of hydrophobic and hydrophilic ILs.

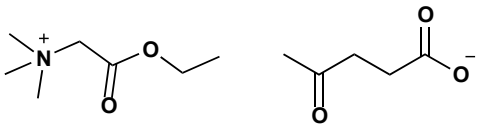
1.1.3 ILs and green chemistry

With the world's increasing population, the demand for medicines, food, clothes and other products is also greatly increasing. Chemistry always has played a crucial role in the development and production of materials for human requirements; however, many chemical processes are responsible for pollution and contamination of the environment. Accordingly, "green chemistry" aims to develop new chemical reactions and technologies, which will have substantially less damaging effects on the ecosystem, human and wild life.[47] While the detrimental effects of traditional solvents on various chemical reactions are well documented in terms of both kinetics and thermodynamics, the search for greener alternatives for some of the more problematic solvents (*e.g.* benzene and carbon tetrachloride – the latter is now banned in many countries) has become a priority. A few alternative solutions and solvents have already been explored that avoid or substitute organic solvents by non-toxic or

'trace-less' alternatives, including solvent-free synthesis,[48-49] using water as reaction media,[50-53] supercritical carbon dioxide[54] and poly(ethylene glycol). In recent years, poly (ethylene glycol) has attracted attention as a green reaction media, which is less hazardous than other organic solvents and has negligible vapour pressure.[55-57] However, drawbacks include cost, limited solubility, and a narrow or limited ease of use. These days, ILs are also marketed as "green" or "sustainable" alternatives to conventional solvents, but such terminology does not necessarily mean that ILs are environmentally friendly. Some ILs are known to be toxic such as [HDMIM][NTf_2] (1-hexadecyl-3-methylimidazolium bis(trifluoromethyl sulfonyl)imide),[58,59] while others are considered to be non-toxic[60] and biodegradable such as [Bet-ester][Lev] (2-ethoxy-*N*,*N*,*N*-trimethyl-2-oxoethanaminium levulinate) (Figure 1.4).[29]



[HDMIM][NTf_2]



[Bet-ester][Lev]

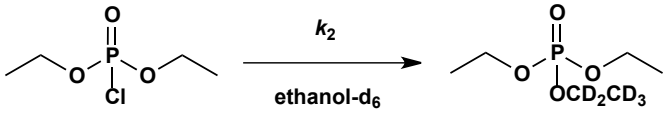
Figure 1.4. Examples of toxic and non-toxic and biodegradable ILs.

Nonetheless, "green chemistry" and ILs are correlated due to the unique properties of the latter, which make ILs alternatives to conventional solvents.

1.1.4 ILs as convenient solvents for synthetic chemistry

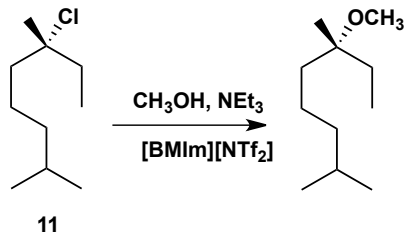
The use of ILs as reaction medium has been widely explored. Consequently, the effects of ILs on the selectivity and kinetics of many organic reactions have been studied in detail. For example, Harper *et al.* found that the rate of the ethanolysis of diethyl chlorophosphate **10** was affected by addition of [BMIm][NTf_2], with the rate

enhancement depending on the mole fraction of the IL used. For example, the ratio of the bimolecular rate constant (k_2) at 0.3 mole fraction of [BMIm][NTf_2] in ethanol to the value in ethanol-d_6 ($k_{2(ethanol)}$) at 25 °C is ($k_2/k_{2(ethanol)}$ = 4.0 ± 0.19). Determination of the activation parameters showed the decrease in both activation enthalpy and entropy. The decrease in both parameters suggests either a decreased organisation about and stabilisation of the starting materials or stabilisation of the transition state through electrostatic interaction with components of [BMIm][NTf_2] (which also involve some ordering). Given the charge development in the transition state, the later has been considered as the origin of the rate enhancement (Scheme 1.1).[61]



Scheme 1.1. Ethanolysis of diethyl chlorophosphite.

It is interesting to note that various reactions have different mole fraction dependencies. For example, an increase of the bimolecular rate constant (k_2) for the reaction between chloride **11** and methanol in the presence of triethylamine at 40 °C to reach a maximum enhancement by a factor of two at 0.02 mole fraction of [BMIm][NTf_2] in methanol was found.[62] In this case, the maximum effect occurred at a much lower proportion of the ionic liquid compared to the ethanolysis of diethyl chlorophosphite described in Scheme 1.2 above.

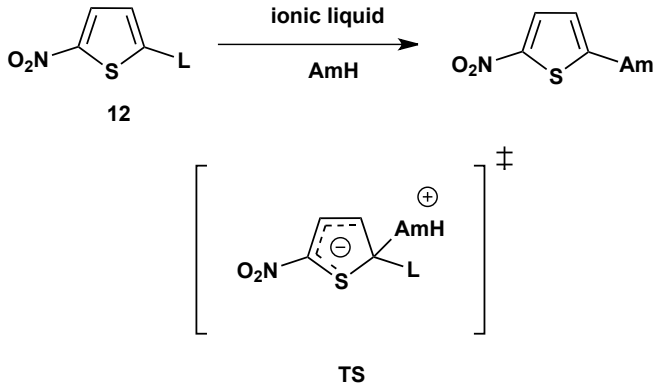


k_2 = (62.5 ± 0.4) × 10^{-5} s^{-1} (methanol at 40 °C)

k_2 = (4.8 ± o.6) × 10^{-5} s^{-1} (0.02 mole fraction of [BMIm][NTf_2] at 40 °C)

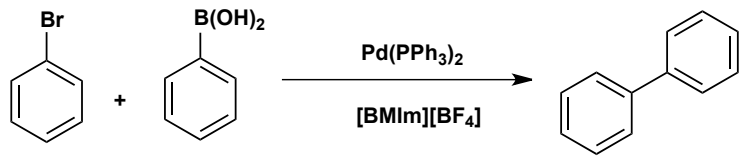
Scheme 1.2. Solvolysis of the chloride **11** to give an ether.

The work of D'Anna *et al.* [63-70] and Welton *et al.* [71-81] are typical examples of kinetic studies on organic processes. D'Anna reported a faster rate (by almost 1 or 3 orders of magnitude in comparison with methanol or benzene) of the nucleophilic aromatic substitution of some 2-L-5-nitrothiophene **12** (L= Br, OMe, OC_6H_5 as leaving groups) with amines such as piperidine, pyrrolidine and morpholine in ILs comparing to organic solvent (benzene, methanol) (Scheme 1.2). This rate enhancement was attributed to an increase in polarity of the solvent, which stabilises the charge separation developed in the transition state.[82]



Scheme 1.2. Aromatic nucleophilic substitution with amines on nitrothiophenes. L = Br, OMe, OC_6H_5. AmH = piperidine, pyrrolidine, morpholine.

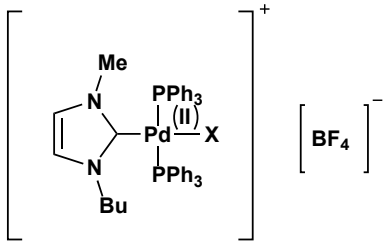
ILs are also useful reaction media for transition metal catalysis processes, where they can be considered as co-catalyst, since organometallic compounds can be dissolved in ILs. Well-studied examples include Heck reactions,[83] Suzuki cross-coupling reactions (Scheme 1.3),[84] hydroformylation and hydrogenation reactions.[85]



Scheme 1.3. Example of Suzuki cross-coupling reaction in [BMIm][NTf_2].

For example, the observed improved efficiency of coupling reactions catalysed by palladium phosphine have been rationalised by *in situ* formation of complex **13** from

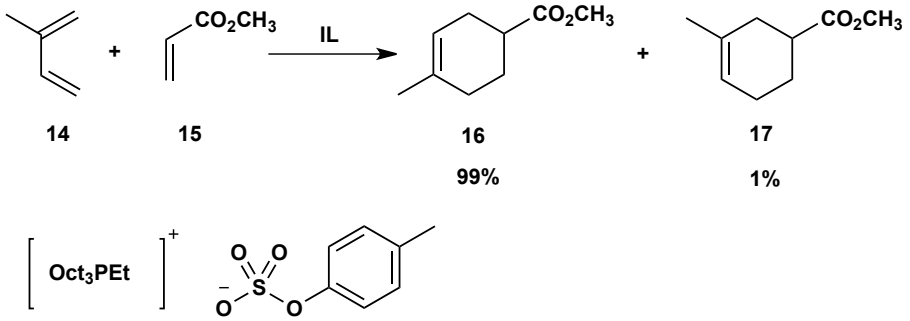
[BMIm][BF_4], which makes the catalyst to exist longer and prevents catalyst decomposition (Figure 1.5).[86, 87]



13 X = Cl, Br

Figure 1.5. *In situ* formation of phosphine-imidazolylidene palladium complex **13**.

Furthermore, ILs have been used as solvents and catalysts for organic syntheses including Diels-Alder reaction,[88] esterifications,[89] stereoselective halogenations,[86] Friedel-Crafts reactions, Fischer-Tropsch syntheses, among others. For example, the Diels-Alder reaction of isoprene **14** with methyl acrylate **15** proceeds in trioctylethylphosphonium tosylate with high regioselectivity leading to practically exclusive formation of the 4-substituted product **16** (Scheme 1.4). The absence of the regioisomeric product **17** has been rationalised by coordination of the carbonyl oxygen in **15** to the phosphorus atom in the IL, which increases the steric bulk at the carbonyl side in methyl acrylate so that isoprene approaches methyl acrylate with its methyl group as far away as possible from the coordinated carbonyl group (Figure 1.6).[91]



IL: trioctylethylphosphonium tosylate

Scheme 1.4. Diels-Alder reaction of methyl acrylate **15** with isoprene **14** in IL as a solvent.

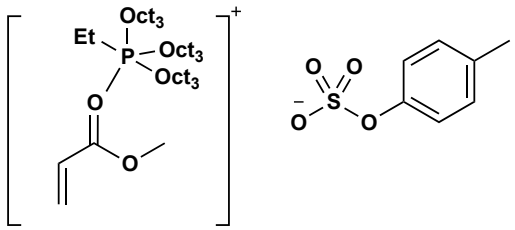
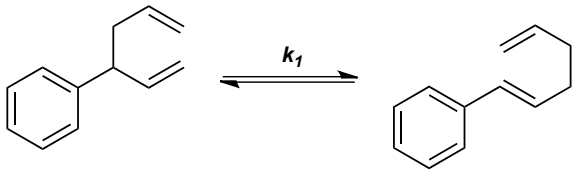


Figure 1.6. Coordination of the carbonyl oxygen to the phosphorus atom in trioctylethylphosphonium tosylate.

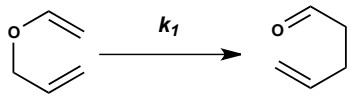
Pericyclic processes such as the Cope and Claisen rearrangements have been shown to perform in ILs with higher efficiency as a result of the high pressure within the solvent caused by strong cohesive interaction between ionic species of the solvent, and stabilising of the transition state in the IL.[92-94] For example, Cope rearrangement of 3-phenyl-1,5-hexadiene increased from $k_1 = (6.2 \pm 2.5) \times 10^{-7}$ s^{-1} in benzene at 150 °C to $k_1 = (61.6 \pm 9.4) \times 10^{-7}$ s^{-1} in [BMIm][NTf$_2$] at 150 °C (Scheme 1.5). Also, Claisen rearrangement of allyl vinyl ether increased from $k_1 = (1.0 \pm 0.1) \times 10^{-8}$ s^{-1} in benzene at 45 °C to $k_1 = (3.2 \pm 0.1) \times 10^{-8}$ s^{-1} in [BMIm][NTf$_2$] at 45 °C (Scheme 1.6).



$k_1 = (6.2 \pm 2.5) \times 10^{-7}$ s^{-1} (in benzene at 150 °C)

$k_1 = (61.6 \pm 9.4) \times 10^{-7}$ s^{-1} (in [Bmim][NTf$_2$] at 150 °C)

Scheme 1.5. Cope rearrangement of 3-phenyl-1,5-hexadiene.



$k_1 = (1.0 \pm 0.1) \times 10^{-8}$ s^{-1} (in benzene at 45 °C)

$k_1 = (3.2 \pm 0.1) \times 10^{-8}$ s^{-1} (in [Bmim][NTf$_2$] at 45 °C)

Scheme 1.6. Claisen rearrangement of allyl vinyl ether.

1.2 Free radicals in organic chemistry

1.2.1 General aspects of free radicals

Free radicals with a singly occupied molecular orbital (SOMO) are usually highly reactive species with unique properties.[95,96] Up to the 1950s, free radical reactions were frequently disdained by synthetic practitioners and often blamed as the main reason for unwanted reaction outcomes.[97] However, from the 1960s onwards, scientists have sought to control free radical reactions in order to take advantage of these reactive species.[98-101] Since the discovery of radical chain reactions and the role of transition metal compounds, such as mercury and tin hydrides in promoting these reactions, radical chemistry has turned into an important tool in organic synthesis,[102] providing methods to make new bonds such as inter-molecular or intramolecular homolytic addition to double bonds,[103,104] intramolecular homolytic substitutions[105] or translocation reactions.[106]

In addition to their inherent reactivity, there are other factors that govern the outcome of free radical reactions, such as electronic, polar, steric and bond strength effects.[107] Understanding these factors allows to control the reaction conditions in order to influence the reaction outcome in terms of regio- or stereoselectivity.[108] Although several rules have been proposed that govern radical reactions, it remains difficult to accurately predict the outcome of free radical reactions.[109] Since these reactions are usually performed under kinetic rather than thermodynamic control, the stability of the product is not determining the reaction outcome, whereas factors that affect the transition state are key.[110]

In the following sections, important radical reactions including intramolecular and intermolecular radical addition to alkene double bonds, alkoxy radical cyclisations and homolytic substitution reactions will be reviewed, since they have become fundamental to the methods of organic synthesis and the formation of new bonds and will therefore be topics of study in this thesis.

1.2.2 Polar effects on radical additions to double bonds

In radical additions to alkenes the regioselectivity and reaction rate depend on the several factors, including the nature of the substituents on the double bond and on the radical. The presence of electron withdrawing groups (EWGs) or electron donating groups (EDGs) on the radical and double bond has a large influence on the rate and regioselectivity of addition.[111]

Carbon radicals, X-C$^{\bullet}$, are considered nucleophilic if X is an electron donor (RO, NR_2, R_3Si or alkyl, etc.) or electrophilic if X is electron withdrawing (NO_2, CN, COR, CO_2R, etc.). Nucleophilic radicals interact faster with electron poor olefins, conversely electrophilic radicals react faster with electron rich olefins. These effects can be explained by frontier molecular orbital theory: the SOMO of the radical can interact with either the highest occupied molecular orbital (HOMO) or lowest unoccupied molecular orbital (LUMO). In a nucleophilic radical, the raised SOMO interacts with the lower LUMO of the electron poor olefin. In an electrophilic radical the lower SOMO of radical interacts with the raised HOMO of the electron rich olefin (Figure 1.7).[112]

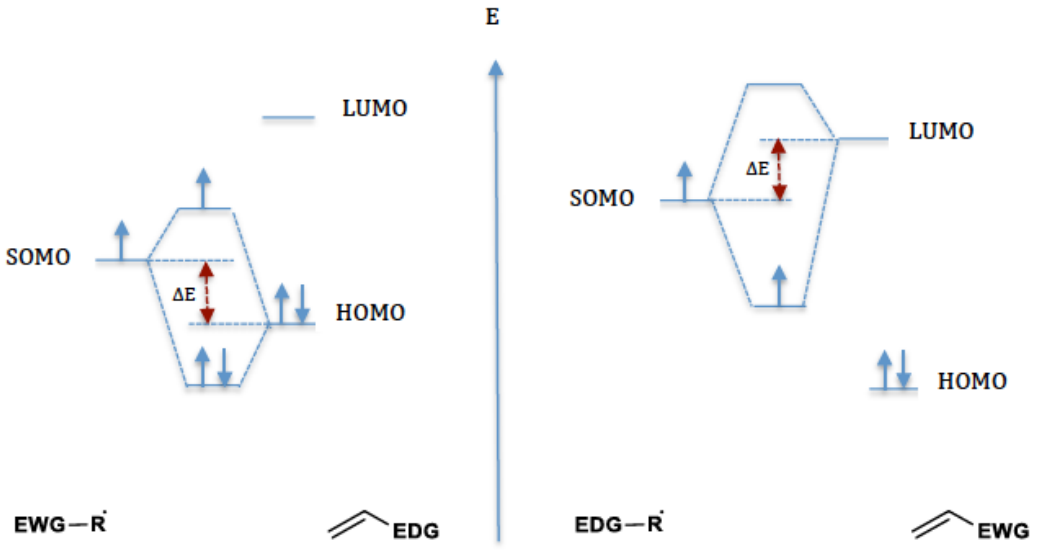
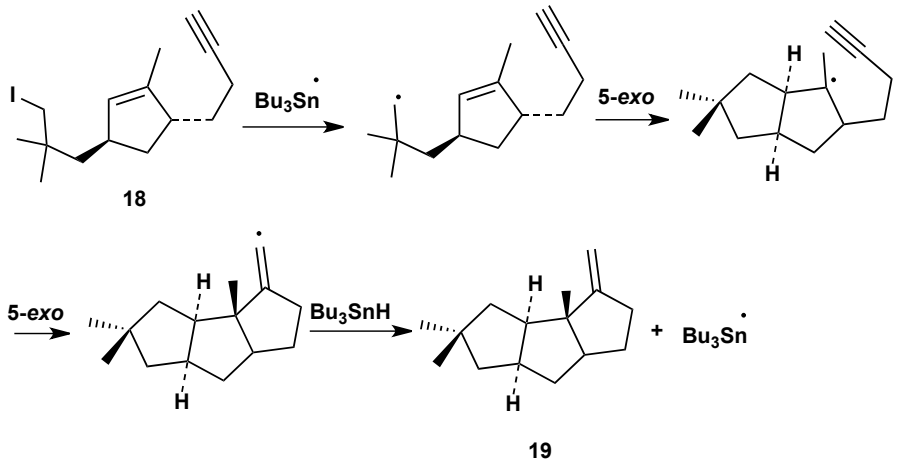


Figure 1.7. Frontier molecular orbitals in electrophilic and nucleophilic radicals.

1.2.3 Intramolecular radical addition to double bonds (radical cyclisations)

The intramolecular carbon radical addition to double bonds, commonly known as radical cyclisations, is an important tool for both mechanistic studies and synthetic applications.[113,114] Numerous examples where radical cyclisations are used as a key step to produce small rings, macrocyclic systems and complex molecules have been reported.[115,116] Hirsutene (**19**) is a linear condensed cyclopantanoid natural product. Scheme 1.7 illustrates the synthesis of hirustene (**19**) by Curran *et al*. from iodide **18** through two consecutive 5-*exo* cyclisation followed by a hydrogen atom abstraction from Bu_3SnH to produce **19**.[117]



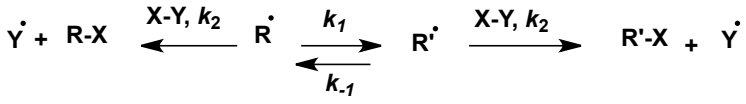
Scheme 1.7. Synthesis of hirsutene (**19**).

Since radical reactions are usually kinetically controlled, knowledge of the kinetics and reaction mechanisms is essential to enable radical reactions in a regio- and stereochemical fashion and to avoid formation of unwanted products.[118,119] The following section provides an overview of common kinetic methods.

1.2.4 Direct and indirect competition kinetic techniques

Both direct and indirect methods can be employed to determine reaction kinetics. Laser flash photolysis techniques enable to directly obtain absolute rate data for individual radical reactions from concentration-time measurements (provided that the

radical can be accessed by photolysis and monitored by UV/Vis spectroscopy or other methods). Indirect methods include competition studies, where relative rates for the competing pathways are obtained. Depending on the availability of absolute rate data for one of these reactions, the absolute rate constant for the other reaction can subsequently be determined. For simplicity, unimolecular and bimolecular reactions that are irreversible are employed. For further simplification, in bimolecular reactions one of the reagents is present in large excess (*e.g.* at least 10 equivalents) so that its concentration changes only negligibly during the course of the experiment, enabling the reaction to be treated as a pseudo-first order process. Scheme 1.8 outlines a competition kinetics experiment in which the unimolecular radical rearrangement of R$^{\bullet}$ to give R′$^{\bullet}$ (rate constant k_1) competes with bimolecular trapping of R$^{\bullet}$ (rate constant k_2) by X-Y to produce R-X. When the unimolecular radical rearrangement is irreversible, the rate of trapping of R′$^{\bullet}$ by X-Y is kinetically unimportant (assuming that k_2 is the same for both R and R′).



Scheme 1.8. A competition kinetic experiments involving a bimolecular and unimolecular process.

Under these conditions, the product distribution provides a ratio of the rate constants for the unimolecular and biomolecular process *via* equation 1.

$$(1) \quad [R'X]/[RX] = k_1/k_2 \times 1/[X\text{-}Y]$$

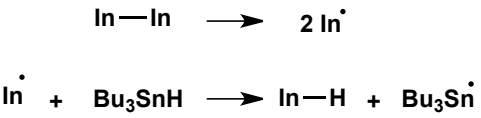
The most common indirect techniques applied for competition kinetic measurements in radical chemistry are tin hydride, nitroxyl radical coupling, and pyridine-2-thione-*N*-oxycarbonyl (PTOC)-thiol techniques, which will be outlined in the following.

1.2.4.1 Tin hydride reductions

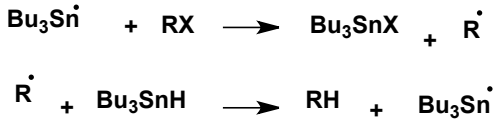
In the tin hydride method, an alkyl halide is used as a radical precursor which is reduced by trialkyl tin hydride (the most common is tri-*n*-butyl tin hydride, Bu_3SnH).[120] One example for the determination of the rate constant for the hydrogen transfer from Bu_3SnH to an alkyl radical R$^{\bullet}$ is outlined in Scheme 1.10. Thermolysis of azobisisobutyronitrile (AIBN) initiates the radical chain process, where the

resulting initiator radical (In$^{\bullet}$) reacts with tin hydride to give the tin-centred radical, $Bu_3Sn^{\bullet}$, which then reacts with the alkyl halide to produce the desired radical, R$^{\bullet}$. Unimolecular rearrangement of R$^{\bullet}$ to R$^{\bullet 1}$, which has a known rate constant (this reaction is called a 'radical clock'; details will be outlined below) competes with the bimolecular hydrogen atom abstraction to give a directly reduced compound R-H (Scheme 1.9).

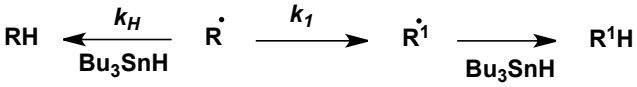
Initiation:



Propagation:



Unimolecular radical rearrangement:



Scheme 1.9. Reactions of the tin hydride technique.

Bu_3SnH reacts with alkyl radicals with the rate of 2.4×10^6 M^{-1} s^{-1} at room temperature.[121] Thus, one can use Bu_3SnH in the experiments with the rate constant in the range of 1×10^4 to 1×10^8 $M^{-1}s^{-1}$. At the upper limit, the competition reaction will predominate over hydrogen atom transfer from Bu_3SnH, and *vice versa*, which leads to lower the accuracy of analytical technique employed to determine products distribution.

Tris(trimethylsilyl)silane $(Me_3Si)_3SiH$, is a non-toxic alternative for tin hydride.[122-124] The hydrogen atom transfer rate constant from $(Me_3Si)_3SiH$ to alkyl radical reported to be an order of magnitude less than Bu_3SnH.[125] Therefore $(Me_3Si)_3SiH$ with lower k_H value is a useful clock that can be used to determine the rate of the reaction in competition kinetic studies, which cannot be studied with Bu_3SnH.

1.2.4.2 Nitroxyl radical couplings

In this method, the desired carbon centred radical is generated by photolysis of either a peroxy ester or a peroxide and the generated radicals are trapped by recombination with nitroxyl radicals such as 2,2,6,6-tetramethyl piperidine-*N*-oxyl (TEMPO). There is no chain reaction in this method (Figure 1.8). The coupling rate constant of nitroxyl radicals with carbon radicals is very fast (generally between 10^8 to 10^9 $M^{-1}s^{-1}$), making this method suitable for the study of very fast radical reactions.[126-131] The negative side of this method is the influence of steric hindrance on both carbon radical and nitroxyl radical on the coupling rate constant, which means that one cannot use a rate constant for coupling of one nitroxyl radical to estimate that for another one.[130]

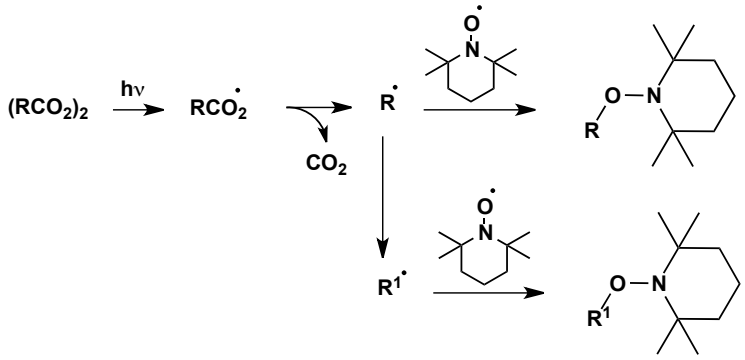


Figure 1.8. Nitroxyl radical coupling reactions.

1.2.4.3 PTOC-thiol cleavage

The PTOC-thiol method[121] employs (*N*-hydroxypyridine-2-thione) esters (PTOC esters) as the source of radicals (Figure 1.9).[100] PTOC esters were first developed by Barton, Crich and Motherwell in 1983.[132] They have a characteristic yellow colour due to their strong chromophore at 350 nm, which extend into the visible light range, enabling initiation of the radical chain with visible light. Homolytic cleavage of the weak N-O bond in the PTOC ester produces an acyloxyl radical that gives the desired carbon radical after rapid decarboxylation. The alkyl radical then goes through either a rearrangement process or hydrogen atom abstraction.

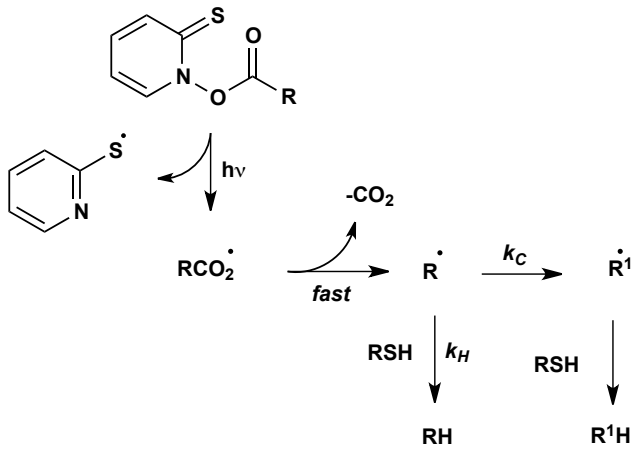


Figure 1.9. The PTOC-thiol method chain sequence in a competition kinetic experiment.

By using the hydrogen atom donor in large excess (*e.g.* at least 10 equivalents), the final product distribution can provide a ratio of the rate constant for the unimolecular rearrangement and bimolecular hydrogen atom abstraction processes (equation 1). Thus, once one rate constant is known for either process, the other can be calculated from the ratio of unimolecular and bimolecular products.

Equation (1)

$$(1) \quad d[R^{\bullet 1}]/d[RH] = k_C/k_H \times 1/[RSH]^{-1}$$

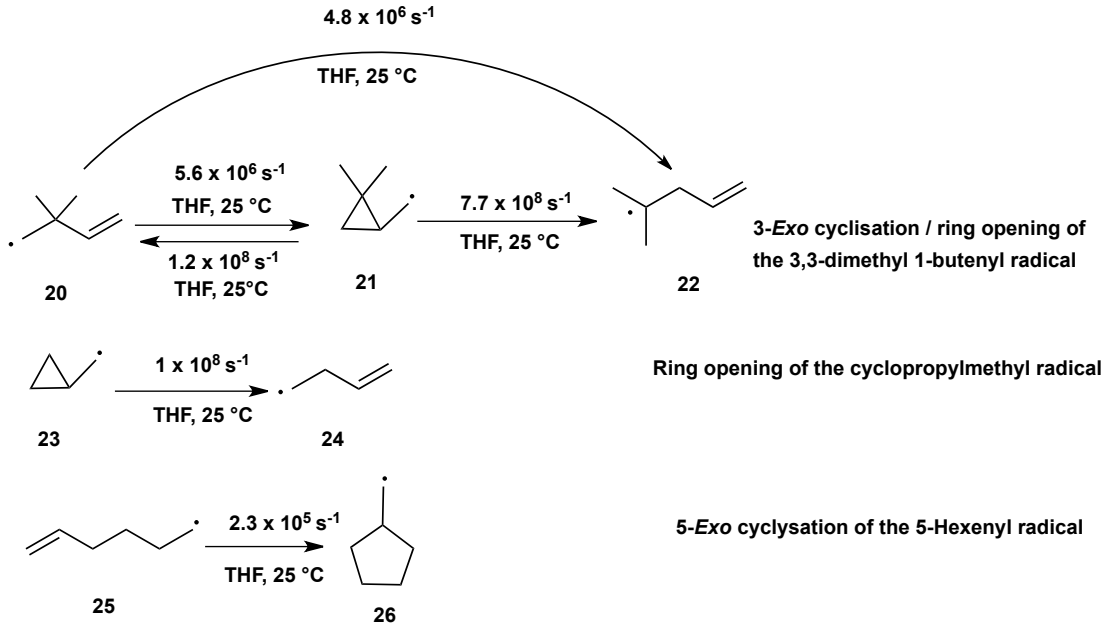
$$(2) \quad [R^1H]/[RH] = k_C/k_H \times 1/[RSH]^{-1}$$

Where [RSH] is the concentration of the trapping agent, k_H is the rate constant for hydrogen atom transfer from RSH to the alkyl radical, and k_C is the cyclisation rate constant.

1.2.5 Well-studied radical clocks

As mentioned above, a radical clock is a radical reaction with a known rate constant, which can be used to determine the rate constants of other radical reactions in competition kinetic experiments. Scheme 1.10 gives some examples for radical clocks. The unimolecular rearrangement of the primary 1-butenyl radical **20** to the tertiary 1-butenyl radical **20** has a rate constant of 4.8×10^6 s^{-1} in THF at 25 °C. This rearrangement occurs through 3-*exo* radical cyclisation to the intermediate

cyclopropylmethyl radical **21**, followed by ring opening.[118] Several radical clocks involve ring opening processes. Ring opening of the cyclopropylmethyl radical **23** to **24** is a well-known clock in this group, which is an example of fast radical rearrangement with a rate constant of nearly 1×10^8 s^{-1} in THF at 25 °C.[133,134] 5-*exo* Radical cyclisations are another radical clock rearrangement. The most prominent example in this group is the ring closure of the 5-hexenyl radical **25** to the cyclopentylmethyl radical **26** with a rate constant of 2.3×10^5 s^{-1} in THF at 25 °C.[135-136] The well-studied cyclisation of the 5-hexenyl radical is one of the most versatile radical clocks,[136-139] which has been used to explore the kinetics of a large number of 5-*exo* radical cyclisation reactions. The latter radical clock will be used in this work and will be therefore outlined in more detail in the next paragraph.

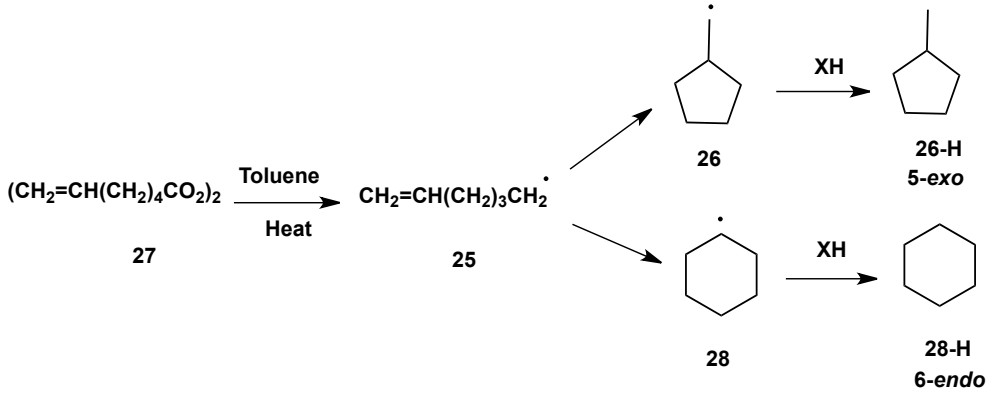


Scheme 1.10. Three well-studied radical clocks.

1.2.5.1 Cyclisation of 5-hexenyl radical

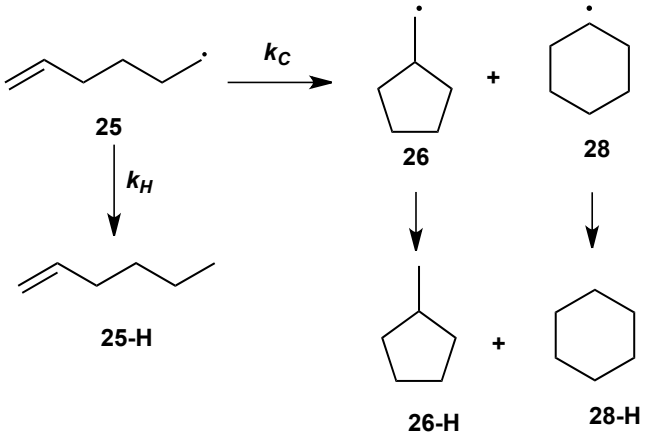
Cyclisation of 5-hexenyl radical first studied by Arai, Sato and Shida in 1960, who observed the formation of methylcyclopentane from mercury-sensitized photolysis of cyclohexane at 400 °C, which was explained by the cyclisation of the intermediate 5-hexenyl radical **25**.[140] Three years later, formation of the less thermodynamically stable compound **26-H** (5-*exo* product) as the major product and compound **28-H** (6-

endo product) as the minor product was confirmed by Lamb, Ayers and Toney using 6-heptenoyl peroxide (**27**) as a source of the 5-hexenyl radical (**25**) (Scheme 1.11).[141]



Scheme 1.11. Thermal decomposition of the 6-heptenoyl peroxide (**27**) in toluene.

The cyclisation of the 5-hexenyl radical **25** is a valuable mechanistic probe[110,118] used to measure the rate constant of reactions in competition experiments. For example, rearrangement to cyclised radicals **26** and **28** can compete with the bimolecular hydrogen atom trapping reaction to produce **25-H** (Scheme 1.12).



Scheme 1.12. Ring closure versus direct reduction of the 5-hexenyl radical (**25**).

There have been many attempts to ascertain the factors affecting the regio-chemistry of free radical cyclisations. At one time the driving forces to obtain the energetically less favourable 5-*exo* product as major product were considered to be the favourable entropy and enthalpy terms.[135] In 1968, Julia proposed that the energy of the transition state is important, rather than the thermodynamic stability of product, in

other words, the reaction proceeds under the kinetic control.[98] The transition state to form a 6-membered ring is higher in energy than the one to form a 5-membered ring, which means that the major product is the kinetic product, not the thermodynamic product (Figure 1.10). According to the theoretical studies by Beckwith and Schiesser[142] in 1985, and two years later by Spellmeyer and Houk,[143] the strain engendered in the transition structure of a 6-*endo* compound is greater than that of a 5-*exo* compound. This strain outweighs the thermodynamic factors that otherwise favour generation of a more stable product,[142] leading to the less thermodynamically stable compound as the major product.

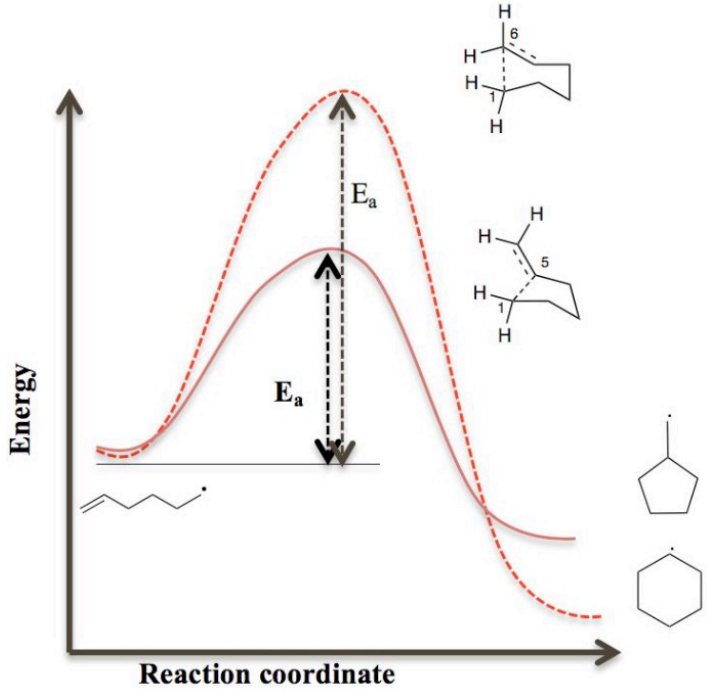
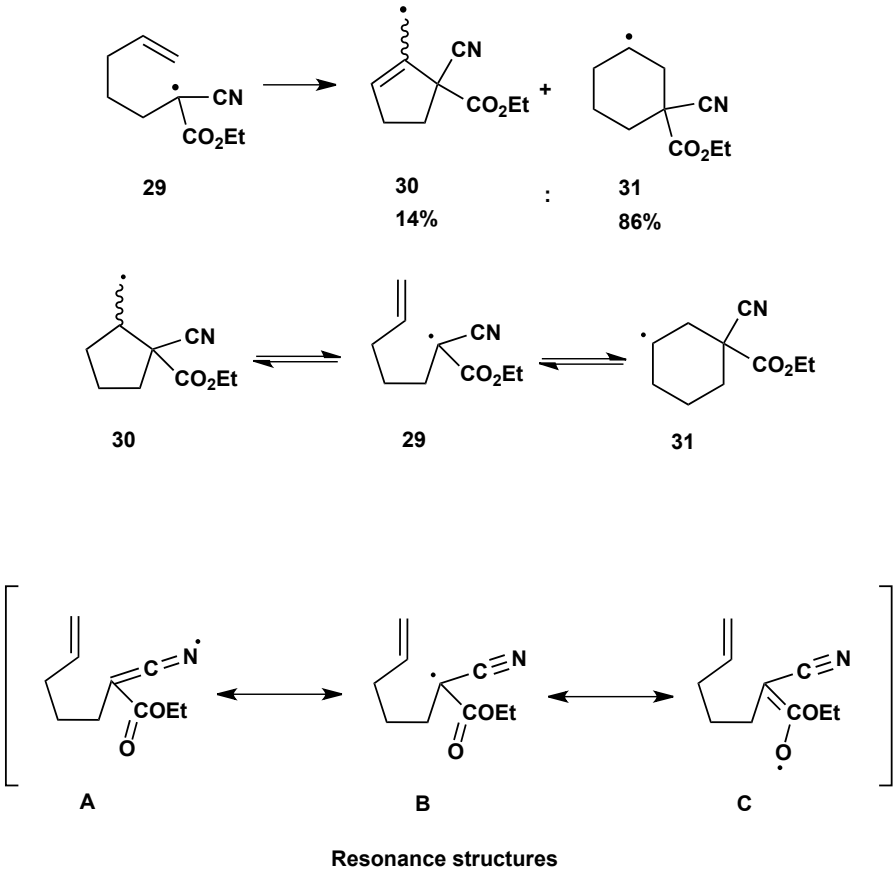


Figure 1.10. Reaction coordinate for the competing cyclisation pathways of 5-hexenyl radical (**25**).

On the other hand, Julia observed that a tertiary resonance-stabilised radical **29** exclusively generates 6-membered compounds **31** (Scheme 1.13 shows the resonance structures of the radical **29**, where structure **B** is more favourable than **A** and **C** and this is because free radicals on tertiary carbons are more stable than radicals on either oxygen or nitrogen atoms). The reason for this different outcome is the reversibility of the reaction under the experimental conditions, which leads to the thermodynamic product **31** (Scheme 1.13),[98] in contrast to radical **24**, which undergoes an

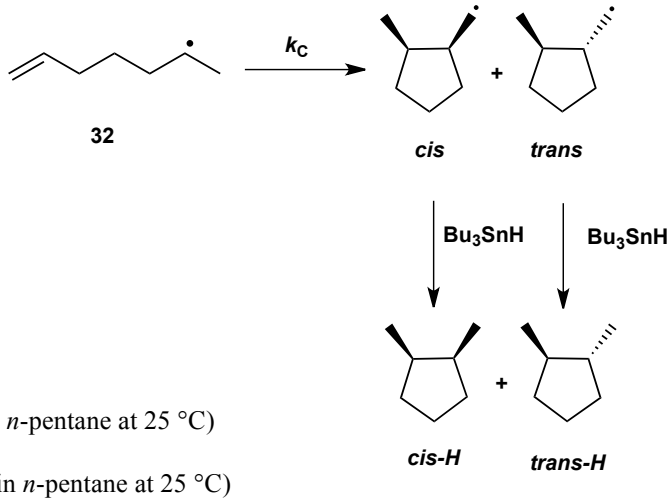
irreversible cyclisation leading to the kinetic product **27** as the major product (Scheme 1.12).



Scheme 1.13. Reversibility of the 5-hexenyl radical cyclisation of radical **29** and the resonance structures.

1.2.6 Stereochemistry of the 5-*exo* cyclisation of substituted 5-hexenyl radicals

The 5-*exo* cyclisation of 1-substituted 5-hexenyl radicals leads to the formation of *cis*-1,2-disubstituted isomer. For example, the *cis*/*trans* ratio in the 5-*exo* cyclisation of the hept-6-en-2-yl radical (**32**) in *n*-pentane at 25 °C is 2.6 (Scheme 1.14).[144-147]



$k_{cis} = 1.1 \times 10^5\ s^{-1}$ (in *n*-pentane at 25 °C)

$k_{trans} = 4.2 \times 10^4\ s^{-1}$ (in *n*-pentane at 25 °C)

Scheme 1.14. Cyclisation of the hept-6-en-2-yl radical (**32**).

An early explanation by Beckwith and co-workers suggested secondary orbital overlap between the σ^* orbital of olefinic bond and CH σ of the alkyl substituent in the transition structure (TS) for the *cis* cyclisation, which is not available in the *trans* mode. The primary interaction involves interaction of the half-filled p orbital with the vacant π^* orbital of the olefinic bond, which is available in both *cis* and *trans* isomers. (Figure 1.11).[148,149]

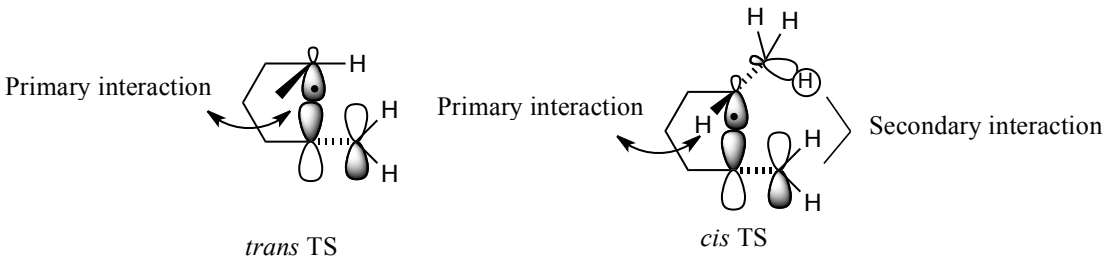


Figure 1.11. Orbital overlap in the transition state (TS) of the 5-*exo* cyclisation of the hept-6-en-2-yl radical (**32**).

However, this hypothesis was not supported by the calculations of Spellmeyer and Houk, who attributed the preference towards the *cis* product to van der Waals interaction between alkene carbon being attacked and carbon radical.[143]

1.2.6.1 Guidelines for radical cyclisation chemistry

Following this early work in the 1960s and 70s several researchers became interested in radical cyclisation chemistry and made significant contributions to this field. These contributions led Beckwith, Easton and Serelis to propose four guidelines for radical reactions:[150]

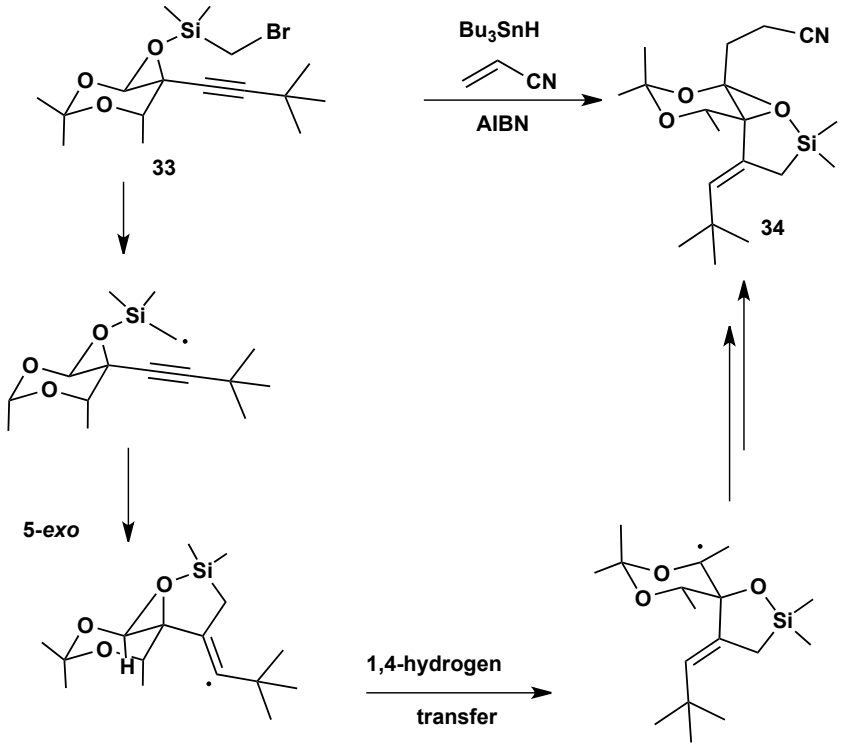
I. Intramolecular addition under kinetic control in lower alkenyl radicals (alkenyls contain less than 8 carbons in the chain including butenyl, hexenyl, heptenyl, octenyl radicals) and lower alkynyl radicals and related species occurs preferentially in the *exo*-mode.
II. Substituents on an olefinic bond disfavour homolytic addition at the substituted position.
III. Homolytic cleavage is favoured when the bond concerned lies close to the plane of an adjacent semi-occupied orbital or of an adjacent filled non-bonding or π-orbital.
IV. 5-Ring closures of substituted 5-hexenyl radicals and related radicals are stereoselective: 1- or 3-substituted systems afford mainly *cis*-disubstituted products, whereas 2- or 4-substituted systems give mainly *trans*-products.

These guidelines provide rules to predict regio- and stereochemistry and have been a most valuable tool to predict the outcome of radical reactions.[151]

1.2.6.2 Synthesis through the cascade radical reactions

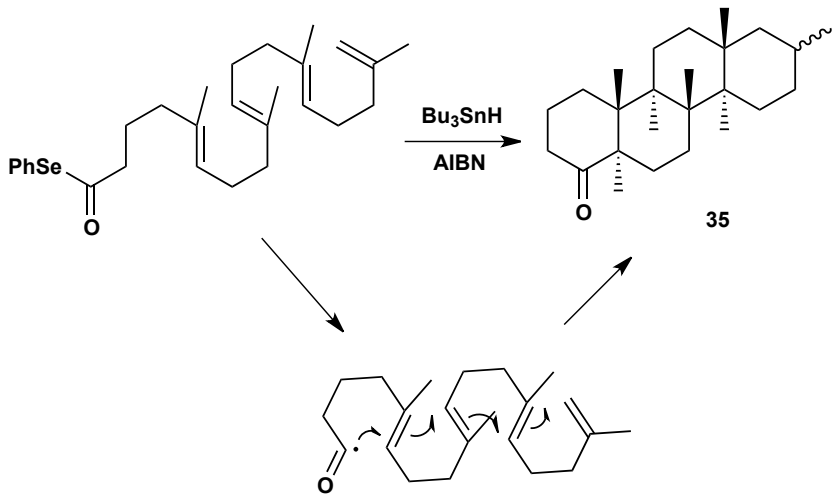
Cascade radical reactions are a methodology that allows formation of the maximum number of bonds with a minimum number of steps. There are many examples of the use of intramolecular homolytic addition to prepare biologically active molecules. Some interesting examples will be outlined in the following.

Scheme 1.15 illustrates the synthesis of heterocyclic complex **34** by Gulea *et al*. through 5-*exo* cyclisation of **33** followed by 1,4-hydrogen atom transfer, finishing with intermolecular addition.[152]



Scheme 1.15. Formation of silacycle **34** from bromomethyldimethylsilyl ether **33**.[152]

Another example of intramolecular homolytic addition is the synthesis of the steroidal skeleton **35** with high regio- and stereo-control through a series of 6-*endo* reactions. In general, acyl radical precursors having linear polyene structure may leads to preferential 6-mode of cyclisation of this type of reactions (Scheme 1.16).[153]



Scheme 1.16. Synthesis of steroidal skeleton **35**.[153]

1.2.7 Alkoxy radical cyclisation

Intramolecular addition of heteroatom radicals to double bonds is an effective approach to prepare complex heterocyclic compounds.[154] Tetrahydrofuran and tetrahydropyran moieties are often found in complex natural products and are considered important building blocks for natural product synthesis.[155-156] Figure 1.12 shows the structure of the two natural products Monensin A and Calcimycin, which have important biological properties including antibacterial and antifungal activities.[156]

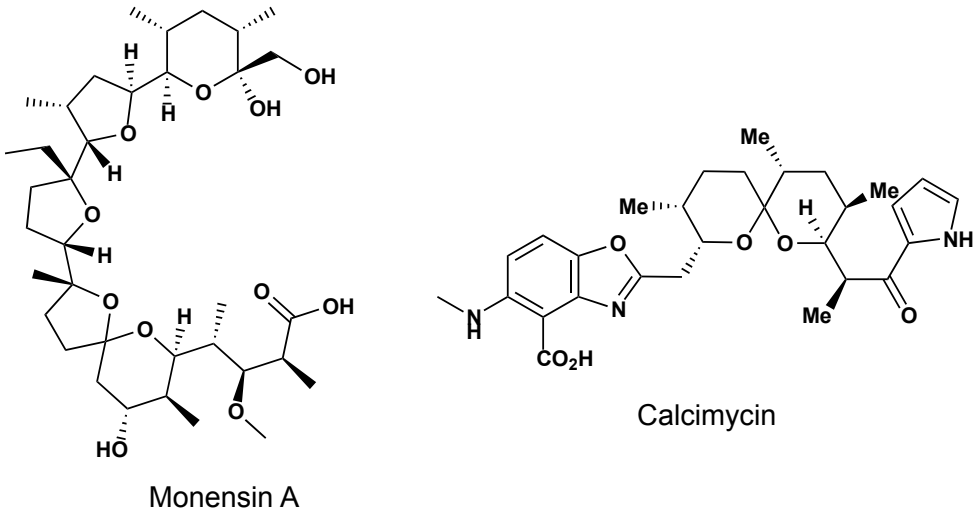
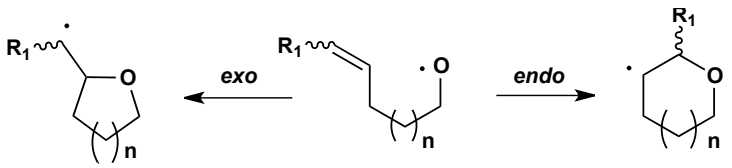


Figure 1.12. Structures of Monensin A and Calcimycin.

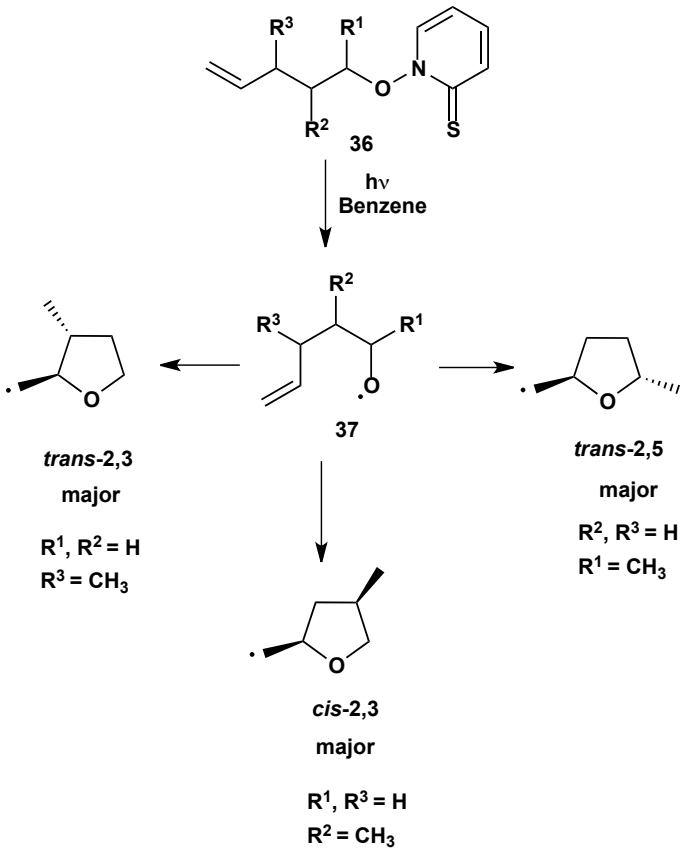
Radical cyclisation of alkoxyl radicals provide an alternative to ionic methods to access O-heterocycles under mild conditions (Scheme 1.17).[157-159]



Scheme 1.17. Oxygen-centred radical cyclisation.

In 1989, the development of alkoxy radical precursors **36** with sufficient shelf life by Hay and Beckwith,[160] paved the way for using free alkoxy radical chemistry in

organic synthesis and mechanistic studies. Hartung *et al*. reported some kinetic data for the cyclisation of the substituted pentenyl-1-oxy radicals **37** (Scheme 1.18). They showed that 5-*exo* cyclisation reactions of alkoxy radicals **37** proceed with excellent stereoselectivity, despite being considerably fast reaction, and the stereoselectivity depends on the steric hindrance of alkyl substituents in the 4-pentenyloxy chain. Figure 1.13 illustrates the chair-like transition state for the cyclisation of the alkoxy radical. The substituents in the transition state preferred to occupy pseudo-equatorial position leading to produce stereoselective products *trans*-2,5-, *cis*-2,4-, *trans*-2,3.[161]



Scheme 1.18. Generation and cyclisation of substituted pentenyl-1-oxy radicals **37**.

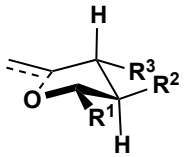
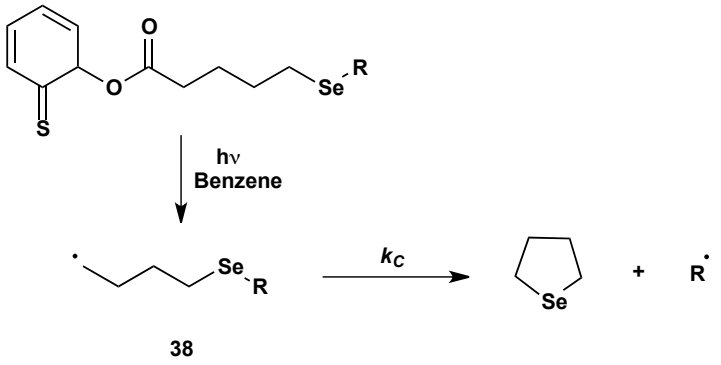


Figure 1.13. TS model for stereoselective alkoxy radical cyclisation.

1.2.8 Intramolecular homolytic substitutions

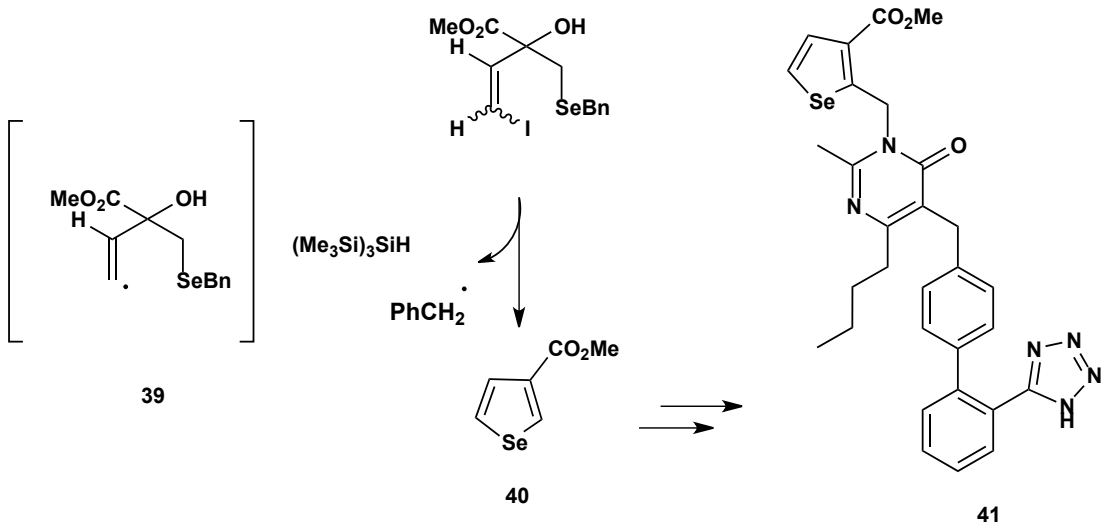
Intramolecular homolytic substitutions are another versatile method to form carbon-heteroatom bonds to access heterocyclic compounds.[105] There are numerous examples of homolytic substitution reactions at sulphur, selenium and silicon and fewer examples involving tellurium and tin. For example, intramolecular homolytic substitution on the sulfur atom can be used to produce carbon-sulfur bonds.[162-164] Likewise, selenium-containing cyclic systems, which are interesting targets, particularly in medicinal chemistry, can be synthesised through intramolecular homolytic substitution of carbon radicals on selenium.[165]

For a long time, the development of new methods to synthesise selenium-containing rings suffered from the lack of accurate kinetic data for homolytic substitution reactions. In 2014, a competitive kinetic and computational study of intramolecular homolytic substitution of radical **38** by Schiesser and co-workers revealed that the type of leaving radical is a main factor that influences the rate of the reaction (Scheme 1.19). For example, the rate constant for cyclisation (k_C) of radical **38** at 22 °C range from 3.4×10^4 s^{-1}(R = *n*-octyl) to 1.1×10^7 s^{-1}(R = Ph_2CH) and correlate with expectations based on leaving group ability.[166,167]



Scheme 1.19. Homolytic substitution at selenium.

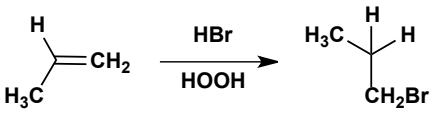
Selenomilfasartan (**41**) is a selenophene analogue of milfasartan, which is an antihypertensive compound. The selenophene ring **40** is synthesised through intramolecular homolytic substitution (involving intermediate **39**) with release of $PhCH_2^{\bullet}$ (Scheme 1.20).[168-169]



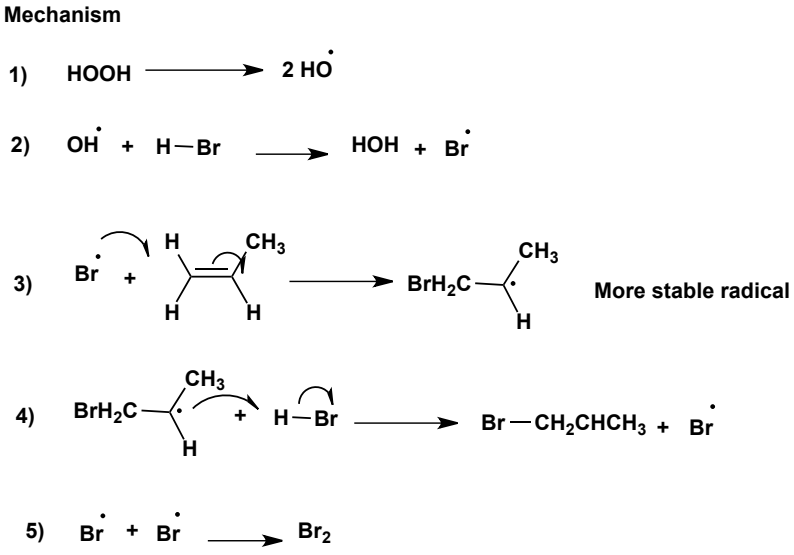
Scheme 1.20. Selenomilfasrtan (**41**) synthesis through intramolecular homolytic substitution chemistry.

1.2.9 Intermolecular addition to alkene

Countless examples for the intermolecular free radical addition to olefins to form new bonds have been reported. One early example is the *anti*-Markovnikov addition of HBr to unsymmetrical alkenes such as propene **42**. In the presence of a peroxide such as hydrogen peroxide (H_2O_2), hydrogen bromide adds to propene *via* a radical mechanism in an *anti*-Markovnikov mode (Scheme 1.21).[170]



42



Scheme 1.21. *Anti*-Markovnikov addition of hydrogen bromide to propene (**42**) in presence of hydrogen peroxide.

Radical polymerisations are an important industrial application of intermolecular free radical addition to alkenes. Similar to *intra*-molecular radical reactions outlined above, there are several factors that affect the rate of addition of carbon-centred radicals to olefins, including substituents on the radical and alkene,[171] steric factors, and likely the nature of the solvent used as the reaction medium.

1.2.10 Solvent effects on radical reactions

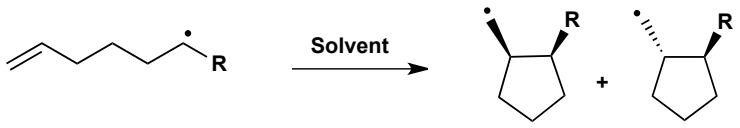
It has been found that solvent polarity affects the rate of the radical addition to double bonds. Solvation energies include non-electrostatic, which does not affect the activation barrier, and the electrostatic force that can be split into a solute polarisation term and solvent-solute interaction. Due to the charge transfer from radical to alkene in the transition state of the radical addition to double bond, the solvation energy of the transition state is larger than that of reactants.[172] Therefore, enhancing solvent polarity should decrease the activation barrier and increase the rate of addition.

However, the influence of the solvent polarity on the activation barrier of a reaction with polar TS is greater than the activation barrier of a reaction with less polar TS.

Supercritical fluids [173] and ILs[174] have been studied as new reaction media in free radical polymerisation. In some cases, higher propagation rate constants[93, 175,176] and lower termination constants[94] in ILs compared to conventional organic solvents have been reported. Lower termination constants in ILs are attributed to the high viscosity of the ILs compared with organic solvents.[92]

In the preceding sections, various free radical reactions that lead to the formation of new bonds in organic synthesis were presented. Yet, the influence of solvent has rarely been considered in free radical reactions. The reason for this gap in research arises from a belief of the non-polarisable nature of free radicals, meaning that free radical reactions were thought not to be affected by the nature of the solvent. In fact, computational studies have shown that the influence of the solvent is insignificant for the addition of the methyl radical to a double bond.[175] However, it has been reported that polar effects and the exothermicity of a reaction can highly affect the activation barrier.[176-177] Therefore, the polarity of the solvent should affect the activation barrier.

Beckwith and Schiesser studied the effect of solvent on the cyclisation of substituted 5-hexenyl radicals. They showed that the *cis*/*trans* stereoselectivity of 5-*exo* cyclisations increased for hexenyl radicals with a bulky *t*-butyl substituent at the radical centre as the solvent polarity increased from benzene to 1-propanol. However, no rationale has been provided (Scheme 1.22 and Table 1.1).[178]



Scheme 1.22. Cyclisation of alkyl substituted 5-hexenyl radicals.

Table 1.1. *Cis*/*trans* stereoselectivity for the 5-*exo* cyclisation of substituted 5-hexenyl radicals in different solvents. Data from ref. 178.

cis/*trans* steroselectivity in solvent			
Substituent (R)	Benzene	DME[a]	1-Propanol
CF_3	1.1	1.9	1.7
t-butyl	3.1	4.4	5.6
Dielectric constant	2.3	7.2	20.1

[a] 1,2-Dimethoxyethane.

1.3 Free radical reactions in ionic liquids

As stated in section 1.2.3.1, radical reactions usually proceed under kinetic control (if the radical is not stabilised), hence, an understanding of radical reaction mechanisms and kinetics[118] is vital to synthesising molecules regio- and stereoselectively. A very versatile solvent for free radical reactions is benzene, due its low reactivity. Unfortunately, benzene is toxic, volatile and flammable. Alternative commonly used less problematic solvents are tetrahydrofuran and *n*-pentane, which are unfortunately also highly volatile and flammable. The unique properties of ILs, as outlined above, and the observation of solvent effects on the stereoselectivity of substituted 5-hexenyl radical cyclisations (see Section 1.2.10), suggest that these alkyl radical reactions should be attempted in ILs as polar and "green" solvents. ILs are potentially greener alternative for these useful organic reactions. There are no comprehensive reviews, but a number of investigations and the most important findings will be summarised in the following.

A recent investigation involving nitroxide spin trap indicated that IL could interact with radicals either through hydrogen bonding or electrostatic interactions. These additional interactions result in slightly reduced mobility of the spin probes. Furthermore, it was found that electrostatic interactions between nitroxide radicals and ionic liquid reduced mobility of radicals more than hydrogen bonding. An example for such interactions is shown for a nitroxide radical and an imidazolium based ionic liquid in Figure 1.14.[179]

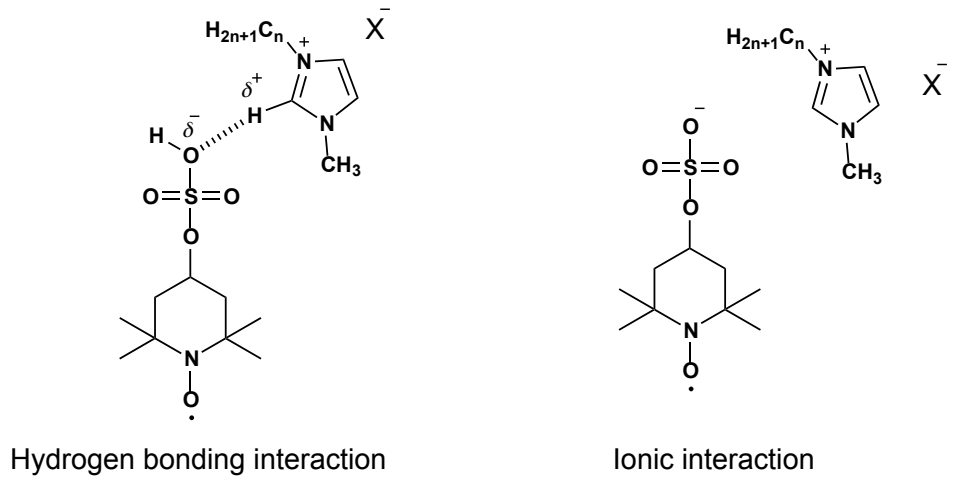


Figure 1.14. Interaction between nitroxide radical and imidazolium based ionic liquid.

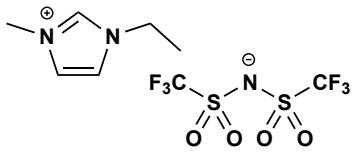
In general, the kinetics of organic reactions are guided by the physiochemical properties of the solvents, including viscosity and polarity. The definition of solvent polarity is not simple. In general, polarity is considered as a measure of the mixed electrostatic and hydrogen bonding interactions.[180] According to molecular spectroscopy and solubility, IL polarity can be defined as electrostatic interactions of ILs that are equal to those of molecular liquids with notably higher dielectric constants.[180c] However, for many well studied ILs, the measured dielectric constants fall in the range of 10–15.[180d]

Variety of reactions proceeds faster in ILs, notably ionic and radical polymerisations. Despite the promise of ILs as a sustainable alternative to conventional solvents, most radical chemistry performed in ILs involves electron transfer or radical recombination rather than traditional radical reactions.[179]

1.3.1 1-Ethyl-3-methylimidazolium bis(trifluoromethylsulfonyl)imide ([EMIm][NTf_2]) as a medium for radical reactions

1-Ethyl-3-methylimidazolium-based ILs have been reported to be moisture and air resistant.[13] The IL used throughout this thesis research, [EMIm][NTf_2] (Figure 1.15), frequently appears in the chemical literature and its physicochemical properties have been studied.[36,181] The dielectric constant of [EMIm][NTf_2] is reported in previous work as 12.2.[181c] Furthermore, it is easy to prepare and purify,[182] is optically

transparent in the spectral region required for photochemical cleavage of PTOC esters, and readily dissolves *t*-BuSH, which was used as the trapping agent in the competition kinetic studies. It is hydrophobic so easy to dry. In general, imidazolium-based ILs have relatively low viscosity, making them easier to work with.



[EMIm][NTf$_2$]

Figure 1.15. Structure of [EMIm][NTf$_2$], the IL used in this thesis.

[EMIm][NTf$_2$] used throughout this study was purchased from IoLiTec-Ionic Liquids Technologies GmbH. The water content reported by the supplier was 66 ppm. Given that the IL bottle was sealed and kept in a desiccator after each use and also considering [EMIm][NTf$_2$] as a moisture and air resistant IL,[13,14] the intake of water should be negligible.

Hydrogen atom transfer trapping reactions have been most commonly employed as basis reactions in the competition kinetic studies of alkyl radical reactions. Several calibrated hydrogen atom donors with known rate constants in conventional organic solvents have been reported.[121] Among these, organotin compounds are widely used in kinetic studies,[183] but are presumed toxic and are insoluble in 1-ethyl-3-methylimidazolium bis(trifluoromethane-sulfonyl)-imide ([EMIm][NTf$_2$]), the IL used in this thesis. Of the readily available H-donors, *t*-butylthiol (*t*-BuSH) is soluble in [EMIm][NTf$_2$]. Therefore, *t*-BuSH was chosen as the H-donor in this work. The thiyl radical generated from the trapping agent (*t*-BuSH), propagates the chain reaction by addition to the PTOC-ester.

PTOC esters can be prepared easily through the reaction of thiohydroxamic acid and a carboxylic acid. They are stable provided they are shielded from light and stored below room temperature.

1.4 Aim and methodology of this thesis

The aim of this thesis is to explore whether and how free radical reactions, which have been shown to be excellent methods for the preparation of complex molecular frameworks with high regio- and stereoselectivities under mild conditions,[184] can be moved away from "conventional" solvents into ILs. Although numerous kinetic data are now available for reactions performed in traditional solvents, there remains a distinct lack of kinetic parameters for reactions of neutral radicals in unconventional solvents such as ILs. This thesis will provide the first unimolecular radical clocks for alkyl radical cyclisation in an IL. In all of the reactions in this thesis the PTOC-thiol method[121] is used to measure the kinetics of cyclisation reactions, and the PTOC ester is employed as the source of radicals (Figure 1.8).[100]

The PTOC-thiol method will be used to perform competition kinetic studies for a series of important radical reaction types, *i.e.* 5-*exo* cyclisations and intramolecular homolytic substitutions, to obtain insight into the fundamental reactivities of neutral alkyl and alkoxyl radicals in imidazolium-based ILs.

To directly compare the influence of the reaction medium on both radical reactivity and stereoselectivity, experiments in this thesis were performed in the non-polar conventional organic solvents of benzene, *n*-hexane or *t*-BuPh and in polar [EMIm][NTf_2] (Figure 1.14). The chosen IL is composed of an organic imidazolium-based cation with a delocalized positive charge, and a relatively big anion with a negative delocalized charge.

This thesis contributes to gaining a fundamental understanding of the effects of ILs on the kinetics of various types of traditional free radical reactions. Specifically, it is interesting to explore whether (i) these reactions take place in ILs; (ii) an IL medium affects selectivity and efficiency; (iii) reaction products can be conveniently isolated from the IL, and; (iv) the IL solvent can be recycled and/or reused. In order to directly compare the influence of the reaction medium on both radical reactivity and stereoselectivity, the experiments will be performed in non-polar conventional organic solvents and [EMIm][NTf_2].

There are various options for following reaction progress in ILs. UV-Visible spectroscopy requires a reaction involving a change in chromophore for it to be practical.[185-189] Mass spectrometric analysis is complicated by the large proportion of ions present in the mixture, which can dominate the spectrum as a result.[190] A common problem for the use of NMR spectroscopy is overlap of the signals of interest with signals due to the ionic liquid.[191]

Use of gas chromatography requires particular care to ensure that the involatile IL does not block the column. This issue can be easily resolve by passing the organic phase used in extraction through a silica plug before injection into the instrument to remove trace amounts of IL. Efficient extraction of the reaction products from the IL phase was required for gas chromatography analysis of the competition kinetic studies, and this will be described in chapter 2.

The research addressing the thesis aim is presented in three chapters:

Chapter 2: DFT calculations performed at the M062X/6-31+G* level of theory using the Gaussian software package to exclude the potential involvement of [EMIm][NTf_2] in radical reactions. Also, the extraction efficiency of the reaction products from the IL phase was investigated to get reliable kinetic data for competition kinetic studies. Kinetic rate data were determined for the cyclisation of a series of primary alkyl radicals in [EMIm][NTf_2] and conventional organic solvent and the results compared. This chapter culminates with a study of the recyclability of ILs.

Chapter 3: Intramolecular homolytic substitution of C-1 substituted 5-hexenyl radicals were explored to determine the role of steric effects on the rate and stereoselectivity of 5-exo radical cyclisation in ILs compared with conventional organic solvents. For this purpose, relative rate coefficients of suitably substituted 5-hexenyl radicals of differing steric demand in ILs and organic solvents were determined. Also, an example for a tandem radical cyclisation was performed on [EMIm][NTf_2].

Chapter 4: Kinetic rate data for alkoxy radical ring closure and homolytic substitution at selenium in [EMIm][NTf_2] and non-polar organic solvent were determined and compared. This is followed by the determination of kinetic rate data

for intermolecular addition of alkyl radical to activated double bonds in [EMIm][NTf_2] and benzene.

1.5 References

[1] Lei, Z.; Chen, B., Koo, Y.-M.; MacFarlane, D. R.,*Chem. Rev*. **2017**, 117, 6633.

[2] Ramsay, W., XXXIV. *Philosophical Magazine Series 5* **1876,** *2*, 269.

[3] (a) Walden, P. *Bull. Acad. Imper. Sci. (St. Petersburg)* **1914**, 1800. (b) Sugden, S.; Wilkins, H., *J. Chem. Soc.* **1929**, 1291.

[4] (a) Schofer, S. H.; Kaftzik, N.; Wasserscheid, P.; Kragl, U., *Chem. Commun.* **2001**, 425. (b) Schroer, K.; Tacha, E.; Lütz, S., *Org. Process Res. Dev.* **2007**, *11*, 836.

[5] Verrelli, R.; Laszczynski, N.; Passerini, S.; Hassoun, J., *Energy. Technol.* **2016**, *4*, 700.

[6] Birbilis, N.; Howlett, P. C.; MacFarlane, D. R.; Forsyth, M., *Surf. Coat. Technol.* **2007**, *201*, 4496.

[7] Hernández-Fernández, F. J.; Pérez de los Ríos, A.; Mateo-Ramírez, F.; Godínez, C.; Lozano-Blanco, L. J.; Moreno, J. I.; Tomás-Alonso, F., *Chem. Eng. J.* **2015**, *279*, 115.

[8] Kuberský, P.; Altšmíd, J.; Hamáček, A.; Nešpůrek, S.; Zmeškal, O., *Sensors.* **2015**, *15*, 28421.

[9] Strehmel, V.; Wetzel, H.; Laschewsky, A., *Macromol. Symp.* **2014**, *342*, 78.

[10] Eshetu, G. G.; Armand, M.; Scrosati, B.; Passerini, S., *Angew. Chem. Int. Ed.* **2014**, *53*, 13342.

[11] Eshetu, G. G.; Armand, M.; Scrosati, B.; Passerini, S., *Angew. Chem.* **2014**, *126*, 13558.

[12] Price, H.; Lüpfert, E.; Kearney, D.; Zarza, E.; Cohen, G.; Gee, R.; Mahoney, R., *J. Sol. Energy Eng.* **2002**, *124*, 109.

[13] Wilkes, J. S.; Zaworotko, M. J., *J. Chem. Soc., Chem. Commun.* **1992**, 965.

[14] Yee, P.; Shah, J. K.; Maginn. E. J., *J. Phys. Chem. B.* **2013**, *117*, 12556.

[15] Davis Jr., J. H., *Chem. Lett.* **2004**, *33*, 1072.

[16] Fedorov, M. V.; Kornyshev, A. A., *Chem. Rev.* **2014**, *114*, 2978.

[17] Chum, H. L.; Koch, V. R.; Miller, L. L.; Osteryoung, R. A., *J. Am. Chem. Soc.* **1975**, *97*, 3264.

[18] Krossing, I.; Slattery, J. M.; Daguenet, C.; Dyson, P. J.; Oleinikova, A.; Weingärtner, H., *J. Am. Chem. Soc.* **2006**, *128*, 13427.

[19] Earle, M. J.; Esperança, J. M. S. S.; Gilea, M. A.; Canongia Lopes, J. N.; Rebelo, L. P. N.; Magee, J. W.; Seddon, K. R.; Widegren, J. A., *Nature* **2006**, *439*, 831.

[20] Taylor, A. W.; Lovelock, K. R. J.; Deyko, A.; Licence, P.; Jones, R. G., *Phys. Chem. Chem. Phys.* **2010**, *12*, 1772.

[21] Galiński, M.; Lewandowski, A.; Stępniak, I., *Electrochim. Acta* **2006**, *51*, 5567.

[22] Lewandowski, A.; Świderska-Mocek, A., *J. Power Sources.* **2009**, *194*, 601.

[23] Freire, M. G.; Santos, L. M. N. B. F.; Fernandes, A. M.; Coutinho, J. A. P.; Marrucho, I. M., *Fluid Phase Equilib.* **2007**, *261*, 449.

[24] Niedermeyer, H.; Hallett, J. P.; Villar-Garcia, I. J.; Hunt, P. A.; Welton, T., *Chem. Soc. Rev.* **2012**, *41*, 7780.

[25] Lu, W.; Fadeev, A. G.; Qi, B.; Smela, E.; Mattes, B. R.; Ding, J.; Spinks, G. M.; Mazurkiewicz, J.; Zhou, D.; Wallace, G. G.; MacFarlane, D. R.; Forsyth, S. A.; Forsyth, M., *Science* **2002**, *297*, 983.

[26] Hallett, J. P.; Welton, T., *Chem. Rev.* **2011**, *111*, No. 5, 3508.

[27] Earle, M. J.; Gordon, C. M.; Plechkova, N. V.; Seddon, K. R.; Welton, T., *Anal. Chem.* **2007**, *79*, 758.

[28] Nockemann, P.; Binnemans, K.; Driesen, K., *Chem. Phys. Lett.* **2005**, *415*, 131.

[29] Abels, C.; Redepenning, C.; Moll, A.; Melin, T.; Wessling, M., *J. Membr. Sci.* **2012**, *405-406*, 1.

[30] Kuchenbuch, A.; Giernoth, R., *ChemistryOpen* **2015**, *4*, 677.

[31] Tochigi, K.; Yamamoto, H., *J. Phys. Chem. C.* **2007**, *111*, 15989.

[32] Zhang, S.; Sun, N.; He, X.; Lu, X.; Zhang, X., *J. Phys. Chem. Ref. Data* **2006**, *35*, 1475.

[33] Deetlefs, M.; Seddon, K. R.; Shara, M., *Phys. Chem. Chem. Phys.* **2006**, *8*, 642.

[34] Seddon Kenneth, R.; Stark, A.; Torres, M.-J., In *Pure Appl. Chem.* **2000**, *72*, 2275.

[35] Perry, R. L.; Jones, K. M.; Scott, W. D.; Liao, Q.; Hussey, C. L., *J. Chem. Eng. Data.* **1995**, *40*, 615.

[36] Huddleston, J. G.; Visser, A. E.; Reichert, W. M.; Willauer, H. D.; Broker, G. A.; Rogers, R. D., *Green Chem.* **2001**, *3*, 156.

[37] Fröba, A. P.; Kremer, H.; Leipertz, A., *J. Phys. Chem. B.* **2008**, *112*, 12420.

[38] Fröba, A. P.; Leipertz, A., *Int. J. Thermophys.* **2003**, *24*, 895.

[39] Beuermann, S., *Macromol. Rapid Commun.* **2009**, *30*, 1066.

[40] Strehmel, V.; Laschewsky, A.; Wetzel, H.; Görnitz, E., *Macromolecules* **2006**, *39*, 923.

[41] Hong, K.; Zhang, H.; Mays, J. W.; Visser, A. E.; Brazel, C. S.; Holbrey, J. D.; Reichert, W. M.; Rogers, R. D., *Chem. Commun.* **2002**, 1368.

[42] Harrisson, S.; Mackenzie, S. R.; Haddleton, D. M., *Macromolecules* **2003**, *36*, 5072.

[43] Qian, W.; Texter, J.; Yan, F., *Chem. Soc. Rev.* **2017,** *46*, 1124.

[44] Gurkan, B. E.; de la Fuente, J. C.; Mindrup, E. M.; Ficke, L. E.; Goodrich, B. F.; Price, E. A.; Schneider, W. F.; Brennecke, J. F., *J. Am. Chem. Soc.* **2010,** *132*, 2116.

[45] Wickramanayake, S.; Hopkinson, D.; Myers, C.; Hong, L.; Feng, J.; Seol, Y.; Plasynski, D.; Zeh, M.; Luebke, D., *J. Membr. Sci.* **2014**, *470*, 52.

[46] Dobler, D.; Schmidts, T.; Klingenhöfer, I.; Runkel, F., *Int. J. Pharm.* **2013**, *441*, 620.

[47] Vekariya, R. L., *J. Mol. Liq*. **2017**, 227, 44.

[48] (a) Reichardt, C. Handbook of Solvents; ChemTec Publishing: Toronto, **2001**. (b) Dolzhenko, A. V.; Dolzhenko, A. V., Elsevier: Boston, **2015**, 101.

[49] Tanaka, K.; Toda, F., *Chem. Rev.* **2000**, *100*, 1025.

[50] Lubineau, A.; Auge, J.; Queneau, Y., *Synthesis* **1994**, 741.

[51] Lindström, U. M., *Chem. Rev.* **2002**, *102*, 2751.

[52] Li, C.-J.; Chen, L., *Chem. Soc. Rev.* **2006**, *35*, 68.

[53] McCluskey, A., *Green Chem.* **1999**, *1*, 167.

[54] Nalawade, S. P.; Picchioni, F.; Janssen, L. P. B. M., *Prog. Polym. Sci.* **2006**, *31*, 19.

[55] Molteni, V.; Annunziata, R.; Cinquini, M.; Cozzi, F.; Benaglia, M., *Tetrahedron Lett.* **1998**, *39*, 1257.

[56] Shou, W. G.; Yang, Y. Y.; Wang, Y. G. Synthesis **2005**, 530.

[57] Jian, S. Z.; Yuan, Q.; Wang, Y. G. Synthesis **2006**, 1829.

[58] Luczak, J.; Jungnickel, C.; Lacka, I.; Stolte, S.; Hupka, J., *Green Chem.* **2010**, *12*, 593.

[59] Coleman, D.; Spulak, M.; Garcia, M. T.; Gathergood, N., *Green Chem.* **2012**, *14*, 1350.

[60] Petkovic, M.; Seddon, K. R.; Rebelo, L. P. N.; Silva Pereira, C., *Chem. Soc. Rev.* **2011**, *40*, 1383.

[61] Bulter, B.J.; Harper, J. B., *New J. Chem.* **2015**, *39*, 213.

[62] Man, B. Y. W.; Hook, J. M.; Harper, J. B., *Tetrahedron lett.*, **2005**, *46*, 7641.

[63] (a) D'Anna, F.; Frenna, V.; Noto, R.; Pace, V.; Spinelli, D., *J. Org. Chem.,* **2006**, *71*, 9637. (b) D'Anna, F.; Frenna, V.; Noto, R.; Pace, V.; Spinelli, D., *J. Org. Chem.,* **2006**, *71*, 5144.

[64] D'Anna, F.; Frenna, V.; Pace, V.; Noto, R., *Tetrahedron*, **2006**, 62, 1690.

[65] D'Anna, F.; Frenna, V.; La Marca, S.; Noto, R.; Pace, V.; Spinelli, D., *Tetrahedron*, **2008**, 64, 672–680.

[66] D'Anna, F.; La Marca, S.; Lo Meo, P.; Noto, R., *Chem. – Eur. J*., **2009**, 15, 7896.

[67] D'Anna, F.; Marullo, S.; Vitale, P.; Noto, R., Eur. *J. Org. Chem.,* **2011**, 5681.

[68] D'Anna, F.; Marullo, S.; Vitale, P.; Noto, R., *Chem. Phys. Chem*. **2012**, 13, 1877.

[69] D'Anna, F.; Nimal Gunaratne, H. Q.; Lazzara, G.; Noto, R.; Rizzo, C.; Seddon, K. R., *Org. Biomol. Chem*. **2013**, 11, 5836.

[70] D'Anna, F.; Marullo, S.; Vitale, P.; Rizzo, C.; Lo Meo, P.; Noto, R., *Appl. Catal*. A. **2014**, 482, 287.

[71] Lancaster, N. L.; Welton, T.; Young, G. B., *J. Chem. Soc., Perkin Trans*. 2. **2001**, 2267.

[72] Lancaster, N. L.; Salter, P. A.; Welton, T.; Young, G. B., *J. Org. Chem.* **2002**, 67, 8855.

[73] Crowhurst, L.; Lancaster, N. L.; P´erezArlandisand, J. M.; Welton, T., *J. Am. Chem. Soc*., **2004**, 126, 11549.

[74] Lancaster, N. L.; Welton, T., *J. Org. Chem*. **2004**, 69, 5986.

[75] Crowhurst, L.; Falcone, R.; Lancaster, N.L.; Llopis-Mestre, V.; Welton, T., *J. Org. Chem*. **2006**, 71, 8847.

[76] Bini, R.; Chiappe, C.; Mestre, V. L.; Pomelli, C. S.; Welton, T., *Org. Biomol. Chem*. **2008**, 6, 2522.

[77] Ranieri, G.; Hallett, J. P.; Welton, T., *Ind. Eng. Chem. Res*. **2008**, 47, 638.

[78] Lui, M. Y.; Crowhurst, L.; Hallett, J. P.; Hunt, P. A.; Niedermeyer, H.; Welton, T., *Chem. Sci*. **2011**, 2, 1491.

[79] Skarmoutsos, I.; Dellis, D.; Matthews, R. P.; Welton, T.; Hunt, P. A., *J. Phys. Chem*. B. **2012**, 116, 4921.

[80] Niedermeyer, H.; Ashworth, C.; Brandt, A.; Welton, T.; Hunt, P. A., *Phys. Chem. Chem. Phys*. **2013**, 15, 11566.

[81] Chen, L.; Sharifzadeh, M.; Mac Dowell, N.; Welton, T.; Shahand, N.; Hallett, J. P., *Green Chem*. **2014**, 16, 3098.

[82] D'Anna, F.; Frenna,V.; Noto,R.; Pace, V.; Spinelli, D., *J. Org. Chem.* **2006**, 71, 5144.

[83] Calò, V.; Nacci, A.; Monopoli, A.; Lopez, L.; di Cosmo, A., *Tetrahedron* **2001**, *57*, 6071.

[84] Mathews, C. J.; Smith, P. J.; Welton, T., *Chem. Commun.* **2000**, 1249.

[85] Steines, S.; Wasserscheid, P.; Drießen-Hölscher, B., *Journal für praktische Chemie* **2000**, *342*, 348.

[86] McLachlan, F.; Mathews, C. J.; Smith, P. J.; Welton, T., *Organometallics* **2003**, *22*, 5350.

[87] Mathews, C. J.; Smith, P. J.; Welton, T.; White, A. J. P.; Williams, D. J., *Organometallics* **2001**, *20*, 3848.

[88] Ludley, P.; Karodia, N., *Tetrahedron Lett.* **2001**, *42*, 2011.

[89] Gu, Y.; Shi, F.; Deng, Y., *J. Mol. Catal. A: Chem.* **2004**, *212*, 71.

[90] Chiappe, C.; Capraro, D.; Conte, V.; Pieraccini, D., *Org. Lett.* **2001**, *3*, 1061.

[91] Ludley, P.; Karodia, N., *Tetrahedron Lett.* **2001**, *42*, 2011.

[92] George, S. R. D.; Edwards, G. L.; Harper, J. B., *Org. Biomol. Chem.* **2010**, *8*, 5354.

[93] Rosella, C. E.; Harper, J. B., *Tetrahedron Lett.* **2009**, *50*, 992.

[94] Harper, J. B.; Haines, R. S.; Keaveney, S. T., *ChemPlusChem* **2017**, *82*, 1.

[95] Phaniendra, A.; Jestadi, D. B.; Periyasamy, L., *Indian. J. Clin. Biochem.* **2015**, *30*, 11.

[96] Robinson, G. W., *J. Am. Chem. Soc*. **1962**, *36*, 10.

[97] Hancock, A. N.; Schiesser, C. H., *Chem. Commun.* **2013**, *49*, 9892.

[98] Julia, M., *Acc. Chem. Res.* **1971**, *4*, 386.

[99] Barton, D. H. R.; McCombie, S. W., *J. Chem. Soc., Perkin Trans. 1* **1975**, *16*, 1574.

[100] Barton, D. H. R.; Crich, D.; Motherwell, W. B., *Tetrahedron* **1985**, *41*, 3901.

[101] Barton, D. H. R.; Crich, D.; Löbberding, A.; Zard, S. Z., *Tetrahedron* **1986**, *42*, 2329.

[102] Gulea, M.; López-Romero, J. M.; Fensterbank, L.; Malacria, M., *Org. Lett.* **2000**, *2*, 2591.

[103] Clive, D. L. J.; Beaulieu, P. L., *J. Chem. Soc., Chem. Commun.* **1983**, *6*, 307.

[104] Porter, N. A.; Magnin, D. R.; Wright, B. T., *J. Am. Chem. Soc.* **1986**, *108*, 2787.

[105] Schiesser, C. H., *Chem. Commun.* **2006**, *39*, 4055.

[106] Curran, D. P.; Shen, W., *J. Am. Chem. Soc.* **1993**, *115*, 6051.

[107] Struble, D. L.; Beckwith, A. L. J.; Gream, G. E., *Tetrahedron Lett.* **1968**, *9*, 3701.

[108] Tedder, J. M., *Angew. Chem. Int. Ed.* **1982**, *21*, 401.

[109] Beckwith, A. L. J., *Tetrahedron* **1981**, *37*, 3073.

[110] Zhang, W., *Tetrahedron* **2001**, *57*, 7237.

[111] Giese, B., *Angew. Chem.* **1983**, 95, 771; Int. Ed. Engl. **1983**, *22*, 753.

[112] Fischer, H.; Radom, L., *Angew. Chem.* **2001**, 113, 1380; Int. Ed. **2001**, *40*, 1340.

[113] Beckwith, A. L. J., *Rev. Chem. Intermed.* **1986**, *7*, 143.

[114] Hart, D. J.; Huang, H. C.; Krishnamurthy, R.; Schwartz, T., *J. Am. Chem. Soc.* **1989**, *111*, 7507.

[115] Curran, D. P.; Chen, M. H.; Kim, D., *J. Am. Chem. Soc.* **1989,** *111*, 6265.

[116] Mehta, G.; Murthy, A. N.; Reddy, D. S.; Reddy, A. V., *J. Am. Chem. Soc.* **1986**, *108*, 3443.

[117] Curran, D. P.; Rakiewicz, D. M., *J. Am. Chem. Soc.* **1985**, *107*, 1448.

[118] Griller, D.; Ingold, K. U., *Acc. Chem. Res.* **1980**, *13*, 317.

[119] Newcomb, M.; Glenn, A. G., *J. Am. Chem. Soc.* **1989**, *111*, 275.

[120] Walling, C.; Cooley, J. H.; Ponaras, A. A.; Racah, E. J., *J. Am. Chem. Soc.* **1966**, *88*, 5361.

[121] Newcomb, M., *Tetrahedron.* **1993**, 49, 1151.

[122] Chatgilialoglu, C.; Griller, D.; Lesage, M. *J. Org. Chem.* **1988**, *53*, 3641.

[123] Ballestri, M.; Chatgilialoglu, C.; Clark, K. B.; Griller, D.; Giese, B.; Kopping, B., *J. Org.* Chem. **1991**, 56, 678.

[124] Chatgilialoglu, C., *Act. Chem. Res.* **1992**, 25,188.

[125] Chatgilialoglu, C.; Dickhaut, J.; Giese, B., *J. Org. Chem*. **1991**, 56, 6399.

[126] Johnston, L. J.; Scaiano, J. C.; Ingold, K. U., *J. Am. Chem. Sot.* **1984**, 4877.

[127] Chateauneuf, J.; Lusztyk, J.; Ingold, K. U. *J. Org. Chem.* **1988**, 53, 1629.

[128] Beckwith, A. L. J.; Bowry, V. W.; Moad.G. *J. Org. Chem.* **1988,** 53, 1632.

[129] Beckwith, A. L. J.; Bowry, V. W.; Ingold, K. U. *J. Am. Chem. Sot.* **1992**, 114, 4983.

[130] Bowry, V. W.; Ingold, K. U., *J. Am. Chem. Soc.* **1992***, 114,* 4992.

[131] Beckwith, A. L. I.; Bowry, V. W., *J. Org. Chem.* **1989***, 54,* 2681.

[132] Barton, D. H. R.; Crich, D.; Motherwell, W. B., *J. Chem. Soc., Chem. Commun.* **1983,** *17*, 939.

[133] Newcomb, M.; Glenn, A. G., *J. Am. Chem. Soc.* **1989**, *111*, 275.

[134] Fenick, D. J.; Falvey, D. E., *J. Org. Chem.* **1994**, 59, 4791.

[135] Beckwith, A. L. J.; Moad, G., *J. Chem. Soc., Chem. Commun.* **1974**, *12*, 472.

[136] Walling, C.; Cioffari, A., *J. Am. Chem. Soc.* **1972**, *94*, 6059.

[137] Schmid, P.; Griller, D.; Ingold, K. U., *Int. J. Chem. Kinet.* **1979**, *11*, 333.

[138] Chatgilialoglu, C.; Ingold, K. U.; Scaiano, J. C., *J. Am. Chem. Soc.* **1981**, *103*, 7739.

[139] Ha, C.; Horner, J. H.; Newcomb, M.; Varick, T. R.; Arnold, B. R.; Lusztyk, J., *J. Org. Chem.* **1993,** *58*, 1194.

[140] Arai, S.; Sato, S.; Shida, S., *J. Chem. Phys.* **1960**, *33*, 1277.

[141] Lamb, R. C.; Ayers, P. W.; Toney, M. K., *J. Am. Chem. Soc.* **1963,** *85*, 3483.

[142] Beckwith, A. L. J.; Schiesser, C. H., *Tetrahedron* **1985,** *41*, 3925.

[143] Spellmeyer, D. C.; Houk, K. N., *J. Org. Chem.* **1987,** *52*, 959.

[144] Beckwith, A. L. J.; Easton, C. J.; Lawrence, T.; Serelis, A. K., *Aust. J. Chem.* **1983,** *36*, 545.

[145] Beckwith, A. L. J.; Cliff, M. D.; Schiesser, C. H., *Tetrahedron* **1992**, *48*, 4641.

[146] Newcomb, M.; Filipkowski, M. A.; Johnson, C. C., *Tetrahedron Lett.* **1995**, *36*, 3643.

[147] Tripp, J. C.; Schiesser, C. H.; Curran, D. P., *J. Am. Chem. Soc.* **2005**, *127*, 5518.

[148] Beckwith, A. L. J.; Gream, G. E.; Struble, D. L., *Aust. J. Chem.* **1972**, *25*, 1081-1105.

[149] Beckwith, A. L. J.; Blair, I.; Phillipou, G., *J. Am. Chem. Soc.* **1974**, *96*, 1613.

[150] Beckwith, A. L. J.; Easton, C. J.; Serelis, A. K., *J. Chem. Soc., Chem. Commun.* **1980**, *11*, 482.

[151] Bischof, P., *Helv. Chim. Acta* **1980,** *63*, 1434.

[152] Gulea, M.; López-Romero, J. M.; Fensterbank, L.; Malacria, M., *Org. Lett.* **2000**, *2*, 2591.

[153] a) Chen, L.; Gill, G. B.; Pattenden, G., *Tetrahedron Lett.* **1994,** *35*, 2593. b) Chatgilialoglu, C.; Crich, D.; Komatsu, M.; Ryu, I., *Chem. Rev.* **1999**, *99*, 1991.

[154] Callier-Dublanchet, A.-C.; Quiclet-Sire, B.; Zard, S. Z., *Tetrahedron Lett.* **1997**, *38*, 2463.

[155] Shaw, D. E.; Fenton, G.; Knight, D. W., *J. Chem. Soc., Chem. Commun.* **1994**, *21*, 2447.

[156] Boivin, T. L. B., *Tetrahedron* **1987**, *43*, 3309.

[157] Rieke, R. D.; Moore, N. A., *J. Org. Chem.* **1972**, *37*, 413.

[158] Johns, A.; A. Murphy, J., *Tetrahedron Lett.* **1988**, *29*, 837.

[159] Avila, D. V.; Ingold, K. U.; Di Nardo, A. A.; Zerbetto, F.; Zgierski, M. Z.; Lusztyk, J., *J. Am. Chem. Soc.* **1995**, *117*, 2711.

[160] Hay, B. P.; Beckwith, A. L. J., *J. Org. Chem.* **1989**, *54*, 4330.

[161] Hartung, J.; Gallou, F., *J. Org. Chem.* **1995**, *60*, 6706.

[162] Tada, M.; Uetake, T.; Matsumoto, M., *J. Chem. Soc., Chem. Commun.* **1990**, *20*, 1408.

[163] Benati, L.; Montevecchi, P. C.; Tundo, A.; Zanardi, G., *J. Chem. Soc., Perkin Trans. 1* **1974**, 1272.

[164] Beckwith, A. L. J.; Duggan, S. A. M., *J. Chem. Soc., Perkin Trans. 2* **1994**, *7*, 1509.

[165] Schiesser, C. H.; Sutej, K., *J. Chem. Soc., Chem. Commun.* **1992**, *1*, 57.

[166] Benjamin, L. J.; Schiesser, C. H.; Sutej, K., *Tetrahedron* **1993**, *49*, 2557.

[167] a) Hancock, A. N.; Kavanagh, Y.; Schiesser, C. H., *Org. Chem. Front.* **2014**, *1*, 645. b) Hancock, A. N.; Lobachevsky, S.; Haworth, N. L.; Coote, M. L.; Schiesser, C. H., *Org. Biomol. Chem.* **2015**, *13*, 2310.

[168] Grange, R. L.; Ziogas, J.; North, A. J.; Angus, J. A.; Schiesser, C. H., *Biorg. Med. Chem. Lett.* **2008**, *18*, 1241.

[169] Benjamin, L. J.; Schiesser, C. H.; Sutej, K., *Tetrahedron* **1993**, *49*, 2557.

[170] Tedder, J. M.; Walton, J. C., *Acc. Chem. Res.* **1976**, *9*, 183.

[171] Giese, B., *Angew. Chem. Int. Ed.* **1983**, *22*, 753.

[172] Lalevée, J.; Allonas, X.; Fouassier, J. P.; Rinaldi, D.; Ruiz Lopez, M. F.; Rivail, J. L., *Chem. Phys. Lett.* **2005,** *415*, 202.

[173] Canelas, D. A.; Desimone, J. M., *Adv. Polym. Sci.* **1997**, *133*, 103.

[174] Kubisa, P., *Prog. Polym. Sci.* **2004,** *29*, 3.

[175] Arnaud, R.; Bugaud, N.; Vetere, V.; Barone, V., *J. Am. Chem. Soc.* **1998**, *120*, 5733.

[176] Fischer, H.; Radom, L., *Angew. Chem. Int. Ed.* **2001**, *40*, 1340.

[177] Wu, J. Q.; Beranek, I.; Fischer, H., *Helv. Chim. Acta* **1995**, *78*, 194.

[178] Beckwith, A. L. J.; Schiesser, C. H., *Org. Biomol. Chem.* **2011**, *9*, 1736.

[179] Strehmel, V.; Berdzinski, S.; Rexhausen, H., *J. Mol. Liq.* **2014**, *192*, 153.

[180] (a) Reichardt, C., *Chem. Rev*., **1994**, 94, 2319. (b) Hanke, C.; Johansson, A.; Harper, J.; Lynden-Bell, R., *Chem. Phys. Lett*., **2003**, 374, 85. (c) Rovere. M.; Tosi, M. P., *Rep. Prog. Phys.,* **1986**, 49, 1001. (d) Weinga¨ rtner, H., *Z. Phys. Chem*., **2007**, 220, 1395.

[181] (a) Moya, C.; Palomar, J.; Gonzalez-Miquel, M.; Bedia, J.; Rodriguez, F., *Ind. Eng. Chem. Res.* **2014**, *53*, 13782. (b) Seoane, R. G.; Corderí, S.; Gómez, E.; Calvar, N.; González, E. J.; Macedo, E. A.; Domínguez, Á., *Ind. Eng. Chem. Res.* **2012**, *51*, 2492. (c) Daguenet, C.; Dyson, P. J.; Krossing, I.; Oleinikova, A.; Slattery, J.; Wakai, C.; Weingartner, H, *J. Phys. Chem. B*, **2006**, 110, 12682.

[182] Burrell, A. K.; Sesto, R. E. D.; Baker, S. N.; McCleskey, T. M.; Baker, G. A., *Green Chemistry* **2007**, *9*, 449.

[183] Kuivila, H. G., *Acc. Chem. Res.* **1968**, *1*, 299.

[184] Selected examples: a) Hart, D. J.; Huang, H. C.; Krishnamurthy, R.; Schwartz, T., *J. Am. Chem. Soc.* **1989**, *111*, 7507; b) Curran, D. P.; Chen, M. H.; Kim, D., *J. Am. Chem. Soc.* **1989**, *111*, 6265; c) Porter, N. A.; Magnin, D. R.; Wright, B. T., *J. Am. Chem. Soc.* **1986**, *108*, 2787; d) Beckwith, A. L. J.; *Tetrahedron* **1981**, *37*, 3073; e) Wille, U., *Chem. Rev.* **2013**, *113*, 813.

[185] Lancaster, N. L.; Welton, T., Young, G. B., *J. Chem. Soc., Perkin Trans. 2* **2001**, 2267.

[186] Lancaster, N. L.; Salter, P. A.; Welton, T.; Young, G. B., *J. Org. Chem.* **2002**, 67, 8855.

[187] Crowhurst, L.; Lancaster, N. L.; Pérez Arlandis, J. M.; Welton, T., *J. Am. Chem. Soc*. **2004**, 126, 11549.

[188] Lancaster, N. L.; Welton, T., *J. Org. Chem*. **2004**, 69, 5986.

[189] Crowhurst, L.; Falcone, R.; Lancaster, N. L.; Llopis-Mestre, V.; Welton, T., *J. Org. Chem.* **2006**, 71, 8847.

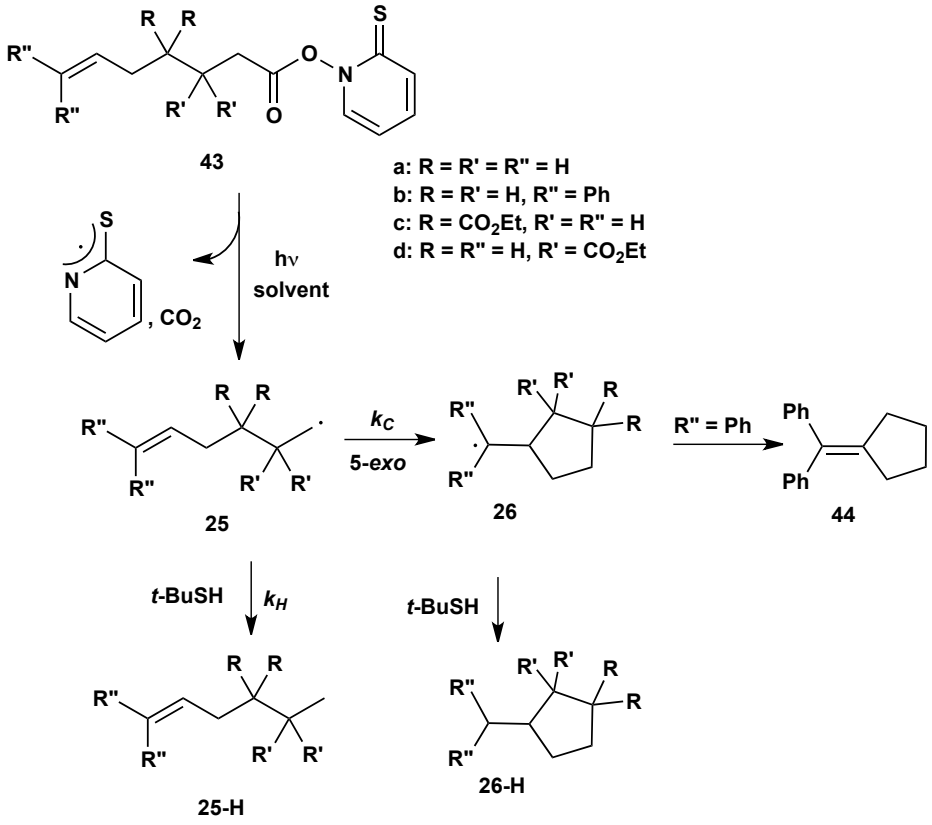
[190] Bini, R.; Bortolini, O.; Chiappe, C.; Pieraccini, D.; Siciliano, T.*, J. Phys. Chem. B* **2007**, 111, 598.

[191] Butler, B. J.; Thomas, D. S.; Hookb, J. M.; Harper, J. B., *Magn. Reson. Chem*. **2016**, 54, 423.

2 5-*Exo* cyclisation of primary alkyl radicals

The structure of the radicals and their precursors studied in this chapter are depicted in Scheme 2.1. The 5-hexenyl radicals **25a-d** were generated in the presence of *t*-BuSH (*t*-butylthiol) by photochemical cleavage of the PTOC-ester **43a-d** using a 250 W broad-spectrum mercury lamp. Competition kinetic experiments[1] were performed in [EMIm][NTf_2], and, in order to directly compare the reactivity, also in the non-polar conventional solvent *t*-butylbenzene (*t*-BuPh) under otherwise identical reaction conditions. Details will be outlined below (section 2.4.)

In all experiments the amount of [EMIm][Ntf_2] (1 ml, 3.88 mmol) was much larger than [*t*-BuSH] with the maximum value of (22 µL, 1.96×10^{-4} mmol), under these conditions dilution of the ionic liquid by the reagent can be excluded (χIL = 1).[2] Quantitative extraction of the reaction products from the IL phase, which is crucial for the competition kinetic studies, will be described in section 2.3.

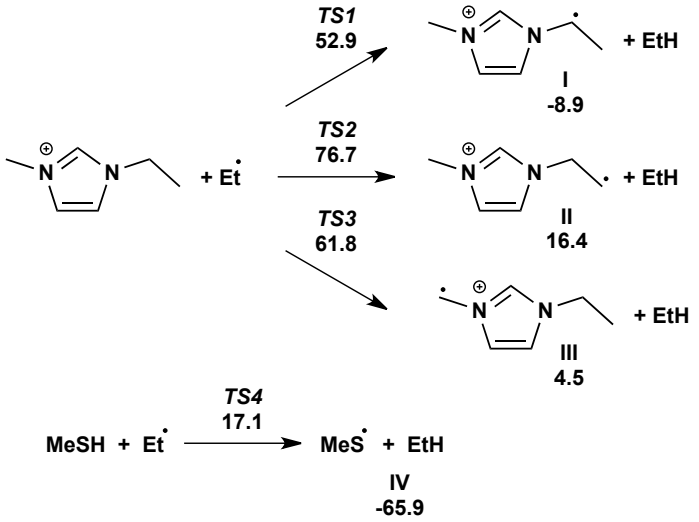


Scheme 2.1. Generation of the 5-hexenyl radicals (**25**) and competing reactions through reduction to **25-H** and 5-*exo* cyclisation to **26**.

2.1 Exploring the compatibility of [EMIm][NTf_2] in radical reactions

Before starting the kinetic experiments, it was required to confirm that [EMIm][NTf_2] is stable under the experimental conditions of the intended radical reactions.[3] In particular, the alkyl side chains in the cationic moiety of [EMIm][NTf_2] could potentially provide a source of hydrogen atoms, which might lead to an apparently faster rate for the terminating radical reduction. The NTf_2 moiety on the other hand does not contain structural motifs susceptible to radical reactions and was considered as inert.

Scheme 2.2 shows the results of gas phase DFT calculations performed at the M062X/6-31+G* level of theory using the Gaussian software package,[4] which used the ethyl radical as a simplified model for the alkyl radicals employed in this study. This level of theory was chosen because it has been previously shown to provide sufficiently accurate energies to enable quantitative assessment of competing pathways in radical reactions.[3b] The kinetically and thermodynamically most favourable pathway is hydrogen abstraction from the ethyl substituent in EMIm *via* the transition state TS1. In fact, formation of the EMIm radical **I** is the only exothermic pathway, whereas hydrogen abstraction from the primary positions to give the isomeric radicals **II** and **III** is not only endothermic, but the transition states associated with these processes, TS2 and TS3, are also considerably higher than TS1.



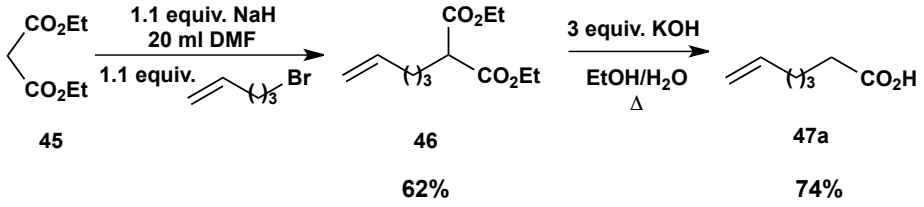
Scheme 2.2. M062X/6-31+G*-calculated barriers and reaction energies (in kJ mol^{-1}) for hydrogen abstractions from EMIm and methylthiol (calculations performed by U. Wille).

Comparison with the data for the hydrogen abstraction of Et$^{\bullet}$ from methyl thiol, which was used as simplified model for *t*-BuSH, clearly revealed that EMIm should not be a competitive hydrogen donor for the radical reactions studied in this work. Not only is TS4 considerably lower than TS1, but the hydrogen abstraction from a thiol to give the product complex **IV** is also thermodynamically significantly more favourable. Thus, based on the computations EMIm should be compatible to the radical reaction conditions studied in this work. The Gaussian archive entries for all calculated ground and transition states are given in the Appendix 1.

2.2 Synthesis of the radical precursors 43 and reference compounds

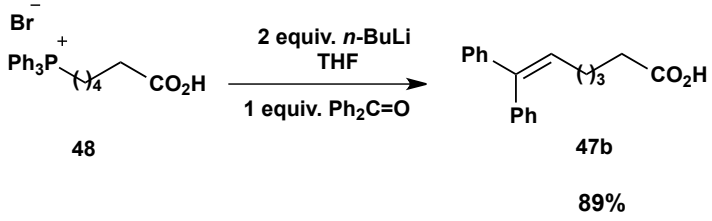
This section describes the synthesis of the radical precursors **43a-d** employed in this Chapter, as outlined Scheme 2.1, and of the authentic samples of the reaction products, which were required to unequivocally identify the product peaks in the gas chromatograms.

All PTOC esters **43** were obtained by reacting the respective mono carboxylic acids with *N*-hydroxypyridine-2-thione. Scheme 2.3 outlines the synthesis of 6-heptenoic acid (**47a**), where commercially available diethylmalonate (**45**) was first alkylated with 1.1 equivalents of 5-bromopentene in anhydrous DMF, using sodium hydride as the base. Diethyl ester **46** was obtained in 62% yield after column chromatography. The ^{1}H NMR spectrum showed a triplet of the methine protons at 3.32 ppm (^{3}J = 7.5 Hz, 1H), in agreement with literature.[5] Subsequent saponification and decarboxylation provided 6-heptenoic acid (**47a**) in 74% yield. The structure was confirmed by ^{1}H NMR data through the loss of the quartet and triplet signals of the ethyl groups at 4.2 ppm and 1.26 ppm respectively, and a new triplet signal at 2.35 ppm (^{3}J = 7.5 Hz, 2H) that can be assigned to the α-methylene protons, in agreement with literature data.[6]



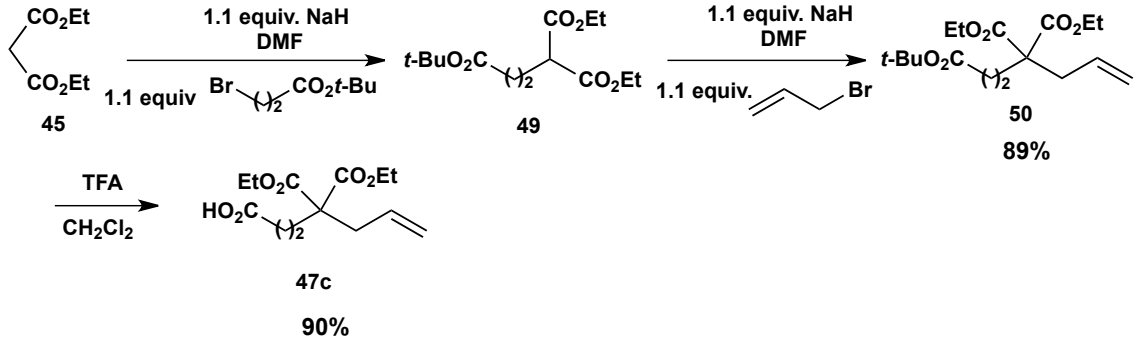
Scheme 2.3. Synthesis of 6-heptenoic acid (**47a**).

7,7-Diphenyl-6-heptenoic acid (**47b**) was synthesised through a Wittig reaction[7] by treating phonium bromide **48**[8] with two equivalents of *n*-butyllithium (*n*-BuLi), followed by addition of benzophenone (Scheme 2.4). Column chromatography gave the acid **47b** in good yield (89%). The ^{1}H NMR spectrum showed the vinylic proton as a triplet at 6.06 ppm. All other signals matched those found in the literature.[9]



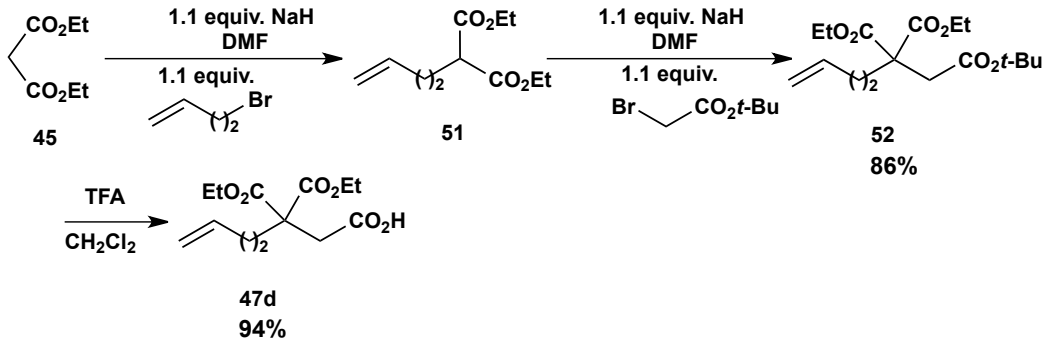
Scheme 2.4. Synthesis of the 7,7-diphenyl-6-heptenoic acid (**47b**).

Carboxylic cid **47c** was synthesised as shown in Scheme 2.5. Diethylmalonate (**45**) was alkylated with *t*-butyl 3-bromopropionate and allyl bromide in anhydrous DMF, using sodium hydride as the base. Tricarboxylate **50** was obtained in 89% yield after column chromatography. The ^{1}H NMR spectrum showed the 9 protons of the *t*-butyl ester group as a singlet at 1.42 ppm and two multiplets signals at 5.61-5.71 and 5.08-5.13 ppm belonging to the olefinic CH and CH_2, thus confirming the successful formation of **49**. Subsequent treatment of **49** with TFA in CH_2Cl_2 at room temperature gave compound **47c** in 90% yield. Loss of the signal of the *t*-butyl group in the ^{1}H NMR spectrum of the product **47c**, with the other signals similar to the spectrum of the compound **50**, confirmed the formation of the product **47c**.



Scheme 2.5. Synthesis of the 4,4-bis(ethoxycarbonyl)hept-6-enoic acid (**47c**).

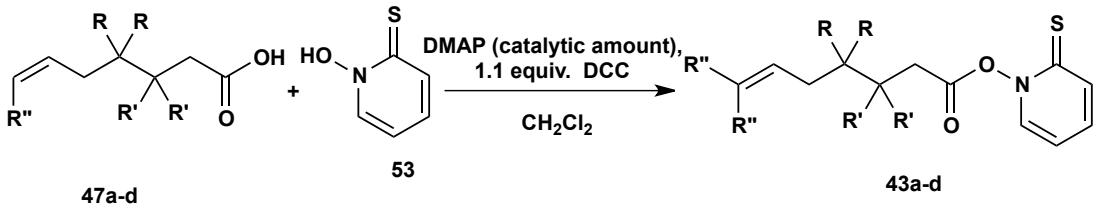
Scheme 2.6 outlines the synthesis of carboxylic acid **47d**, which was prepared in a similar way from diethylmalonate (**45**), 4-bromobutene and *t*-butyl bromoacetate in anhydrous DMF, using sodium hydride as the base. Tricarboxylate **51** was obtained in 86% yield after column chromatography. The ^{1}H NMR spectrum displayed a characteristic singlet of methylene protons attached to the *t*-butyl carboxylate group at 2.9 ppm, a singlet of the *t*-butyl group at 1.42 ppm and two multiplets of the olefinic protons at 5.73- 5.82 and 4.95- 5.05 ppm, confirming the successful formation of the compound **52**. Liberation of the acid using TFA in CH_2Cl_2 at room temperature gave compound **47d** in 94% yield. The structure was confirmed by ^{1}H NMR data through the disappearance of the singlet of *t*-butyl group at 1.42 ppm.



Scheme 2.6. Synthesis of the 3,3-bis (ethoxycarbonyl) hept-6-enoic acid (**47d**).

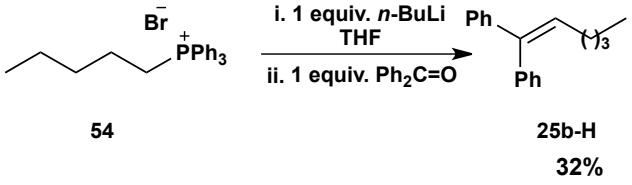
Coupling of the mono acids **47a-d** to provide the PTOC esters **43a-d** was achieved following the literature procedure (Scheme 2.7).[10] Treatment of **47a-d** with 0.95 equivalents of *N*-hydroxypyridine-2-thione (**53**) was performed under exclusion of

light by covering the reaction flask with aluminium foil in the presence of a catalytic amounts of 4-dimethylaminopyridine (DMAP) and 1.1 equivalents of dicyclohexylcarbodiimide (DCC) in CH_2Cl_2. Purification by column chromatography gave the respective thiohydroxamic esters **47a** (69%), **47b** (64%), **47c** (90%), and **47d** (65%). ^{1}H NMR data analysis in C_6D_6 showed the four aromatic hydrogen atoms at 5.4, 6.0, 6.4 and 7.4 ppm, respectively, with the other spectral data being similar to those of the corresponding monoacids. The HRMS data of **43a-d** confirmed the molecular formula in all cases (Scheme 2.7).



Scheme 2.7. Synthesis of the PTOC ester **43a-d**.

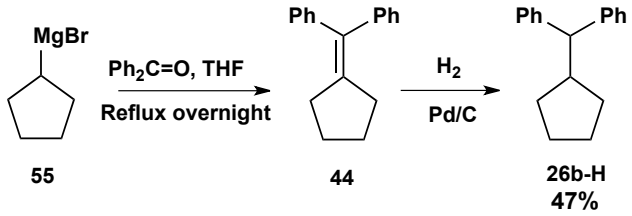
1,1-Diphenyl-1-hexene (**25b-H**) was synthesised as a GC standard through a Wittig reaction by treating (1-pentyl) triphenylphosphonium bromide (**54**) with *n*-butyllithium followed by addition of benzophenone (Scheme 2.8). Column chromatography gave compound **25b-H** in 32% yield. The ^{1}H NMR spectrum showed a triplet at 6.11 ppm that can be assigned to the olefinic CH, in agreement with the literature data.[8]



Scheme 2.8. Synthesis of the 1,1-diphenyl-1-hexene (**25b-H**).

(Diphenylmethyl)cyclopentane (**26b-H**) was synthesised through a Grignard reaction,[11,12] using benzophenone and cyclopentylmagnesium bromide (**55**) (prepared by addition of bromocyclopentane to Mg chips in anhydrous THF and activation by a few drops of 1,2-dibromoethane) in dry THF, and refluxing overnight. Subsequent

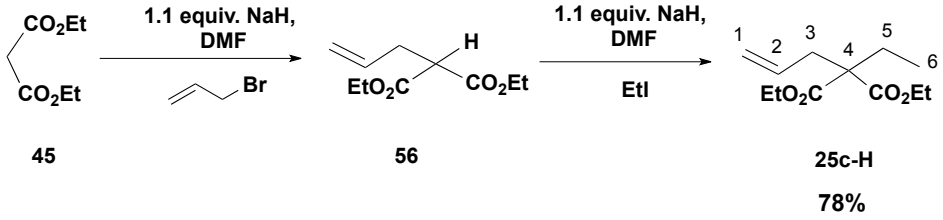
work up and column chromatography gave (diphenylmethylene) cyclopentene (**44**) as a white solid. Hydrogenation using 5% Pd/C under H_2 (100 psi) afforded the title compound **26b-H** in 47% yield over two steps (Scheme 2.9). The ^{1}H NMR spectrum displayed a characteristic doublet of the benzylic methine proton at 3.5 ppm and a multiplet of the methine proton attached to cyclopentane at 2.63-2.74 ppm, in agreement with the literature.[8]



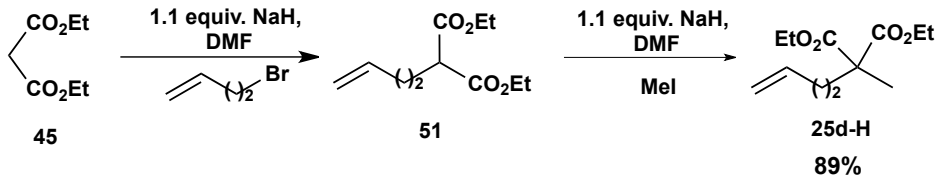
Scheme 2.9. Synthesis of the (diphenylmethyl)cyclopentane (**26b-H**).

Diethyl allylethylmalonate (**25c-H**) was synthesised as shown in Scheme 2.10. Diethylmalonate (**45**) was first alkylated with ally and then with ethyl iodide in anhydrous DMF, using sodium hydride as the base. Diethyl allylethylmalonate (**25c-H**) was obtained in 78% yield after column chromatography. The ^{1}H NMR spectrum showed a quartet of protons attached to C-2 at 1.94 ppm and doublet of triplets of the allylic protons at 2.66 ppm (^4J = 1.1 Hz, ^3J = 7.4 Hz).

Diethyl ester **25d-H** was prepared in a similar way, using 4-bromobutene and methyl iodide (Scheme 2.11). Diethyl ester **25d-H** was obtained in 89% yield after column chromatography.

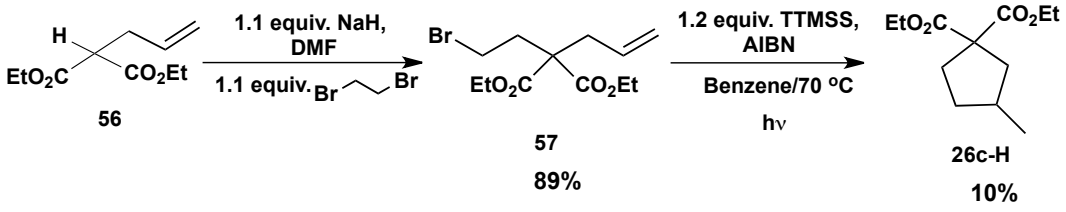


Scheme 2.10. Synthesis of the diethyl allylethylmalonate (**25c-H**).



Scheme 2.11. Synthesis of the diethyl 2-(but-3-enyl)-2-methylpropanedioate (**25d-H**).

Diethyl ester (**26c-H**) was prepared from diethyl diester **56**, which was alkylated with 1,2-dibromoethane in anhydrous DMF, using sodium hydride as the base. Diethyl 2-allyl-2-(2-bromoethyl) malonate (**57**) was obtained in 89% yield. The ^{1}H NMR spectrum was in agreement with literature.[13] Compound **57** was irradiated with a mercury lamp at 70°C in benzene in the presence of tris(trimethyl silyl)silane and catalytic amounts of AIBN to furnish diethyl ester (**26c-H**) as a pale yellow oil in 10% yield (Scheme 2.12). The ^{1}H NMR spectrum was in agreement with literature.[13]



Scheme 2.12. Synthesis of the 3-methyl-cyclopentane-1,1-dicarboxylic acid diethyl ester (**26c-H**).

2.3 Extraction procedure

One of the key challenges to using ILs as solvents in organic synthesis is the efficient recovery of reaction products from these solvents. Several product recovery techniques from ILs have been reported in the literature, for example:

1. Distillation of volatile products from an IL.[14]
2. Extraction of hydrophilic products from hydrophobic ILs using water.[15]
3. Utilizing supercritical carbon dioxide (CO_2) for the extraction of non-volatile or thermally sensitive products from an IL.[16,17]
4. Extraction of products from an IL using organic solvents.[18,19]

Obtaining reliable kinetic data in competition kinetic studies requires determination of accurate product ratios, which in turn requires a reliable and reproducible extraction procedure to recover all products from the IL. Established methods, such as distillation[14] or extraction using supercritical CO_2,[16,17] were not feasible for the small-scale kinetic experiments in this work. Therefore, it was explored which organic solvent could enable quantitative extraction of the reaction products from the IL after the kinetic experiments.

It was found that extraction of the ionic liquid phase with *t*-BuPh (three times) enabled quantitative recovery of the non-polar reaction products **25a-H** and **26a-H** from [EMIm][NTf_2]. Other solvents, such as dichloromethane, ethyl acetate, and ethanol are miscible in [EMIm][NTf_2] and could not be used for the extraction. In order to verify that all products from the competition kinetics studies were quantitatively extracted from [EMIm][NTf_2], solutions of 1 equivalent of methylcyclopentane (**26a-H**) and 1-hexene (**25a-H**) (the products of 5-hexenyl radical **25a** cyclisation), in both *t*-BuPh and in [EMIm][NTf_2] were prepared (Figure 2.1).

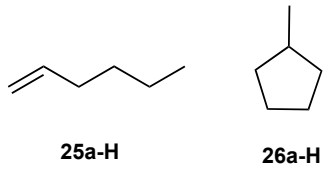


Figure 2.1. Products of 5-hexenyl radical (**25a**) cyclisation.

The standard solution in *t*-BuPh was directly analysed by GC, whereas the one in [EMIm][NTf_2] was analysed after extraction with *t*-BuPh. The organic phase used in the extraction passed through a short silica plug to remove trace amounts of IL.

Measuring the peak area (PA) is one of the common ways to quantify the composition of reaction mixtures by GC. In this experiment, solutions of methylcyclopentane (**26a-H**) and 1-hexene (**25a-H**) with similar concentration (1 molar) gave different peak areas in gas chromatogram, which is due to the different response of the detector (FID detector) to those compounds. Similar ratio of the peaks area obtained from extraction with *t*-BuPh (1.14) compared to those from the standard solution (1.13)

provide confidence that the products of the 5-hexenyl radical cyclisation can be successfully extracted with *t*-BuPh from the IL phase (Table 2.1).

Table 2.1. The ratio of GC peak areas of methylcyclopentane (**26a-H**) and 1-hexene (**25a-H**) in *t*-BuPh and after extraction from [EMIm][NTf_2].

Solvent	[**26a-H**]/M^{-1}	[**25a-H**]/M^{-1}	PA (**25a-H**)/PA (**26a-H**)[a]
t-BuPh	1	1	1.1 ± 0.1
[EMIm][NTf_2]	1	1	1.1 ± 0.1[b]

[a]PA: Peak area; error represents deviation from the average result of three experiments. [b]After extraction with *t*-BuPh.

For more polar compounds (including the products of the cyclisation of radical **25c** and **25d**) (Figure 2.2), several literature procedures were attempted, including extraction with diethyl ether,[18] mixtures of petroleum ether and ethyl acetate (5:1),[19] and first dilution of the IL phase with ethyl acetate, followed by extraction with diethyl ether (three times).[20] The latter method turned out to enable quantitative isolation of polar compounds from [EMIm][NTf_2]. The data are shown in Table 2.2.

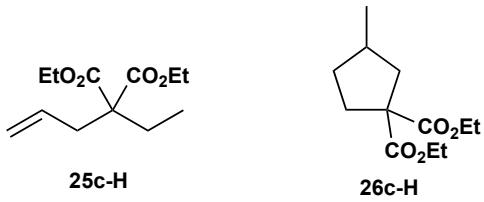


Figure 2.2. Products of radical **25c** cyclisation.

Table 2.2. The ratio of GC peak areas of compounds **26c-H** and **25c-H** in *t*-BuPh and after extraction from [EMIm][NTf_2].

Solvent	[**26c-H**]/M^{-1}	[**25c-H**]/M^{-1}	PA (**25c-H**)/PA (**26c-H**)[a]
t-BuPh	1	1	1.1 ± 0.1
[EMIm][NTf_2]	1	1	1.1± 0.2[b]

[a]PA: Peak area; error represents deviation from the average result of three experiments. [b]After extraction with ethyl acetate and diethyl ether.

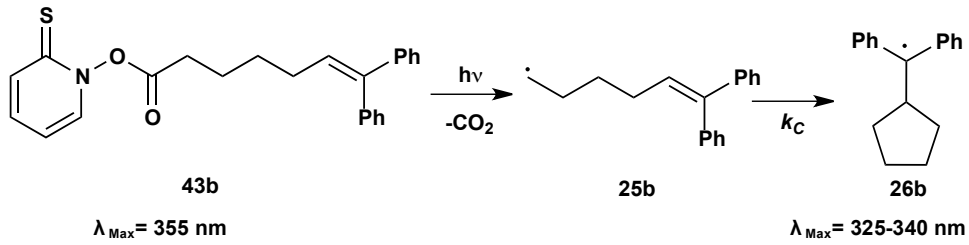
2.4 Kinetic experiments

So far, a large number of radical clocks have been calibrated in different conventional solvents, but not for ionic liquids. The first step in this work was therefore to calibrate the first unimolecular radical clock for alkyl radicals in [EMIm][NTf_2].

Determination of the rate constants for the cyclisation of the primary alkyl radicals from competition kinetic experiments requires knowledge of absolute rate data for at least one reference reaction. The 5-*exo* radical cyclisation of the primary diphenyl substituted 5-hexenyl radical **25b** was selected as reference reaction (Scheme 2.1), since the absolute rate coefficient k_C could be determined by monitoring the time-dependent formation of the resonance stabilised radical **26b** in [EMIm][NTf_2] through transient UV absorption spectroscopy. In a second step, the ratio of cyclisation versus reduction, k_C/k_H for **25b** was obtained through competition kinetic studies by determining k_H for the hydrogen abstraction of a primary alkyl radical from a thiol in [EMIm][NTf_2]. More details are given in the following section.

2.4.1 Determination of the absolute rate constant, k_C, in [EMIm][NTf_2] using the direct method

The absolute rate constant for the 5-*exo* cyclisation of radical **25b**, k_C, to form radical **26b** was determined using laser flash photolysis (LFP).[21] The PTOC-ester **43b** has an absorption band at 355 nm. Laser excitation leads to homolytic cleavage of the N-O bond, followed by rapid decarboxylation to form radical **25b**, which can undergo cyclisation to radical **26b**. The latter was monitored at 325-340 nm (Scheme 2.13).



Scheme 2.13. Generation and cyclisation of the 6,6-diphenyl-5-hexenyl radical (**25b**).

The laser flash photolysis experiments were performed with an Edinburgh Instrument LP920 spectrometer using the third harmonic of a Quantel Brilliant B Nd:YAG laser (6 ns pulse, 25 mJ, λ = 355 nm). The detector system employed a Hamamatsu R2856 photomultiplier tube (PMT) interfaced with a Tektronix TDS 3012C Digital Phosphor oscilloscope for transient absorption spectra. Solutions of the PTOC ester **43b** ([**43b**] ca. 2×10^{-4} M) in [EMIm][NTf_2] were studied in a static cell (10 × 10 mm). Control experiments were performed in acetonitrile using the same concentration of **43b**. The solutions were purged with Argon for 15 minutes before the experiments and the spectra were obtained 60 ns after the laser pulse.[8] To minimise the effects from photobleaching, the laser was operated in single-shot mode, where the cell was shaken manually after each laser pulse. The transient absorption spectra in both acetonitrile and [EMIm][NTf_2] were averaged over five of such measurements and are shown in Figure 2.3.

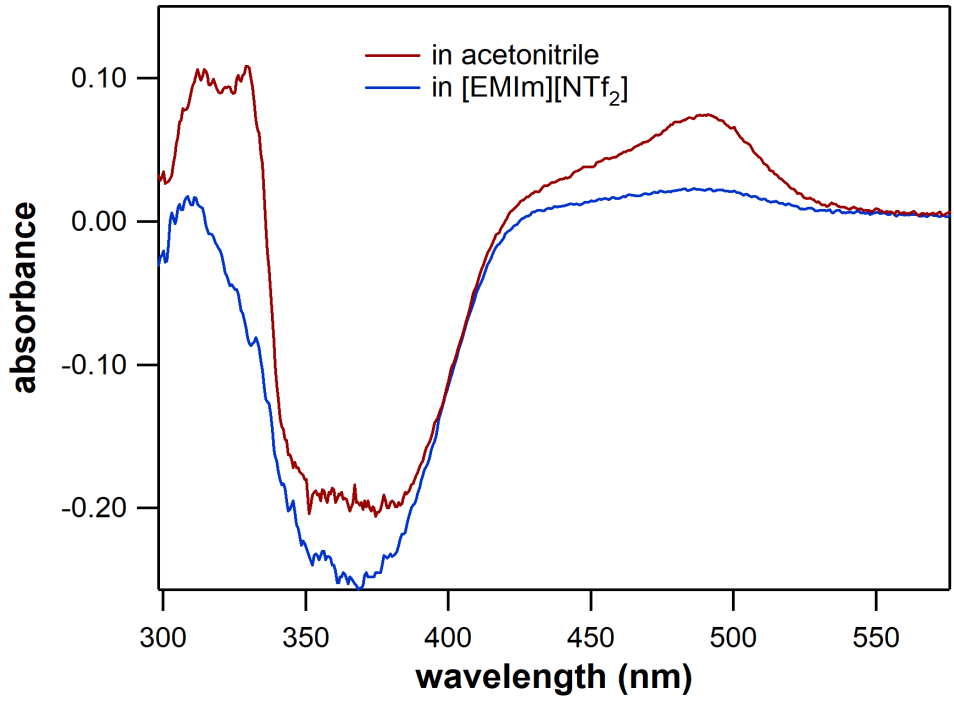


Figure 2.3. Time-resolved spectrum of transients produced by photolysis of PTOC ester **43b** obtained 60 ns after irradiation with 355 nm light in acetonitrile (red line) and [EMIm][NTf_2] (blue line). Experiments performed by Dr J. Nathanael.

Overall, the intensity of the absorptions in the two different solvent systems suggest that after 60 ns less **26b** is formed in [EMIm][NTf_2] than in acetonitrile, which might

indicate that photochemical generation of **25b** is slower in the ionic liquid. While the absorption maximum of **26b** in acetonitrile is characterised by two maxima at 330[8] and 314 nm, in [EMIm][NTf_2], only one absorption maximum at 310 nm was found. It is not possible to state whether the longer wavelength maximum in acetonitrile disappears in the ionic liquid, or whether both maxima undergo a hypsochromic shift in [EMIm][NTf_2], because the strong PTOC **43b** depletion makes mesurements of transient absorptions at wavelengths below 300 nm impossible. Time-dependent formation of the signal at 310 nm in [EMIm][NTf_2] showed first order behaviour (Figure 2.4) to reveal k_C for the formation of **26b** of $(10.0 \pm 0.8) \times 10^7$ s^{-1} (298 K). However, it should be pointed out that the kinetic measurements in the ionic liquid were very challenging. In order to obtain a measurable signal of **26b** in [EMIm][NTf_2], it was required to use a concentration of the PTOC ester **43b** that was about a five times higher than Newcomb *et al*. used in their laser flash photolysis studies in acetonitrile (0.08 mM), where they determined $k_C = (4.5 \pm 0.1) \times 10^7$ s^{-1} from the growth of the signal of **26b** in the range of 310 - 342 nm (295 K).[8] With the higher [**43b**] in this work, k_C was measured in acetonitrile as $(7.5 \pm 0.3) \times 10^7$ s^{-1} from the growth of the signal at 330 nm (298 K), which is 1.7 times larger than Newcomb's value. However, irrespective of this discrepancy, which was not further investigated, the k_C value for the 5-*exo* cyclisation of **25b** in [EMIm][NTf_2] was more than twice as high than in acetonitrile (based on Newcomb's value). It should be noted that the red-shifted transient with an absorbance around 490 nm was formed within the time period of the laser pulse and could be assigned to the 2-pyridinethiyl radical, the by-product from the photochemical PTOC cleavage, in agreement with literature.[8]

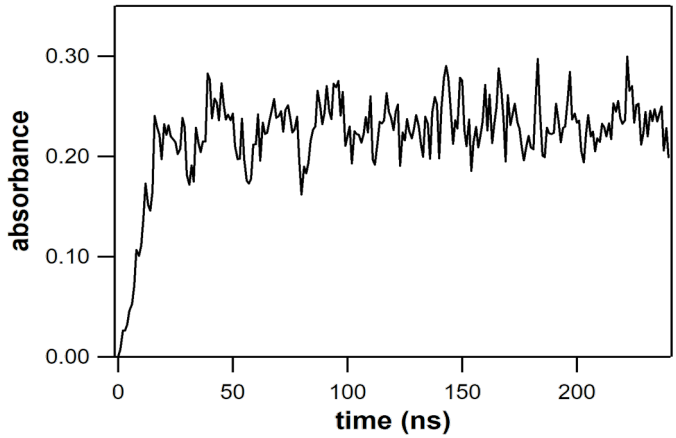
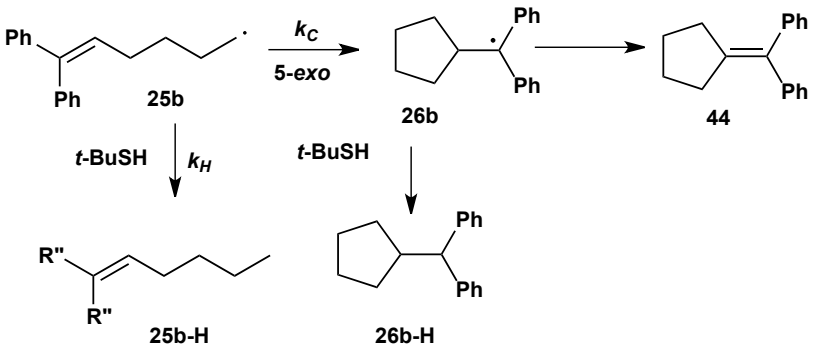


Figure 2.4. Time-dependent formation of (diphenylmethylene)cyclopentyl radical **26b** at 310 nm in [EMIm][NTf_2] ([PTOC] = 0.23 mM). Experiments performed by Dr J. Nathanael.

The obtained k_C value was subsequently used to determine the k_H value from *t*-BuSH to primary alkyl radicals in competition kinetic studies.

2.4.2 Competition kinetic studies

In order to calibrate the experimental methodology, the competition kinetic studies were first performed with the well-studied 6,6-diphenyl-5-hexenyl radical **25b**.[8] A series of competition kinetic experiments of the 5-*exo* cyclisation of the 6,6- diphenyl-5-hexenyl radical **25b** in *t*-BuPh and [EMIm][NTf_2] at 24 ± 1 °C with concentrations of *t*-BuSH ranging from 0.1-0.25 M were carried out (Scheme 2.14).



Scheme 2.14. Competition kinetic studies of the 5-*exo* cyclisation of the 6,6-diphenyl-5-hexenyl radical (**25b**) and the reduction through hydrogen abstraction from *t*-BuSH.

According to the GC analysis, no additional products than those shown in Scheme 2.14 were found in the reactions performed in [EMIm][NTf_2], indicating no

interfering reactions of radical intermediates with the solvent. The identity of the products was confirmed by comparison with authentic samples, which were prepared as described in section 2.2.1.

With *t*-BuSH present in excess (10 equivalents), its concentration can be considered as constant during the course of the reaction, enabling the system to be treated as a pseudo-first order process. Under these conditions, the final product distribution provides a ratio of rate constants for the unimolecular and bimolecular processes *via* equation 1.

As outlined in chapter 1, when the radical cyclisation is irreversible, trapping of radical **25b** by *t*-BuSH (k_H) is kinetically irrelevant.[22]

$$(1) \qquad [\mathbf{26b\text{-}H}]/[\mathbf{25b\text{-}H}] = k_C/k_H \times [t\text{-BuSH}]^{-1}$$

The ratio of the product concentration was determined by GC analysis of the reaction mixture from the relative peak areas (after extraction with *t*-BuPh (3X) in the case of the experiments performed in [EMIm][NTf_2]).

In the cyclisation of radical **25b**, since the *t*-BuSH was relatively poor trapping agent for the stabilised radical **26b-H** and that relatively high concentration of this radical accumulated leading to radical-radical reaction to produce the cyclised alkene **44** as a by-product, as reported previously.[8] k_C/k_H for this reaction was therefore determined using ([**26b-H**]+[**44**])/[**25b-H**] = $k_C/k_H \times [t\text{-BuSH}]^{-1}$.

The results of the competition experiment in *t*-BuPh and [EMIm][NTf_2] are compiled in Table 2.3. The data for the k_C/k_H determination are shown graphically in Figure 2.5.

Table 2.3. GC results of the competition kinetic experiments for the 5-*exo* cyclisation of the 6,6-diphenyl-5-hexenyl radical (**25b**) at 24 ± 1 °C.[a],[b]

Solvent	[*t*-BuSH] M	1/[*t*-BuSH] M^{-1}	[26b-H]/[25b-H]
t-BuPh	0.100	10.0	45.08 ± 2.45
	0.120	8.3	41.22 ± 7.56
	0.140	7.1	32.28 ± 0.41
	0.175	5.7	27.78 ± 0.76
	0.18	5.6	23.66 ± 0.55
	0.210	4.7	19.87 ± 0.10
	0.245	4.1	20.33 ± 1.52
	0.280	3.5	18.80 ± 1.45
	0.315	3.2	15.42 ± 0.43
[EMIm][NTf_2]	0.100	10.0	31.53 ± 0.89
	0.120	8.3	27.37 ± 0.97
	0.140	7.1	26.96 ± 1.27
	0.160	6.3	22.58 ± 0.51
	0.180	5.6	20.02 ± 1.35
	0.200	5.0	19.92 ± 1.61

[a] Error represents deviation from the average of two experiments. [b] [**43b**] = 0.1[*t*-BuSH].

According to the equation ([**26b-H**] + [**44**])/[**25b-H**] = k_C/k_H × [*t*-BuSH]$^{-1}$, the product ratio versus of the inverse thiol concentration was plotted. The linearity of the data shown in Figure 2.5, provides confidence that the kinetic model shown in Scheme 2.14 is correct.

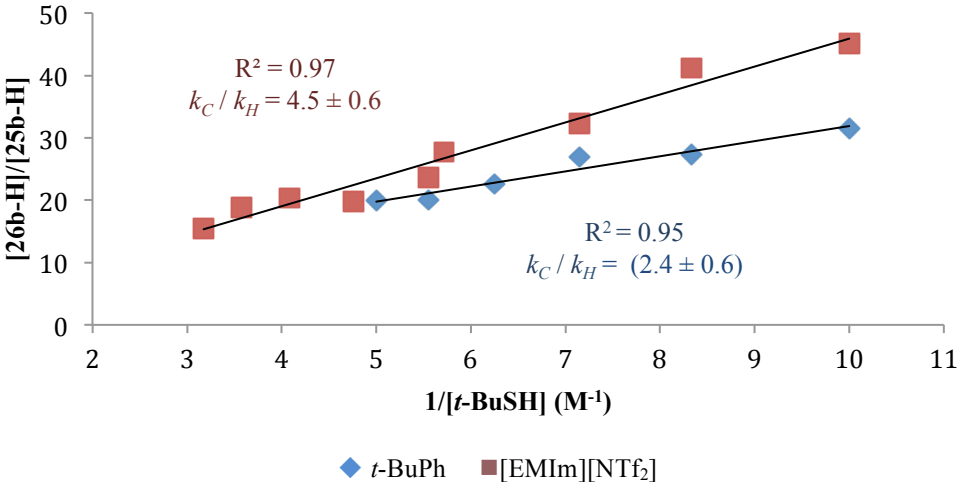


Figure 2.5. Dependence of [**26b-H**]/[**25b-H**] on *t*-BuSH concentration at 24 ± 1 °C for the cyclisation of the 6,6-diphenyl-5-hexenyl radical (**25b**). Uncertainties are calculated from the linear regression (2σ).

From the slope of the lines the ratio of the rate constant (k_C/k_H) is (4.5 ± 0.6) in *t*-BuPh and (2.4 ± 0.6) in [EMIm][NTf_2]. Using the value for k_C in [EMIm][NTf_2] determined from the direct kinetic measurement in this work of (10.0 ± 0.8) × 10^7 s^{-1}, k_H for HAT from *t*-BuSH to the primary alkyl radical is (4.2 ± 0.3) × 10^7 M^{-1} s^{-1}.

The measured k_H value of (1.0 ± 0.2) × 10^7 M^{-1} s^{-1} in *t*-BuPh (the value for k_C = (4.5 ± 0.1) × 10^7 s^{-1} taken from literature)[8] is in good agreement with the literature value in THF at 25 ± 1 °C, (8.0 ± 0.3)× 10^6 M^{-1} s^{-1}, which was calculated from the Arrhenius function log (k/$M^{-1}s^{-1}$) = (8.37 ± 0.08) - (2.00 ± 0.09) (Table 2.4).[3] Comparison of k_H obtained in [EMIm][NTf_2] and in THF reveals that the hydrogen atom transfer rate constant in [EMIm][NTf_2] is about four times higher than in the organic solvent.

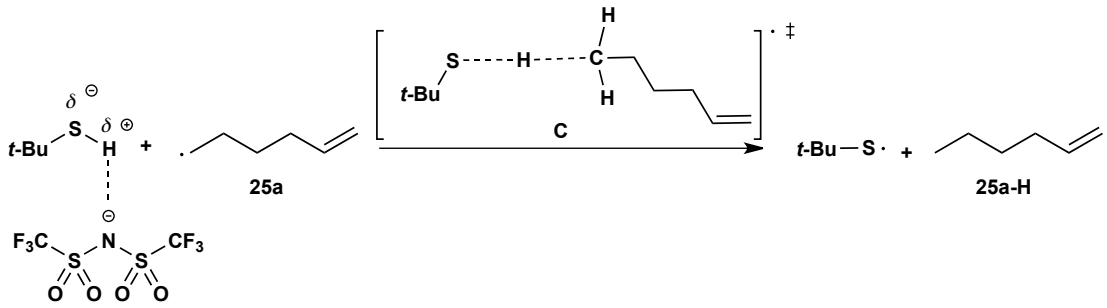
Table 2.4. Kinetic data for the 5-*exo* cyclisation of the 6,6-diphenyl 5-hexenyl radical **25b**.[a]

Solvent	k_C/k_H [b]	k_C (s^{-1}) $\times 10^7$	k_H ($M^{-1} s^{-1}$) $\times 10^7$
t-BuPh	4.5 ± 0.6	(4.5 ± 0.1) [c]	(1.0 ± 0.2)
[EMIm][NTf_2]	2.4 ± 0.6	(10.0 ± 0.8)	(4.2 ± 0.3)

[a] Errors are from the fit of the linear regression (2σ). [b] Determined from the slope of the line in Figure 2.5. [c] Taken from ref. [8].

The observed rate accelerating effect of the ionic liquid on the hydrogen transfer from the thiol to the hexenyl radical, compared to the aprotic organic solvent, could potentially be rationalised by an interplay between enthalpic and entropic effects.

Scheme 2.15 illustrates the proposition for the reduction of the hexenyl radical **25a** → **25a-H**, where hydrogen bonding between the positively polarised H in the thiol and the anion of the ionic liquid leads to stabilisation of the ground state. This H bonding is broken when moving to the transition state, which increases disorder. It is possible that the entropic benefit of the latter might outweigh the enthalpic cost associated with breaking the hydrogen bonding, which should lead to a faster hydrogen transfer in the ionic liquid.



Scheme 2.15. Proposed rationale of the higher rate coefficient for hydrogen rtransfer in IL. Hydrogen bonding between the thiol and the anion of [EMIm][NTf_2] stabilises the ground state. The enthalpic cost of breaking this H bond is outweighed by the entropic benefit resulting from a less ordered transition state, resulting in rate acceleration for hydrogen transfer in the ionic liquid.

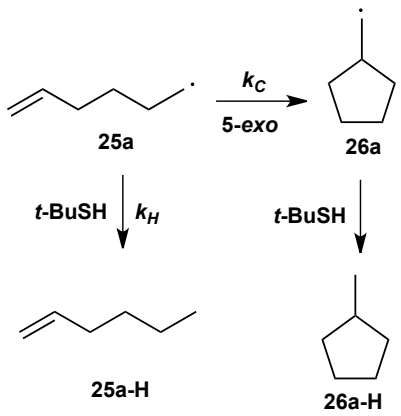
After having obtained rate data for the 5-*exo* cyclisation of the 6,6-diphenyl 5-hexenyl radical at 298 K, which also enabled determination of the rate constant for the reduction of this primary radical through hydrogen transfer from *t*-BuSH, it is now

possible to determine rate coefficients for the cyclisation of other 5-hexenyl radicals. The results will be described in the following.

2.4.2.1 5-Hexenyl radical cyclisation

Knowing the value of the rate constant for the hydrogen atom transfer from *t*-BuSH to primary alky radicals, the cyclisation rate constants of different primary alkyl radicals can be measured. The same experimental methodology of the competition kinetic studies described in the previous section, was used for this part of the study.

Photolysis of precursor **43a** in the presence of *t*-BuSH gave similar products in both *t*-BuPh and [EMIm][NTf_2]. The identity of the products was confirmed by comparison with authentic samples (Sigma Aldrich), and the ratio of the product concentration was determined by GC analysis of the reaction mixture from the relative peak areas (after extraction with *t*-BuPh (3X) in the case of the experiments performed in [EMIm][NTf_2]) (Scheme 2.16).



Scheme 2.16. Competition kinetic studies of the 5-*exo* cyclisation of the 5-hexenyl radical (**25a**) and reduction through hydrogen abstraction from *t*-BuSH.

The competition kinetic experiments were carried out in both solvents at 24 ± 1 °C employing a variety of thiol concentrations. The experimental data are listed in Table 2.5. The data for the k_C/k_H determination are shown graphically in Figure 2.6.

Table 2.5. GC results of the competition kinetic experiments for the 5-*exo* cyclisation of the 5-hexenyl radical (**25a**) at 24 ± 1 °C in *t*-BuPh and [EMIm][NTf_2].[a],[b]

Solvent	[*t*-BuSH] (M)	1/[*t*-BuSH] (M^{-1})	[26a-H]/[25a-H]
t-BuPh	0.200	5.0	0.21 ± 0.01
	0.100	10.0	0.37 ± 0.02
	0.050	20.0	0.71 ± 0.02
	0.040	25.0	0.74 ± 0.04
	0.030	33.3	0.87 ± 0.07
	0.015	66.6	1.57 ± 0.01
[EMIm][NTf_2]	0.200	5.0	0.12 ± 0.01
	0.120	8.3	0.21 ± 0.02
	0.080	12.5	0.27 ± 0.02
	0.050	20.0	0.39 ± 0.05
	0.045	22.2	0.45 ± 0.07
	0.040	25.0	0.48 ± 0.07
	0.035	28.6	0.54 ± 0.02

[a] Errors represent deviation from the average of three experiments. [b] [**43a**] = 0.1[*t*-BuSH].

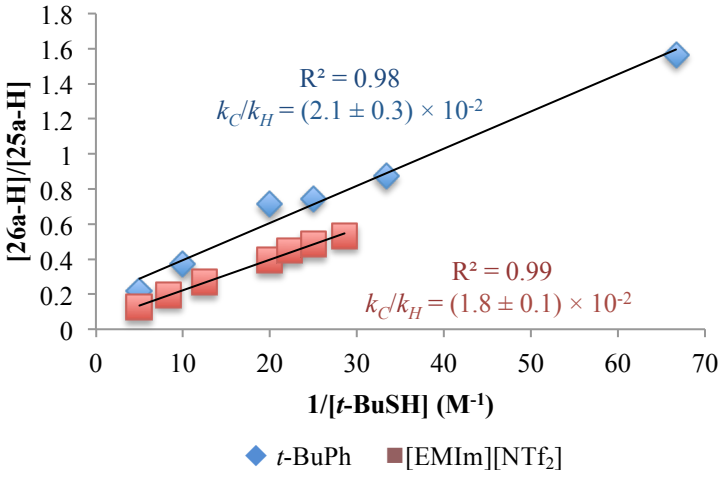


Figure 2.6. Dependence of [**26a-H**]/[**25a-H**] on *t*-BuSH concentration at 24 ± 1 °C for the cyclisation of the 5-hexenyl radical (**25a**). Uncertainties are calculated from the linear regression (2σ).

The data measured in *t*-BuPh are from the average of three experiments. The slope of the straight line provides the ratio of rate constants (k_C/k_H) as $(2.1 \pm 0.3) \times 10^{-2}$ in *t*-BuPh. Thus, using the literature rate coefficient for the reduction of primary C-centred radicals by *t*-BuSH of $k_H = (8.0 \pm 0.3) \times 10^6$ M^{-1} s^{-1} in THF,[3] k_C for the 5-*exo* cyclisation **25a** → **26a** can be calculated as $(1.7 \pm 0.2) \times 10^5$ s^{-1}. This value is sufficiently close to the reported value of k_C in organic solvents of $(2.2 \pm 0.1) \times 10^5$ s^{-1},[23] further supporting the above finding that the experimental methodology is correct. The small differences might be due to employing different solvents.

When the reaction of **25a** was performed in [EMIm][NTf_2], a slightly smaller k_C/k_H value of $(1.8 \pm 0.1) \times 10^{-2}$ was obtained. With the rate coefficient for the reduction of primary C-centred radicals by *t*-BuSH of $k_H = (4.2 \pm 0.3) \times 10^7$ M^{-1} s^{-1} obtained in [EMIm][NTf_2] in the previous section, the cyclisation rate coefficient is calculated to be $k_C = (7.5 \pm 0.1) \times 10^5$ s^{-1}, which is about four times faster in the ionic liquid than in conventional organic solvents.

Relative activation parameters for the 5-*exo* cyclisation and the radical reduction were determined by measuring k_C/k_H for the reaction of **25a** in [EMIm][NTf_2] over the temperature range of 23-70 °C.[24] According to the linear form of the Eyring equation, a plot of ln (k_C/k_H) versus 1/T should produce a straight line, providing $\Delta\Delta S^{\ddagger}$ (the activation entropy difference: $\Delta\Delta S^{\ddagger} = \Delta S_C^{\ddagger} - \Delta S_H^{\ddagger}$) from the intercept and $\Delta\Delta H^{\ddagger}$ (the

activation enthalpy difference: $\Delta\Delta H^{\ddagger} = \Delta H_C^{\ddagger} - \Delta H_H^{\ddagger}$) from the slope (more details are given in Appendix 2).

The values for $\Delta\Delta H^{\ddagger}$ and $\Delta\Delta S^{\ddagger}$ can be determined from kinetic data from ln (k_C/k_H) versus 1/T plot. The equation is a straight line with negative slope, - ($\Delta\Delta H^{\ddagger}$)/R and an intercept, $\Delta\Delta S^{\ddagger}$/R. (using R = 8.314 J K^{-1} mol^{-1}).

The kinetic data in [EMIm][NTf_2] are compiled in Table 2.6 and the plot to determine the Arrhenius parameter is shown graphically in Figure 2.7.

Table 2.6. GC results of the competition kinetic experiments for the 5-*exo* cyclisation of the 5-hexenyl radical **25a** at different temperatures in [EMIm][NTf_2].[a],[b]

T/^{o}C	[*t*-BuSH]/M^{-1}	[26a-H]/[25a-H]
23	0.1	0.27 ± 0.01
35	0.1	0.36 ± 0.02
40	0.1	0.45 ± 0.03
50	0.1	0.49 ± 0.02
60	0.1	0.61 ± 0.07
70	0.1	0.78 ± 0.14

[a] Errors represent deviation from the average of three experiments. [b] [**43a**] = 0.01 M.

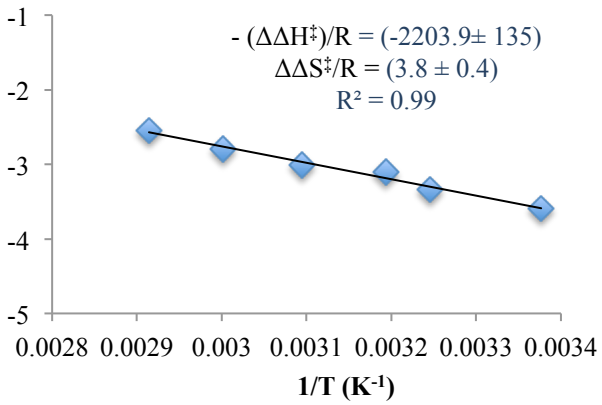


Figure 2.7. A plot of ln (k_C/k_H)) *vs*.1/T for the cyclisation of the 5-hexenyl radical (**25a**) and reduction through hydrogen abstraction from *t*-BuSH in [EMIm][NTf_2] (R = 8.314 J K^{-1} mol^{-1}). Uncertainties are calculated from the linear regression (2σ).

The values for $\Delta\Delta S^{\ddagger}$ of (32.0 ± 7.1) J mol^{-1} K^{-1} and $\Delta\Delta H^{\ddagger}$ of (18.3 ± 1.1) kJ mol^{-1} obtained in [EMIm][NTf_2] are within error similar to those in the conventional organic solvent (data taken from literature)[24,3], which are included in Table 2.7 for comparison. Since the kinetic measurements have shown that the cyclisation rate coefficient is higher in the ionic liquid, this finding suggests changes in the activation parameters of both hydrogen atom transfer and cyclisation processes that lead to small changes in the relative kinetic data.

Table 2.7. Kinetic rate data for the 5-*exo* cyclisation of the 5-hexenyl radical (**25a**).

Solvent	k_C/k_H[a],[b]	k_C (s^{-1})	$\Delta\Delta S^{\ddagger}$	$\Delta\Delta H^{\ddagger}$[a]
	× 10^{-2}	× 10^{5}	(J mol^{-1} K^{-1})	(kJ mol^{-1})
t-BuPh	2.1 ± 0.3	(1.7 ± 0.2) [c]	34.1 ± 1.4[f]	19.2 ± 0.3[f]
[EMIm][NTf_2]	1.8 ± 0.1	(7.5 ± 0.1) [d]	32.0 ± 7.1[a]	18.3 ± 1.1[a]

[a] Errors are from the fit of the linear regression (2σ). [b] Determined from the slope of the line in Figure 2.6, at 24 ± 1 °C. [c] Using k_H = (8.0 ± 0.3) × 10^6 M^{-1} s^{-1}; ref. [3]. [d] Using k_H = (4.1 ± 0.1) × 10^7 M^{-1} s^{-1} determined in this work. [f] Taken from refs. [25] and [3].

2.4.2.2 The role of electronic effects

Previous sections provide evidence that IL's have accelerating effects on both HAT and cyclisation of nucleophilic alkyl radicals. In order to expand the scope of synthetic radical reactions, electrophilic radicals will be studied in this section. Diester substituted systems **25c** and **25d** were chosen for this purpose, which are expected to undergo ring-closure with a faster rate constant compare to the unsubstituted "parent" system (due to the Thorpe-Ingold effect, where large substituents on the alkyl chain caused the intramolecular cyclisation reactions proceed faster).[25, 26] The presence of the two electron-withdrawing ester substituents on the alkyl chain of the radical **25c** should increase the electrophilicity of the radical compared to the unsubstituted hexenyl radicals **25a**. The electrophilicity should increase even more when the diester group moves adjacent to the radical centre in **25d**. Since ^{1}H NMR data of the radicals could not be obtained to confirm the proposition of increasing electrophilicity going from **25a** -> **25b** -> **25d**, the chemical shift of the future C-radical centre (C-6) in the ^{1}H NMR spectra of the radical precursors **43a**, **43c** and **43d** was used as a proxy (Figure 2.8). Thus, the signal of the protons at C-6 of compound **43a** appeared at 2.35 ppm; this signal slightly deshielded in compound **43c** at 2.56 ppm and considerably deshielded in compound **43d** at 3.47 ppm, clearly revealing the impact of the electron-withdrawing substituents at the adjacent C on the electron density at this atom. To our knowledge the kinetics of these two radicals has never been studied before.

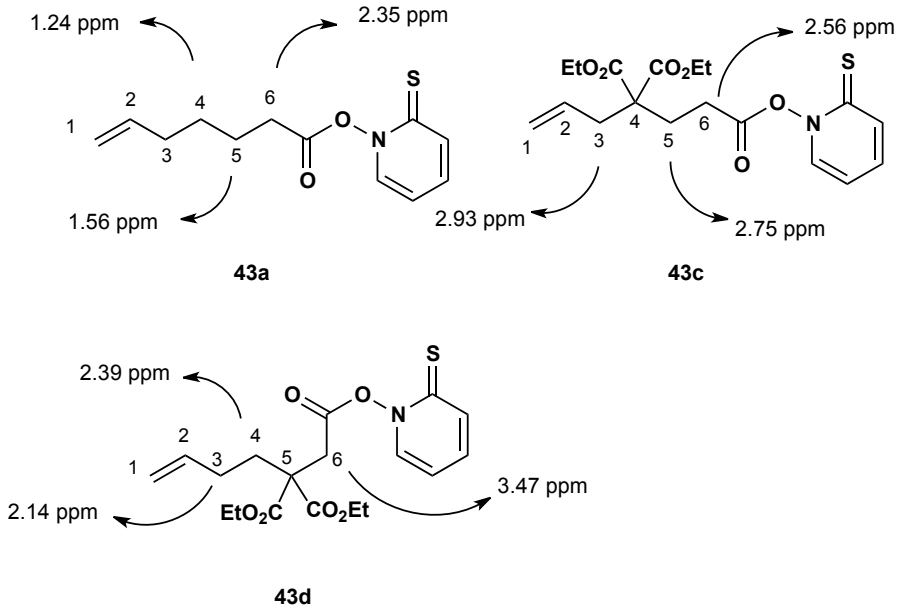
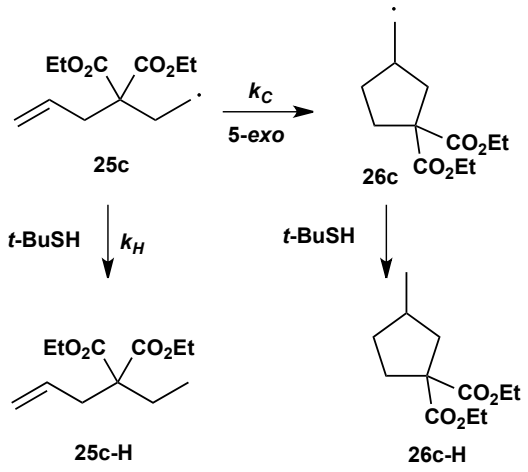


Figure 2.8. Structures and chemical shifts of compound **43a**, **43c** and **43d**.

2.4.2.2.1 Reaction of the 3,3-diester substituted 5-hexenyl radical 25c

Following the method described above, competition studies with the diester substituted radical **25c** were carried out in both [EMIm][NTf_2] and *t*-BuPh (Scheme 2.17). Compounds **25c-H** and **26c-H** were prepared as a GC standard as described in section 2.2.1. Because of the higher polarity of the reaction products, the reaction mixture in [EMIm][NTf_2] was diluted with ethyl acetate and extracted with diethylether (3X), followed by GC analysis, as described in section 2.3.



Scheme 2.17. Competition kinetic studies of the 5-*exo* cyclisation of the radical **25c** and reduction through hydrogen abstraction from *t*-BuSH.

The ratio of rate constants (k_C/k_H) was determined in *t*-BuPh and IL employing various concentrations of *t*-BuSH at 24 ± 1 °C. The experimental data are reported in Table 2.8. The data for the k_C/k_H determination are shown graphically in Figure 2.9.

Table 2.8. GC results of the competition kinetic experiments for the 5-*exo* cyclisation of the 5-hexenyl radical **25c** at 24 ± 1 °C.[a],[b]

Solvent	[*t*-BuSH] (M)	1/[*t*-BuSH] (M^{-1})	[26c-H]/[25c-H]
t-BuPh	0.2	5	15.1 ± 0.2
	0.16	6.3	19.3 ± 0.4
	0.14	7.1	21.9 ± 0.4
	0.12	8.3	28.4 ± 0.4
	0.08	12.5	51.0 ± 3.3
[EMIm][NTf_2]	0.2	5	8.1 ± 0.3
	0.18	5.5	10.2 ± 0.9
	0.16	6.3	10.5 ± 0.6
	0.14	7.1	12.2 ± 0.1
	0.12	8.3	13.9 ± 0.1

[a] Errors represent deviation from the average of three experiments; errors are [b] [**43c**] = 0.1[*t*-BuSH].

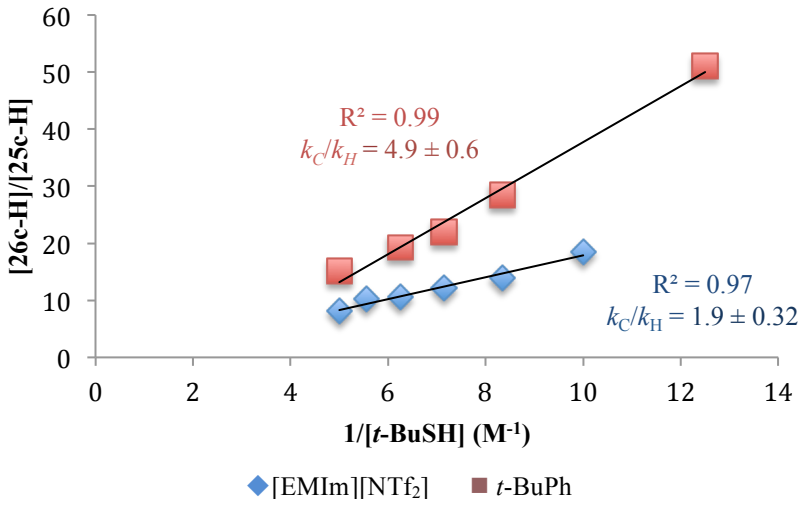
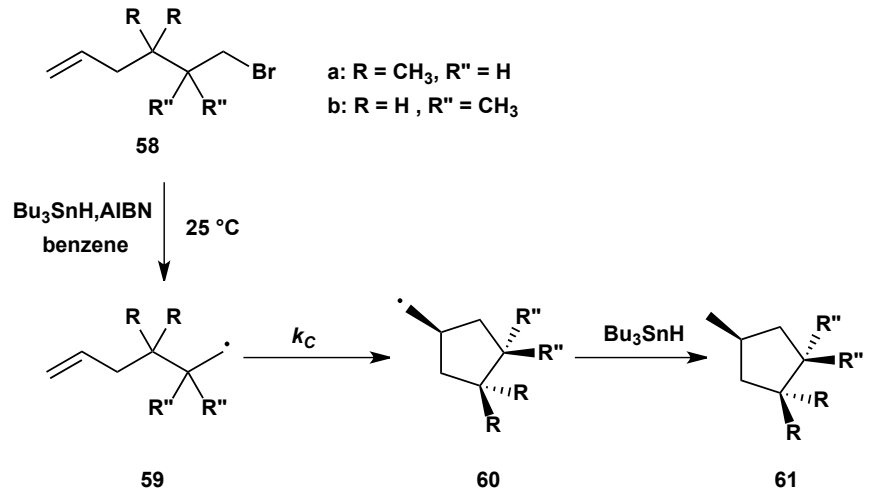


Figure 2.9. Dependence of [**26c-H**]/[**25c-H**] on *t*-BuSH concentration at 24±1 °C for the cyclisation of the 5-hexenyl **25c** radical and reduction through hydrogen abstraction from *t*-BuSH. Uncertainties are calculated from the linear regression (2σ).

From the k_C/k_H value of (4.9 ± 0.6) obtained for the reaction of the 3,3-diester substituted radical **25c** in *t*-BuPh, the 5-*exo* cyclisation rate coefficient of k_C = (3.9 ± 0.5) × 10^7 s^{-1} is calculated, which is about two orders of magnitude faster than for the unsubstituted radical **25a**.

The 5-*exo*-cyclisation rate constants of the dimethyl substituted 5-hexenyl radicals **59a** and **59b** in benzene at 25 °C is reported in previous work as k_C = (5.2 × 10^6 s^{-1}) and k_C = (3.6 × 10^6 s^{-1}) respectively (Scheme 2.18),[7] indicating that radicals **59a** and **59b** cyclised faster than the unsubstituted radical **25a** (due to the Thorpe-Ingold effect). However, the cyclisation reactions of radicals **59a** and **59b** proceed by one order of magnitude slower than radical **25c**, suggesting that, for the cyclisation of the radical **25c**, in addition to the rate accelerating Thorpe-Ingold effect due to the geminal diester substituents, the electrophilic nature of the radical centre further increases the cyclisation rate by one order of magnitude.



Scheme 2.18. Cyclisation of radicals **59a** and **59b**.[7]

In [EMIm][NTf_2] a k_C/k_H value of (1.9 ± 0.3) was obtained, leading to a rate coefficient for the 5-*exo* cyclisation of **25c** of k_C = (7.8 ± 0.2) × 10^7 s^{-1} in [EMIm][NTf_2], which is about two times faster than in *t*-BuPh (Table 2.10).

Further insight into the factors affecting the rate of the cyclisation can be deduced from the data obtained through temperature dependent studies, which are presented in

Table 2.9. The experimental data for the activation parameters determination are shown graphically in Figure 2.10.

Table 2.9. GC results of the competition kinetic experiments for the 5-*exo* cyclisation of the 5-hexenyl radical **25c** at different temperature.[a],[b]

Solvent	**T/^{o}C**	**[*t*-BuSH] (M)**	**[26c-H]/[25c-H]**
t-BuPh	25	0.12	28.4 ± 0.4
	35	0.12	28.9 ± 0.1
	45	0.12	31.2 ± 0.3
	55	0.12	41.2 ± 1.4
	65	0.12	42.6 ± 0.9
	75	012	49.5 ± 1.2
[EMIm][NTf_2]	25	0.12	13.9 ± 0.1
	35	0.12	26.3 ± 0.1
	45	0.12	30.4 ± 2.2
	55	0.12	41.2 ± 5.0
	65	0.12	63.3 ± 3.1

[a] Error represents deviation from the average of three experiments; errors are 2σ. [b] [**43c**] = 0.012 M.

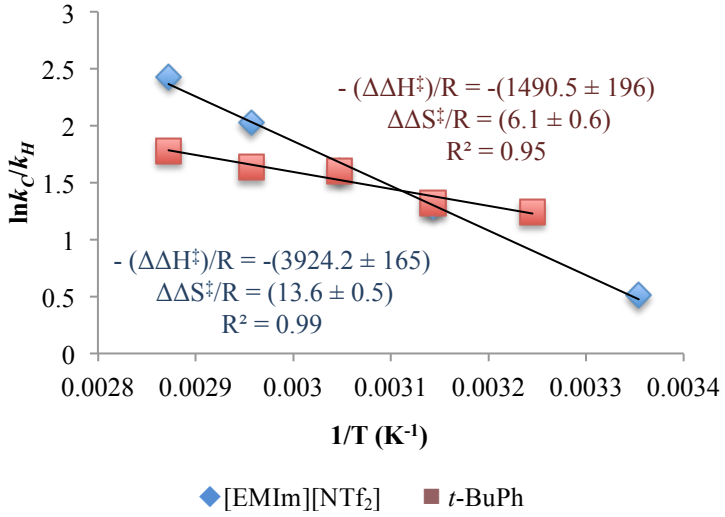


Figure 2.10. (ln (k_C/k_H)) *vs*.1/T for the ring closure of the 5-hexenyl radical **25c** and reduction through hydrogen abstraction from *t*-BuSH (R = 8.314 J K^{-1} mol^{-1}). Uncertainties are calculated from the linear regression (2σ).

From slope of the line $\Delta\Delta H_C^{\ddagger}$ could be calculated as (12.4 ± 3.3) kJ mol^{-1} in *t*-BuPh and (32.6 ± 2.8) kJ mol^{-1} in [EMIm][NTf_2] and $\Delta\Delta S^{\ddagger}$ from the intercept calculated as (50.4 ± 9.7) J mol^{-1} K^{-1} in *t*-BuPh and (113.4 ± 8.5) J mol^{-1} K^{-1} in [EMIm][NTf_2] (Table 2.10).

Table 2.10. Kinetic rate data for the 5-*exo* cyclisation of the 3,3-diester-5-hexenyl radical**.**

Solvent	k_C/k_H [a],[b]	k_C (s^{-1}) × 10^7	$\Delta\Delta S^{\ddagger}$ [a] (J mol^{-1} K^{-1})	$\Delta\Delta H^{\ddagger}$ [a] (kJ mol^{-1})
t-BuPh	4.9 ± 0.6	(3.9 ± 0.48) [c]	50.4 ± 9.7	12.4 ± 3.3
[EMIm][NTf_2]	1.9 ± 0.32	(7.9 ± 0.24) [d]	113.4 ± 8.5	32.6 ± 2.8

[a] Errors are from the fit of the linear regression (2σ).[b] Determined from the slope of the line in Figure 2.9, at 24 ± 1 °C. [c] Using k_H = (8.0 ± 0.3) × 10^6 M^{-1} s^{-1}; ref. [3]. [d] Using k_H = (4.1 ± 0.1) × 10^7 M^{-1} s^{-1} determined in this work.

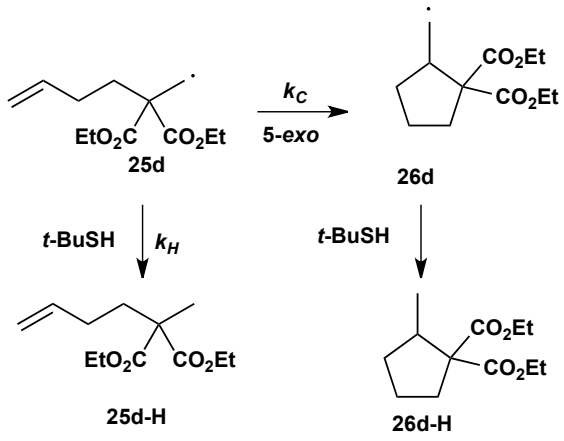
In *t*-BuPh, the $\Delta\Delta S^{\ddagger}$ values for the reaction of the diester substituted radical **25c** are considerably more positive (113.4 ± 8.5) J mol^{-1} K^{-1} compared to the unsubstituted radical **25a** (34.1 ± 1.4) J mol^{-1} K^{-1} (data for the latter are shown in Table 2.7). Under the reasonable assumption that $\Delta S_H^{\ddagger}$ and $\Delta H_H^{\ddagger}$ in the respective solvents are approximately the same for the alkyl radicals studied in this work,[23a] this finding

indicates a less negative $\Delta S_C^{\ddagger}$ for the cyclisation of **25c**, compared with **25a**. This suggests earlier, less organised transition states for **25c**, in line with the higher cyclisation rate of this radical due to the electrophilicity of the radical and the Thorpe-Ingold effect.[26] $\Delta\Delta S^{\ddagger}$ is even more positive in [EMIm][NTf_2] for **25c** (113.4 ± 8.5) J mol^{-1} K^{-1}, clearly suggesting that the favourable entropy term $\Delta S_C^{\ddagger}$ is mainly responsible for cyclisation rate enhancement of these radicals, compared with the unsubstituted radical **25a**, where the small positive $\Delta S_C^{\ddagger}$ value is indicative for a more ordered, later transition state.

The $\Delta\Delta H^{\ddagger}$ value for the reaction of the substituted radical **25c** in *t*-BuPh (12.4 ± 3.3) kJ mol^{-1} is similar to the values of radical **25a (**19.2 ± 0.3) kJ mol^{-1}. However, this value is larger in [EMIm][NTf_2] (32.6 ± 2.8) kJ mol^{-1}, indicating a more positive $\Delta H^{\ddagger}_C$ for **25c** in [EMIm][NTf_2] compared with in *t*-BuPh. In total, it appears that the entropic benefit outweighs the enthalpic cost, which leads to lower the energy of the transition state, leading to an overall rate enhancement for the 5-*exo* cyclisation of **25c** in [EMIm][NTf_2] compared with in *t*-BuPh.

2.4.2.2.2 Reaction of the 2,2-diester substituted 5-hexenyl radical 25d

Radical **25d** was generated from precursor **43d** as described in section 2.2.1 (Scheme 2.19).



Scheme 2.19. Competition kinetic studies of the 5-*exo* cyclisation of the radical **25d** and reduction through hydrogen abstraction from *t*-BuSH.

k_C/k_H was determined using concentrations of *t*-BuSH ranging from 0.1-0.2 M (consistent with other experimental conditions) at 24 ± 1 °C. Unfortunately, under

such conditions it was impossible to obtain a straight line in the plot due to high cyclisation rate of **25d,** resulting in a large signal of the cyclised compound **26d-H** in the GC, compared to only small amounts of the reduced radical **25d-H**, which caused scattered data points with larger errors. Therefore, the experiments were performed at higher concentrations of *t*-BuSH (0.4-0.8 M) to promote radical reduction and to reduce the error of the competition kinetic experiments. The results are listed in Table 2.11. The data for the k_C/k_H determination are shown graphically in Figure 2.11.

Table 2.11. GC results of the competition kinetic experiments for the 5-*exo* cyclisation of the 5-hexenyl radical **25d** at 24 ± 1 °C.[a],[b]

Solvent	**[*t*-BuSH] (M)**	**1/[*t*-BuSH] (M^{-1})**	**[26d-H]/[25d-H]**
t-BuPh	0.8	1.25	14.0 ± 0.3
	0.72	1.39	15.4 ± 1.0
	0.64	1.60	17.0 ± 0.5
	0.56	1.79	19.6 ± 0.7
	0.48	2.08	25.2 ± 0.9
	0.4	2.5	29.7 ± 1.2
[EMIm][NTf_2]	0.8	1.25	22.6 ± 1.4
	0.72	1.39	23.3 ± 0.7
	0.64	1.60	27.9 ± 3.7
	0.56	1.79	30.9 ± 4.2
	0.48	2.08	38.3 ± 1.6
	0.4	2.5	45.3 ± 1.9

[a] Errors represent deviation from the average of three experiments. [b] [**43d**] = 0.1[*t*-BuSH].

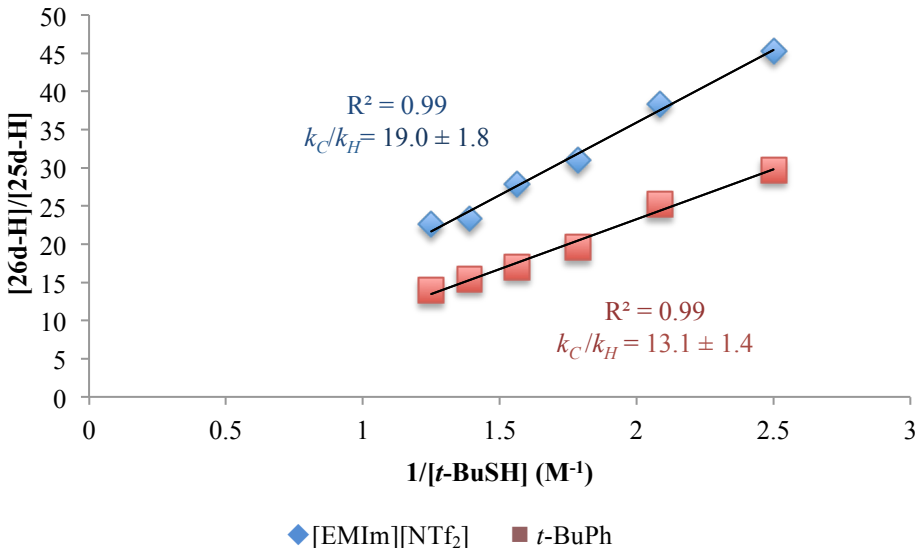
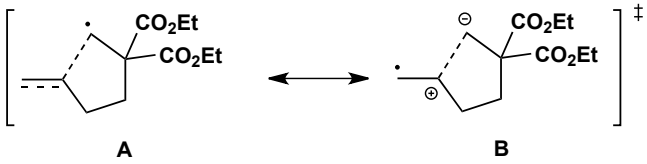


Figure 2.11. Dependence of [**26d-H**]/[**25d-H**] on *t*-BuSH concentration at 24 ± 1 °C for the cyclisation of the 5-hexenyl radical **25d**. Uncertainties are calculated from the linear regression (2σ).

With k_C/k_H ratios of (13.1 ± 1.3) obtained in *t*-BuPh and of (19.0 ± 1.8) in [EMIm][NTf$_2$], values for k_C of (1.0 ± 0.1) × 10^8 s^{-1} in *t*-BuPh and (7.9 ± 0.2) × 10^8 s^{-1} in [EMIm][NTf$_2$], respectively, can be calculated under the reasonable assumption that k_H for **25d** → **26d-H** should be similar as for the other primary alkyl radicals in the respective solvent.[27] These data indicate that by moving the diester group adjacent to the radical centre in radical **25d** to increase its electrophilicity, the cyclisation rate further increases by one order of magnitude. This finding could be rationalised by the structure of the transition state, which can be described by the canonical forms **A** and **B** (Scheme 2.19), where **B** is characterised by charge transfer from the alkene to the electrophilic radical centre. This additional stabilisation of the transition state, compared to those for the nucleophilic radical **25a**, **59a**, **59b** and less electrophilic radical **25c** leads to an increased cyclisation rate of this radical in the organic solvent.



Scheme 2.19. Canonical forms of the transition state for the 5-*exo* cyclisation of the electrophilic 5-hexenyl radical **25d**.

The particularly rapid 5-*exo* cyclisation of **25d** in [EMIm][NTf_2], which is about one order of magnitude faster than **25c** and eight times faster than in the conventional organic solvent, suggests additional stabilising effects by the ionic liquid.

It should be noted that in the case of **25d** the reaction temperature could not be increased beyond 50 °C due to the fast cyclisation of this radical, which made GC determination of k_C/k_H by GC very difficult at temperatures higher than room temperature, leading to the large error of the relative activation parameters. The experimental results from the competition kinetic studies for the 5-hexenyl radicals **25d** are compiled in Table 2.12.

Table 2.12. Kinetic rate data for the 5-*exo* cyclisation of the 2,2-diester-5-hexenyl radical **25d**.[a]

Solvent	k_C/k_H [a],[b]	k_C (s^{-1}) $\times 10^8$	$\Delta\Delta S^{\ddagger}$ [a] (J mol^{-1} K^{-1})	$\Delta\Delta H^{\ddagger}$ [a] (kJ mol^{-1})
t-BuPh	13.1 ± 1.4	(1.0 ± 0.1) [c]	nd.	nd.
[EMIm][NTf_2]	19.0 ± 1.8	(7.9 ± 0.2) [d]	nd.	nd.

[a] Errors are from the fit of the linear regression (2σ). [b] Determined from the slope of the line in Figure 2.11, at 24 ± 1 °C. [c] Using $k_H = (8.0 \pm 0.3) \times 10^6$ M^{-1} s^{-1}; ref. [3]. [d] Using $k_H = (4.1 \pm 0.1) \times 10^7$ M^{-1} s^{-1} determined in this work.

2.5 Recyclability

The reaction involving radical precursor **43a** was also used to explore the recyclability of [EMIm][NTf_2] as solvent for radical chemistry. After consumption of the precursor was complete (using reaction conditions and times similar to those of the kinetic studies), the products were extracted with *t*-BuPh and the ionic liquid solvent was reused directly without further purification. Using 1-heptene as internal standard for the quantitative GC analysis (due to its chemical similarity with the reaction products) revealed a combined yield of 84% for **25a-H** and **26a-H** after the first cycle. The yield slightly dropped to 78% in the second cycle and to 74% in the third cycle, which demonstrates that ILs can be reused several times in radical reactions without significant loss of efficiency. However, we observed that the color of the solvent turned to pale yellow after the first cycle, which is likely due to the

accumulation of polar by-products (*e.g.*, pyridyl sulfides resulting from the PTOC precursor, see Scheme 2.1) that cannot be extracted from the [EMIm][NTf_2] phase, but since the outcome after 3 reaction cycles was still good, analysis of potential degradation of the IL was not performed. It cannot be excluded that the presence of these by-products might prevent quantitative extraction of the reaction products, which could explain the slight drop in yield with increasing recirculation of the solvent.

2.6 Summary

In this chapter it was demonstrated that ionic liquids can be successfully used in intramolecular homolytic additions of primary alkyl radicals. Laser flash photolysis studies were performed to reveal the absolute rate coefficient for the 5-*exo* radical cyclisation of the diphenyl substituted primary alkyl radical **25b** in [EMIm][NTf_2] of $k_C = (10.0 \pm 0.8) \times 10^7$ s^{-1}. This value was used in PTOC-thiol competition kinetic studies to determine the rate coefficient for the hydrogen abstraction from *t*-BuSH by primary alkyl radicals of $k_H = (4.1 \pm 0.1) \times 10^7$ M^{-1} s^{-1} in [EMIm][NTf_2], which is about five times higher than in conventional organic solvents. This finding could be rationalised by a hydrogen bond between the thiol and the anion of the ionic liquid in the ground state. The enthalpic cost associated with breaking the hydrogen bond upon progression to the transition state is outweighed by the entropic benefit caused by the increase in disorder, resulting in an overall increase of the hydrogen transfer rate. Through competition kinetic studies k_C was determined for the 5-*exo* cyclisations of the primary alkyl radicals **25a, 25c** and **25d**. Overall, these processes proceed faster by up to one order of magnitude in the ionic liquid than in organic solvents. From the Arrhenius parameters it appears that the rate accelerating effect is due to a favorable $\Delta S^{\ddagger}_C$ term for all radicals, which can be rationalised by earlier, less-organised transition states of the radical cyclisation. The particularly fast cyclisation rate of **25d**, which is the most electrophilic radical in this study, suggests additional stabilisation of the transition state through interaction with the ionic liquid.

No interfering reactions between [EMIm][NTf_2] and radical intermediates were observed. All products were quantitatively extracted from the ionic liquid phase, which can be reused without purification for several cycles.

2.7 References

[1] Newcomb, M.; Glenn, A. G.; Manek, M. B., *J. Org. Chem.* **1989**, *54*, 4603.

[2] (a) Bulter, B.J.; Harper, J. B., *New J. Chem.* **2015**, *39*, 213. (b) Man, B. Y. W.; Hook, J. M.; Harper, J. B., *Tetrahedron lett*., **2005**, *46*, 7641.

[3] (a) Shkrob, I. A.; Wishard, J. F., *Encyclopedia of Radicals in Chemistry, Biology and Materials*, John Wiley & Sons, Ltd., **2012**. (b) Andrikopoulos, B.; Sidhu, P. K.; Taggert, B. I.; Nathanael, J. G.; O′Hair, R. A. J.; Wille, U., *ChemPlusChem*, **2020**, 85, 195.

[4] Frisch, M. J.; Trucks, G. W.; Schlegel, H. B.; Scuseria, G. E.; Robb, M. A; Cheeseman, J. R.; Scalmani, G.; Barone, V.; Mennucci, B.; Petersson, G. A.; Nakatsuji, H.; Caricato, M.; Li, X.; Hratchian, H. P.; Izmaylov, A. F.; Bloino, J.; Zheng, G.; Sonnenberg, J. L.; Hada, M.; Ehara, M.; Toyota, K.; Fukuda, R.; Hasegawa, J.; Ishida, M.; Nakajima, T.; Honda, Y.; Kitao, O.; Nakai, H.; Vreven, T.; Montgomery, J. A.; Jr.; Peralta, J. E.; Ogliaro, F.; Bearpark, M.; Heyd, J. J.; Brothers, E.; Kudin, K. N.; Staroverov, V. N.; Keith, T.; Kobayashi, R.; Normand, J.; Raghavachari, K.; Rendell, A.; Burant, J. C.; Iyengar, S. S.; Tomasi, J.; Cossi, M.; Rega, N.; Millam, J. M.; Klene, M.; Knox, J. E.; Cross, F. B.; Bakken, V.; Adamo, C.; Jaramillo, J.; Gomperts, R.; Stratmann, R. E.; Yazyev, O.; Austin, A. J.; Cammi, R.; Pomelli, C.; Ochterski, J. W.; Martin, R. L.; Morokuma, K.; Zakrzewski, V. G.; Voth, G. A.; Salvador, P.; Dannenberg, J. J.; Dapprich, S.; Daniels, A. D.; Farkas, O.; Foresman, J. B.; Ortiz, J. V.; Cioslowski, J.; Fox, D. J.; *Gaussian 09*, Revision B.01, Gaussian, Inc., Wallingford CT, **2010**.

[5] Salomon, R. G.; Coughlin, D. J.; Ghosh, S.; Zagorski, M. G., *J. Am. Chem. Soc.* **1982,** *104*, 998.

[6] Bailey, W. F.; Nurmi, T. T.; Patricia, J. J.; Wang, W., *Am. Chem. Soc.* **1987,** *109*, 2442.

[7] Crich, D.; Jiao, X.-Y.; Yao, Q.; Harwood, J. S., *J. Org. Chem.* **1996**, *61*, 2368.

[8] Deroose, F. D.; De Clercq, P. J. D., *J. Org. Chem.* **1995**, *60*, 321.

[9] Ha, C.; Horner, J. H.; Newcomb, M.; Varick, T. R.; Arnold, B. R.; Lusztyk, J., *J. Org. Chem.* **1993**, *58*, 1194.

[10] (a) Barton, D. H. R.; Crich, D.; Mother ll, W. B., *J. Chem. Soc., Chem. Commun.* **1983**, *17*, 939. (b) Benjamin, L. J.; Schiesser, C. H.; Sutej, K., *Tetrahedron* **1993**, *49*, 2557.

[11] Lébl, T.; Zoufalá, P.; Bruhn, C., *Eur. J. Inorg. Chem.* **2005**, *2005*, *12*, 2536.

[12] Qi, W.; Wang, P.; Fan, L.; Zhang, S., *J. Org. Chem.* **2013**, *78*, 5918.

[13] Kyne, S. H.; Lévêque, C.; Zheng, S.; Fensterbank, L.; Jutand, A.; Ollivier, C., *Tetrahedron* **2016**, *72*, 7727.

[14] Blanchard, L. A.; Brennecke, J. F., *Ind. Eng. Chem. Res.* **2001**, *40*, 287.

[15] Huddleston, J. G.; Willauer, H. D.; Swatloski, R. P.; Visser, A. E.; Rogers, R. D., *Chem. Commun.* **1998**, *16*, 1765.

[16] Jessop, P. G.; Ikariya, T.; Noyori, R., *Chem. Rev.* **1999**, *99*, 475.

[17] Zhang, W., *Chem. Rev.* **2004**, *104*, 2531.

[18] Chrobok, A., *Tetrahedron* **2010**, *66*, 2940.

[19] Candeias, N. R.; Branco, L. C.; P.Gois, P. M.; Afonso, C. A. M.; Trindade, A. F., *Chem. Rev.* **2009**, *109*, 2703.

[20] Gordon, C. M.; McCluskey, A., *Chem. Commun.* **1999**, *15*, 1431.

[21] Bohne, C.; Boch, R.; Scaiano, J. C., *J. Org. Chem.* **1990**, *55*, 5414.

[22] Newcomb, M., *Tetrahedron* **1993**, *49*, 1151.

[23] Selected examples: a) Beckwith, A. L. J.; Moad, G., *J. Chem. Soc., Chem. Commun.* **1974**, 472; b) Walling, C.; Cioffari, A., *J. Am. Chem. Soc.* **1972**, *94*, 6059; c) Schmid, P.; Griller, D.; Ingold, K. U., *Int. J. Chem. Kinet.* **1979**, *11*, 333; d) Beckwith, A. L. J.; Blair, I.; Phillipou, G., *J. Am. Chem. Soc.* **1974**, *96*, 1613; e) Beckwith, A. L. J.; Cliff, M. D.; Schiesser, C.H., *Tetrahedron* **1992**, *48*, 4641; f) Tripp, J. C.; Schiesser, C. H.; Curran, D. P., *J. Am. Chem. Soc.* **2005**, *127*, 5518; g) Beckwith, A. L. J.; Schiesser, C. H., *Org. Biomol. Chem.* **2011**, *9*, 1736; h) Beckwith, A. L. J.; Schiesser, C. H., *Tetrahedron* **1985**, *41*, 3925; i) M. Julia, *Acc. Chem. Res*. 1971, *4*, 386.

[24] Chatgilialoglu, C.; Ingold, K. U.; Scaiano, J. C., *J. Am. Chem. Soc.* **1981**, *103*, 7739.

[25] a) Beckwith, A. L. J.; Lawrence, T., *J. Chem. Soc., Perkin Trans. 2* **1979**, 1535; b) Beckwtih, A. L. J.; Lawrence, T.; Serelis, A. K., *J. Chem. Soc., Chem. Commun*. **1980**, 484.

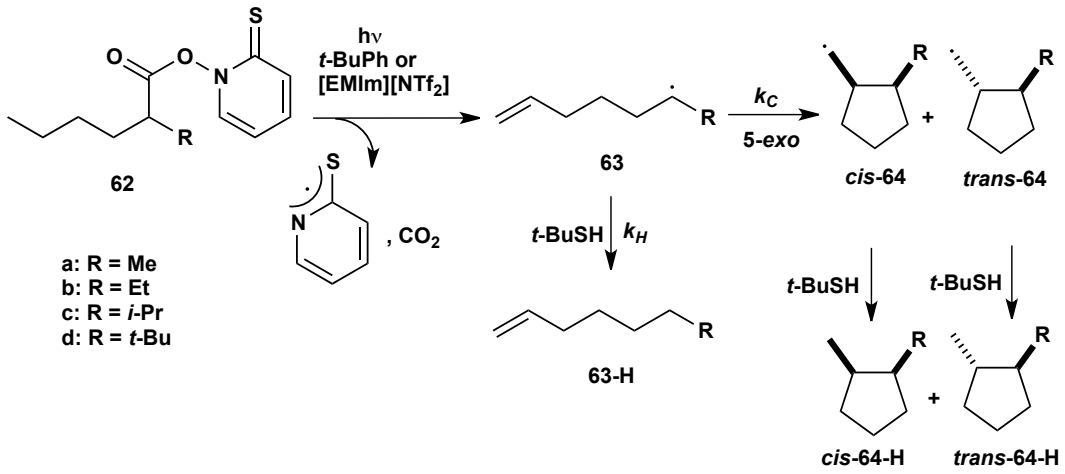
[26] a) Jung, M. E., *Synlett* **1999**, 843; b) Jung, M. E.; Piizzi, G., *Chem. Rev*. **2005**, *105*, 1735; c) Eliel, E. L.; Allinger, N. L.; Angyal, S. J.; Morrison, G. A., Wiley, New York, **1965**, 165.

[27] In the absence of available rate data for reductions by thiols, this assumption is made on the basis of similar rate coefficients obtained for the reduction of primary alkyl radicals and the more nucleophilic α-carbethoxy radicals by tin hydrides in organic solvents; see ref. [24a] and Newcomb, M.; Horner, J. H.; Filipkowksi, M. A.; Ha, C.; Park, S.-U., *J. Am. Chem. Soc*. **1995**, *117*, 3674.

3 Cyclisation of secondary 5-hexenyl radicals

Many examples have shown that cyclisations of substituted alkenyl radicals are an excellent method to prepare complex molecular frameworks with high regio- and stereoselectivity under usually mild conditions.[1-7] However, it is complicated to determine the factors controlling the stereochemical outcome of these reactions. Beckwith proposed a guideline, as described in Chapter 1, suggesting that cyclisation of C-1 substituted 5-hexenyl radicals is predominantly *cis*-selective.[8,9]

In order to explore the role of steric effects on the rate and stereoselectivity of the 5-*exo* radical cyclisation in ionic liquids, the reactions of the C-1 substituted 5-hexenyl radicals **63a–d** will be studied in this chapter (Scheme 3.1). Also, solvent-effect data for radical **63d** published in previous work,[10] showing that stereoselectivity of the cyclised product is sensitive to solvent polarity (described in Chapter 1), open up the possibility to explore the effects of ILs on the stereochemical outcome of the C-1 substituted 5-hexenyl radicals.

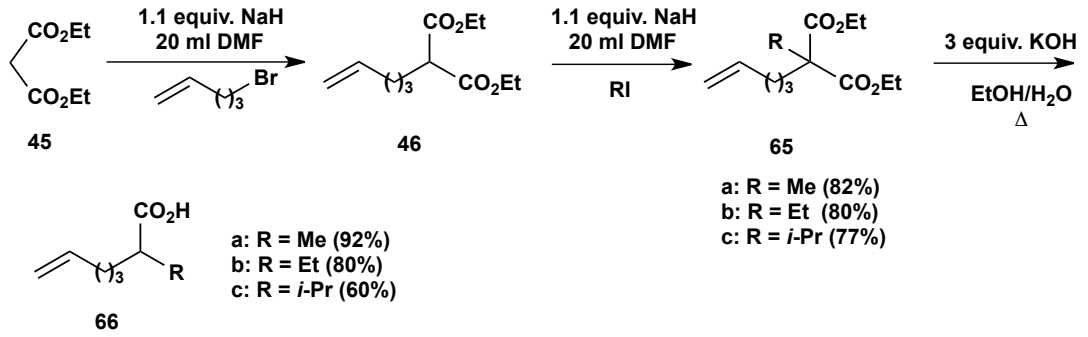


Scheme 3.1. Generation of the 5-hexenyl radicals **63** and competing reactions through reduction to **63-H** and 5-*exo* cyclisation to *cis*-**64** and *trans*-**64**.

3.1 Synthesis of the radical precursors 62a-d and reference compounds

This section describes the synthesis of the radical precursors **62a-d** employed in this chapter and of the authentic samples, which were required to identify the product peaks in the gas chromatograms. All PTOC esters **62a-d** were obtained by reacting the respective carboxylic acids **62a-d** with *N*-hydroxypyridine-2-thione (**53**).

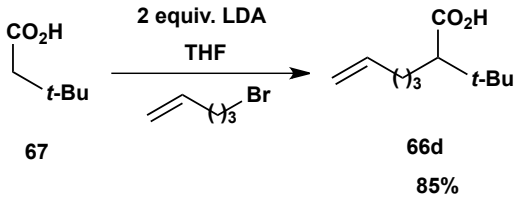
Scheme 3.2 shows the synthesis of the first three carboxylic acids **66a-c**. A procedure similar to that used in the preparation of 6-heptenoic acid (**66a**), which was described in Section 2.2.1, was followed and extended by an additional alkylation step. Diethyl ester **46** was alkylated with alkyl iodide in anhydrous DMF, using sodium hydride as the base. The alkyl substituted diesters **65a-c** were obtained in 82%, 80% and 77% yield, respectively, after column chromatography. Subsequent saponification and decarboxylation provided the α-alkylated 6-heptenoic acids **66a-c** in 92%, 80% and 60% yield, respectively. The identity of the compounds was confirmed by ^{1}H NMR spectroscopy, which showed a doublet of the methyl protons at 1.2 ppm in **66a**, a triplet and multiplet of ethyl protons attached to C-2 in **66b** at 0.94 and 1.55 ppm, a doublet of methyl protons at 0.97 ppm and a multiplet of CH of the isopropyl group in **66c** at 1.9 ppm, with other signals matching those of 6-heptenoic acid **47a**.[11]



Scheme 3.2. Synthesis of the carboxylic acids **66a-c**.

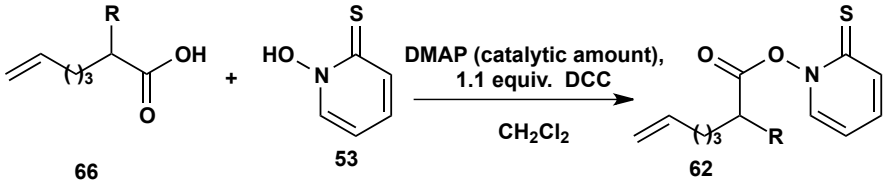
The *t*-butyl-substituted carboxylic acid **66d** was synthesised in 85% yield according to literature[12] by treating the *t*-butylacetic acid (**67**) with freshly prepared LDA in THF, followed by addition of 5-bromopentene (Scheme 3.3). The ^{1}H NMR spectrum

included a singlet of 9 chemically equivalent methyl protons attached to the quaternary carbon at 0.99 ppm. HRMS of the acid **66d** resulted in a peak at *m*/*z* 185.1537 [M + H^+], which is consistent with the molecular formula of $C_{11}H_{19}O_2$.



Scheme 3.3. Synthesis of the carboxylic acid **66d**.

Coupling of the acids **66a-d** to provide PTOC esters **66a-d** was achieved following the literature procedure.[13] Treatment of **66a-d** with 0.95 equivalents of *N*-hydroxypyridine-2-thione **53** was performed under exclusion of light (in an aluminium-foil-covered reaction flask) in the presence of catalytic amounts of dimethylaminopyridine (DMAP) and 1.1 equivalents of dicyclohexylcarbodiimide (DCC) in dichloromethane. Purification by column chromatography gave the PTOC esters **62a** (69%), **62b** (64%), **62c** (90%) and **62d** (63%). ^{1}H NMR data analysis in C_6D_6 showed the four aromatic hydrogen atoms at 5.4, 6.0, 6.4 and 7.4 ppm, with the rest of the spectra being similar to those of the corresponding acids **66a-d**. The HRMS data of **60a-d** confirmed the molecular formula in all cases (Scheme 3.4).



Scheme 3.4. Synthesis of the PTOC esters **62a-d**.

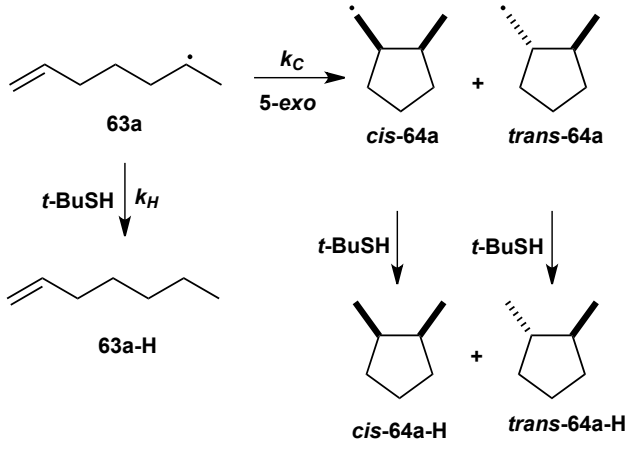
3.2 Kinetic experiments

With the required radical precursors in hand, the reaction of secondary 5-hexenyl radicals **63a-d** in [EMIm][NTf_2] can be explored and compared with results from reactions performed in organic solvents.

GC analysis of the reaction mixtures obtained from photolysis of the PTOC esters **62a-d** in the presence of 10 equivalents of *t*-BuSH revealed formation of three major products in both *t*-BuPh (or *n*-hexane in the case of **63d**) and [EMIm][NTf_2]. In all experiments the amount of [EMIm][Ntf_2] (1 ml, 3.88 mmol) was much larger than [*t*-BuSH] with the maximum value of (22 μL, 1.96×10^{-4} mmol), under these conditions dilution of the ionic liquid by the reagent can be excluded (χIL = 1). The products from the radical reductions, *i.e.*, **63a-d-H**, were identified by GC through treatment of the reaction mixtures with excess bromine, which reacted with the alkene moiety to form the dibromide, leading to disappearance of the peaks of **63a-d-H** in the GC chromatogram. The two other products were the *cis*- and *trans*-isomers of the cyclised products **64a-d-H**. Since 5-*exo* cyclisations of C-1 substituted 5-hexenyl radicals generally occur with high *cis*-selectivity in organic solvents,[8,14-17] the product with the larger GC peak area was assigned as *cis*-**64a-d-H** and the product with the smaller GC peak area as *trans*-**64a-d-H**. The results of the competition kinetic studies will be discussed individually for each radical.

3.2.1 Cyclisation of 1-methyl-5-hexenyl radical (63a)

Competition kinetic experiments with radical **63a** in *t*-BuPh and [EMIm][NTf_2] at 24 ± 1 °C, which were performed according to the experimental procedure described in Chapter 2, gave 1-heptene (**63a-H**) and the stereoisomeric1,2-dimethyl cyclopentanes *cis*-**64a-H** and *trans*-**64a-H**, as depicted in Scheme 3.5.



Scheme 3.5. Competition kinetic studies of the 5-*exo* cyclisation of the 1-methyl-5-hexenyl radical (**61a**) and reduction through hydrogen abstraction from *t*-BuSH.

1-Heptene (**63a-H**) was identified by comparison with an authentic sample (Sigma Aldrich). The two other peaks were assigned as described above. The detailed kinetic data are provided in Table 3.1. The data for the k_C/k_H determination are shown graphically in Figure 3.1.

Table 3.1. GC results of the competition kinetic experiments for the 5-*exo* cyclisation of the 1-methyl-5-hexenyl radical (**63a**) at 24 ± 1 °C.[a],[b]

Solvent	[*t*-BuSH] (M)	1/[*t*-BuSH] (M^{-1})	*cis*/*trans*	[64a-H]/[63a-H]
t-BuPh	0.2	5	3.83 ± 0.10	0.164 ± 0.006
	0.18	5.6	3.88 ± 0.10	0.181 ± 0.003
	0.16	6.25	3.88 ± 0.03	0.206 ± 0.006
	0.14	7.1	3.87 ± 0.03	0.239 ± 0.005
	0.12	8.3	3.85 ± 0.10	0.290 ± 0.011
	0.1	10	3.83 ± 0.01	0.339 ± 0.008
[EMIm][NTf_2]	0.2	5	4.12 ± 0.08	0.094 ± 0.006
	0.18	5.6	4.12 ± 0.07	0.099 ± 0.005
	0.16	6.25	4.18 ± 0.04	0.108 ± 0.005
	0.14	7.1	4.11 ± 0.01	0.125 ± 0.005
	0.12	8.3	4.12 ± 0.01	0.135 ± 0.005
	0.1	10	4.14 ± 0.05	0.164 ± 0.007

[a] Errors represent deviation from the average of three experiments . [b] [**62a**] = 0.1[*t*-BuSH].

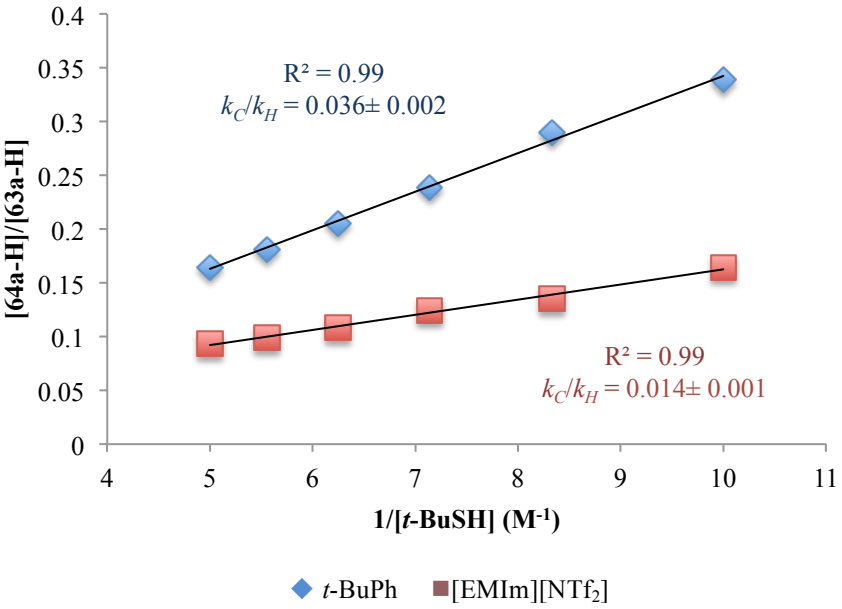


Figure 3.1. Dependence of [**64a-H**]/[**63a-H**] on *t*-BuSH concentration at 24 ± 1 °C for the cyclisation of the 5-hexenyl radical **63a** and reduction through hydrogen abstraction from *t*-BuSH. Uncertainties are calculated from the linear regression (2σ).

The data in Table 3.1 revealed that the *cis*/*trans* ratio remained constant in both solvents at 24 °C with slightly more *cis* selectivity in [EMIm][NTf_2] (*cis*/*trans* = 4.1 ± 0.1) compared to that in *t*-BuPh (*cis*/*trans* = 3.8 ± 0.1).

The gradient of the straight line provides the ratio of the rate constants (k_C/k_H) as (3.6 ± 0.2) × 10^{-2} in *t*-BuPh and (1.4 ± 0.1) × 10^{-2} in [EMIm][NTf_2]. It is apparent that the ratio of k_C/k_H almost halves in value by moving from *t*-BuPh to [EMIm][NTf_2] for this particular radical. It is reasonable to assume that k_H from *t*-BuSH to primary alkyl radicals, which was determined in Chapter 2 as k_H = (4.16 ± 0.3) × 10^7 M^{-1} s^{-1} in [EMIm][NTf_2] and reported previously to be k_H = 8 × 10^6 M^{-1} s^{-1} in organic solvents,[18] should be similar for secondary alkyl radicals. Under this assumption k_C of (2.9 ± 0.2) × 10^5 s^{-1} in *t*-BuPh and k_C = (5.8 ± 0.1) × 10^5 s^{-1} in [EMIm][NTf_2] (Table 3.3) is obtained, clearly showing that the cyclisation rate constant increased by almost a factor of two moving from *t*-BuPh to [EMIm][NTf_2].

Relative activation parameters for the 5-*exo* cyclisation and the reduction of radical **63a** were determined by measuring k_C/k_H in [EMIm][NTf_2] and *t*-BuPh over the temperature range of 23-70 °C. The experimental data in *t*-BuPh and [EMIm][NTf_2]

are compiled in Table 3.2, and the plot to determine the Arrhenius parameter is shown in Figure 3.2.

Table 3.2. GC results of the competition kinetic experiments for the 5-*exo* cyclisation of the 1-methyl-5-hexenyl radical (**63a**) at different temperatures.[a],[b],[c]

Solvent	**T/^{o}C**	**[64a-H]/[63a-H]**
t-BuPh	25	0.164 ± 0.006
	40	0.179 ±0.006
	45	0.184 ± 0.009
	55	0.192 ± 0.006
	60	0.202 ± 0.017
	65	0.216 ± 0.011
[EMIm][NTf_2]	4	0.133 ± 0.018
	25	0.161 ± 0.007
	45	0.308 ± 0.085
	65	0.585 ± 0.047
	85	0.806 ± 0.051
	95	1.250 ± 0.053
	115	1.706 ± 0.053

[a] Errors represent deviation from the average of three experiments. [b] [**62a**] = 0.01 M. [c] [*t*-BuSH] = 0.1 M.

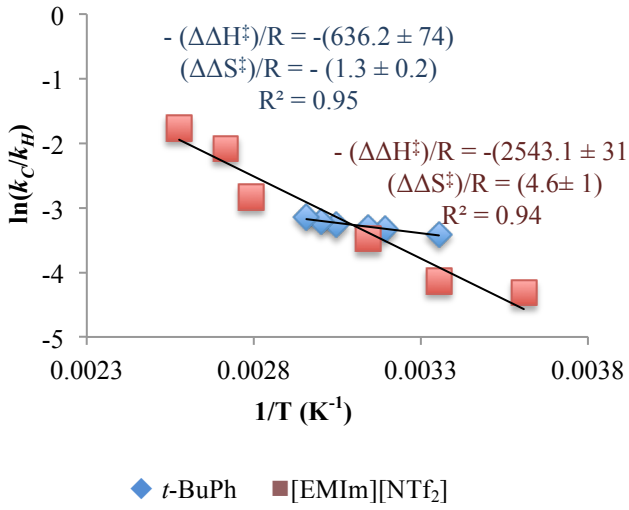


Figure 3.2. (ln (k_C/k_H)) *vs*.1/T for the 5-*exo* ring closure of the 5-hexenyl radical **63a** and reduction through hydrogen abstraction from *t*-BuSH in [EMIm][NTf_2] and *t*-BuPh (R = 8.314 kJ mol^{-1}). Uncertainties are calculated from the linear regression (2σ).

Figure 3.2 reveals that an increase in temperature leads to a considerable acceleration of the 5-*exo* cyclisation in [EMIm][NTf_2], whereas in *t*-BuPh the temperature effect on k_C/k_H is only small. Figure 3.3 shows the viscosity data for [EMIm][NTf_2], which are taken from literature,[19] and the temperature dependence of the 5-*exo* cyclisation of **63a** *vs*. the direct reduction by *t*-BuSH in *t*-BuPh and [EMIm][NTf_2] measured in this work. These data clearly suggest that the faster cyclisation at elevated temperatures is likely due to the decrease of the viscosity of [EMIm][NTf_2], which should increase radical mobility and should therefore facilitate the conformational changes required for a successful radical cyclisation. Furthermore, increasing the temperature allows for a greater movement of the solute particles resulting in the intermolecular interactions between the solute and solvent being broken. Therefore, a reduction in any unfavorable interactions between IL and starting material **63a** could also be considered as the origin of the increased rate constant at elevated temperatures. Thus, it appears that solvent viscosity is likely one of the main factors responsible for the different relative kinetic data obtained in the IL, compared to conventional organic solvents, where a temperature-independent product distribution would be expected.

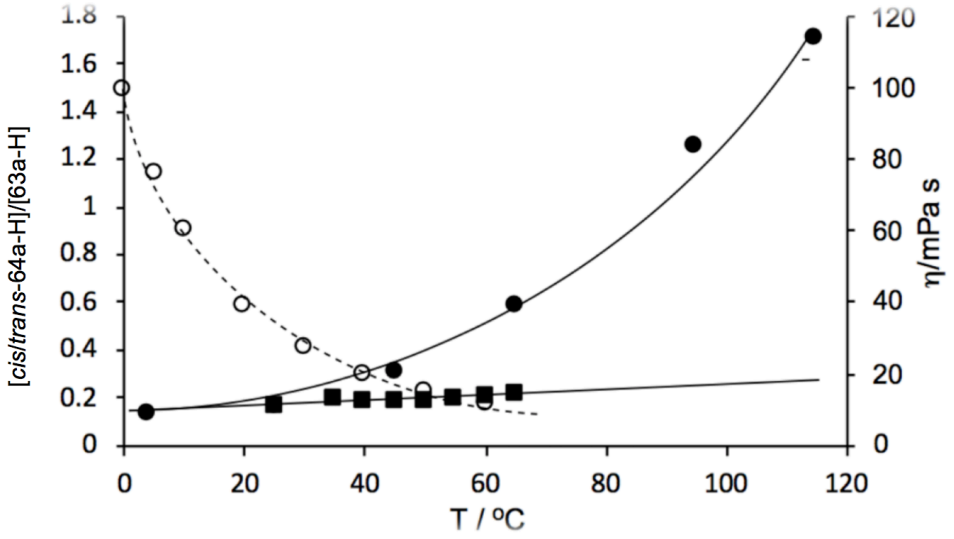


Figure 3.3. Temperature dependence of the 5-*exo* cyclisation of **63a** ([*cis*/*trans*-**64a-H**]) *vs*. the direct reduction by *t*-BuSH in *t*-BuPh (■) and [EMIm][NTf_2] (●); with [*t*-BuSH]/[**62a**] = 10 (left axis). Viscosity data for [EMIm][NTf_2] (○) are taken from ref. [19] (right axis).

In [EMIm][NTf_2], a $\Delta\Delta S^{\ddagger}$ ($\Delta\Delta S^{\ddagger} = \Delta S^{\ddagger}_C - \Delta S^{\ddagger}_H$) value of (38.3 ± 15.8) J mol^{-1} K^{-1} was obtained, which is more positive compared to the $\Delta\Delta S^{\ddagger}$ value in *t*-BuPh of (-10.8 ± 15.8) J mol^{-1} K^{-1}. Under the assumption that $\Delta S_H^{\ddagger}$ and $\Delta H_H^{\ddagger}$ in both solvents are approximately the same for the alkyl radicals studied in this work, this finding indicates a less negative $\Delta S^{\ddagger}_C$ for the cyclisation of radical **63a** in [EMIm][NTf_2], compared with *t*-BuPh. The increased entropy of activation could be due to either: a) increased ordering of [EMIm][NTf_2] about the starting material **63a**; or b) decreased ordering about the transition state, relative to *t*-BuPh. Due to the charge transfer from the radical to the double bond occuring in the transition state, it can be considered as unlikely that [EMIm][NTf_2] with larger polarisability decreases ordering in the transition state (especially compared to the non-polar solvent *t*-BuPh). Therefore, it can be suggested that the increased entropy of activation is due to [EMIm][NTf_2] ordering about the starting material **63a** to greater extent than that observed in *t*-BuPh.

A similar trend was found for $\Delta H^{\ddagger}_C$. The values for $\Delta\Delta H^{\ddagger}$ ($\Delta\Delta H^{\ddagger} = \Delta H^{\ddagger}_C - \Delta H^{\ddagger}_H$) of (21.1 ± 5.2) kJ mol^{-1} in [EMIm][NTf_2] and (5.3 ± 1.2) kJ mol^{-1} in *t*-BuPh indicate a more positive $\Delta H^{\ddagger}_C$ for cyclisation of radical **63a** in [EMIm][NTf_2]. The increased enthalpy of activation could arise from either: a) stabilisation of the starting material **63a**; or b) destabilisation of the transition state, relative to *t*-BuPh. Once again, it can

be considered as unlikely that [EMIm][NTf_2] with its larger polarisability destabilises the transition state (especially compared to the non-polar solvent *t*-BuPh). Hence, it was considered more likely that [EMIm][NTf_2] is stabilising, and hence deactivating the starting material **63a**. As there is a rate enhancement in [EMIm][NTf_2], relative to *t*-BuPh, clearly the entropic benefit outweighs the enthalpic cost, which leads to lower the energy of the transition state, leading to an overall rate enhancement for the 5-*exo* cyclisation of **63a** in [EMIm][NTf_2] compared with in *t*-BuPh (Table 3.3).

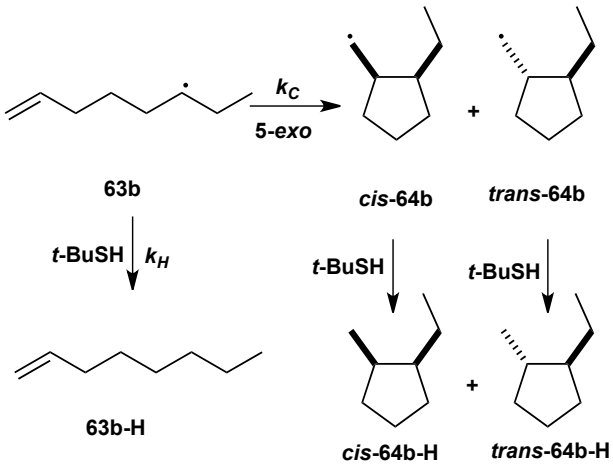
Table 3.3. Kinetic data for the 5-*exo* cyclisation of the 5-hexenyl radical **63a**.

Solvent	***cis*/*trans*** [a]	k_C/k_H [b],[c] $\times 10^{-2}$	k_C (s^{-1}) $\times 10^{5}$	$\Delta\Delta S^{\ddagger}$ [c] (J mol^{-1} K^{-1})	$\Delta\Delta H^{\ddagger}$ [c] (kJ mol^{-1})
t-BuPh	3.8 ± 0.1	3.6 ± 0.2	2.9 ± 0.2	-10.8 ± 3.8	5.3 ± 1.2
[EMIm][NTf_2]	4.1 ± 0.1	1.4 ± 0.1	5.8 ± 0.1	38.3 ± 15.8	21.1 ± 5.2

[a] Error represents deviation from the average of six experiments, at 24 ± 1 °C. [b] Determined from the slope of the line in Figure 3.1, at 24 ± 1 °C. [c] Errors are from the fit of the linear regression (2σ).

3.2.2 Cyclisation of the 1-ethyl-5-hexenyl radical (63b)

The PTOC-ester **62b** was irradiated in the presence of *t*-BuSH in *t*-BuPh at 24 ± 1 °C to produce the uncyclised compound **63b-H** and cyclised compounds, *cis*-**64b-H** and *trans*-**64b-H**, as depicted in Scheme 3.6. The same products were obtained in [EMIm][NTf_2] as a reaction medium. The product identification was performed as described in the previous section for the methyl substituted 5-hexenyl radical **63a**.



Scheme 3.6. Competition kinetic studies of the 5-*exo* cyclisation of the 1-ethyl-5-hexenyl radical (**63b**) and reduction through hydrogen abstraction from *t*-BuSH.

The detailed kinetic data are listed in Table 3.4 and the plot to determine the k_C/k_H is shown in Figure 3.4.

Table 3.4. Results of the competition kinetic experiments for the 5-*exo* cyclisation of the 1-ethyl-5-hexenyl radical (**63b**) at 24 ± 1 °C.[a],[b]

Solvent	[*t*-BuSH] (M)	1/[*t*-BuSH] (M^{-1})	*cis*/*trans*	[64b-H]/[63b-H]
t-BuPh	0.2	5	2.87 ± 0.02	0.187 ± 0.002
	0.18	5.6	2.87 ± 0.01	0.209 ± 0.005
	0.14	7.14	2.97 ± 0.01	0.281 ± 0.016
	0.12	8.3	2.97 ± 0.05	0.319 ± 0.011
	0.1	10	2.98 ± 0.04	0.362 ± 0.024
[EMIm][NTf_2]	0.2	5	2.61 ± 0.05	0.106 ± 0.001
	0.18	5.6	2.60 ± 0.02	0.116 ± 0.002
	0.16	6.3	2.64 ± 0.04	0.122 ± 0.003
	0.12	8.3	2.78 ± 0.03	0.159 ± 0.004
	0.1	10	2.79 ± 0.01	0.180 ± 0.004

[a] Errors represent deviation from the average of three experiments. [b] [**62b**] = 0.1[*t*-BuSH].

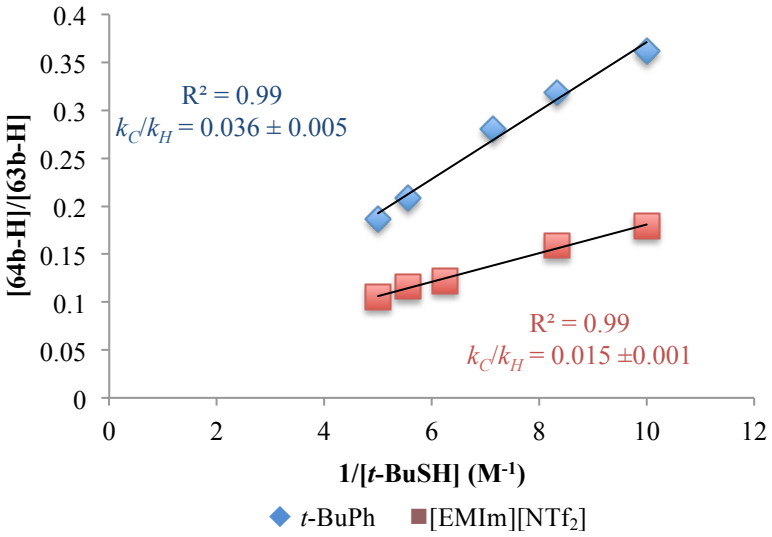


Figure 3.4. Dependence of [**64b-H**]/[**63b-H**] on *t*-BuSH concentration at 24 ± 1 °C for the cyclisation of the 1-ethyl-5-hexenyl radical (**63b**). Uncertainties are calculated from the linear regression (2σ).

The data in Table 3.4 show that the *cis*/*trans* ratio remained constant in both solvents at 24 ± 1 °C within the experimental error, with the average of (2.9 ± 0.1) in *t*-BuPh and (2.7 ± 0.1) in [EMIm][NTf_2]. Also, it is obvious that the *cis*-selectivity decreased with increasing the size of the C-1 substituents moving from methyl (*cis*/*trans* = 3.8) to ethyl (*cis*/*trans* = 2.9) substituted 5-hexenyl radicals in *t*-BuPh, possibly due to increasing unfavourable steric interaction of the transition state of *cis*-**64b-H** between methyl and ethyl group compared with the smaller interaction in the transition state of *cis*-**64a-H** between two methyl group (Figure 3.5). Similar trend was found in IL.

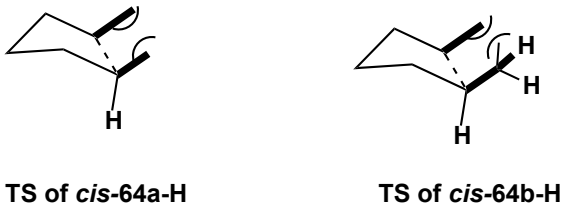


Figure 3.5. Structures of *cis*-**64a-H** and *cis*-**64b-H**.

From the k_C/k_H value of (3.6 ± 0.5) × 10^{-2} for the reaction of the ethyl substituted radical **63b** in *t*-BuPh, the 5-*exo* cyclisation rate coefficient of k_C = (2.9 ± 0.4) × 10^5 s^{-1} is calculated, which is similar to the methyl substituted radical **63a** reported in the previous section. In [EMIm][NTf_2] a k_C/k_H value of (1.5 ± 0.1) × 10^{-2} was obtained,

leading to rate coefficient for the 5-*exo* cyclisation of **63b** as $k_C = (6.2 \pm 0.2) \times 10^5$ s^{-1}, which is about two times faster than in *t*-BuPh (Table 3.6).

Further insight into the factors affecting the rate of the cyclisation can be deduced from the data obtained through temperature dependent studies, which are presented in Table 3.5. The plot to determine the Arrhenius parameter is shown in Figure 3.6.

Table 3.5. GC results of the competition kinetic experiments for the 5-*exo* cyclisation of the 1-ethyl-5-hexenyl radical (**63b**) at different temperatures.[a],[b],[c]

Solvent	T/^{o}C	*cis*/*trans*	[64b-H]/[63b-H]
t-BuPh	25	2.87 ± 0.02	0.187 ± 0.002
	40	2.79 ± 0.01	0.205 ± 0.002
	50	2.77 ± 0.03	0.206 ± 0.002
	60	2.66 ± 0.03	0.306 ± 0.023
	70	2.60 ± 0.01	0.364 ± 0.016
[EMIm][NTf_2]	25	2.79 ± 0.01	0.180 ± 0.004
	40	2.64 ± 0.03	0.253 ±0.059
	50	2.51 ± 0.10	0.292 ± 0.017
	60	2.48 ± 0.06	0.399 ± 0.065
	70	2.40 ± 0.03	0.499 ± 0.051

[a] Errors represent deviation from the average of three experiments. [b] [**62b**] = 0.01 M. [c] [*t*-BuSH] = 0.1 M.

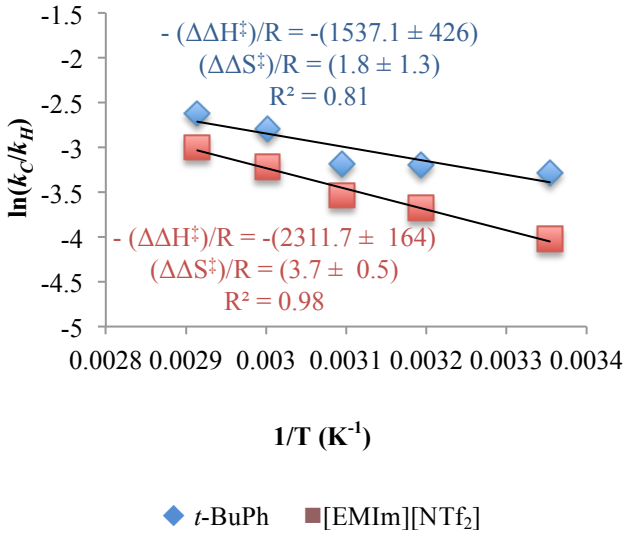


Figure 3.6. (ln (k_C/k_H)) *vs*.1/T for the ring closure of the 5-hexenyl radical **63b** in [EMIm][NTf_2] and *t*-BuPh (R = 8.314 kJ mol^{-1}). Uncertainties are calculated from the linear regression (2σ).

Figure 3.6 shows that temperature effect on k_C/k_H in [EMIm][NTf_2] is larger than in *t*-BuPh, which can be explained by the lower viscosity of [EMIm][NTf_2] at higher temperatures.[19] The 5-*exo* cyclisation of the 1-ethyl 5-hexenyl radical (**63b**) proceeds with similar *cis*-selectivity in both *t*-BuPh and [EMIm][NTf_2] (Table 3.5).

$\Delta\Delta S^{\ddagger}$ calculated from the intercept and $\Delta\Delta H^{\ddagger}$ from the slope of the line from the plot of ln (k_C/k_H) versus 1/T.

The values for $\Delta\Delta S^{\ddagger}$ of (30.8 ± 8.5) J mol^{-1} K^{-1} and $\Delta\Delta H^{\ddagger}$ of (19.2 ± 2.7) kJ mol^{-1} obtained in [EMIm][NTf_2] are bigger than those in *t*-BuPh that are $\Delta\Delta S^{\ddagger}$ of (14.7 ± 22.0) J mol^{-1} K^{-1} and $\Delta\Delta H^{\ddagger}$ of (12.8 ± 7.1) kJ mol^{-1} (Table 3. 6). This trend is similar as for the radical **63a**, indicating that the favourable entropy term is responsible for cyclisation rate enhancement of radical **63b** in [EMIm][NTf_2] compared with in *t*-BuPh. However, the large uncertainties in the activation parameters for the cyclisation of radical **63b** in both solvents, making it difficult to confirm such a trend.

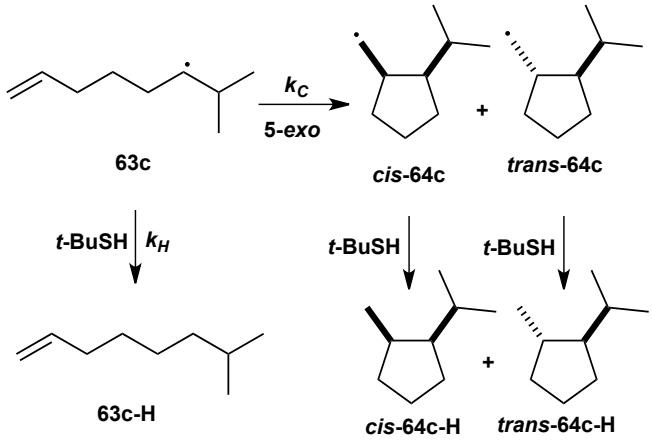
Table 3.6. Kinetic rate data for the 5-*exo* cyclisation of the 5-hexenyl radical **63b**.

Solvent	*cis*/*trans*[a]	k_C/k_H[b],[c] $\times 10^{-2}$	k_C (s^{-1}) $\times 10^{5}$	$\Delta\Delta S^{\ddagger}$[c] (J mol^{-1} K^{-1})	$\Delta\Delta H^{\ddagger}$[c] (kJ mol^{-1})
t-BuPh	2.9 ± 0.1	3.6 ± 0.5	2.9 ± 0.4	14.7 ± 22.0	12.8 ± 7.1
[EMIm][NTf_2]	2.7 ± 0.1	1.5 ± 0.1	6.2 ± 0.1	30.8 ± 8.5	19.2 ± 2.7

[a] Error represents deviation from the average of six experiments, at 24 ± 1 °C. [b] Errors are from the fit of the linear regression (2σ).[c] Determined from the slope of the line in Figure 3.4, at 24 ± 1 °C.

3.2.3 Cyclisation of 1-isopropyl-5-hexenyl radical (63c)

Competition kinetic experiments with radical **63c** in *t*-BuPh at 24 ± 1 °C, which were performed according to the experimental procedure described in Chapter 2, gave the uncyclised compound **63c-H**, and cyclised compounds, *cis*-**64c-H** and *trans*-**64c-H**, as depicted in Scheme 3.7. The same products were obtained in [EMIm][NTf_2] as a reaction medium.



Scheme 3.7. Competition kinetic studies of the 5-*exo* cyclisation of the 1-isopropyl-5-hexenyl radical **63c** and reduction through hydrogen abstraction from *t*-BuSH.

The experimental data are provided in Table 3.7 and the plot to determine the k_C/k_H is shown in Figure 3.7.

Table 3.7. GC results of the competition kinetic experiments for the 5-*exo* cyclisation of the 1-isopropyl-5-hexenyl radical (**63c**) at 24 ± 1 °C.[a],[b]

Solvent	[*t*-BuSH] (M)	1/[*t*-BuSH] (M^{-1})	*cis*/*trans*	[64c-H]/[63c-H]
t-BuPh	0.2	5	2.82 ± 0.02	0.180 ± 0.004
	0.18	5.6	2.81 ± 0.03	0.216 ± 0.004
	0.16	6.3	2.93 ± 0.12	0.243 ± 0.006
	0.14	7.1	2.88 ± 0.05	0.277 ± 0.002
	0.12	8.3	2.90 ± 0.08	0.324 ± 0.006
	0.1	10	2.88 ± 0.03	0.383 ± 0.009
[EMIm][NTf_2]	0.2	5	2.84 ± 0.05	0.108 ± 0.002
	0.18	5.6	2.82 ± 0.08	0.115 ± 0.002
	0.16	6.3	2.82 ± 0.02	0.126 ± 0.001
	0.14	7.1	2.96 ± 0.08	0.139 ± 0.003
	0.12	8.3	2.87 ± 0.04	0.167 ±0.003
	0.1	10	2.78 ± 0.07	0.196 ± 0.001

[a] Errors represent deviation from the average of three experiments. [b] [**62c**] = 0.1[*t*-BuSH].

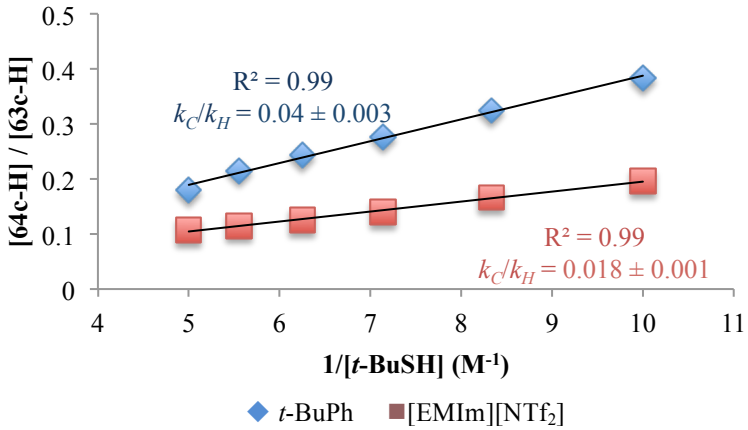


Figure 3.7. Dependence of [**64c-H**]/[**63c-H**] on *t*-BuSH concentration at 24 ± 1 °C for the cyclisation of the 5-hexenyl radical **63c** and reduction through hydrogen abstraction from *t*-BuSH. Uncertainties are calculated from the linear regression (2σ).

According to the data presented in Table 3.7, the *cis*/*trans* ratio remained constant at 24 ± 1 °C within the experimental error, with the average of (2.9 ± 0.1) in *t*-BuPh and (2.8 ± 0.1) in [EMIm][NTf_2]. This finding indicates that the stereoselectivity of the 5-*exo* cyclisation of radical **63c** at room temperature is not affected by the nature of the solvent.

The ratio of the rate constants (k_C/k_H) is (3.9 ± 0.3) × 10^{-2} in *t*-BuPh and (1.8 ± 0.1) × 10^{-2} in [EMIm][NTf_2] at 24 ± 1 °C. The 5-*exo* cyclisation rate coefficient of k_C = (7.5 ± 0.1) × 10^5 s^{-1} in [EMIm][NTf_2] is calculated, which is about two times faster than the cyclisation rate coefficient in *t*-BuPh (k_C = (3.1 ± 0.2) × 10^5 s^{-1}) (Table 3.9). Competition experiments at elevated temperatures are presented in Table 3.8. The plot to determine the Arrhenius parameters is shown in Figure 3.8.

Table 3.8. GC results of the competition kinetic experiments for the 5-*exo* cyclisation of the 1-isopropyl-5-hexenyl radical (**63c**) at different temperatures.[a],[b],[c]

Solvent	T/°C	*cis*/*trans*	[64c-H]/[63c-H]
t-BuPh	25	2.82 ± 0.02	0.180 ± 0.004
	35	2.78 ± 0.02	0.219 ± 0.013
	40	2.77 ± 0.03	0.226 ± 0.001
	50	2.72 ± 0.04	0.248 ± 0.004
	55	2.68 ± 0.02	0.280 ± 0.011
[EMIm][NTf_2]	25	2.77 ± 0.07	0.196 ± 0.001
	35	2.71 ± 0.05	0.341 ± 0.078
	40	2.66 ± 0.02	0.367 ± 0.031
	45	2.59 ± 0.06	0.373 ± 0.026
	58	2.51 ± 0.01	0.520 ± 0.031
	70	2.30 ± 0.15	-

[a] Error represents deviation from the average of three experiments. [b] [**62c**] = 0.01 M. [c] [*t*-BuSH] = 0.1 M.

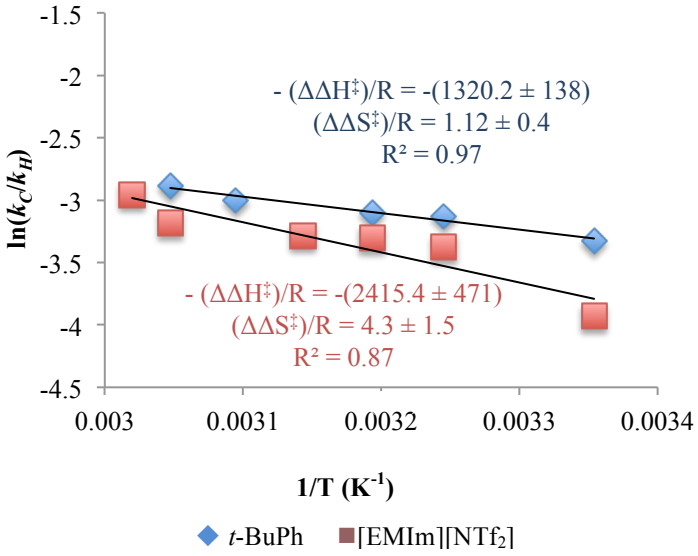


Figure 3.8. (ln (k_C/k_H)) *vs*.1/T for the ring closure of the 5-hexenyl radical **63c** in [EMIm][NTf_2] and *t*-BuPh (R = 8.314 kJ mol^{-1}). Uncertainties are calculated from the linear regression (2σ).

The values for $\Delta\Delta S^{\ddagger}$ of (30.8 ± 8.5) J mol^{-1} K^{-1} and $\Delta\Delta H^{\ddagger}$ of (19.2 ± 2.7) kJ mol^{-1} obtained in [EMIm][NTf_2] are bigger than those in *t*-BuPh that are $\Delta\Delta S^{\ddagger}$ of (14.7 ± 22.0) J mol^{-1} K^{-1} and $\Delta\Delta H^{\ddagger}$ of (12.8 ± 7.1) kJ mol^{-1} (Table 3. 6). This trend is similar as for the radical **63a** and **63b**, indicating that the favourable entropy term is responsible for cyclisation rate enhancement of radical **63c** in [EMIm][NTf_2] compared with in *t*-BuPh. However, the large uncertainties in the activation parameters for the cyclisation of radical **63c** in both solvents, making it difficult to confirm such a trend.

Table 3.9. Kinetic rate data for the 5-*exo* cyclisation of the 1-isopropyl-5-hexenyl radical (**63c**).

Solvent	*cis*/*trans*[a]	k_C/k_H[b],[c] × 10^{-2}	k_C (s^{-1}) ×10^5	$\Delta\Delta S^{\ddagger}$[b] (J mol^{-1} K^{-1})	$\Delta\Delta H^{\ddagger}$[b] (kJ mol^{-1})
t-BuPh	2.9 ± 0.1	3.9 ± 0.3	3.1 ± 0.24	9.3 ± 7.3	11.0 ± 2.3
[EMIm][NTf_2]	2.8 ± 0.1	1.8 ± 0.1	7.5 ± 0.13	35.8 ± 24.8	20.1 ± 7.8

[a] Error represents deviation from the average of six experiments, at 24 ± 1 °C. [b] Errors are from the fit of the linear regression (2σ). [c] Determined from the slope of the line in Figure 3.6, at 24 ± 1 °C.

3.2.4 Cyclisation of 1-*t*-butyl-5-hexenyl radical (63d)

The stereochemistry and influence of temperature on the cyclisation of 5-hexenyl radicals bearing a bulky substituent at the radical centre has been controversial for decades. As mentioned above, the preferential formation of the *cis* isomer in the 5-*exo* ring closure of C-1 substituted alkenyl radicals has been established as early as in 1972.[9] However, in 1992 Beckwith *et al*. reported that the ring closure of the *t*-butyl-substituted radical **63d** is *trans*-selective with a *trans*/*cis* ratio of 3:1 at 25 °C,[20] and the high steric hindrance caused by *t*-butyl substituent was believed to be the reason of breaching the general stereoselectivity trend (Figure 3.9).[15,16]

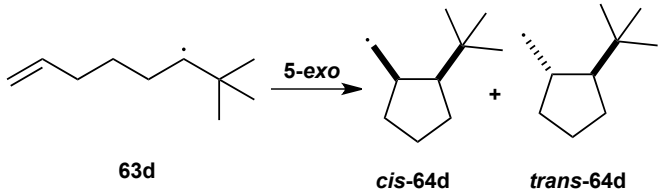


Figure 3.9. Cyclisation of the 1-*t*-butyl-5-hexenyl radical (**63d**).

Some years later, in 2005, Curran *et al.* demonstrated that 1-*t*-butyl-5-hexenyl radical (**63d**), like other C-1 substituted hexenyl radicals follows the general "1,2 *cis* selectivity" rules in 5-*exo* radical cyclisations.[21] However, the role of the solvent in controlling the stereoselectivity of the ring closure of C-1 substituted 5-hexenyl radicals still remains unclear. Beckwith published solvent effect data for 1-*t*-butyl-5-hexenyl radical (**63d**) showing that the stereochemistry in the cyclised product depended on solvent polarity, where the *cis*/*trans* ratio increased as the solvent polarity increased from hexane or benzene to *n*-propanol. Similar solvent effects on the stereoselectivity of other secondary radicals **68** and **69** (shown in Figure 3.10) were not observed (Table 3.10).[10]

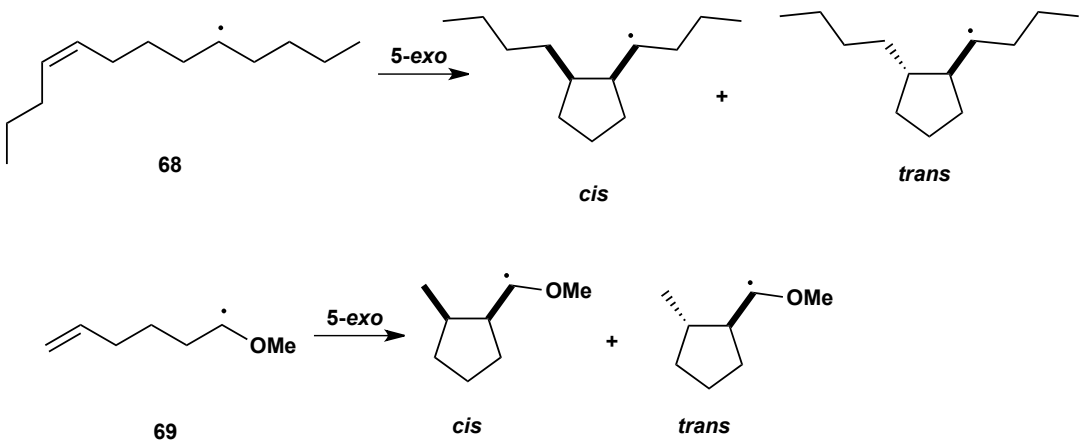


Figure 3.10. The 5-*exo* cyclisation of substrates **68** and **69**.

Table 3.10. *Cis*/*trans* ratio for the 5-*exo* cyclisation of the substrates 68, 69 and **63d** in different solvents.[a]

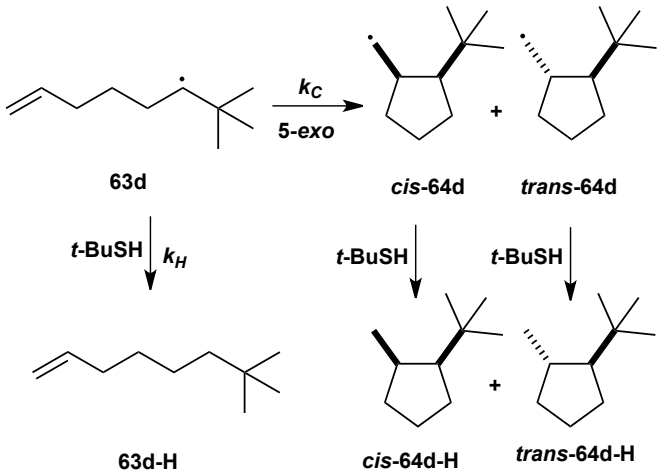
	cis/trans		
Radical	Benzene or hexane	DME[b]	1-propanol
68	1.0	0.9	0.9
63d	3.1	4.4	5.9
69	0.6	0.6	0.6

[a] Data taken from ref. [17]. [b]1,2-dimethoxyethane.

Furthermore, the computational methods employed in the study of Curran *et al.* predict that the stereochemical outcome should follow the general "1,2 *cis* selectivity" rules, also in the case of the 5-*exo* cyclisation of 1-*t*-butyl-5-hexenyl radical (**61d**). However, there is disagreement between the activation energy differences for formation of the *cis* and *trans* isomers, with the experimental value of ΔE_a = 12.97 kJ mol^{-1},[20] being considerably higher than the 2.7 kJ mol^{-1} calculated using the BHLYP/cc-pVDZ method.[17] This discrepancy warrants to revisit the stereochemical outcome of the 5-*exo* cyclisation of radical **63d** and the effects of temperature and solvent on the stereochemistry outcome of this radical.

For these experiments instead of using *t*-BuPh as the organic solvent, the reaction of radical **63d** was performed in the likewise non-polar *n*-hexane, since the signals of

***cis*-64d-H** signal and *t*-BuPh overlapped in the GC. The competition kinetic experiments were carried out at 24 ± 1 °C to produce the uncyclised compound **64d-H** and cyclised compounds, *cis*-**64d-H** and *trans*-**64d-H**, as depicted in Scheme 3.8. The same products were obtained in [EMIm][NTf_2] as a reaction medium. The product identification was performed similar to that outlined for the methyl and ethyl substituted radicals and the masses of the products were confirmed by GC-MS.



Scheme 3.8. Competition kinetic studies of the 5-*exo* cyclisation of 1-*t*-butyl-5-hexenyl radical (**63d**) and reduction through hydrogen abstraction from *t*-BuSH.

The experimental data are listed in Table 3.11 and the plot to determine the k_C/k_H is shown in Figure 3.11.

Table 3.11. GC results of the competition kinetic experiments for the 5-*exo* cyclisation of the 1-*t*-butyl-5-hexenyl radical (**63d**) at 24 ± 1 °C.[a],[b]

Solvent	[*t*-BuSH] (M)	1/[*t*-BuSH] (M^{-1})	*cis*/*trans*	[64d-H]/[63d-H]
n-hexane	0.20	5.0	1.61 ± 0.05	0.109 ± 0.010
	0.18	5.6	1.58 ± 0.02	0.123 ± 0.011
	0.16	6.3	1.58 ± 0.01	0.131 ± 0.013
	0.14	7.1	1.56 ± 0.05	0.156 ± 0.022
	0.12	8.3	1.58 ± 0.07	0.174 ± 0.010
	0.10	10.0	1.56 ± 0.13	0.187 ± 0.020
[EMIm][NTf_2]	0.20	5.0	1.71 ± 0.01	0.055 ± 0.002
	0.18	5.6	1.73 ± 0.12	0.059 ± 0.001
	0.16	6.3	1.73 ± 0.02	0.064 ± 0.002
	0.14	7.1	1.71 ± 0.04	0.072 ± 0.002
	0.12	8.3	1.66 ± 0.04	0.081 ± 0.001
	0.10	10.0	1.67 ± 0.03	0.093 ± 0.007

[a] Errors represent deviation from the average of three experiments. [b] [**62d**] = 0.1[*t*-BuSH].

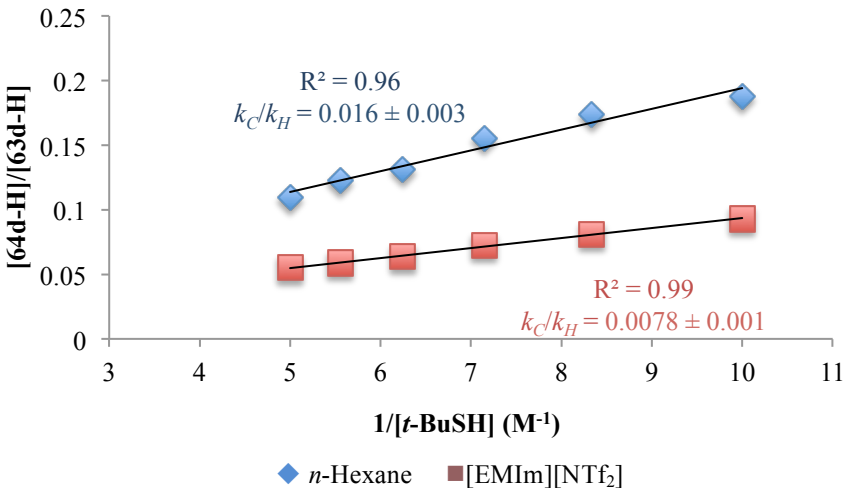
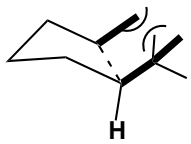


Figure 3.11. Dependence of [**64d-H**]/[**63d-H**] on *t*-BuSH concentration at 24 ± 1 °C for the cyclisation of the 1-*t*-butyl-5-hexenyl radical **63d**. Uncertainties are calculated from the linear regression (2σ).

From the k_C/k_H value of (1.6 ± 0.3) × 10^{-2} obtained for the reaction of the radical **63d** in *n*-hexane, the 5-*exo* cyclisation rate coefficient of k_C = (1.3 ± 0.2) × 10^5 s^{-1} is calculated. In [EMIm][NTf_2] a k_C/k_H value of (0.8 ± 0.1) was obtained, leading to a value of k_C as (6.4 ± 0.2) × 10^5 s^{-1}. It is apparent that radical **63d** undergoes ring closure slower than the less hindered radicals **63a**, **63b** and **63c** in both [EMIm][NTf_2] and *n*-hexane. The lower k_C for radical **63d** might be due to steric hindrance in the transition state of the cyclisation process (Figure 3.12). Similar to the results obtained for radicals **63a**, **63b** and **63c**, the k_C for the *t*-butyl substituted 5-hexenyl radical **63d** increased moving from *n*-hexane to [EMIm][NTf_2].



TS *cis*-64d

Figure 3.12. Transition structure for the ring closure of radical **63d**.

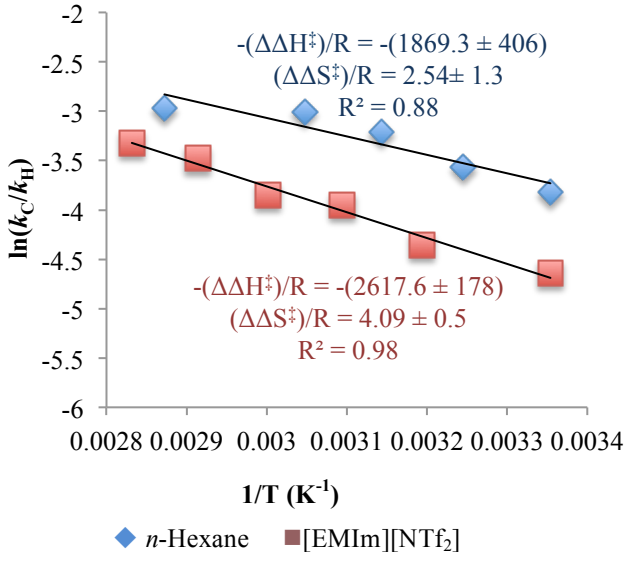
According to the data provided in Table 3.11, the average of the *cis*/*trans* ratio obtained as (1.6 ± 0.1) in *n*-hexane and as (1.7 ± 0.1) in [EMIm][NTf_2] indicates that the stereoselectivity of the 5-*exo* cyclisation of the *t*-butyl-5-hexenyl radical at room temperature is not affected by the nature of the solvent, consistent with those obtained for the other C-1 substituted hexenyl radicals reported in this chapter. Furthermore, it is obvious that the cyclisation of the *t*-butyl-5-hexenyl radical is *cis*-selective in both solvents, however the *cis* selectivity is much lower than in the case of the less hindered methyl, ethyl and isopropyl substituted 5-hexenyl radicals which are 3.8, 2.9 and 2.9 respectively in *t*-BuPh. This finding indicates that the steric hindrance is a main factor controlling the stereoselectivity of the alkyl substituted radicals and *t*-butyl substituted 5-hexenyl radical **63d** is not excepted.

For further insight into the factors affecting the rate and stereoselectivity of the reaction, the experiments performed at various temperatures ranging from 25-80 ^oC. The detailed kinetic data are provided in Tables 3.12 and the plot to determine the Arrhenius parameter is shown in Figure 3.13.

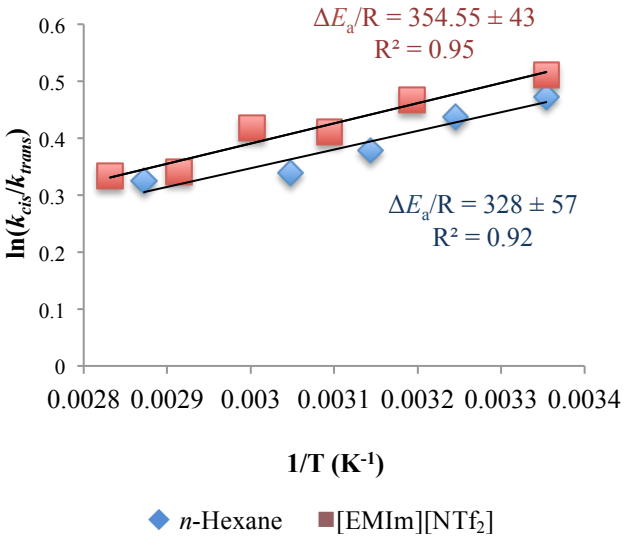
Table 3.12. GC results of the competition kinetic experiments for the 5-*exo* cyclisation of the 1-*t*-butyl-5-hexenyl radical (**63d**) at different temperatures.[a],[b],[c]

Solvent	T/^{o}C	*cis*/*trans*	[64d-H]/[63d-H]
n-Hexane	25	1.60 ± 0.06	0.109 ± 0.010
	35	1.53 ± 0.01	0.141 ± 0.005
	45	1.46 ± 0.01	0.201 ± 0.012
	55	1.40 ± 0.01	0.214 ± 0.014
	75	1.38 ±0.01	0.256 ± 0.018
[EMIm][NTf_2]	25	1.67 ± 0.03	0.097 ± 0.007
	40	1.60 ± 0.01	0.129 ± 0.011
	50	1.51 ±0.02	0.192 ± 0.018
	60	1.52 ±0.01	0.214 ± 0.013
	70	1.41 ±0.02	0.310 ± 0.009
	80	1.39 ±0.01	0.361 ± 0.021

[a] Error represents deviation from the average of three experiments. [b] [**62d**] = 0.01 M. [c] [*t*-BuSH] = 0.1 M.



a



b

Figure 3.13. a: (ln (k_C/k_H)) *vs*.1/T and b: (ln (k_{cis}/k_{trans})) *vs*.1/T for the ring closure of the 5-hexenyl radical **63d** in [EMIm][NTf_2] and *t*-BuPh (R = 8.314 kJ mol^{-1}). Uncertainties are calculated from the linear regression (2σ).

Relative activation parameters were determined by measuring k_C/k_H for the reaction of **63d** in each solvent over the 25-80 °C temperature range. The values for $\Delta\Delta S^{\ddagger}$ of (34.0 ± 9.1) J mol^{-1} K^{-1} and $\Delta\Delta H^{\ddagger}$ of (21.8 ± 3.0) kJ mol^{-1} obtained in [EMIm][NTf_2] are bigger than those in *n*-hexane that are $\Delta\Delta S^{\ddagger}$ of (21.1 ± 21.2) J mol^{-1} K^{-1} and $\Delta\Delta H^{\ddagger}$

of (15.5 ± 6.8) kJ mol^{-1} (Table 3.13). This trend is similar as for the radicals **63a**, **63b** and **63c**, which described above.

Looking at the temperature profile of the different mode of cyclisation of radical **63d** in Figure 3.13.b, reveals that the stereoselectivity of radical **63d** is similar in both *n*-hexane and [EMIm][NTf$_2$] and it does not display any solvent dependence. Apparently, for radical **63d,** with the large steric effect, the influence of the solvent on the stereochemical outcome of the reaction becomes negligible.

Table 3.13. Kinetic data for the ring closure of 5-hexenyl radical **63d**.

Solvent	***cis*/*trans*[a]**	k_C/k_H[b],[c] × 10^{-2}	k_C (s^{-1}) × 10^5	ΔΔS‡ [b] (J mol^{-1} K^{-1})	ΔΔH‡ [b] (kJ mol^{-1})
n-Hexane	1.6 ± 0.1	1.6 ± 0.3	1.3 ± 0.2	21.1 ± 21.2	15.5 ± 6.8
[EMIm][NTf$_2$]	1.7 ± 0.1	0.8 ± 0.1	6.4 ± 0.2	34.0 ± 9.1	21.8 ± 3.0

[a] Error represents deviation from the average of six experiments, at 24 ± 1 °C. [b] Errors are from the fit of the linear regression (2σ). [c] Determined from the slope of the line in Figure 3.11, at 24 ± 1 °C; errors are 2σ.

Linear regression over the temperature range of 25 °C to 80 °C of the *cis/trans* ratio at several temperatures provided the values for the differences in the activation energies. The kinetic data are shown graphically in Figure 3.13.b. Based on the experimental data reported in this section, the differences of the activation energies for formation of the *cis* and *trans* isomers in the 5-*exo* cyclisation of the 1-*t*-butyl 5-hexenyl radical (**63d**) in *n*-hexane can be calculated as 2.7 kJ mol^{-1}.

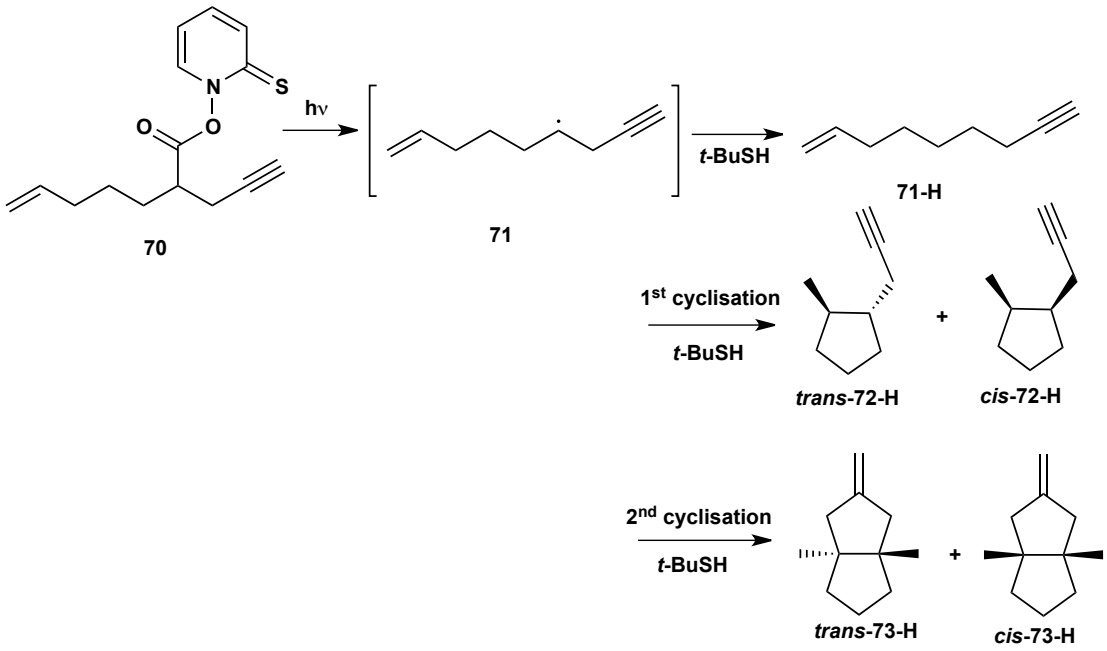
ΔE_a= Slope×8.314×10^{-3} kJ mol^{-1}

ΔE_a= 328×8.314×10^{-3} = 2.7 kJ mol^{-1}

Indeed, the origin of the discrepancy between the previous experimental studies,[20] and the one in this work is not clear. However, the experimental values obtained in this work are consistent with the theoretical outcome reported in the literature using BHLYP/cc-pVDZ method which is 2.7 kJ mol^{-1}.[17]

3.3 Tandem radical cyclisations

Having established that 5-*exo* radical cyclisations can be successfully performed in ionic solvents and with similar stereoselectivities than in organic solvents, a tandem radical cyclisation of 1-propargyl-5-hexenyl radical (**71**) was explored (Scheme 3.9). This radical was chosen because the corresponding PTOC radical precursor is readily available in few synthetic steps and also because the additional alkyne moiety on the structure of the radical **71** enables the reaction to proceed through two consecutive 5-*exo* cyclisations to generate bicyclic alkenes **73**.



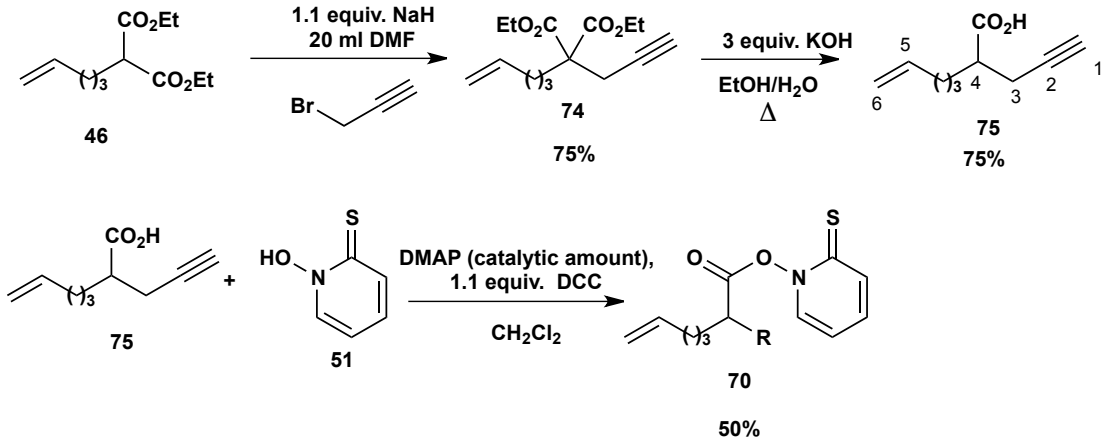
Scheme 3.9. Tandem radical cyclisation of 1-propargyl-5-hexenyl radical **71.**

3.3.1 Synthesis of the radical precursor 70

Scheme 3.10 outlines the synthesis of acid **75** and PTOC ester **70**. Diethyl 5-hexenyl-1,1-dicarboxylate (**46**) was alkylated with propargyl bromide in anhydrous DMF, using sodium hydride as the base. Compound **74** was obtained in 75% yield after column chromatography. Subsequent saponification and decarboxylation provided the propargyl substituted monoacid **75** in 75% yield. The ^{1}H NMR spectrum showed a triplet of acetylenic proton at 2.02 ppm, one doublet of doublet of doublet proton at

2.43 ppm and another one at 2.54 ppm, which are assigned to the two chemically non-equivalent hydrogen atoms attached to C-3.

Coupling of monoacid **75** to provide PTOC ester **70** in 50% yield was achieved following the literature procedure (Scheme 3.10),[13] as described in Section 2.2.1. ^{1}H NMR data analysis in C_6D_6 showed the four aromatic hydrogen atoms at 5.4, 6.0, 6.4 and 7.4 ppm, with the rest of the spectra being similar to those of the corresponding monoacid **75**. The high-resolution mass spectrometry of **70** featured a peak at *m*/*z* 276.10538 consistent with the molecular formula of **70** ($C_{15}H_{16}NO_2S$).

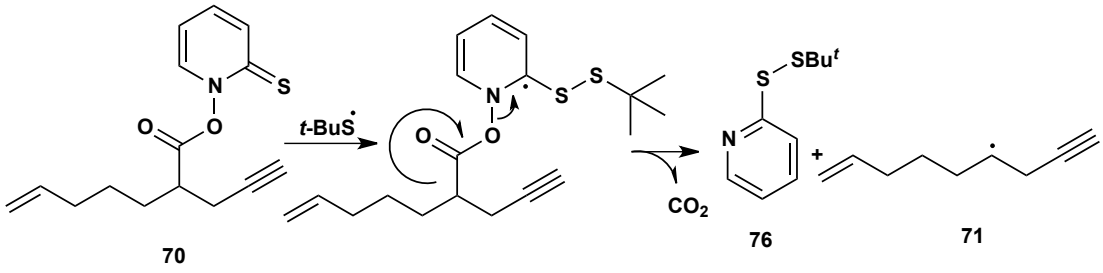


Scheme 3.10. Synthesis of the PTOC ester **70**.

3.3.2 Product assignment

Product assignment of this reaction was performed by GC analysis of the crude reaction mixture, since the anticipated products are very complex and difficult to access. Also, preparative separation of the products by column chromatography or HPLC was impossible due to the lack of a UV chromophore in these compounds.

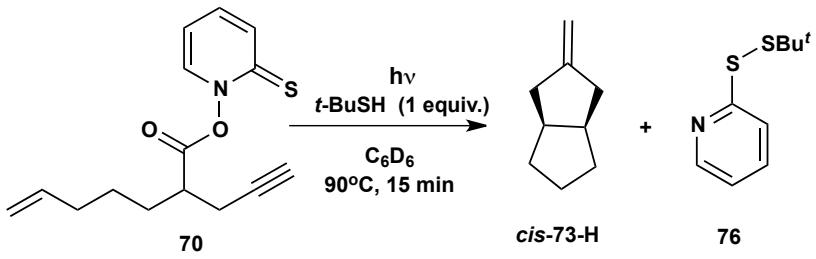
The experiments were performed first in *n*-hexane at 80 °C, where at least 6 major products were obtained. Scheme 3.11 illustrates the generation of the by-product produced in PTOC-thiol experiments from the reaction of the thiyl radical (*t*-BuS$^\bullet$) with the PTOC ester **70** in a radical propagation step.[22]



Scheme 3.11. Generation of the by-product **76** when the thiyl radical reacts with PTOC esters.

Therefore, the product at R_t = 16.7 min can be assigned as the by-product **76**. The assignment of the other products was made by variation of [*t*-BuSH], where increasing concentrations of the thiol results in trapping of early radical intermediates. At very high thiol concentration ([*t*-BuSH] = 10 eq.) the product with the lowest retention time (R_t = 4.35 min) was the most dominant peak, which was, therefore, tentatively identified as the directly reduced product **71-H**. Lowering [*t*-BuSH] resulted in increasing signal intensities at R_t = 4.57 min and R_t = 5.33 min, which were assigned as the monocyclic products ***trans*-72-H** and ***cis*-72-H** (Scheme 3.9). In addition to this, two products at R_t = 5.79 min and R_t = 6.26 min were detected, which had their highest intensity at low thiol concentrations ([*t*-BuSH] = 1 eq.). Because of the high *cis*-selectivity of such 5-*exo* cyclisations,[16-17] the more abundant product at R_t = 6.26 min was assigned as ***cis*-73-H**, whereas the less abundant product at R_t = 5.79 min was tentatively attributed to ***trans*-73-H**.

The assignment of *cis*-**73-H** was further confirmed by performing the reaction in C_6D_6 at 90 °C using 1 equivalent of *t*-BuSH (Scheme 3.12). Performing the experiments at higher temperatures increases the 5-*exo* cyclisation rate constants, as described in Chapter 2, enabling the reaction to proceed faster through two consecutive 5-*exo* cyclisation to generate bicyclic compounds *cis*-**73-H** as the major product. Under these conditions two major peaks appeared in the GC of which the product at R_t = 6.26 min can be assigned as *cis*-**73-H** and the product at R_t = 16.7 min can be assigned as the by-product **76**, which was described above.



Scheme 3.12. Cyclisation of 1-propargyl-5-hexenyl radical (**71**) in C_6D_6 at 90 ^oC.

Additional analysis of the reaction mixture using DEPT ^{13}C NMR spectroscopy further supported this assignment. The sp^2-CH_2 signal at 105.1 ppm and a quaternary carbon at 153.2 ppm could be identified, which correspond to the vinylic carbons (-C=CH_2) of the exocyclic alkene moiety in *cis*-**73-H**. The three aliphatic methylene carbon signals appear at 40.4, 34.1 and 25.9 ppm, whereas a signal at 48.4 could be assigned to the quaternary aliphatic carbon at the ring fusion in *cis*-**73-H**. The by-product **76** features the aromatic CH at 149.1, 135.9, 119.8 and 119.0 ppm, the quaternary C-S carbon at 162.0 ppm and the *t*-butyl group at 29.5 and 18.9 (from cis-**73-H**) ppm (Figure 3.14 and 3.15)

^{13}C NMR (500 MHz, C_6D_6): 162.0, *153.2, 149.1, *135.9, 119.8, *119.0, **105.1, 48.4, 42.2, **40.4, **34.1, 29.5, **25.9, 18.9 ppm.

* = CH carbons (all from **76**); 149.1, 135.9, 119.8, 119.0 ppm.

** = CH_2 carbons (all from *cis*-**73-H**); 105.1, 40.4, 34.1, 25.9 ppm

*** =CH_3 carbons: 29.5 (from **76**), 18.9 (from cis-7) ppm.

**** =C carbons: 162.0 (from **76**), 153.2 (from cis-7), 48.4 (from 19), 42.2 (from cis-**73**) ppm.

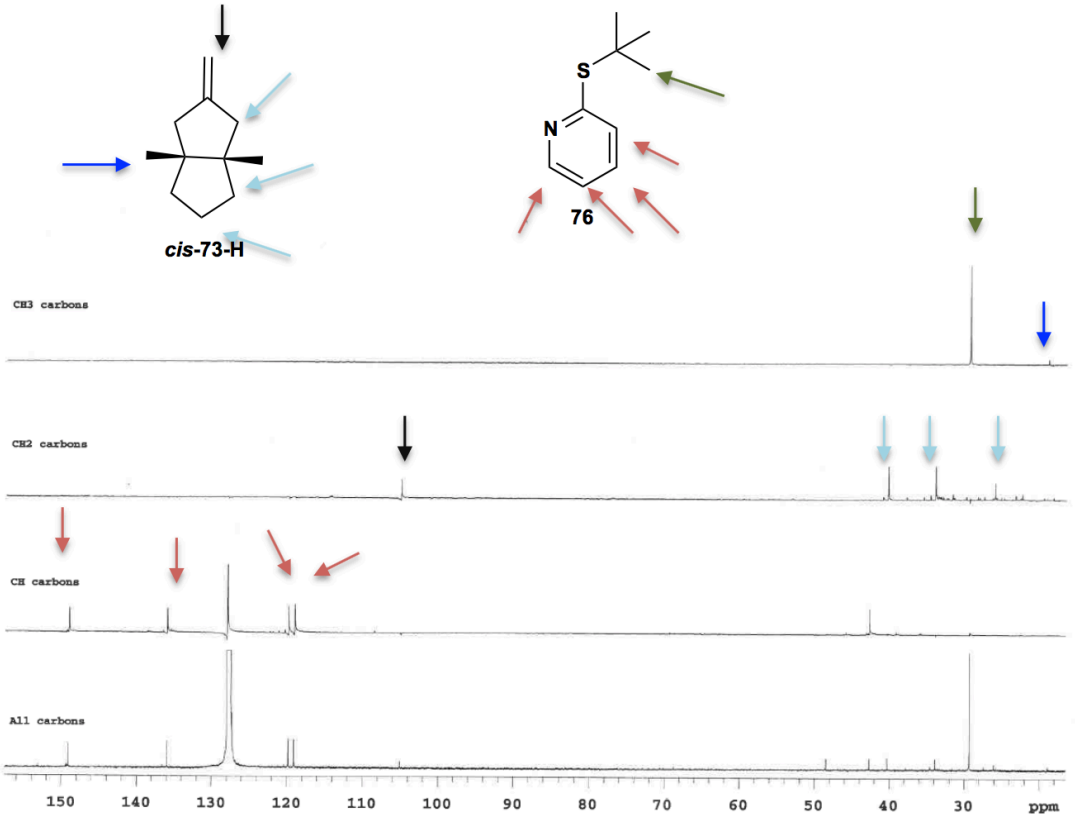


Figure 3.14. DEPT ^{13}C NMR spectra of the reaction mixture resulting from cyclisation of 1-propargyl-5-hexenyl radical (**71**) in C_6D_6 at 90 ^{o}C.

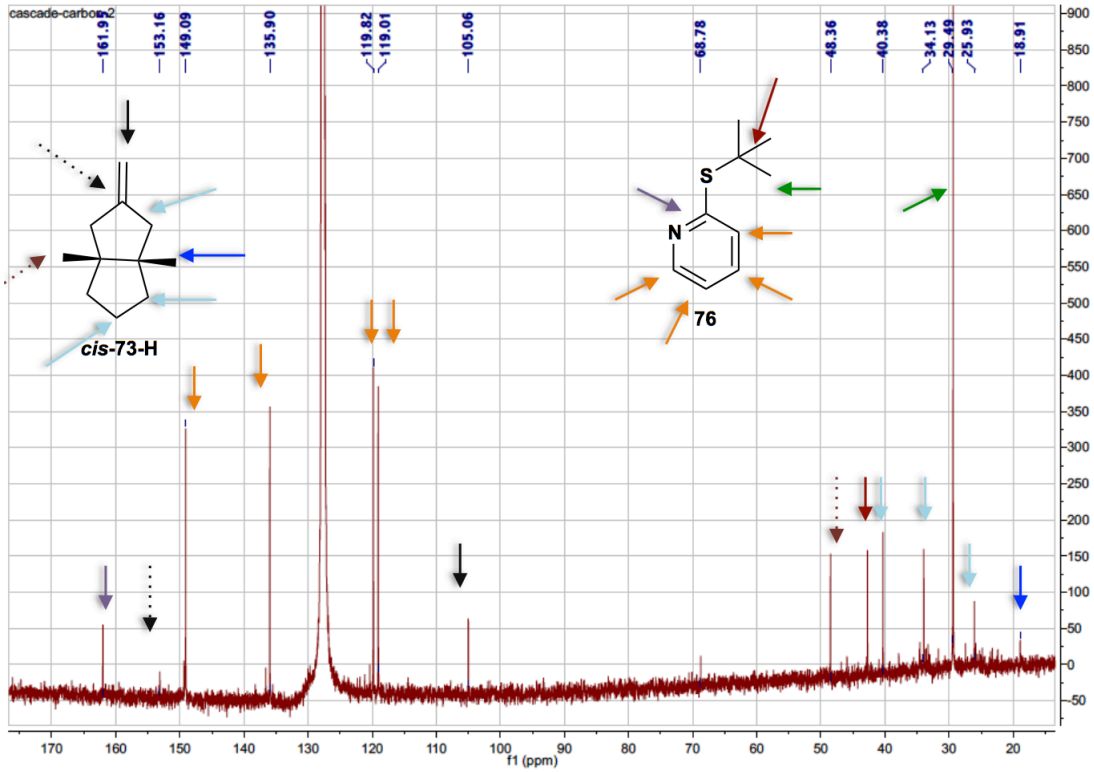
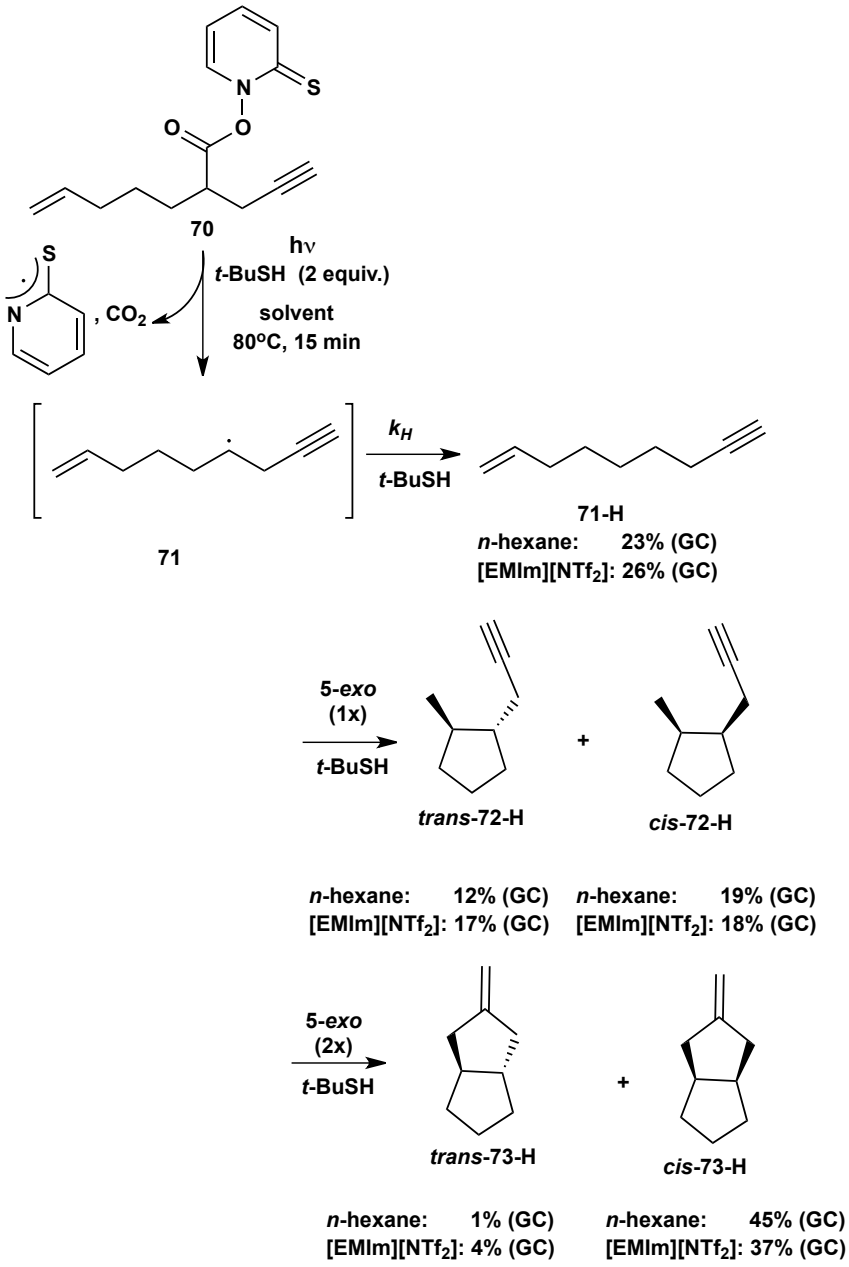


Figure 3.15. ^{13}C NMR(500 MHz, C_6D_6) of the reaction mixture resulting from cyclisation of 1-propargyl-5-hexenyl radical (**71**).

Obviously, *cis*-**73-H** is the product of two consecutive *cis* selective 5-*exo* cyclisations (first cyclisation to the alkene, followed by cyclisation to the alkyne), which could be formed in [EMIm][NTf_2], although the yield was slightly lower than that obtained in *n*-hexane (37% *vs*. 45%, determined by GC from the relative peak areas). The major by-product **71-H** resulted from direct reduction of **71**. The by-procucts from reduction of the radical intermediate after the first cyclisation produced *cis*-**72-H** and *trans*-**72-H** with less than 20% (GC) (Scheme 3.13).



Scheme 3.13. Tandem radical cyclisation of 5-hexenyl radical **71**.

3.4 Summary

In order to explore the role of steric effects on the rate and stereo-selectivity of the 5-*exo* radical cyclisation in ionic liquids, the reactions of the secondary 5-hexenyl radicals **63a-d** have been studied.

It is obvious that the 5-*exo* cyclisation proceeds with similar *cis*-selectivity in both [EMIm][NTf_2] and in the organic solvent at ambient temperature. As expected, due to unfavorable interactions in the transition state, the *cis*-selectivity decreases with increasing size of the C-1 substituent in both solvent systems.

Furthermore, it has been found that ionic liquids enhance the rate of the cyclisation of the secondary radicals similar to primary radicals.

Also, considerable 5-*exo* cyclisation rate enhancements (compared to the direct reduction) have been observed by increasing the temperature in [EMIm][NTf_2], whereas in *t*-BuPh the temperature effect on k_C/k_H was only small. The faster cyclisation at elevated temperatures is likely due to a decrease of the viscosity of [EMIm][NTf_2], which increases radical mobility and facilitates the conformational changes required for successful radical cyclisations. Therefore, one can conclude that solvent viscosity is one of the main factors responsible for the different relative kinetic data obtained in the IL, compared to conventional organic solvents.

Analysis of the activation parameter showed that the values of $\Delta\Delta S^{\ddagger}$ were larger in [EMIm][NTf_2] in comparison with organic solvent for all secondary radicals, Therefore, with the assumption that the activation entropy and enthalpy for HAT is the same in both solvents, one can conclude that entropy changes of the secondary 5-hexenyl radical for cyclisation is more favoured than hydrogen atom transfer in [EMIm][NTf_2] compare to organic solvent. Suggesting [EMIm][NTf_2] ordering about the starting material, to greater extent than that observed in *t*-BuPh. Also, the values of $\Delta\Delta H^{\ddagger}$ were observed to be larger in [EMIm][NTf_2] in comparison with organic solvents, which mean larger value of ΔH_C compare to ΔH_H in [EMIm][NTf_2]. Therefore, one can conclude that either the energy barrier of the T.S for the cyclisation is higher or for the hydrogen atom transfer is lower in [EMIm][NTf_2] compare to organic solvent that caused larger $\Delta\Delta H^{\ddagger}$ in [EMIm][NTf_2].

3.5 References

[1] Porter, N. A.; Magnin, D. R.; Wright, B. T., *J. Am. Chem. Soc.* **1986**, *108*, 2787.

[2] Bischof, P., *Helv. Chim. Acta.* **1980**, *63*, 1434.

[3] Curran, D. P.; Chen, M. H.; Kim, D., *J. Am. Chem. Soc.* **1986**, *108*, 2489.

[4] Bachi, M. D.; Denenmark, D., *J. Org. Chem.* **1990**, *55*, 3442.

[5] Hart, D. J.; Huang, H. C.; Krishnamurthy, R.; Schwartz, T., *J. Am. Chem. Soc.* **1989**, *111*, 7507.

[6] Mehta, G.; Murthy, A.N.; Reddy,D.S.; Reddy, A.V., *J. Am. Chem. Soc.* **1986**, *108*, 3443.

[7] Bachi, M. D.; Denenmark, D., *J. Org. Chem.* **1990**, *55*, 3442.

[8] Beckwith, A. L. J.; Blair, I.; Phillipou, G., *J. Am. Chem. Soc.* **1974**, *96*, 1613.

[9] Beckwith, A. L. J.; Moad, G.; *J. Chem. Soc., Chem. Commun.* **1974**, 472.

[10] Beckwith, A. L. J.; Schiesser, C. H., *Org. Biomol. Chem.* **2011**, *9*, 1736.

[11] Bailey, W. F.; Nurmi, T. T.; Patricia, J. J.; Wang, W., *J. Am. Chem. Soc.* **1987**, *109*, 2442.

[12] Shimshoni, J. A.; Bialer, M.; Wlodarczyk, B.; Finnell, R. H.; Yagen, B., *J. Med. Chem.* **2007**, *50*, 6419.

[13] a) Barton, D. H. R.; Crich, D.; Motherwell, W. B., *J. Chem. Soc., Chem. Commun.* **1983**, 939. b) Benjamin, L. J.; Schiesser, C. H.; Sutej, K., *Tetrahedron* **1993**, *49*, 2557.

[14] Beckwith, A. L. J.; Lawrence, T.; Serelis, A. K., *J. Chem. Soc., Chem. Commun.* **1980**, 484.

[15] Beckwith, A. L. J.; Easton, C. J.; Lawrence, T.; Serelis, A. K., *Aust. J. Chem.* **1983**, *36*, 545.

[16] Beckwith, A. L. J.; Schiesser, C. H., *Tetrahedron* **1985**, *41*, 3925.

[17] Spellmeyer, D. C.; Houk, K. N., *J. Org. Chem.* **1987**, *52*, 959.

[18] Newcomb, M.; Glenn, A. G.; Manek, M. B., *J. Org. Chem.* **1989**, *54*, 4603.

[19] Fröba, A. P.; Kremer, H.; Leipertz, A., *J. Phys. Chem. B* **2008**, *112*, 12420.

[20] Beckwith, A. L. J.; Cliff, M. D.; Schiesser, C, H., Tetrahedron **1992**, 48, 4641.

[21] Tripp, J. C.; Schiesser, C. H.; Curran, D. P., *J. Am. Chem. Soc.* **2005**, *127*, 5518.

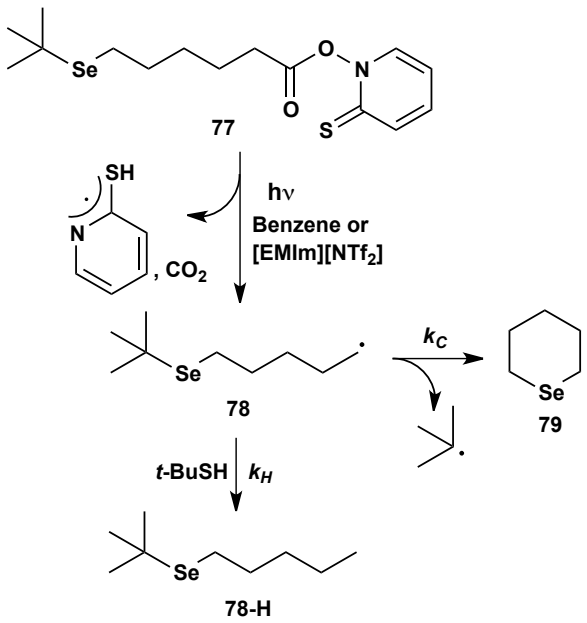
[22] Barton, D. H. R.; Crich, D.; Motherwell, W. B., *J. Chem. Soc., Chem. Commun.* **1983**, 109, 939.

4 Miscellaneous reactions: Intramolecular homolytic substitutions, 5-*exo* alkoxy radical cyclisations and intermolecular homolytic addition to alkenes

4.1 Intramolecular homolytic substitution

Intramolecular homolytic substitution chemistry provides a versatile method for accessing heterocyclic compounds.[1] In particular, selenium-containing cyclic systems, which are interesting targets in medicinal chemistry, can be conveniently synthesised through intramolecular homolytic substitution of *C*-radicals at selenium.[2] While kinetic data for a series of intramolecular substitutions of primary alkyl radicals at selenium have been recently determined in benzene,[2c] no such investigations have been performed in ILs. The results from the competition kinetic experiments in the previous chapters, which revealed accelerating effects on 5-*exo* radical cyclisations in [EMIm][NTf_2], suggest that similar behavior could also be found in intramolecular homolytic substitutions. Since the rate coefficient for the homolytic substitution of radical **78** in benzene is known, this radical was chosen as a candidate to explore the intramolecular homolytic substitution chemistry in [EMIm][NTf_2].[2c]

Scheme 4.1 shows the generation of the radical **78** from the PTOC ester **77** in the presence of *t*-BuSH. Intramolecular homolytic substitution leads to formation of tetrahydroselenopyran (**79**) with the release of *t*-Bu·, which competes with the direct reduction to the selenoether **78-H**.

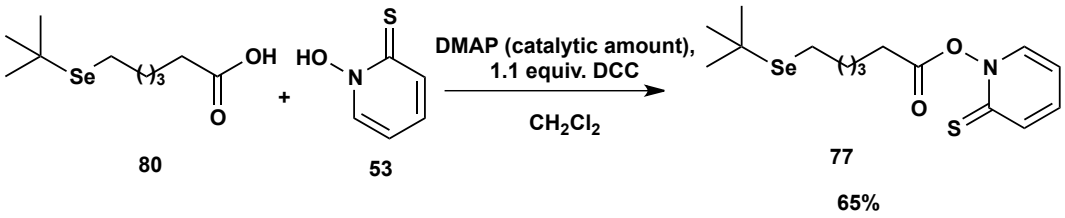


Scheme 4.1. Generation of the Se-containing radical **78** and competing reactions through reduction to **78-H** and cyclisation to **79** through homolytic substitution.

4.1.1 Synthesis of the PTOC ester 77 and pentamethylene selenide (79) as reference compound

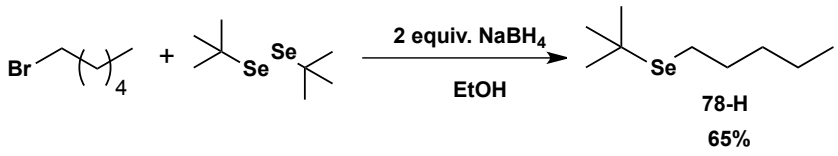
The PTOC ester **77** was obtained by reacting the Se-containing carboxylic acid **80** with *N*-hydroxypyridin-2-thione (**53**), as described in Section 2.2.1 (Scheme 4.2). Synthesis of the carboxylic acid **80** was performed as described previously.[3] ^{1}H NMR data analysis in C_6D_6 showed the four aromatic hydrogen atoms at 7.4, 6.5, 6.0 and 5.4 ppm and a triplet of the methylene protons α to the carboxyl group at 2.4 ppm and a singlet of the 9 protons of three chemically equivalent methyl groups at 1.3 ppm.

The HRMS of **77** featured a peak at *m*/*z* 362.0696 $[M + H]^+$ consistent with the molecular formula $C_{15}H_{23}NO_2SSe$, further supporting successful synthesis of this PTOC ester **77**.



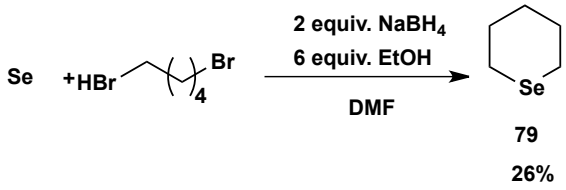
Scheme 4.2. Synthesis of the PTOC ester **77**.

The reference compound *t*-butyl pentyl selenide (**78-H**) was prepared as described previously[3] using 1-bromohexane, sodium borohydride and bis-(*t*-butyl) diselenide in anhydrous ethanol in 65% yield (Scheme 4.3).



Scheme 4.3. Synthesis of the *t*-butyl pentyl selenide (**78-H**).

Pentamethylene selenide **79** was prepared as authentic sample following the literature procedure,[4] using two equivalents of $NaBH_4$, elemental selenium, six equivalents of EtOH and 1,5-dibromopentane in DMF as a colourless liquid in 26% yield (Scheme 4.4).[5]



Scheme 4.4. Synthesis of the pentamethylene selenide (**79**).

Competition kinetic studies were performed in a similar way to those used for the 5-*exo* radical cyclisations outlined in Chapter 2, by measuring the product ratio [**79**]/[**78-H**] to determine k_C/k_H. Because of the polarity of the products, quantitative extraction from the ionic-liquid phase was achieved by using a mixture of ethyl acetate and diethyl ether (as described in Chapter 2). In all experiments the amount of [EMIm][Ntf_2] (1 ml, 3.88 mmol) was much larger than [*t*-BuSH] (11 μL, 9.8×10^{-5}

mmol), under these conditions dilution of the ionic liquid by the reagent can be excluded (χIL = 1).

The results of the competition experiments in [EMIm][NTf_2] and the literature data for the reaction in benzene[2c] are compiled in Table 4.1. The plot to determine the Arrhenius parameter is shown graphically in Figure 4.1.

Table 4.1. GC results of the competition experiments for the intramolecular homolytic substitution of the radical **78** at different temperatures.[a],[b],[c]

T/°C	[79]/[78-H] × 10^{-2}	k_C/k_H × 10^{-3}	k_C/k_H[d] × 10^{-3}
	in [EMIm][NTf_2]		in Benzene
24	3.29 ± 0.34	3.29 ± 0.34	2.5
59	7.01 ± 0.55	7.01 ± 0.55	5.3
81	12.60 ± 0.41	12.60 ± 0.41	7.8
100	24.70 ± 0.47	24.70 ± 0.47	11.3

[a] Errors represent deviation from the average of three experiments. [b] [**77**] = 0.01 M. [c] [*t*-BuSH] = 0.1 M. [d] Data from ref. [1].

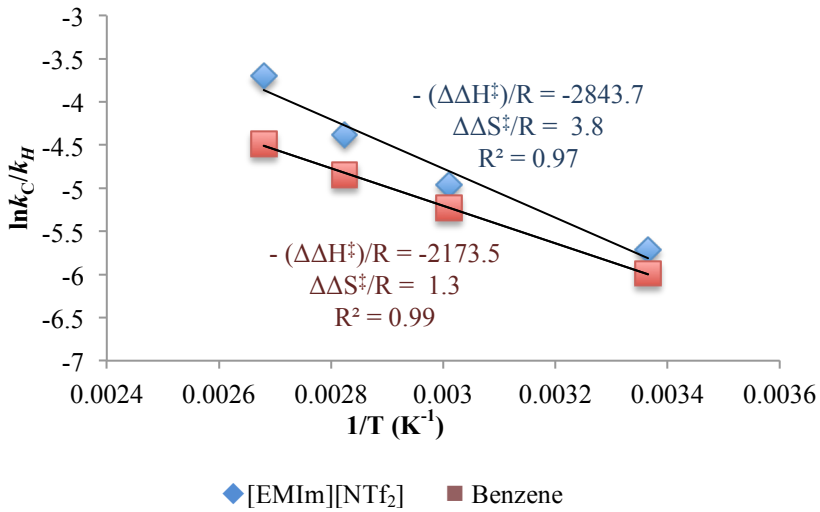


Figure 4.1. (ln (k_C/k_H)) *vs*.1/T for the homolytic substitution of radical **78** in [EMIm][NTf_2] and benzene (R = 8.314 J K^{-1} mol^{-1}). Uncertainties are calculated from the linear regression (2σ).

The data in Table 4.1 suggest that an increase in temperature leads to acceleration of the intramolecular homolytic substitution in [EMIm][NTf_2] much more than in benzene. This finding can be rationalised by the lower viscosity of [EMIm][NTf_2] at higher temperatures, which enables the conformational changes required for the cyclisation. [6]

In [EMIm][NTf_2] a (k_C/k_H) value of $(3.3 \pm 0.7) \times 10^{-3}$ was obtained, which reveals a rate coefficient for the homolytic substitution of $k_C = (1.4 \pm 0.2) \times 10^5$ s^{-1} (using the value for the reduction of primary alkyl radicals by *t*-BuSH of $k_H = (4.1 \pm 0.1) \times 10^7$ M^{-1} s^{-1} determined in Chapter 2). Compared to the literature value for k_C in benzene (2×10^4 s^{-1}), this result clearly shows that the ionic liquid leads to a rate enhancement by one order of magnitude (Table 4.2). Whilst the large uncertainties prevents identification the origin for the rate enhancement, it is likely that the increased entropy of activation is due to [EMIm][NTf_2] ordering about the starting material **78**, to greater extent than that observed in *t*-BuPh, similar to those described for the 5-*exo* cyclisation of **63a** in the previous chapter.

Table 4.2. Kinetic data for the homolytic substitution of the radical **78** in benzene and in [EMIm][NTf_2].[a],[b]

Solvent	k_C/k_H × 10^{-3}	k_C (s^{-1})	$\Delta\Delta S^{\ddagger}$ (J mol^{-1} K^{-1})	$\Delta\Delta H^{\ddagger}$ (kJ mol^{-1})
Benzene	n.d. [d]	2.0×10^4 [c]	10.9 ± 2.3	18.1 ± 0.8
[EMIm][NTf_2]	(3.3 ± 0.7) [e]	$(1.4 \pm 0.1) \times 10^5$ [f]	31.2 ± 18.3	23.6 ± 6.1

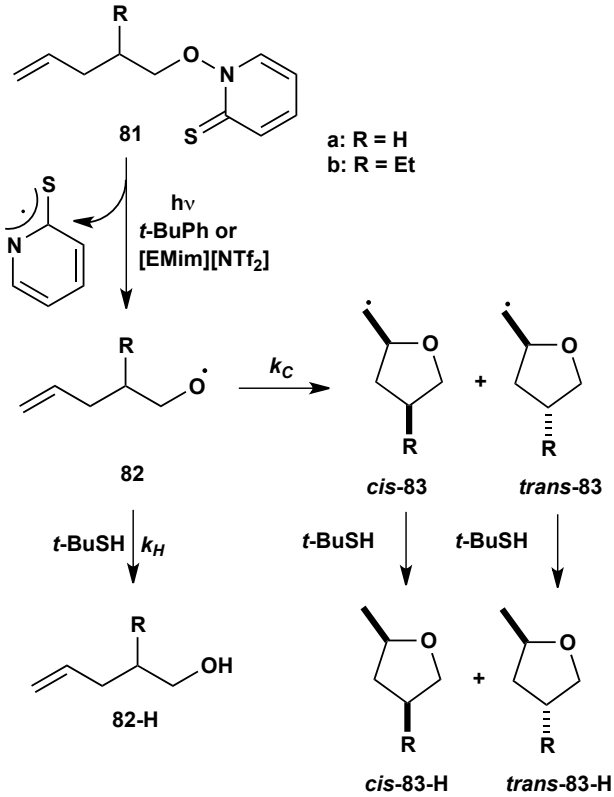
[a] Errors are 2δ. [b] Conditions: [*t*-BuSH]/[**77**] = 10. [c] Data from ref. [2a]. [d] not determined. [e] Single-concentration experiment at 24°C, error represents deviation from the average of multiple experiments. [f] Using $k_H = (4.1 \pm 0.1) \times 10^7$ M^{-1} s^{-1} determined in Chapter 2.

4.2 Alkoxy radical cyclisations

In contrast to the alkyl radicals studied in previous chapters, alkoxyl radicals, $RO^{\bullet}$, are strongly electrophilic species. It was therefore interesting to explore whether their reactivity is impacted when the reactions are performed in [EMIm][NTf_2]. Alkoxy radicals **82a** and **82b** (Scheme 4.5) were used to study the 5-*exo* cyclisation chemistry

of alkoxy radicals in [EMIm][NTf_2]. These radicals were chosen because (i) the corresponding PTOC radical precursors are readily available in few synthetic steps and (ii) because the reaction is expected to produce small molecules that could be detected by GC chromatography (see Scheme 4.5). Furthermore, the kinetic rate data for the 5-*exo* cyclisation of radical **82a** are known in *t*-BuPh.[7]

To that end **81a** and **81b** were synthesised as precursors for the alkoxyl radicals **82a** and **82b**, respectively (Scheme 4.5). The competition kinetic studies were then carried out, similar to those described in previous chapters. It should be noted that, due to the polar nature of the products, extraction from the [EMIm][NTf_2] phase was achieved using a mixture of ethyl acetate and diethyl ether (as described in Chapter 2).

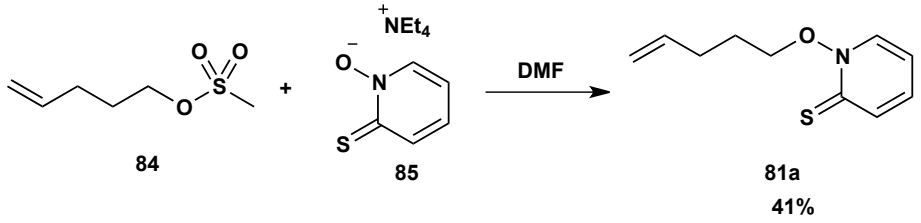


Scheme 4.5. Generation of the alkoxy radicals **82** and competing reactions through reduction to **82-H** and 5-*exo* cyclisation to *cis*-**83** and *trans*-**83**.

This section describes the synthesis of the radical precursors **81a-b** and of the authentic samples **82a-H** and **82b-H**, which were required to identify the product peaks in the gas chromatograms.

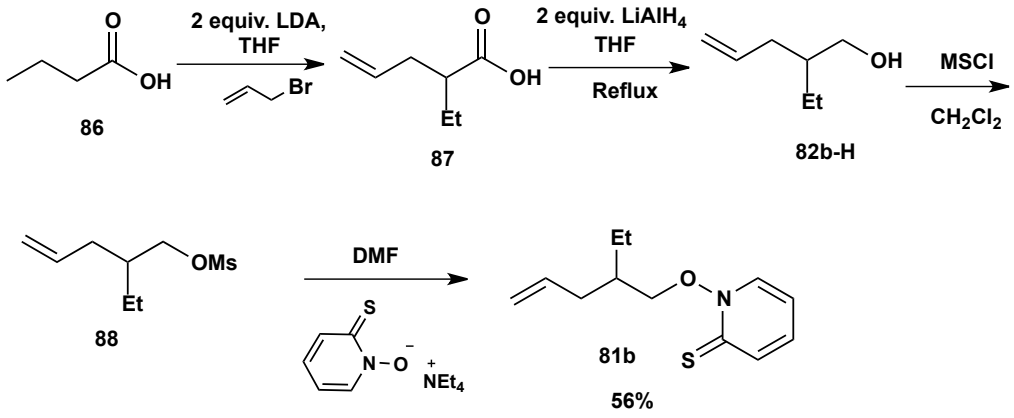
The PTOC ester **81a** was obtained following the literature procedure (Scheme 4.6),[8] by reacting tetraethylammonium pyridine-2(1H)-thione *N*-oxide (**85**) with pent-4-enyl

methane sulfonate **84** in DMF to obtain PTOC ester **81a** in 41% yield after column chromatography. The ^{1}H NMR spectrum in C_6D_6 showed four aromatic signals at 5.6, 6.0, 6.6 and 7.5 ppm. The spectrum showed the vinylic protons as two multiplets and one triplet at 4.9 and 4.2 ppm, respectively.



Scheme 4.6. Synthesis of the PTOC ester **81a**.

Scheme 4.7 outlines the synthesis of precursor **81b**. Commercially available *n*-butyric acid (**86**) was first alkylated with allyl in anhydrous THF, using two equivalents of LDA as the base. The obtained acid **87** was reduced to the alcohol **82b-H** using two equivalents of $LiAlH_4$. The alcohol **82b-H** was mesylated using mesyl chloride to give 2-ethylpent-4-enyl mesylate (**88**), which was then treated with tetraethylammonium pyridine-2(1H)-thione *N*-oxide in DMF to obtain *N*-(4-pentenyl-2-ethyl-1-oxy) pyridine-2-(1H)-thione (**81b**) in 56% yield. The ^{1}H NMR spectrum showed four aromatic signals at 7.4, 6.6, 6.0 and 5.6 ppm and a doublet of the α-methylene protons at 4.0 ppm.



Scheme 4.7. Synthesis of the PTOC ester **81b**.

Competition kinetic studies were performed in a similar way to those used for the 5-*exo* radical cyclisations outlined in Chapter 2. The reaction of the unsubstituted alkoxyl radical **82a** was performed in *t*-BuPh with *t*-BuSH as the hydrogen atom donor to form the cyclised product **83a-H** and uncyclised alcohol **82a-H**, as confirmed by GC using commercially available authentic samples purchased from Sigma Aldrich. In all experiments the amount of [EMIm][NTf_2] (1 ml, 3.88 mmol) was much larger than [*t*-BuSH] (11 μL, 9.8×10^{-5} mmol), excluding dilution of the ionic liquid by the reagent as a feature that must be considered ($\chi IL = 1$).[2]

Unfortunately, accurate product ratios could not be obtained because the GC signals of **82a-H** and *t*-BuSH partially overlapped. Using the heavier *t*-nonanethiol or *t*-dodecanethiol as hydrogen donor enabled separation of the product signals by GC in *t*-BuPh. However, due to insolubility of both *t*-nonanethiol and *t*-dodecanethiol in [EMIm][NTf_2], competition kinetic studies could not be performed in this ionic liquid.

The complications arising from overlapping GC signals could be remedied through the use of an alkoxyl radical with a higher molecular mass, which would increase the retention time in the GC. Therefore, the ethyl-substituted alkoxyl radical **82b**, which was obtained by irradiating the precursor **81b** in the presence of *t*-BuSH, was then attempted. This reaction led to formation of three major products that did not overlap with any of the by-products and starting materials in the GC, allowing to obtain the accurate k_C/k_H ratio.

Three major products were detected in the GC analysis of the reaction (see Scheme 4.7); the reduced alcohol **82b-H** was identified by comparison with an authentic sample, whereas the two remaining products were assigned to be the stereoisomeric 2,4-disubstituted tetrahydrofurans ***cis*-83b-H** (major) and ***trans*-83b-H** (minor) on the basis of literature data, which show that β-alkyl-substituted alkoxyl radicals undergo 5-*exo* cyclisation with high *cis*-selectivity.[7] The results of the competition experiments in *t*-BuPh and [EMIm][NTf_2] are compiled in Table 4.3. The plot to determine the Arrhenius parameter is shown in Figure 4.2.

Table 4.3. GC results of the competition kinetic experiments for the 5-*exo* cyclisation of the alkoxyl radical **82b** at different temperatures.[a],[b],[c]

Solvent	T/°C	*cis*/*trans*	[83b-H]/[82b-H]	k_C/k_H × 10^{-2}
t-BuPh	24	3.40 ± 0.01	10.58 ± 0.25	52.9 ± 1.2
	35	3.35 ± 0.02	10.61 ± 0.38	58.0 ± 1.8
	40	3.37 ± 0.01	11.28 ± 0.24	56.4 ± 1.2
	45	3.30 ± 0.01	12.09 ± 0.52	60.4 ± 2.6
	50	3.36 ± 0.01	12.14 ± 0.61	60.7 ± 0.7
[EMIm][NTf_2]	24	3.07 ± 0.01	7.87 ± 0.29	39.4 ± 1.4
	35	3.00 ± 0.01	8.05 ± 0.09	40.3 ± 0.5
	40	2.98 ± 0.01	8.14 ± 0.58	40.7 ± 2.9
	45	2.93 ± 0.01	8.40 ± 0.93	42.0 ± 0.5
	50	2.91 ± 0.02	8.43 ± 0.12	42.2 ± 0.6
	70	2.75 ± 0.01	9.00 ± 0.85	45.0 ± 4.3

[a] Errors represent deviation from the average of three experiments (2σ). [b] [**81b**] = 0.005 M. [c] [*t*-BuSH] = 0.05 M.

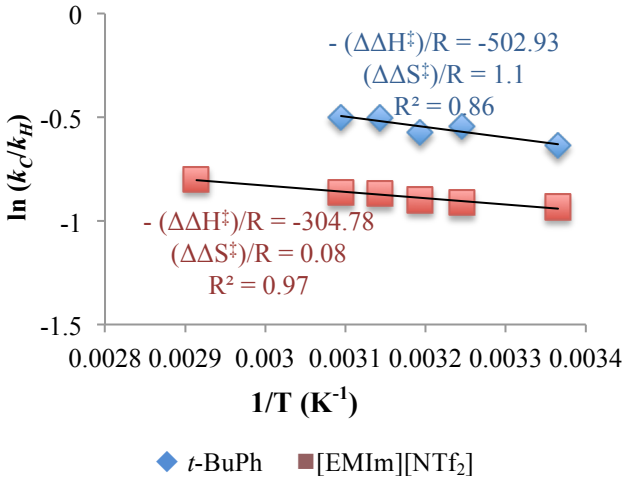


Figure 4.2. (ln (k_C/k_H)) *vs*.1/T for the ring closure of the alkoxy radical **82b** in [EMIm][NTf_2] and *t*-BuPh (R = 8.314 kJ mol^{-1}). Uncertainties are calculated from the linear regression (2σ).

The data in Table 4.4 show that the *cis*/*trans* ratio almost remained constant in both solvents at 24 °C, which is (*cis*/*trans* = 3.1) in [EMIm][NTf_2] and (*cis*/*trans* = 3.4) in *t*-BuPh.

As expected, the alkoxyl radical **82b** undergoes rapid 5-*exo* cyclisation in *t*-BuPh,[7] as reflected by a value of k_C/k_H of 52.9 × 10^{-2} at 24 ± 1 °C, which is about one order of magnitude higher than that for the 5-hexenyl radical (k_C/k_H = (2.1 ± 0.3) × 10^{-2}; see Chapter 2). The k_C/k_H value obtained for the reaction of **82b** in [EMIm][NTf_2] is 39.4×10^{-2}, which is 25% less than that of in *t*-BuPh (Table 4.4). Because k_H for the reduction of alkoxyl radicals by *t*-BuSH in both the organic solvent and in the ionic liquid was not available, it was impossible to obtain k_C for the cyclisation of the alkoxy radical. However, based on the findings for the alkyl radicals, it is reasonable to assume that k_H from *t*-BuSH to oxygen-centred radicals, *i.e.*, RO$^{\bullet}$ + *t*-BuSH → ROH + *t*-BuS$^{\bullet}$, should be faster in [EMIm][NTf_2] than in *t*-BuPh. Therefore, the data suggest that [EMIm][NTf_2] leads to increase of the 5-*exo* cyclisation of the oxygen-centred radicals more than the 5-*exo* cyclisation of the carbon-centred radicals. (The reduction of the value of k_C/k_H of carbon-centred radicals was up to 50% less in ionic liquid comparing to organic solvent, while this value is about 25% for the alkoxyl radical).

The values for $\Delta\Delta S^{\ddagger}$ of (0.7 ± 1.3) J mol^{-1} K^{-1} and $\Delta\Delta H^{\ddagger}$ of (2.5 ± 0.4) kJ mol^{-1} obtained in [EMIm][NTf_2] are within error similar to those in the conventional organic solvent that are $\Delta\Delta S^{\ddagger}$ of (8.8 ± 6.3) J mol^{-1} K^{-1} and $\Delta\Delta H^{\ddagger}$ of (4.2 ± 2.0) kJ mol^{-1} (Table 4.4). Since the kinetic measurements have shown that the cyclisation rate coefficient is higher in the ionic liquid, this finding suggests changes in the activation parameters of both hydrogen atom transfer and cyclisation processes that lead to small changes in the relative kinetic data, which prevents the origin of the rate enhancement being determined.

Table 4.4. Kinetic data for the 5-e*xo* cyclisation of the alkoxy radical **82b**.[a]

Solvent	*cis*-83b-H/*trans*-83b-H[b]	k_C/k_H[b] × 10^{-2}	$\Delta\Delta S^{\ddagger}$[c] (J mol^{-1} K^{-1})	$\Delta\Delta H^{\ddagger}$[c] (kJ mol^{-1})
t-BuPh	3.4 ± 0.1	52.9 ± 1.2	8.8 ± 6.3	4.2 ± 2.0
[EMIm][NTf_2]	3.1 ± 0.1	39.4 ± 1.5	0.7 ± 1.3	2.5 ± 0.4

[a] Conditions: [*t*-BuSH]/[**81b**] = 10. [b] Errors represent deviation from the average of three experiments at 24 ± 1 °C. [c] Errors are from the fit of the linear regression (2σ).

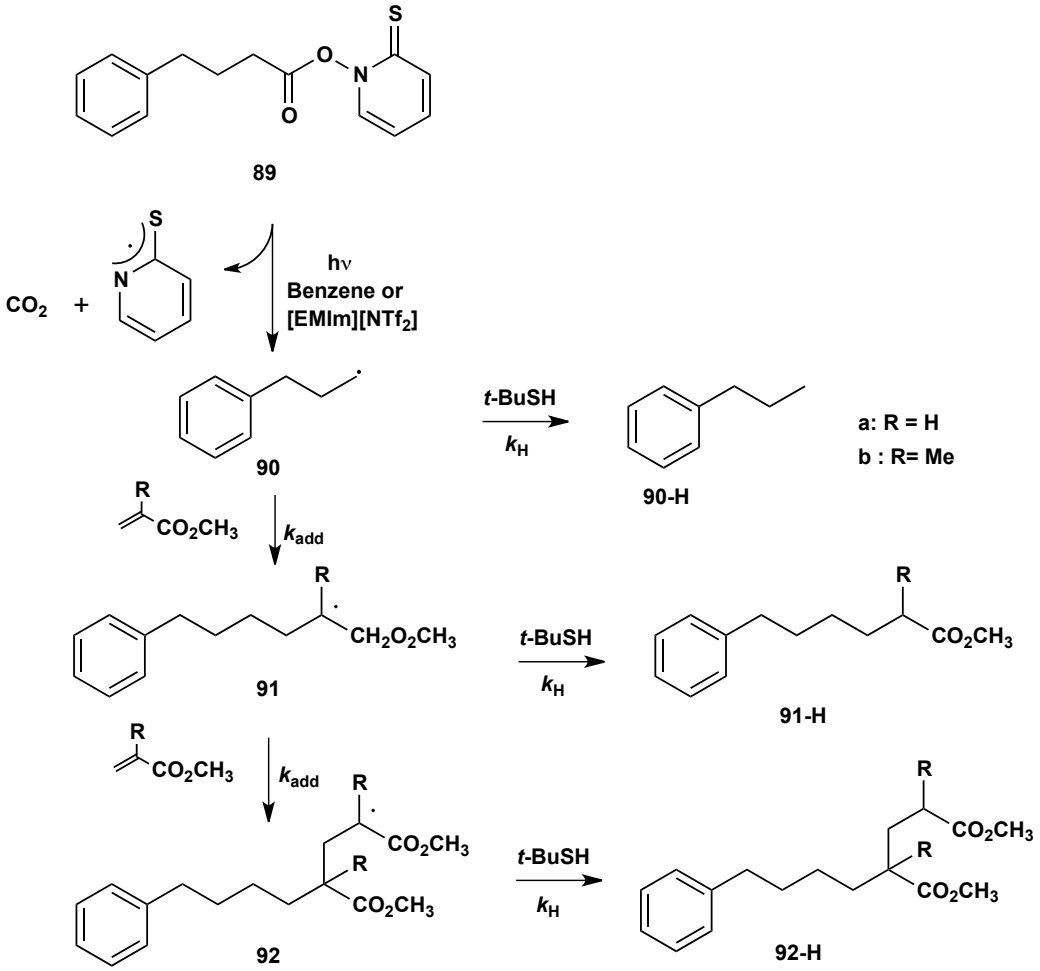
4.3 Intermolecular addition of alkyl radicals to alkenes

The free radical polymerisation is the most important industrial application of free radical chemistry in organic synthesis. This reaction enables the synthesis of macromolecular carbon chains by addition of alkyl radicals to alkenes. Previous works[9] indicated that alkyl radicals are more reactive with electron deficient alkenes (*i.e.,* acrylic monomers) than with electron rich alkenes (styrene). In order to explore the effect of an IL solvent on intermolecular alkyl radical additions, the rate constant for the intermolecular radical addition onto electron-deficient alkenes including methylacrylate (MA) and methyl methacrylate (MMA) was determined.[9-11]

To that end the reaction of the 3-phenylpropyl radical **(90**) to vinyl monomers (*i.e*., MA and MMA) will be studied in this section (Scheme 4.8). This radical was chosen because the corresponding precursor, PTOC-ester **89,** is synthetically readily available. Also the anticipated products produced through the direct reduction and of the first and second addition reactions can be detected by GC-MS analysis (see Scheme 4.8).

This experiment uses two bimolecular competing reactions, of which one reaction has a known rate constant (the rate constant for the hydrogen atom transfer from *t*-BuSH to primary alky radical (k_H) in organic solvents,[12] and in [EMIm][NTf_2], which determined in Chapter 2). The reaction was performed under pseudo-first order conditions where the concentration of alkene and *t*-BuSH are in large excess compared to the concentration of radical precursor **89** (*i.e.,* at least 10 equivalents).

Scheme 4.8 outlines a competition kinetic experiment in which the bimolecular radical addition of 3-phenylpropyl radical (**90**) to an electron deficient alkene to give **91-H** (rate constant k_{add}) competes with the bimolecular trapping of 3-phenylpropyl radical **(90**) (rate constant k_H) by *t*-BuSH to produce **90-H**. Theoretically, a mixture of higher oligomers should be produced in this reaction, but in practice the k_H ((8.0 ± 0.3) × 10^6 M^{-1} s^{-1} in THF at 25 °C)[12] is larger by one order of magnitude than the addition rate constant k_{add} (6.2 × 10^5 M^{-1} s^{-1} in neat MA at 25 °C)[13], so that the formation of products arising from further addition reactions of radical **92** is negligible.



Scheme 4.8. Generation of the 3-phenyl propyl radical **90** and competing reactions through reduction to **90-H** and addition to alkene to produce **91-H** and **92-H**.

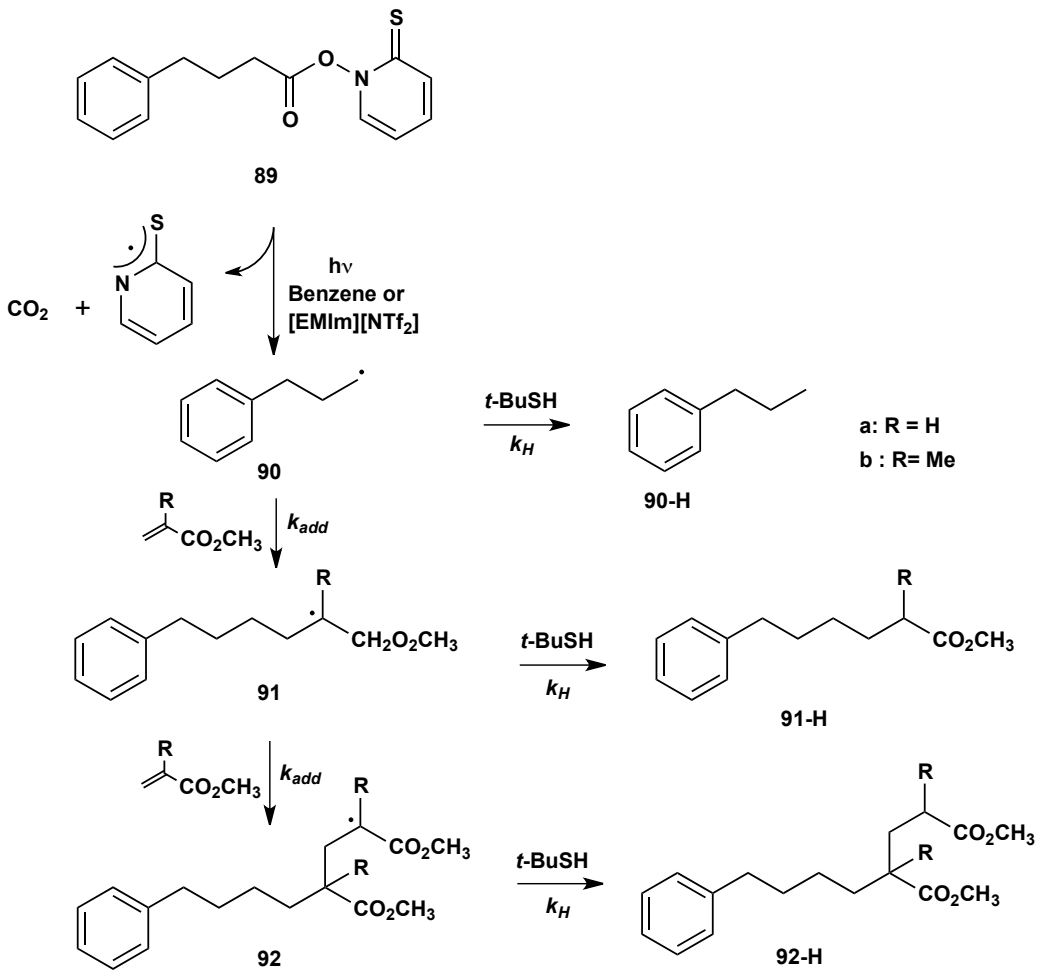
Under these conditions, the product distribution provides the ratio of the rate constants for two biomolecular processes *via* equation 1.

(1) $([\mathbf{91\text{-}H}]+[\mathbf{92\text{-}H}])/[\mathbf{90\text{-}H}]=k_{add}/k_H \times [\text{alkene}]/[t\text{-BuSH}]$

More details are given in the following sections.

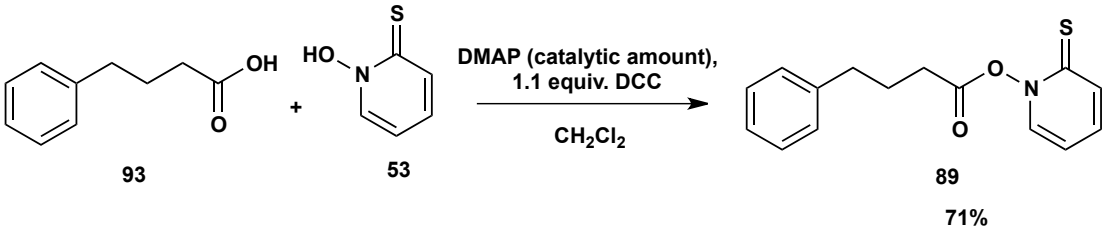
4.3.1 Intermolecular addition of 3-phenylpropyl radical (90) to methylacrylate (MA)

Scheme 4.9 illustrates the competition experiments that occur under the conditions when alkyl radical **90** was generated in the presence of 10 equivalents of *t*-BuSH and variety of MA concentrations with [MA]/[*t*-BuSH] ranging from 2-6.6 (MA was purchased from Sigma Aldrich and the stabiliser was removed by column purification).



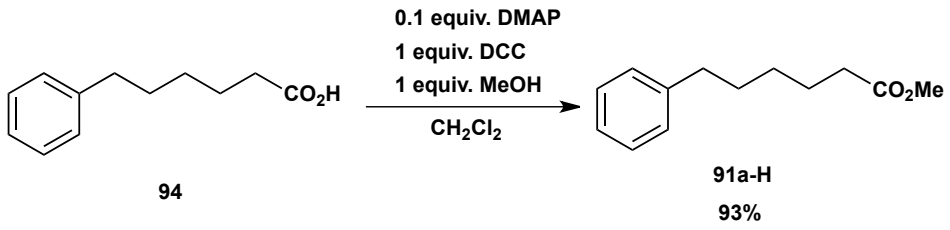
Scheme 4.9. Generation of the 3-phenyl propyl radical (**90**) and competing reaction through the addition of the radical **90** to MA and reduction through hydrogen abstraction from *t*-BuSH to produce **90-H**.

The PTOC ester **89** was prepared through the procedure described in Section 2.2.1 (Scheme 4.10), which was synthesised from commercially available 4-phenylbutanoic acid (**93**) in 71% yield. ^{1}H NMR data analysis in C_6D_6 showed the four aromatic hydrogen atoms at 5.5, 6.1, 6.5 and 7.5 ppm, 5 aromatic hydrogen atoms of the phenyl ring at 7.2 ppm and 6 aliphatic hydrogen atoms of the three aliphatic CH_2 at 2-2.5 ppm. The HRMS of **89** featured a peak at *m*/*z* 274.0894 $[M + H]^+$ consistent with the molecular formula of $C_{15}H_{15}NO_2S$.



Scheme 4.10. Synthesis of the PTOC ester **89**.

Ethyl 6-phenylhexanoate (**91-H**) was synthesised as a GC standard following the literature procedure (Scheme 4.11).[14] Treatment of 6-phenylhexanoicacid (**94**) with methanol was performed in the presence of 0.1 equivalents of DMAP and 1 equivalent of DCC in dichloromethane. Purification by column chromatography gave methyl 6-phenylhexanoate (**91a-H**) in 93% yield. The ^{1}H NMR spectrum displayed a singlet of methyl protons at 3.6 ppm and 5 aromatic hydrogen atoms at 7.2 ppm, with the other spectral data being similar to those found in the literature.[15]



Scheme 4.11. Synthesis of the methyl 6-phenylhexanoate (**91a-H**).

Competition kinetic experiments were carried out in benzene and $[EMIm][NTf_2]$ at 24 ± 1 °C. GC analysis of the reaction mixtures obtained from photolysis of the PTOC

ester **89**, revealed formation of three major products in both solvents. The directly reduced product **90-H** was identified using the authentic sample purchased from Sigma Aldrich. The product produced from the first addition reaction **91a-H** was prepared as described above. Since the product produced from the second addition reaction **92a-H** was difficult to access, the assignment of this compound was performed by GC-MS analysis of the crude reaction mixture, which displayed a signal showing the mass of 292.1.

The experiments were performed by employing a constant concentration of *t*-BuSH (10 equivalents) and variety of methylacrylate concentrations. It turned out that the proportion of the methyl acrylate and *t*-BuSH concentrations was very crucial in this experiment. Thus, at a very high ratio of [MA]/[*t*-BuSH] formation of higher oligomers could occur, whereas in the case of very low ratio of [MA]/[*t*-BuSH] direct reduction to product **90-H** could be the dominant pathway Therefore the experiments were performed with [MA]/[*t*-BuSH] ranging from 2-6.6, and the only products formed in detectable concentrations under these conditions are **90-H**, **91a-H** and **92a-H**. From the product distribution the ratio of the rate constants for two biomolecular processes *via* equation 1 can be obtained.

$$([\mathbf{91a\text{-}H}]+[\mathbf{92a\text{-}H}])/[\mathbf{90\text{-}H}]=k_{add}/k_H \times [\mathrm{MA}]/[t\text{-BuSH}] \quad (1)$$

The results of the competition experiment in benzene and [EMIm][NTf_2] are compiled in Table 4.5.

Table 4.5. GC results of the competition experiments for intermolecular addition of radical **90** to MA at 24 ± 1 °C.[a],[b],[c]

Solvent	[MA]/[*t*-BuSH]	[Add]/[90-H]
Benzene	2.0	0.036 ± 0.001
	3.0	0.050 ± 0.02
	4.0	0.064 ± 0.011
	6.0	0.099 ± 0.032
	6.6	0.095 ± 0.033
[EMIm][NTf_2]	2.0	0.068 ± 0.006
	3.0	0.083 ± 0.006
	4.0	0.093 ± 0.008
	5.0	0.092 ± 0.004
	6.0	0.099 ± 0.003
	6.6	0.110 ± 0.002

[a] Errors represent deviation from the average of three experiments (2σ). [b] [*t*-BuSH] = 0.1; [*t*-BuSH]/[**89**] = 10. [c] [Add] = [**91a-H**] + [**92a-H**].

According to the above equation, the products ratio versus of the [MA]/[*t*-BuSH] was plotted. The linearity of the data shown in Figure 4.3 provides confidence that the kinetic model shown in Scheme 4.9 is correct.

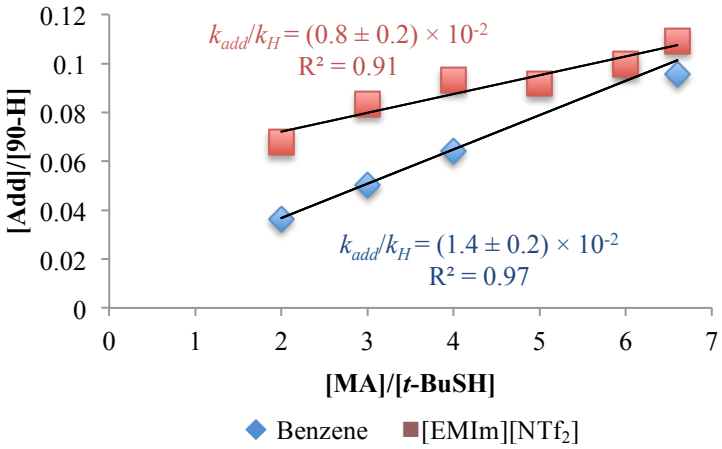


Figure 4.3. Dependence of [Add]/[**90-H**] on [MA]/[*t*-BuSH] at 24 ± 1°C for the addition of radical **90** to MA. [Add] = [**91a-H**] + [**92a-H**]. Uncertainties are calculated from the linear regression (2σ).

The addition of radical **90** to MA in [EMIm][NTf_2] can either occur within the solvent cage, caused by the anion and cation of the solvent or radical can escape from the solvent cage and reacts with another MA. Figure 4.3 shows that an increase in [MA] leads to a considerable acceleration of the radical addition in benzene, whereas in [EMIm][NTf_2] the [MA] effect on k_{add}/k_H is small. This result may be explained by the radical addition occurring within the solvent cage of the [EMIm][NTf_2] to a high extend, which is less dependent on the [MA].

From the slope of the lines the ratio of the rate constants (k_{add}/k_H) is $(1.4 \pm 0.2) \times 10^{-2}$ in benzene. Thus, using the literature rate coefficient for the reduction of primary C-centred radicals by *t*-BuSH of $k_H = (8.0 \pm 0.3) \times 10^6$ M^{-1} s^{-1} in THF,[12] the k_{add} for the addition rate constant of radical **90** to MA (**90 → 91a**) can be calculated as $(1.1 \pm 0.2) \times 10^5$ M^{-1} s^{-1}, which is sufficiently close to the reported rate constant for the addition of the primary *n*-pentyl radical to MA in neat MA at 25 °C ($k_{add} = 6.2 \times 10^5$ M^{-1} s^{-1}) as they are of the same order of magnitude.[15]

When the reactions performed in [EMIm][NTf_2] resulted a smaller k_{add}/k_H value of $(0.8 \pm 0.2) \times 10^{-2}$ that is almost half of the value obtained in benzene. With the rate coefficient for the reduction of primary C-centred radicals by *t*-BuSH of $k_H = (4.2 \pm 0.3) \times 10^7$ M^{-1} s^{-1} obtained in [EMIm][NTf_2] (measured in Chapter 2), the addition rate coefficient calculated as $(3.2 \pm 0.3) \times 10^5$ s^{-1}, which is about three times faster in the ionic liquid than in conventional organic solvents.

Unfortunately, the reaction temperature could not be increased beyond room temperature in benzene due to the generation of the higher oligomers in the reaction vessel, which could not be detected by gas chromatography. The temperature-dependent experiments in [EMIm][NTf_2] also produced a line with relatively large error of the activation parameters. The results of the competition experiments in [EMIm][NTf_2] are presented in Table 4.6 and the plot to determine the activation parameters is shown graphically in Figure 4.4.

Table 4.6. GC results of the competition experiments for the intermolecular addition of radical **90** to MA at different temperatures in [EMIm][NTf_2].[a],[b],[c]

T/°C	[MA]/[*t*-BuSH]	[Add]/[90-H]
23	4	0.093 ± 0.008
33	4	0.116 ± 0.002
45	4	0.125 ± 0.004
55	4	0.127 ± 0.005
60	4	0.148 ± 0.001
65	4	0.136 ± 0.007

[a] Errors represent deviation from the average of three experiments (2σ). [b] [*t*-BuSH] = 0.1; [*t*-BuSH]/[**89**] = 10. [c] [Add] = [**91a-H**] + [**92a-H**].

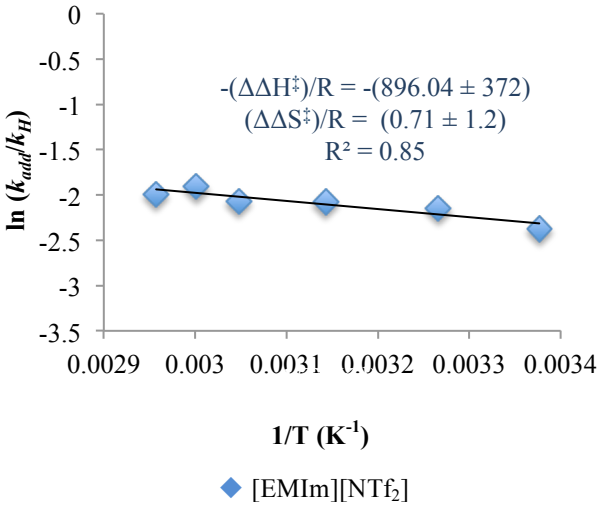


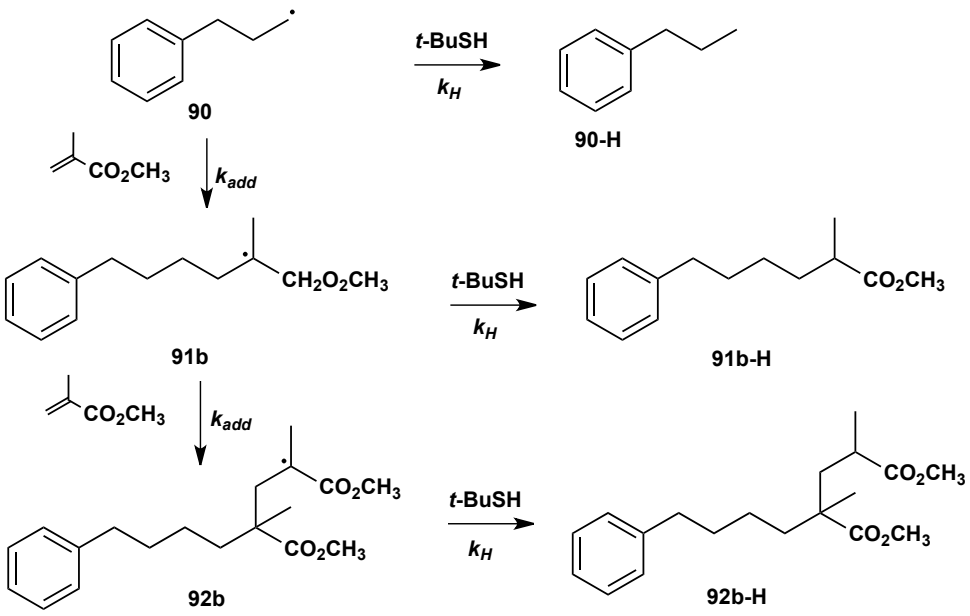
Figure 4.4. (ln (k_{add}/k_H)) *vs*.1/T for the addition of radical **90** to MA in [EMIm][NTf_2]. Uncertainties are calculated from the linear regression (2σ).

The data in Table 4.6 shows that [Add]/[90-H] increase by a factor of two in [EMIm][NTf_2] with increasing the temperature from 23 to 65 ^oC.

The values for $\Delta\Delta S^{\ddagger}$ of (5.9 ± 9.7) J mol^{-1} K^{-1} and $\Delta\Delta H^{\ddagger}$ of (7.5 ± 3.1) kJ mol^{-1} obtained in [EMIm][NTf_2] (Table 4.9). Due to the absence of the data in benzene, results could not be discussed for this reaction.

4.3.2 Intermolecular addition of 3-phenylpropyl radical (90) to methyl methacrylate (MMA)

Following the experimental methodology described in the previous section, the competition experiments for the addition of the 3-phenylpropyl radical **90** to MMA were performed in benzene and [EMIm][NTf_2] at 24 ± 1 °C (Scheme 4.12).



Scheme 4.12. Competition kinetic studies of the addition of the radical **90** to MMA and reduction through hydrogen abstraction from *t*-BuSH to produce **90-H**.

In this experiment the assignment of the products **91b-H** and **92b-H** produced from the first and second addition reactions was performed by GC-MS analysis of the crude reaction mixture. Formation of three major products in both benzene and [EMIm][NTf_2] occurred, which displayed a signal showing the mass of 220.1 and 320.2 respectively.

The results of the competition experiments are presented in Table 4.7 and the kinetic data for the k_{add}/k_H determination are shown in Figure 4.5.

Table 4.7. Results of the competition experiments for the intermolecular addition of radical **90** to MMA at 23 °C.[a],[b]

Solvent	[MMA]/[*t*-BuSH]	[Add][c]/[90-H]
Benzene	1.0	0.033 ± 0.002
	1.5	0.050 ± 0.005
	2.0	0.061 ± 0.002
	2.5	0.070 ± 0.001
	3.0	0.078 ± 0.003
[EMIm][NTf_2]	1.0	0.044 ± 0.005
	1.5	0.055 ± 0.007
	2.0	0.060 ± 0.010
	2.5	0.062 ± 0.010
	3.0	0.064 ± 0.011

[a] Errors represent deviation from the average of three experiments (2σ). [b] [*t*-BuSH] = 0.1; [*t*-BuSH]/[**89**] = 10. [c] [Add] = [**91b-H**] + [**92b-H**].

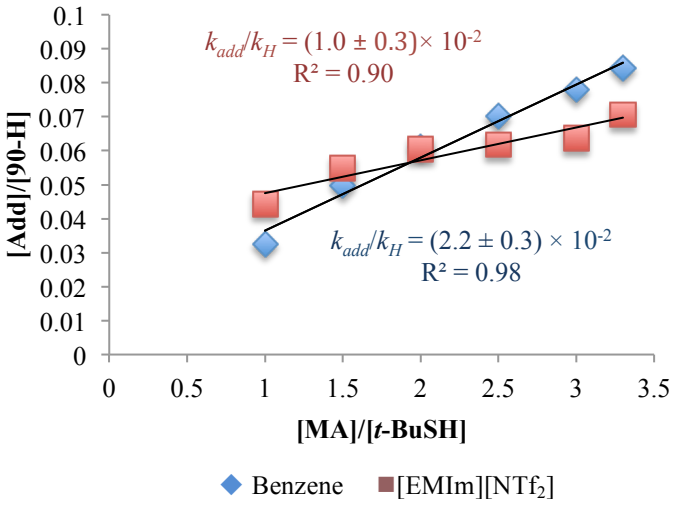


Figure 4.5. Dependence of [Add]/[**90-H**] on [MMA]/[*t*-BuSH] at 24 ± 1 °C for the addition of radical **90** to MMA. Uncertainties are calculated from the linear regression (2σ).

Figure 4.5 shows that [MMA] effect on k_{add} in benzene is larger than in [EMIm][NTf_2].

With k_{add}/k_H ratio of (2.2 ± 0.3) × 10^{-2} obtained in benzene, using the literature rate coefficient of k_H = (8.0 ± 0.3) × 10^6 M^{-1} s^{-1} in THF,[12] value for k_{add} of (1.8 ± 0.2) × 10^5 M^{-1} s^{-1} was calculated in benzene. In [EMIm][NTf_2] a k_{add}/k_H value of (1 ± 0.3) × 10^{-2} was obtained, leading to the rate coefficient for the addition of the radical **90** to MMA of k_{add} = (4.2 ± 0.4) × 10^5 M^{-1} s^{-1} in [EMIm][NTf_2], which is about two times faster than in benzene.

The results of the competition experiments at elevated temperatures are presented in Table 4.8. The plot to determine the Arrhenius parameters is shown in Figure 4.6.

Table 4.8. Results of the competition experiments for the intermolecular addition of radical **90** to MMA at different temperatures.[a],[b],[c]

Solvent	T/°C	[MMA]/[*t*-BuSH]	[Add]/[90-H]
Benzene	23	2	0.061 ± 0.002
	44	2	0.064 ± 0.002
	55	2	0.065 ± 0.003
	65	2	0.067 ± 0.003
	75	2	0.071 ± 0.001
[EMIm][NTf_2]	23	2	0.060 ± 0.010
	44	2	0.097 ± 0.006
	55	2	0.107 ± 0.005
	65	2	0.123 ± 0.004
	75	2	0.131 ± 0.028

[a] Errors represent deviation from the averaged from three experiments (2σ). [b] [*t*-BuSH] = 0.1. [c] [Add] = [**91b-H**] + [**92b-H**].

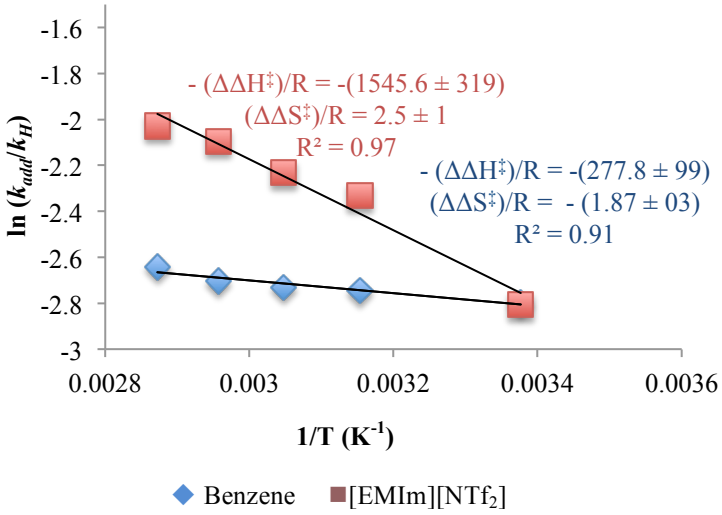


Figure 4.6. (ln (k_{add}/k_{Red})) *vs*.1/T for the addition of radical **90** to MMA in [EMIm][NTf_2] and benzene (R = 8.314 kJ mol^{-1}). Uncertainties are calculated from the linear regression (2σ).

The data in Table 4.8 reveal that an increase in temperature leads to a considerable increase of the addition rate of radical **90** to MMA in [EMIm][NTf_2], whereas in benzene the temperature effect on k_{add} is only small. This finding can be explained by the lower viscosity of [EMIm][NTf_2] at elevated temperature, which should enable faster diffusion of the reactants, and therefore, faster rate constant.

The values for $\Delta\Delta S^{\ddagger}$ of (20.5 ± 8.2) J mol^{-1} K^{-1} and $\Delta\Delta H^{\ddagger}$ of (12.9 ± 2.7) kJ mol^{-1} obtained in [EMIm][NTf_2] are bigger than those in benzene that are $\Delta\Delta S^{\ddagger}$ of (-15.5 ± 2.6) J mol^{-1} K^{-1} and $\Delta\Delta H^{\ddagger}$ of (2.3 ± 0.8) kJ mol^{-1}(Table 4.9). This trend is similar as for the intramolecular cyclisation of alkyl substituted 5-hexenyl radicals studied in chapter 3, indicating that the favourable entropy term is responsible for intermolecular addition rate enhancement of radical **90** in [EMIm][NTf_2] compared with in *t*-BuPh.

Table 4.9. Kinetic rate data for the addition of radical **90** to alkenes.[a]

Solvent	Alkene	k_{add}[b] (s^{-1})	$\Delta\Delta S^{\ddagger}$	$\Delta\Delta H^{\ddagger}$
		$\times 10^5$	(J mol^{-1} K^{-1})	(kJ mol^{-1})
Benzene	MA	1.1 ± 0.2	n.d	n.d
[EMIm][NTf_2]		4.2 ± 0.3	5.9 ± 9.7	7.5 ± 3.1
Benzene	MMA	1.8 ± 0.2	-15.5 ± 2.6	2.3 ± 0.8
[EMIm][NTf_2]		4.2 ± 0.4	20.5 ± 8.2	12.9 ± 2.7

[a] Errors are from the fit of the linear regression (2σ). [b] Determined from the slope of the line in Figure 4.3 and Figure 4.5, at 24 ± 1 °C.

4.4 Summary

In this chapter it was demonstrated that alkoxyl radical cyclisations, intramolecular homolytic substitutions as well as intermolecular addition of alkyl radical at electron-deficient alkenes could be successfully performed in ionic liquids with better or similar outcomes compared to the conventional organic solvents.

Through competition kinetic studies the intramolecular homolytic substitution on Se involving radical **78** was determined. Overall, these processes proceed faster by up to one order of magnitude in the ionic liquid than in organic solvents. From the Arrhenius parameters it appears that the rate accelerating effect is due to a favorable $\Delta S^{\ddagger}_C$ term, which can be rationalized by earlier, less-organised transition states of the radical cyclisation.

In the case of the electrophilic alkoxyl radical **82b**, unlike the nucleophilic alkyl radicals described in Chapter 1 and 2, the higher rate of the 5-*exo* cyclisation in [EMIm][NTf_2] was due to the enthalpy term $\Delta H^{\ddagger}_C$, which was more favourable in [EMIm][NTf_2] comparing to *t*-BuPh, which suggests more stable transition state for the 5-*exo* cyclisation of the O-centred radicals in [EMIm][NTf_2].

Furthermore, the rate of the intermolecular addition to double bond was also observed to be faster in ionic liquid comparing to organic solvent, which was due to favourable entropy term.

4.5 References

[1] Schiesser, C. H., *Chem. Commun.* **2006**, 4055.

[2] Selected examples: a) Hancock, A. N.; Lobachevsky, S.; Haworth, N. L.; Coote, M. L.; Schiesser, C. H., *Org. Biomol. Chem*. **2015**, *13*, 2310; b) Benjamin, L. J.; Schiesser, C. H.; Sutej, K., *Tetrahedron* **1993**, *49* 12, 2557; c) Hancock, A. N.; Kavanagh, Y.; Schiesser, C. H., *Org. Chem. Front*. **2014**, *1*, 645; d) Schiesser, C. H., *Chem. Commun*. **2006**, 4055.

[3] Hancock, A. N.; Kavanagh, Y.; Schiesser, C. H., *Org. Chem. Front.* **2014**, *1*, 645.

[4] Kang, Y.-B.; Chen, X.–M.; Yao, C.-Z.; Ning, X.-S.; X. *Chem. Commun.* **2016,** *52*, 6193.

[5] Levanova, E. P.; Grabel'nykh, V. A.; Elaev, A. V.; Russavskaya, N. V.; Klyba, L. V.; Albanov, A. I.; Korchevin, N. A., *Chem. Heterocycl. Compd.* **2012,** *4*, 1345.

[6] Fröba, A. P.; Kremer, H.; Leipertz, A., *J. Phys. Chem. B* **2008**, *112*, 12420.

[7] Hartung, J.; Gallou, F., *J. Org. Chem.* **1995**, *60*, 6706.

[8] Hay, B. P.; Beckwith, A. L. J., *J. Org. Chem.* **1989**, *54*, 4330.

[9] Giese, B., *Angew Chem. Int. Ed. Engl.* **1983**, *22*, 753.

[10] Caronna, T.; Citterio, A.; Ghirardini, M.; Minisci, F., *Tetrahedron* **1977**, *33*, 793.

[11] Tedder, J. M.; Walton, J. C, *Acc. Chem. Res.* **1976**, *9*, 183-191.

[12] Newcomb, M;. Glenn, A. G.; Manek, M. B., *J. Org. Chem.* **1989**, *54*, 4603.

[13] Beckwith, A. L. J.; Poole, J. S., *J. Am. Chem. Soc.* **2002**, *124*, 9489.

[14] Alliot, J.; Gravel, E.; Doris, E., Synthesis **2013**, *45*, 2861.

[15] Topley, A. C.; Isoni, V.; Logothetis,T. A.; Wynn, D.; Wadsworth, H.; Gibson, A. M. R.; Khan, I.; Wells, N. J.; Perrio, C.; Brown, R. C. D., *Eur. J. Chem.* **2013**, *19*, 1720.

5 Conclusion and perspective

5.1 Conclusion

Free radical chemistry has become extensively used for preparation of complex molecules. There is need for green alternative solvents to perform radical reactions. Ionic liquids are green alternatives to traditional organic solvents. In this study intramolecular homolytic additions of alkyl- and alkoxyl radicals, intramolecular homolytic substitutions as well as intermolecular homolytic additions to alkene have been shown that can be successfully performed in ionic liquids with similar to better outcomes. Competition-kinetic studies, using [EMIm][NTf_2] as an example of a frequently used ionic liquid, revealed that the rates of cyclisation at room temperature are generally greater in the ionic liquid by up to 60%, depending on the nature of the radical. Generally, this is due to the favourable $\Delta S^{\ddagger}_{C}$ term for all radicals, which suggests a less-organised transition state for cyclisation, compared to the reactions in conventional organic solvents. While ionic liquid did not affect the stereo-selectivity of the reactions.

Lowering the viscosity of [EMIm][NTf_2] by performing the reaction at elevated temperatures leaded to a significant acceleration of the cyclisation rate, in contrast to conventional organic solvents, where the temperature effect was much less pronounced.

No interfering reactions between [EMIm][NTf_2] and radical intermediates were observed. All products were quantitatively extracted from the ionic liquid phase, which can be directly reused without purification. Studies on radical cyclisations and intramolecular homolytic substitutions clearly showed that ionic liquids can be used as a suitable alternative media for radical reactions when conventional organic solvents may be problematic.

5.2 Future directions

A number of interesting questions have been provoked as a result of the work described in this thesis and will provide some solid grounds for future work in this area.

i. Can radical cyclisation reaction be done in a more viscous IL, *e.g.,* [BMIm][NTf_2]?
ii. How does this medium affect the reaction outcome and efficiency?
iii. Is it possible to synthesise a bioactive compound in IL through the cascade radical synthesis?
iv. Can radical cyclisation reaction be done in glycerol as another green solvent?

6 Experimental

6.1 General materials, equipment and methods

Unless otherwise stated, all starting materials, reagents and HPLC grade solvents were purchased from commercial sources and used without further purification. The reactions were carried out under argon atmosphere in oven-dried glassware. Ethanol was dried by distillation over magnesium. Tetrahydrofuran, dichloromethane and diethyl ether were dried using the Glass Contour solvent system.

Solvent removal *'in vacuo'* refers to distillation using a rotary evaporator attached to a vacuum pump. Analytical TLC was performed on Merck aluminium-backed 2 μm thick silica gel plates (Kieselgel 60 GF_{254}). Compounds were visualised under a 254 nm UV lamp or by staining with $KMnO_4$ (0.063 M $KMnO_4$, 0.48 M K_2CO_3 and 0.021 M NaOH in H_2O), phosphomolybdic acid (PMA) (30 mM in ethanol) or bromocresol green (solution of 0.04 g bromocresol green in 100 mL absolute ethanol was added dropwise into a 0.1 M solution of NaOH until the solution becomes pale blue). Scharlau silica gel 60 (particle size 0.04 × 0.06 mm) was used for column chromatography.

NMR spectra were recorded on an Agilent MR400 (^{1}H NMR: 400 MHz, ^{13}C NMR: 100 MHz) or Agilent DD2 (^{1}H NMR: 500 MHz, ^{13}C NMR: 126 MHz, ^{77}Se NMR 95 MHz) in deuterated chloroform ($CDCl_3$) or benzene (C_6D_6) as indicated at 25.0 °C. Chemical shifts (δ) are reported in parts per million (ppm) relative to either $CDCl_3$ (^{1}H NMR: 7.26 ppm; ^{13}C NMR: 77.0 ppm) or C_6D_6 (^{1}H NMR: 7.66 ppm; ^{13}C NMR: 128.06 ppm). ^{1}H NMR spectral data are reported as follows: chemical shift (δ), relative integral, multiplicity, and coupling constant/s (*J*) in Hertz (Hz, if any).

High resolution mass spectroscopy (HRMS) was conducted on a Finnigan hybrid linear triple-quadrupole (LTQ) Fourier Transform ion cyclotron resonance (FTICR) mass spectrometer. Parent ions are denoted by $[M + H]^+$.

Analytical GC experiments were performed using a Shimadzu GC 17-A fitted with very non-polar SPB®-Octyl Capillary GC column (SGE) (L × I.D. 30 m × 0.32 mm,

d_f 0.25 μm) or Agilent GC/Mass (EI, 70 eV), fitted with HP-5ms (L × I.D. 30 m × 0.25 mm, d_f 0.25 μm) capillary column.

6.2 Synthesis library

6.2.1 Synthesis of the acids 47a-d and 66a-d

6-Heptenoic acid (47a)

*Diethyl hex-5-ene-1,1-dicarboxylate (**46**)*:[1] To a mixture of sodium hydride (0.5 g, 21.0 mmol) and anhydrous dimethylformamide (20 mL) under argon atmosphere was added dropwise diethyl malonate (**45**, 3.0 g, 18.8 mmol), and the reaction mixture was stirred at room temperature until evolution of hydrogen gas ceased. 5-Bromopent-1-ene (2.9 g, 19.5 mmol) was added and the reaction mixture stirred for 1 hour at 70 ^{o}C. The reaction was quenched by addition of water (200 mL) and extracted with diethyl ether (3 x 50 mL). The combined organic extracts were dried over magnesium sulfate and the solvent was removed *'in vacuo'*. Purification by column chromatography (SiO_2, 95:5 Pet. ether/EtOAc) afforded the intermediate **46** as a colourless oil (2.6 g, 62%), which was directly used in the next step. ^{1}H NMR (400 MHz, $CDCl_3$): δ 5.74-5.81 (1H, m), 4.95-5.03 (2H, m), 4.19 (4H, qd, ^{3}J = 2.7, 7.1 Hz), 3.32 (1H, t, ^{3}J = 7.5 Hz), 1.40-2.10 (6H, m), 1.26 ppm (6H, t, ^{3}J = 7.1 Hz). ^{13}C NMR (100 MHz, $CDCl_3$): 169.44, 137.93, 114.97, 61.26, 51.90, 33.25, 28.16, 26.52, 14.06 ppm.

*6-Heptenoic acid (**47a**)*:[2] Decarboxylation of diethyl ester **46** (8.7 mmol, 2.0 g) was performed according to the literature procedure.[3] Compound **46** was hydrolysed by dissolving it in a solution of potassium hydroxide (1.5 g, 27.3 mmol) in water (12 mL)/ethanol (24 mL), and then decarboxylated by heating to 150-160 °C. Acid **47a** was obtained as a yellow oil (0.8 g, 74%). ^{1}H NMR (400 MHz, $CDCl_3$): 5.76-5.86 (1H, m), 4.96-5.05 (2H, m), 2.38 (2H, t, ^{3}J = 7.5 Hz), 2.07-2.12 (2H, m), 1.64-1.71 (2H, m), 1.43-1.50 ppm (2H, m).

7,7-Diphenyl-6-hexenoic acid (47b):[4] This compound was prepared according to the literature procedure[5] from 6-bromohexanoic acid (1.7 g, 9.0 mmol), triphenyl phosphine (2.4 g, 9.0 mmol) in benzene (15 mL). The resulting (5-carboxypentyl) triphenylphosphonium bromide **48** (4.0 g, 9.0 mmol) was then reacted with *n*-butyllithium (9.0 mL, 18.0 mmol, 2 M in hexane) and benzophenone (1.6 g, 9.0 mmol) in anhydrous tetrahydrofuran (10 mL). The reaction was quenched by addition of water (20 mL) and washed with diethyl ether (3 x 10 mL) to remove unreacted starting materials. The solution was then acidified with concentrated hydrochloric acid and extracted with diethyl ether (3 x 10 mL). The solvent was removed *'in vacuo'* to afford acid **47b** as a white solid (2.2 g, 89%). ^{1}H NMR (400 MHz, $CDCl_3$): 7.16-7.38 (10H, m), 6.06 (1H, t, ^{3}J = 7.5 Hz), 2.31 (2H, t, ^{3}J = 7.4 Hz), 2.14 (2H, dd, ^{3}J = 7.4 Hz, 14.8 Hz), 1.61-1.67 (2H, m), 1.53-1.47 ppm (2H, m).

4,4-Bis(ethoxycarbonyl)hept-6-enoic acid (47c)

1-t-*Butyl-3,3-diethyl hex-5-ene-1,3,3-tricarboxylate (**50**):* Diethyl malonate (**45**, 3.0 g, 18.8 mmol) was added to a suspension of sodium hydride (0.5 g, 20.8 mmol) in dimethylformamide (20 mL), and the mixture was stirred under argon until evolution of hydrogen gas ceased. *t*-Butyl 3-bromopropionate (4.0 g, 19.5 mmol) was added and the resulting mixture heated at 80 °C for 2 hours. After cooling the reaction mixture was poured into water (50 mL), extracted with diethyl ether (3 x 20 mL), dried over magnesium sulfate, and the solvent was removed *'in vacuo'*. Purification by column chromatography (SiO_2, 97:3 Pet. ether/EtOAc) gave compound **49** (4.1 g, 76%). The intermediate **49** (4.1 g, 14.2 mmol) was then reacted with sodium hydride (0.4 g, 16.2 mmol) and allyl bromide (1.8 g, 15.2 mmol) in dimethylformamide (20 mL) similar to the procedure above. The ester **50** was obtained after purification by column chromatography (SiO_2, 97:3 Pet. ether/EtOAc) as colourless oil (3.8 g, 81%). ^{1}H NMR (400 MHz, $CDCl_3$): 5.61-5.71 (1H, m), 5.08-5.13 (2H, m), 4.12-4.21 (4H, m), 2.62 (2H, d, ^{3}J = 7.4 Hz), 2.12-2.23 (4H, m), 1.42 (9H, s), 1.24 ppm (6H, t, ^{3}J = 7.1 Hz). ^{13}C NMR (100 MHz, $CDCl_3$): 172.7, 171.47, 132.80, 119.85, 81.10, 61.95, 57.35, 38.16, 31.21, 28.71, 28.32, 14.73 ppm. HRMS (ESI) *m*/*z* calcd. for $[C_{17}H_{28}O_6]^{+}$: 329.1959 $[M + H]^{+}$, found 329.1956.

*4,4-Bis(ethoxycarbonyl)hept-6-enoic acid (**47c**):* The acid **47c** was obtained according to the literature procedure[6] through treatment of the ester **50** (3.8 g, 11.5 mmol) with

trifluoroacetic acid (3 mL) in dichloromethane (3 mL) as a white solid (3.3 g, 90%). ^{1}H NMR (400 MHz, $CDCl_3$): 5.61-5.71 (1H, m), 5.10-5.15 (2H, m), 4.13-4.25 (4H, m), 2.65 (2H, d, ^{3}J = 7.4 Hz), 2.37-2.41 (2H, m), 2.18-2.22 (2H, m), 1.25 ppm (6H, t, ^{3}J = 7.1 Hz). ^{13}C NMR (100 MHz, $CDCl_3$): 177.54, 170.50, 131.79, 119.28, 61.29, 56.33, 37.60, 28.84, 27.20, 13.90 ppm. HRMS (ESI) *m*/*z* calcd. for $[C_{13}H_{20}O_6]^+$: 273.1332 $[M + H]^+$, found 273.1333.

3,3-Bis(ethoxycarbonyl)hept-6-enoic acid (**47d**)

1-t-*Butyl 2,2-diethylhex-5-ene-1,2,2-tricarboxylate (**52**):* Diethyl malonate **45** (3.0 g, 18.8 mmol) was treated with 4-bromobutene (2.5 g, 18.5 mmol) similar to the synthesis of diester **46**, to yield the diester **51** as a colourless oil (3.1 g, 75%). Diester **51** was subsequently treated with *t*-butyl bromoacetate (2.7 g, 13.7 mmol) as described for the synthesis of the intermediate **46** to produce tricarboxylate **52** as a colourless oil (2.6 g, 76%) after column chromatography (SiO_2, 95:5 Pet. ether/EtOAc). ^{1}H NMR (500 MHz, $CDCl_3$): 5.73-5.82 (1H, m), 4.95-5.05 (2H, m), 4.20 (4H, q, ^{3}J = 7.1 Hz), 2.9 (2H, s), 1.98-2.10 (4H, m), 1.42 (9H, s), 1.25 ppm (6H, t, ^{3}J = 7.1 Hz). ^{13}C NMR (100 MHz, $CDCl_3$): 170.52, 137.51, 115.31, 81.31, 61.61, 55.49, 38.85, 32.33, 28.81, 28.11, 14.16 ppm. HRMS (ESI) *m*/*z* calcd. for $[C_{17}H_{28}O_6]^+$: 329.1959 $[M + H]^+$, found 329.1957.

*3,3-Bis(ethoxycarbonyl)hept-6-enoic acid (**47d**):* Following the literature procedure,[6] compound **47d** was obtained from tricarboxylate **52** (4.0 g, 12.1 mmol,) through treatment with trifluoroacetic acid (3 mL) in dichloromethane (3 mL) as a yellow oil (2.8 g, 86%). ^{1}H NMR (400 MHz, $CDCl_3$): 5.71-5.81 (1H, m), 4.97-5.06 (2H, m), 4.21 (4H, q, ^{3}J = 7.0Hz), 3.03 (2H, s), 1.99-2.14 (4H, m), 1.25 ppm (6H, t, ^{3}J = 7.1 Hz). ^{13}C NMR (100 MHz, $CDCl_3$): 175.00, 170.16, 137.01, 115.42, 61.79, 55.17, 37.18, 32.42, 28.70, 13.92 ppm. HRMS (ESI) *m*/*z* calcd. for $[C_{13}H_{20}O_6S]^+$: 273.1332 $[M + H]^+$, found 273.1333.

2-Methyl-6-heptenoic acid (66a)

*Diethyl 1-methylhex-5-ene-1,1-dicarboxylate (**65a**):* Diethyl ester **46** (3.0 g, 13.0 mmol) was treated with methyl iodide (1.2 g, 14.0 mmol) similar to the synthesis of compound **46**, to yield the diester **65a** as a colourless oil (2.6 g, 82%).^{1}H NMR (400 MHz, $CDCl_3$): 5.73-5.83 (1H, m), 4.94-5.04 (2H, m), 4.17 (4H, q, ^{3}J = 7.1 Hz), 2.06

(2H, q, ^3J = 7.2 Hz), 1.86-1.88 (2H, m), 1.4 (3H, s), 1.24 ppm (6H, t, ^3J = 7.1 Hz). ^{13}C NMR (100 MHz, $CDCl_3$): 172.65, 138.4, 115.11, 61.35, 53.83, 35.24, 34.07, 23.85, 20.11, 14.29 ppm. HRMS (ESI) *m*/*z* calcd. for $[C_{13}H_{22}O_4]^+$: 243.1590 $[M + H]^+$, found 243.1591.

2-Methyl-6-heptenoic acid ***(66a):***[7] Decarboxylation of diethyl ester **65a** (2.0 g, 8.3 mmol) was performed similar to the procedure described for the decarboxylation of diester **46**. The acid **66a** was obtained as a yellow oil (0.9 g, 76%). ^{1}H NMR (400 MHz, $CDCl_3$): 5.76 (1H, m), 4.99 (2H, m), 2.47 (1H, m), 2.07 (2H, m), 1.40-1.74 (4H, m), 1.19 ppm (3H, m). ^{13}C NMR (100 MHz, $CDCl_3$): 183.02, 138.92, 115.29, 39.7, 34.11, 33.49, 26.93, 17.39 ppm. HRMS (ESI) *m*/*z* calcd. for $[C_8H_{14}O_2]^+$: 143.10666 $[M + H]^+$, found 143.10674.

2-Ethylhept-6-enoic acid (66b)

Diethyl 1-ethylhex-5-ene-1,1-dicarboxylate ***(65b)****:* Diester **46** (3.0 g, 13.0 mmol,), was treated with ethyl iodide (2.2 g, 14.0 mmol) similar to the synthesis of compound **46**, to yield the diester **65b** as a colourless oil (2.7 g, 80%). ^{1}H NMR (400 MHz, $CDCl_3$): 5.73-5.83 (1H, m), 4.95-5.04 (2H, m), 4.18 (4H, q, ^3J = 7.1 Hz), 2.06 (2H, q, ^3J = 7.2 Hz), 1.86.1.96 (4H, m), 1.21-1.30 (8H, m), 0.82 ppm (3H, t, ^3J = 7.6 Hz). ^{13}C NMR (100 MHz, $CDCl_3$): 171.80, 138.13, 114.88, 60.93, 57.84, 33.80, 31.08, 25.19, 23.25, 14.09, 8.39 ppm. HRMS (ESI) *m*/*z* calcd. for $[C_{14}H_{24}O_4]^+$: 257.1747 $[M + H]^+$, found 257.1749.

2-Ethylhept-6-enoic acid ***(66b)****:* Decarboxylation of diester **65b** (2.0 g, 8.0 mmol) was performed similar to the procedure described for the decarboxylation of diester **46**. The acid **66b** was obtained as a yellow oil (0.9 g, 78%). ^{1}H NMR (400 MHz, $CDCl_3$): 5.74-5.82 (1H, m), 4.94-5.04 (2H, m), 2.26-2.32 (1H, m), 2.04-2.09 (2H, m), 1.37-1.72 (6H, m), 0.94 ppm (3H, t, ^3J = 7.4 Hz). ^{13}C NMR (100 MHz, $CDCl_3$): 138.36, 114.7, 46.85, 33.57, 31.11, 26.54, 25.15, 11.71 ppm. HRMS (ESI) *m*/*z* calcd. for $[C_9H_{16}O_2]^+$: 157.1223 $[M + H]^+$, found 157.1224.

2-Isopropyl-6-heptenoic acid (66c)

Diethyl 1-isopropylhex-5-ene-1,1-dicarboxylate ***(65c)***: Diester **46** (3.0 g, 13.2 mmol) was treated with isopropyl iodide (2.4 g, 14.0 mmol) similar to the synthesis of

diester **46,** to yield the diester **65c** as a colourless oil (2.7 g, 77%). ^{1}H NMR (400 MHz, $CDCl_3$): 5.73-5.84 (1H, m), 4.95-5.05 (2H, m), 4.20 (4H, q, ^{3}J = 7.1 Hz), 2.82 (2H, d, ^{3}J = 2.6 Hz), 2.04-2.12 (4H, m), 1.99 (1H, t, ^{3}J = 2.6 Hz), 1.23-1.33 ppm (5H, m). ^{13}C NMR (100 MHz, $CDCl_3$): 171.20, 138.21, 114.81, 61.56, 60.62, 33.98, 33.19, 31.84, 23.90, 18.57, 14.15 ppm. HRMS (ESI) *m*/*z* calcd. for $[C_{15}H_{26}O_4]^+$: 271.19039 $[M + H]^+$, found 271.19045.

*2-Isopropyl-6-heptenoic acid **(66c)*:** Decarboxylation of diester **65c** (2.0 g, 8.0 mmol) was performed similar to the procedure described for the decarboxylation of diester **46**. compound **66c** was obtained as a yellow oil (0.8 g, 66%). ^{1}H NMR (400 MHz, $CDCl_3$): 5.76-5.82 (1H, m), 4.94-5.03 (2H, m), 1.36-2.16 (8H, m), 0.96-0.97 ppm (6H, m). ^{13}C NMR (100 MHz, $CDCl_3$): 138.38, 114.67, 52.26, 33.6, 30.41, 28.71, 26.94, 20.42, 20.05 ppm. HRMS (ESI) *m*/*z* calcd. for $[C_{10}H_{18}O_2]^+$: 171.1379 $[M + H]^+$, found 171.1380.

2-*t*-Butyl-6-heptenoic acid (66d)

t-*Butylacetic acid* **(67)** (1.0 g, 8.6 mmol) was treated with 5-bromo-1-pentene (1.3 g, 9.0 mmol) according to literature[8] to obtain compound **66d** as a yellow oil (1.3 g, 85%). ^{1}H NMR (400 MHz, $CDCl_3$): 5.74-5.84 (1H, m), 4.94-5.03 (2H, m), 2.42 (1H, dd, ^{3}J = 11.7, 2.6 Hz), 2.05-2.11 (2H, m), 1.27-1.70 (4H, m), 0.99 ppm (9H, s). ^{13}C NMR (100 MHz, $CDCl_3$): 180.44, 138.37, 114.67, 55.95, 33.57, 32.70, 27.78, 27.62, 26.96 ppm. HRMS (ESI) *m*/*z* calcd. for $[C_{11}H_{20}O_2]^+$: 185.1536 $[M + H]^+$, found 185.1537.

6.2.2 Synthesis of the PTOC esters (43a-d) and (62a-d)

The acids **47a-d** and **66a-d** were converted to the respective PTOC esters through reaction with thiohydroxamic acid **53**, as described in the literature.[9] Due to instability of the PTOC esters melting point could not be obtained.

1-[[(5-Hexenyl)carbonyl]oxy]-2(1*H*)-pyridinethione (43a): Green viscous liquid (0.2 g, 30%). ^{1}H NMR (400 MHz, C_6D_6): 7.44 (1H, dd, ^{3}J = 1.8, 8.9 Hz), 6.46 (1H, dd, ^{3}J = 0.6, 7.0 Hz), 6.01- 6.05 (1H, m), 5.61-5.69 (1H, m), 5.40-5.42 (1H, m), 4.94-5.00 (2H, m), 2.35 (2H, t, ^{3}J =7.5 Hz), 1.81- 1.87 (2H, m), 1.53-1.61 (2H, m), 1.19-

1.27 ppm (2H, m). ^{13}C NMR (126 MHz, C_6D_6): 168.8, 138.4, 137.6, 137, 132.3, 115.2, 110.9, 33.6, 31.7, 28.4, 24.1 ppm. HRMS (ESI) *m*/*z* calcd. for $[C_{12}H_{15}NO_2S]^+$: 238.08963 $[M + H]^+$, found 238.08948.

1-[[(6,6-Diphenyl-5-hexenyl)carbonyl]oxy]-2(1*H*)-pyridinethione (43b): Yellow solid (0.7 g, 53 %). ^{1}H NMR (400 MHz, C_6D_6): 7.43 (1H, dd, ^3J = 2.0, 9.1 Hz), 7.14 (10H, m), 7.3-7.32 (1H, m), 6.46 (1H, dd, ^3J = 7.0 Hz), 6.00-6.04 (1H, m), 5.38-5.40 (1H, t, ^3J = 6.9 Hz), 2.31 (2H, t, ^3J = 7.4 Hz), 2.03 (2H, q, ^3J = 7.4 Hz), 1.52-1.58 (2H, m), 1.28-1.34 ppm (2H, m). ^{13}C NMR (126 MHz, C_6D_6): 176.9, 168.8, 143.2, 142.9, 140.7, 137.7, 137, 132.2, 130.3, 129.4, 127.3, 31.6, 29.6, 29.4, 24.1 ppm. HRMS (ESI) *m*/*z* calcd. for $[C_{24}H_{23}NO_2S]^+$: 390.15223 $[M + H]^+$, found 390.15192.

1-[[(4,4-Bis(ethoxycarbonyl)-5-hexenyl)carbonyl]oxy]-2(1*H*)-pyridinethione (43c): Yellow solid (50%). ^{1}H NMR (500 MHz, C_6D_6): 7.40-7.42 (1H, m), 6.6 (1H, dd, ^3J = 1.5, 7.0 Hz), 6.01- 6.04 (1H, m), 5.67-5.72 (1H, m), 5.40-5.43 (1H, m), 4.97-5.01 (2H, m), 3.94 (2H, q, ^3J = 7.1 Hz), 2.91- 2.94 (2H, m), 2.75-2.76 (2H, m), 2.55-2.58 (2H, m), 0.91 ppm (6H, t, ^3J = 7.1 Hz). Due to the instability of this compound a ^{13}C NMR could not be obtained. HRMS (ESI) *m*/*z* calcd. for $[C_{18}H_{23}NO_6S]^+$: 382.13188 $[M + H]^+$, found 382.13200.

1-[[(3,3-Bis(ethoxycarbonyl)-5-hexenyl)carbonyl]oxy]-2(1*H*)-pyridinethione (43d): Yellow solid (0.8 g, 61 %). ^{1}H NMR (500 MHz, C_6D_6): 7.39 (1H, ddd, ^3J = 8.8, 1.8, 0.6 Hz), 6.72 (1H, ddd, ^3J = 7.0, 1.6, 0.6 Hz), 6.00-5.96 (1H, m), 5.72 (1H, ddt, ^3J = 16.8,10.2, 6.6 Hz), 5.35 (1H, td, ^3J = 6.9, 1.8 Hz), 5.07 (1H, dq, ^3J = 17.1, 1.6 Hz), 4.93 (1H, dq, ^3J = 10.2, 1.3 Hz), 3.98 (4H, q, ^3J = 7.1 Hz), 3.47 (2H, s), 2.43-2.37 (2H, m), 2.18-2.11 (2H, m), 0.92 ppm (6H, t, ^3J = 7.1 Hz). Due to the instability of this compound a ^{13}C NMR could not be obtained. HRMS (ESI) *m*/*z* calcd. for $[C_{18}H_{23}NO_6S]^+$: 382.1319 $[M + H]^+$, found 382.1324.

1-[[(1-Methyl-5-hexenyl)carbonyl]oxy]-2(1*H*)-pyridinethione (62a): Yellow viscous liquid (1.0 g, 64%). ^{1}H NMR (500 MHz, C_6D_6): 7.38-7.40 (1H, m), 6.40-6.42 (1H, m), 5.97-5.99 (1H, m), 5.63-5.72 (2H, m), 5.35-5.36 (1H, m), 4.93-4.99 (1H, m), 2.55-2.59 (1H, m), 1.86-1.89 (2H, m), 1.75-1.78 (1H, m), 1.30-1.34 (3H, m), 1.17 ppm (3H, d, ^3J = 7.0 Hz). ^{13}C NMR (126 MHz, C_6D_6): 176.24, 171.56, 137.98,

137.47, 136.97, 131.48, 114.56, 110.33, 37.43, 33.17, 32.43, 26.20, 16.47 ppm. HRMS (ESI) *m*/*z* calcd. for $[C_{13}H_{17}NO_2S]^+$: 252.10528 $[M + H]^+$, found 251.92429.

1-[[(1-Ethyl-5-hexenyl)carbonyl]oxy]-2(1*H*)-pyridinethione (62b): Yellow viscous liquid (1.4 g, 82%). ^{1}H NMR (500 MHz, C_6D_6): 7.46-7.48 (1H, m), 6.61-6.63 (1H, m), 6.11-6.14 (1H, m), 5.73-5.80 (1H, m), 5.49-5.52 (1H, m), 5.00-5.09 (2H, m), 2.53-2.58 (1H, m), 1.42-2.1 (8H, m), 0.95 ppm (3H, t, ^3J = 7.5 Hz). ^{13}C NMR (126 MHz, C_6D_6): 177.11, 171.64, 138.63, 137.9, 137.43, 132.34, 115.25, 111.17, 44.94, 34.0, 31.09, 26.91, 25.28, 11.98 ppm. HRMS (ESI) *m*/*z* calcd. for $[C_{14}H_{19}NO_2S]^+$: 266.12093 $[M + H]^+$, found 266.12065.

1-[[(1-Isopropyl-5-hexenyl)carbonyl]oxy]-2(1*H*)-pyridinethione (62c): Yellow viscous liquid (0.9 g, 75%). ^{1}H NMR (500 MHz, C_6D_6): 7.45-7.47 (1H, m), 6.57-6.59 (1H, m), 6.01-6.05 (1H, m), 5.74-5.81 (1H, m), 5.39-5.42 (1H, m), 4.98-5.05 (2H, m), 2.47-2.51 (1H, m), 1.44-2.15 (7H, m), 0.95 ppm (3H, dd, ^3J = 6.8, 13.5 Hz). Due to the instability of this compound a ^{13}C NMR could not be obtained. HRMS (ESI) *m*/*z* calcd. for $[C_{15}H_{21}NO_2S]^+$: 280.13658 $[M + H]^+$, found 280.13663.

1-[[(1-*t*-Butyl-5-hexenyl)carbonyl]oxy]-2(1*H*)-pyridinethione (62d): Yellow viscous liquid (0.8 g, 78%). ^{1}H NMR (500 MHz, C_6D_6): 7.46-7.48 (1H, m), 6.68 (1H, d, ^3J = 7.0 Hz), 6.01-6.04 (1H, m), 5.79-5.85 (1H, m), 5.39-5.42 (1H, m), 5.00-5.11 (2H, m), 2.44 (1H, dd, ^3J = 2.7, 11.4 Hz), 1.42-2.1 (6H, m), 0.96 ppm (9H, s). Due to the instability of this compound the ^{13}C NMR spectrum could not be obtained. HRMS (ESI) *m*/*z* calcd. for $[C_{16}H_{23}NO_2S]^+$: 294.15223 $[M + H]^+$, found 294.14713.

6.2.3 Synthesis of the radical precursor 70 and 77

2-(2-Propynyl)-6-heptenoic acid (75)

Diethyl 1-propargylhex-5-ene-1,1-dicarboxylate (74): Diester **74** was synthesised similar to the synthesis of diester **46**, using diester **46** (3.0 g, 13.2 mmol), propargyl bromide (1.6 g, 14.0 mmol), sodium hydride (0.36 g, 15.0 mmol) in DMF (20 mL). After purification by column chromatography (SiO_2, 5:95 Pet. ether/EtOAc) compound **74** was obtained as colourless oil (2.6 g, 75%). ^{1}H NMR (400 MHz, $CDCl_3$): 5.73-5.84 (1H, m), 4.95-5.05 (2H, m), 4.20 (4H, q, ^3J = 7.1 Hz), 2.82 (2H, d,

^{3}J = 2.6 Hz), 2.04-2.12 (2H, m), 1.99 (1H, t, ^{3}J = 2.6 Hz), 1.23-1.33 ppm (8H, m). ^{13}C NMR (100 MHz, $CDCl_3$): 170.44, 138.13, 115.14, 79.1, 71.34, 61.7, 56.87, 33.84, 31.48, 23.41, 22.88, 14.21 ppm. HRMS (ESI) *m*/*z* calcd. for $[C_{15}H_{22}O_4]^+$: 267.1590 $[M + H]^+$, found: 267.1591.

*2-(2-Propynyl)-6-heptenoic acid (**75**):* Decarboxylation of compound **74** (2.0 g, 7.5 mmol) was performed similar to the procedure described for decarboxylation of diester **46** to yield the carboxylic acid **75** as a yellow oil (0.9 g, 75%). ^{1}H NMR (400 MHz, $CDCl_3$): 5.74-5.84 (1H, m), 4.96-5.04 (2H, m), 2.6-2.66 (1H, m), 2.54 (1H, ddd, ^{3}J = 2.5, 6.9, 16.7 Hz), 2.43 (1H, ddd, ^{3}J = 2.5, 6.8, 16.8 Hz), 2.09 (2H, dd, ^{3}J = 7.1,14.2 Hz), 2.02 (1H,t, ^{3}J = 2.4 Hz), 1.65-1.78 (2H, m), 1.4-1.52 ppm (2H, m). ^{13}C NMR (100 MHz, $CDCl_3$): 179.46, 138.06, 114.94, 81.03, 70.07, 43.97, 33.41, 30.38, 26.01, 20.77 ppm. HRMS (ESI) *m*/*z* calcd. for $[C_{10}H_{14}O_2]^+$: 167.1067 $[M + H]^+$, found 167.1067.

1-[[(1-(2-Propynyl)-5-hexenyl)carbonyl]oxy]-2(1*H*)-pyridinethione (70): The acid **75** was converted to the PTOC ester as outlined in Section 2.1.2 to yield a yellow solid (0.5 g, 72%). ^{1}H NMR (500 MHz, C_6D_6): 7.41-7.43 (1H, m), 6.68-6.69 (1H, m), 6.01-6.04 (1H, m), 5.67-5.76 (1H, m), 5.39-5.42 (1H, m), 4.96-5.04 (2H, m), 2.74-2.79 (1H, m), 2.48-2.53 (1H, m), 2.32-2.37 (1H, m), 1.32-1.98 (7H, m) ppm. ^{13}C NMR (126 MHz, C_6D_6): 177.21, 170.21, 138.68, 138.05, 137.55, 132.58, 115.52, 111.29, 81.18, 71.39, 43.03, 34.04, 30.76, 26.72, 21.58 ppm. HRMS (ESI) *m*/*z* calcd. for $[C_{15}H_{17}NO_2S]^+$: 276.1053 $[M + H]^+$, found 276.1054.

2-Thioxopyridin-1(2*H*)-yl 6-(*t*-butylselanyl)hexanoate (77): This compound was prepared following the literature procedure,[10] using 6-(*t*-butylseleno) hexanoic acid **80.** Yellow solid (0.8 g, 73%).[9] ^{1}H NMR (500 MHz, C_6D_6): 7.42-7.44 (1H, m), 6.49-6.51 (1H, m), 6.01-6.04 (1H, m), 5.39-5.42 (1H, m), 2.41 (2H, t, ^{3}J = 7.4 Hz), 2.35 (2H, t, ^{3}J = 7.4 Hz), 1.48-1.59 (4H, m), 1.36 (9H, s), 1.22-1.28 ppm (2H, m). Due to the instability of this compound a ^{13}C NMR and ^{77}Se NMR spectrum could not be obtained. HRMS (ESI) *m*/*z* calcd. for $[C_{16}H_{23}NO_2S]^+$: 362.0688 $[M + H]^+$, found 362.0688.

6.2.4 Synthesis of the radical precursor (81a-b)

***N*-(4-Pentenyl-1-oxy) pyridine-2-(1H)-thione (81a):**[11] This compound was prepared by reacting of tetraethylammonium pyridine-2(1H)-thione *N*-oxide **85** (0.5 g, 2.0 mmol) with *n*-pentenyl mesylate **84** (0.5 g, 2.0 mmol) in DMF (15 mL), as described in the literature;[11] a yellow oil (0.2 g, 41%). ^{1}H NMR (500 MHz, C_6D_6): 7.49 (1H, d, ^3J = 8.8 Hz), 6.65 (1H, d, ^3J = 6.7 Hz), 6.05-6.09 (1H, m), 5.62-5.70 (1H, m), 5.42 (1H, t, ^3J = 6.5 Hz), 4.93-4.99 (2H, m), 4.07 (2H, t, ^3J = 6.5 Hz), 2.00-2.04 (2H, m), 1.58-1.64 ppm (2H, m).

***N*-(4-Pentenyl-2-ethyl-1-oxy) pyridine-2-(1H)-thione (81b)**

*2-Ethylpent-4-enoic acid **(87)***:[13] *n*-Butyric acid (1.6 g, 18.0 mmol) was treated with allyl bromide (2.4 g, 20.0 mmol) in tetrahydrofuran as described in the literature,[8] to yield acid **87** as a colourless liquid (2.2 g, 97%). ^{1}H NMR (500 MHz, $CDCl_3$): 5.73-5.82 (1H, m), 5.03-5.11 (2H, m), 2.35-2.43 (2H, m), 2.23-2.30 (1H, m), 1.55-1.71 (2H, m), 0.95 ppm (3H, t, ^3J = 7.5 Hz).

*2-Ethylpent-4-en-1-ol **(82b-H)***:[14] Acid **87** (1.0 g, 8.0 mmol) was reduced to alcohol **82b-H** using $LiAlH_4$ (0.6 g, 16.0 mmol) as described in the literature[14] to obtain a colourless liquid (0.9 g, 97%). ^{1}H NMR (500 MHz, $CDCl_3$): 5.77-5.88 (1H, m); 5.01-5.09 (2H, m); 3.56-3.58 (2H, dd, ^3J = 2.1, 5.62 Hz); 2.12 (2H, t, ^3J = 6.8 Hz); 1.3-1.57 (3H, m); 0.92 ppm (3H, t, ^3J = 7.5 Hz). ^{13}C NMR (126 MHz, $CDCl_3$): 137.13, 116.08, 65.21, 41.94, 35.37, 23.23, 11.24 ppm.

N-*(4-Pentenyl-2-ethyl-1-oxy) pyridine-2-(1H)-thione **(81b)**:* Tetraethylammonium pyridine-2(1H)-thione *N*-oxide (0.5 g , 2.0 mmol) was treated with 2-ethylpent-4-enyl mesylate **88** (0.4 g, 2.0 mmol) in DMF (15 mL) as described in the literature[15] to obtain a yellow oil (0.3 g, 56%). ^{1}H NMR (500 MHz, C_6D_6): 7.45-7.48 (1H, m); 6.68-6.69 (1H, m); 6.03-6.06 (1H, m); 5.67-5.75 (1H, m); 5.39-5.42 (1H, m); 4.95-5.01 (2H, m); 4.00-4.06 (2H, m); 2.02- 2.17 (2H, m); 1.64-1.71 (1H, m); 1.26- 1.48 (2H, m); 0.84 ppm (3H, t, ^3J = 7.5 Hz). ^{13}C NMR (126 MHz, C_6D_6): 176.80, 138.44, 137.22, 136.76, 131.34, 116.64, 11.35, 77.66, 38.83, 35.43, 23.72, 11.48 ppm.

Synthesis of radical precursor 89: 4-Phenylbutanoic acid **93** (0.4 g, 2.7 mmol) was converted to the PTOC ester **89** as described in the literature[9] to yield compound **89** as a yellow viscous oil (0.5 g, 71%). ^{1}H NMR (500 MHz, C_6D_6): 7.42-7.44 (1H, m), 7.01-7.14 (5H, m), 6.39-6.41 (1H, m), 6.01-6.05 (1H, m), 5.38-5.42 (1H, m), 2.45 (2H, t, ^{3}J = 7.5 Hz), 2.36 (2H, t, ^{3}J = 7.4 Hz), 1.87-1.93 ppm (2H, m). ^{13}C NMR (126 MHz, C_6D_6): 176.83, 168.82, 141.25, 137.58, 137.58, 137.17, 132.23, 128.92, 128.78, 126.43, 110.78, 34.95, 30.98, 26.20 ppm. HRMS (ESI) *m/z* calcd. for $[C_{15}H_{15}NO_2S]^{+}$: 274.0896 $[M + H]^{+}$, found 274.0894.

6.3 Synthesis of the reference compounds

The authentic samples **23a-H**, **24a-H**, **53a-H**, **71a-H**, **72a-H** and **79-H** were commercially available and purchased from Sigma-Aldrich.

1,1-Diphenyl-1-hexene (25b-H):[4] According to literature procedure,[16,17] (pentyl)triphenylphosphonium bromide **54** (3.7 g, 9.0 mmol) (prepared by addition of 1-bromopentane (1.3 g, 9.0 mmol) to triphenyl phosphine (2.4 g, 9.0 mmol) in benzene (15 mL)) was reacted with *n*-butyllithium (4.5 mL, 9.0 mmol) and benzophenone (1.6 g, 9.0 mmol) in anhydrous tetrahydrofuran (15 mL) to afford compound **25b-H** after purification by column chromatography (SiO_2, *n*-hexane) as a colourless oil (1.5 g, 68%). ^{1}H NMR (400 MHz, $CDCl_3$): 7.18-7.41 (10H, m); 6.11 (1H, t, ^{3}J = 7.5 Hz), 2.11- 2.16 (2H, dd, ^{3}J = 7.4, 14.8 Hz), 1.41-1.48 (2H, m), 1.28-1.38 (2H, m), 0.88 ppm (3H, t, ^{3}J = 7.3 Hz).

(Diphenylmethyl)cyclopentane (26b-H):[4,17] A flame-dried round bottom flask was charged with magnesium chips (0.6 g, 24.0 mmol). Bromocyclopentane (2.3 mL, 21.0 mmol) was dissolved in anhydrous tetrahydrofuran (45 mL) and about one fifth of this solution was added to the flask, followed by a few drops of 1,2-dibromoethane. The remaining solution was then added dropwise, and the reaction mixture was refluxed for further 5 hours until the magnesium was dissolved. Under ice-cooling, a solution of benzophenone (1.3 g, 7.0 mmol) in anhydrous tetrahydrofuran (10 mL) was added dropwise to the Grignard reagent and the mixture was refluxed overnight. The reaction was poured into 10% hydrochloric acid (5 mL), extracted with diethylether (3 x 15 mL), and the combined organic fractions were dried over magnesium sulfate and

concentrated *'in vacuo'*. The residue was purified by column chromatography (SiO_2, 95:5 Pet. ether/EtOAc) to afford compound **44** as a white solid, which was directly used in the next step. ^{1}H NMR (400 MHz, $CDCl_3$): 7.22-7.46 (10H, m), 2.44-2.48 (4H, m), 1.72-1.76 ppm (4H, m).

Compound **44** (350 mg, 1.5 mmol) was dissolved in ethanol (35 mL) and 5% palladium on carbon (0.4 mg) was added. The mixture was hydrogenated (100 Psi of H_2) at room temperature for 20 hours, filtered through celite and washed with diethyl ether (20 mL). The solvent was evaporated '*in vacuo'* to give compound **26b-H** as colourless oil (275 mg, 46% over two steps). ^{1}H NMR (400 MHz, $CDCl_3$): 7.10-7.30 (10H, m), 3.55 (1H, d, ^3J = 11.3 Hz), 2.65- 2.75 (1H, m), 1.55-1.69 (6H, m), 1.13-1.19 ppm (2H, m).

Diethyl allylethylmalonate (**25c-H)**: Diester **56** was prepared from diethylmalonate (**45)**, similar to the synthesis of diester **46**, using allyl bromide (2.3 g, 19.5 mmol) and obtained as colourless oil (2.5 g, 66%). Diester **56** was subsequently treated in a similar way with iodoethane (2.0 g, 13.5 mmol) to produce compound **25c-H** as colourless oil (2.5 g, 87%) after column chromatography (SiO_2, 95:5 Pet. ether/EtOAc). ^{1}H NMR (500 MHz, $CDCl_3$): 5.61-5.70 (1H, m), 5.07-5.14 (2H, m), 4.20 (4H, q, ^3J = 7.1 Hz), 2.66 (2H, dt, ^3J = 7.4 Hz, ^4J = 1.1 Hz), 1.94 (2H, q, ^3J = 7.6 Hz), 1.26 (6H, t, ^3J = 7.1 Hz), 0.85 ppm (3H, t, ^3J = 7.6 Hz). ^{13}C NMR (126 MHz, $CDCl_3$): 171.2, 132.5, 118.6, 61.0, 57.7, 36.2, 25.0, 14.0, 8.2 ppm. HRMS (ESI) *m*/*z* calcd. for $[C_{12}H_{20}O_4]^+$: 229.1434 $[M + H]^+$, found 229.1436.

3-Methyl-cyclopentane-1,1-dicarboxylic acid diethyl ester (26c-H)

*Diethyl 2-allyl-2-(2-bromoethyl)malonate (**57**)*:[18] Diethyl 2-allyl-2-(2-bromoethyl)malonate (**57**) was prepared from compound **56** (1.0 g, 5.0 mmol), similar to the synthesis of diester **46**, using 1,2-dibromoethane (1.0 g, 5.5 mmol) to produce compound **57** as a pale yellow oil (1.5 g, 89%) after column chromatography (SiO_2, 95:5 Pet. ether/EtOAc). ^{1}H NMR (500 MHz, $CDCl_3$): 5.62-5.71 (1H, m), 5.14-5.18 (2H, m), 4.22 (4H, q, ^3J = 7.1 Hz), 3.36-3.39 (2H, m), 2.66 (2H, d, ^3J = 7.4 Hz), 2.44-2.48 (2H, m), 1.28 ppm (6H, t, ^3J = 7.1 Hz).

*3-Methyl-cyclopentane-1,1-dicarboxylic acid diethyl ester (**26c-H**)*:[18] A sealable tube was charged with benzene (20 mL), diester **57** (0.6 g, 2.0 mmol), tris(trimethyl silyl)silane (0.6 g, 2.4 mmol) and a single crystal of AIBN. The mixture was degassed by passing a slow stream of nitrogen through the solution for 1-2 minutes. The tube was then immersed in oil bath at 70 °C for 3 hours, while it was irradiated with a 250 W mercury lamp at a distance of 18 cm. Evaporation of the solvent '*in vacuo*' followed by column chromatography ((SiO_2, 98:2 Pet. ether/EtOAc) afforded compound **26c-H** as pale-yellow oil (0.5 g, 10%). ^{1}H NMR (500 MHz, $CDCl_3$): 4.17 (4H, q, ^3J = 7.1 Hz), 1.64-2.64 (6H, m), 1.24 (6H, t, ^3J = 7.1 Hz), 1.21-1.29 (1H, m), 1.01 ppm (3H, d, ^3J = 6.6 Hz).

Diethyl 2-(but-3-enyl)-2-methylpropanedioate (25d-H):[19] Synthesis was performed similar to the synthesis of compound **25c-H** from diester **51** (0.5 g, 2.3 mmol) and iodomethane (0.4 g, 2.5 mmol) to provide **25d-H** as a colourless oil (0.5 g, 89%). ^{1}H NMR (500 MHz, $CDCl_3$): 5.75-5.81 (1H, m), 4.95-5.05 (2H, m), 4.15 (4H, q, ^3J = 7.1 Hz), 1.93-2.04 (4H, m), 1.41 (3H, s), 1.24 ppm (6H, t, ^3J = 7.1 Hz). ^{13}C NMR (126 MHz, $CDCl_3$): 172.22, 137.6, 114.8, 61.1, 53.3, 34.6, 28.5, 19.8, 14.0 ppm.

Methyl 6-phenylhexanoate (91a-H):[20] Ester **91a-H** was synthesised from 6-phenylhexanoicacid (**94**) (1.0 g, 5.2 mmol) and methanol (0.2 g, 5.4 mmol) in the presence of DCC (1.1 g, 5.2 mmol) and DMAP (0.1 g, 0.5 mmol) as described in literature[21] to afford a colourless oil (1.0 g, 93%). ^{1}H NMR (400 MHz, $CDCl_3$): 7.15-7.35 (5H, m), 3.65 (3H, s), 2.60 (2H, t, ^3J = 7.7 Hz), 2.30 (2H, t, ^3J = 7.5 Hz), 1.59-1.69 (4H, m), 1.31-1.39 ppm (2H, m). ^{13}C NMR (126 MHz, $CDCl_3$): 174.20, 142.33, 128.21, 128.09, 125.49, 51.30, 35.55, 33.85, 30.91, 28.59, 24.64 ppm.

***t*-Butyl(pentyl)selane (78-H):**[22] The title compound was prepared according to literature and obtained as a colourless liquid (65%). ^{1}H NMR (500 MHz, $CDCl_3$): 2.58 (2H, t, ^3J = 7.5 Hz), 1.66-1.80 (2H, m), 1.44 (9H, s), 1.32-1.37 (4H, m), 0.89 ppm (3H, t, ^3J = 7.0 Hz). ^{77}Se NMR (95 MHz, $CDCl_3$): 376.9 ppm.

Selenane (79):[23] This compound was prepared following the literature procedure,[24] using $NaBH_4$ (0.4 g, 10.0 mmol), elemental selenium (0.4 g, 5.0 mmol), EtOH (1.4 g, 30.0 mmol), 1,5-dibromopentane (2.3 g, 10.0 mmol) in DMF (10 mL). Purification by

column chromatography (SiO_2, 90:10 Pet. ether/EtOAc) gave compound **79** as a colourless liquid (0.2 g, 26%). ^{1}H NMR (500 MHz, $CDCl_3$): 2.64-2.66 (4H, m), 1.91-1.96 (4H, m), 1.56-1.60 ppm (2H, m).

6.4 Competition kinetic experiments

An aliquot (1.0 mL) of a standard solution of *t*-BuSH (usually 0.1 M in the respective solvent, 10 equivalents) and the radical precursor (1 equivalent) was placed in a 1 mL volumetric flask and the mixture was topped up to 1 mL with the solvent (*t*-BuPh, *n*-hexane, benzene or [EMIm][NTf_2]). The solution was divided into three small Pyrex tubes (300 μL) and degassed by either passing a stream of argon through the solutions for 1 min or by freeze-thawing, where the samples were frozen using liquid nitrogen, vacuumed, thawed, refrozen and sealed under vacuum. The reaction temperature was controlled using a water condenser (23-25 °C) or an oil bath for higher temperature. The samples were irradiated using a 250 W mercury lamp that was held at a constant distance of 18 cm to ensure similar photon absorption in all experiments. The reactions performed in conventional solvents were directly analysed by a GC (Shimadzu GC-17A) fitted with a non-polar SPB®-Octyl Capillary GC column or an Agilent GC/MS, fitted with HP-5ms capillary column (Table 5.1). In the reactions performed in the ionic liquid [EMIm][NTf_2], the products were extracted with suitable organic solvent (3 times), which specified in each section for each reaction. The combined organic layers were passed through the silica plug to get rid of the remaining ILs in organic layer. Then the organic layer was subjected to the GC analysis. In the reactions involving **25a** in Chapter 2, the organic phase was washed with bleach before GC analysis, to move *t*-BuSH signal, which overlapped with directly reduced product peak. The products were identified by GC through comparison with authentic samples, which were either commercially available or prepared as described above.

Table 6.1. Temperature program used for the analysis of the radical reactions studied in this work.

Radical	Instrument	Temperature program
25a	Shimadzu GC-17A	50 ^{o}C (10 mins hold), 20 ^{o}C/min. to 250 ^{o}C, 20 mins. Hold
25b	Agilent GC/MS	100 ^{o}C (no hold), 10 ^{o}C/min. to 250 ^{o}C, 20 mins. Hold
25c	Agilent GC/MS	100 ^{o}C (no hold), 10 ^{o}C/min. to 250 ^{o}C, 20 mins. Hold
25d	Agilent GC/MS	100 ^{o}C (no hold), 10 ^{o}C/min. to 250 ^{o}C, 20 mins. Hold
63a	Shimadzu GC-17A	60 ^{o}C (10 mins hold), 20 ^{o}C/min. to 250 ^{o}C, 20 mins. Hold
63b	Shimadzu GC-17A	67 ^{o}C (10 mins hold), 20 ^{o}C/min. to 250 ^{o}C, 20 mins. Hold
63c	Shimadzu GC-17A	80 ^{o}C (10 mins hold), 20 ^{o}C/min. to 250 ^{o}C, 20 mins. Hold
63d	Shimadzu GC-17A	90 ^{o}C (10 mins hold), 20 ^{o}C/min. to 250 ^{o}C, 20 mins. Hold
71	Shimadzu GC-17A	90 ^{o}C (10 mins hold), 20 ^{o}C/min. to 250 ^{o}C, 20 mins. Hold
78	Shimadzu GC-17A	90 ^{o}C (10 mins hold), 20 ^{o}C/min. to 250 ^{o}C, 20 mins. Hold
82b	Shimadzu GC-17A	70 ^{o}C (10 mins hold), 20 ^{o}C/min. to 250 ^{o}C, 20 mins. Hold
90	Agilent GC/MS	70 ^{o}C (5 mins hold), 20 ^{o}C/min. to 250 ^{o}C, 20 mins. Hold

6.5 References

[1] Salomon, R. G.; Coughlin, D. J.; Ghosh, S.; Zagorski, M. G., *J. Am. Chem. Soc.* **1982**, *104*, 998.

[2] Bailey, W. F.; Nurmi, T. T.; Patricia, J. J.; Wang, W. J., *Am. Chem. Soc.* **1987**, *109*, 2442.

[3] Clive, D. L. J.; Hisaindee, S.; *J. Org. Chem.* **2000**, *65*, 4923.

[4] Ha, C.; Horner, J. H.; Newcomb, M.; Varick, T. R.; Arnold, B. R.; Lusztyk, J., *J. Org. Chem.* **1993**, *58*, 1194.

[5] Crich, D.; Jiao, X-Y.; Yao, X. Q.; Harwood, J. S. , *J. Org. Chem.* **1996**, *61*, 2368.

[6] Plattner, J. J.; Marcotte, P. A.; Kleinert, H. D., Stein, H. H.; Greer, J.; Bolis, G.; Fung, A. K. L.; Bopp, B. A.; Luly, J. R., *J. Med. Chem.* **1988**, *31*, 2277.

[7] Curran, D. P.; Yu, H.; Liu, H., *Tetrahedron* **1994**, *50*, 7343.

[8] Shimshoni, J. A.; Bialer, M.; Wlodarczyk, B.; Finnell, R. H.; Yagen, B., *J. Med. Chem.* **2007**, *50*, 6419.

[9] Barton, D. H. R.; Crich, D.; Mother ll, W. B., *J. Chem. Soc., Chem. Commun.* **1983**, 939.

[10] Benjamin, L. J.; Schiesser, C. H.; Sutej, K., *Tetrahedron* **1993**, *49*, 2557.

[11] Hay, B. P.; Beckwith, A. L. J., *J. Org. Chem.* **1989**, *54*, 4330.

[12] Hamilton, D. S.; Nicewicz, D. A., *J. Am. Chem. Soc.* **2012**, *134*, 18577.

[13] Rudler, H.; Harris, P.; Parlier, A.; Cantagrel, F.; Denise, B.; Bellassoued, M.; Vaissermann, J., *J. Organomet. Chem.* **2001**, *624*, 186.

[14] Crimmins, M. T.; O'Mahony, R., *J. Org. Chem.* **1989**, *54*, 1157.

[15] Hartung, J.; Gallou, F., *J. Org. Chem.* **1995**, *60*, 6706.

[16] Lébl, T.; Zoufalá, P.; Bruhn, C., *Eur. J. Inorg. Chem.* **2005**, *2005*, 2536.

[17] Qi, W.; Wang, P.; Fan, L.; Zhang, S., *J. Org. Chem.* **2013**, *78*, 5918.

[18] Kyne, S. H.; Lévêque, C.; Zheng, S.; Fensterbank, L.; Jutand, A.; Ollivier, C., *Tetrahedron* **2016**, *72*, 7727.

[19] Li, Z.; Wang, Z.; Zhu, L.; Tan, X.; Li, C., *J. Am. Chem. Soc.* **2014**, *136*, 16439.

[20] Topley, A. C.; Isoni, V., Logothetis, T. A.; Wynn, D.; Wadsworth, H.; Gibson, A. M. R.; Khan, I.; Wells, N. J.; Perrio, C.; Brown, R. C. D., *Chem – Eur. J.* **2013**, *19*, 1720.

[21] Alliot, J.; Gravel, E.; Doris, E., *Synthesis* **2013**, *45*, 2861.

[22] Hancock, A. N.; Kavanagh, Y.; Schiesser, C. H., *Org. Chem. Front.* **2014**, *1*, 645.

[23] Levanova, E. P.; Grabel'nykh, V. A.; Elaev, A. V.; Russavskaya, N. V.; Klyba, L. V.; Albanov, A. I.; Korchevin, N. A., *Chem. Heterocyc. Compd.* **2012**, *47*, 1345.

[24] Krief, A.; Trabelsi, M.; Dumont, W.; Derock, M., *Synlett* **2004**, *10*, 1751.

7 Appendix 1

Gaussian archive entries for the calculations shown in Scheme 2.2

Reactant association complex [EMIm – Et•]

1\1\GINC-SPARTAN-RC145\FOpt\UM062X\6-
31+G(d)\C8H16N2(1+,2)\UWILLE\12-S

ep-2017\0\\#p M062X/6-31+G* nosymm scf=(qc,direct) opt=(calcfc,z-matri

x,maxcycle=500) freq=noraman\\geom&freq\\1,2\C,-1.7922073093,0.6198314

451,0.1378714637\C,-0.5854699109,1.251560699,0.1222683237\C,-2.1562414

508,2.7782768204,-0.0886407662\N,-2.7572889467,1.5932506969,0.00191959

48\H,-2.054283416,-0.4260750194,0.2176663001\H,0.4196946645,0.86412575

46,0.1956130825\H,-2.6549496499,3.7305926507,-0.2028044404\N,-0.836345

8398,2.5986634946,-0.0197351\C,-4.2145978705,1.354293162,-0.001903829\

H,-4.6862055721,2.2968950747,-0.2889275984\H,-4.410554267,0.6163389112

,-0.783550085\C,0.1809064106,3.6521433181,-0.0864517091\H,0.7610296952

,3.6509480878,0.836972121\H,0.830985816,3.4694926708,-0.942911913\H,-0

.3168197871,4.614251184,-0.2044181893\C,-4.6942350627,0.8713551098,1.3

582880823\H,-5.7707471622,0.6870645959,1.3159234584\H,-4.2023416943,-0

.0651426719,1.6368640357\H,-4.5012372439,1.6176179287,2.1337279152\C,-

3.0742877957,-2.9793868408,0.4490070037\H,-3.3581088602,-4.0425670431,

0.4236296714\H,-3.1898495791,-2.6569744507,1.4901930373\H,-2.012163041

1,-2.9389983458,0.1844763077\C,-3.9192789125,-2.1802752953,-0.48637062

02\H,-4.956261462,-1.9854444628,-0.2304147345\H,-3.6694597523,-2.14774

64729,-1.542264414\\Version=AM64L-G09RevB.01\HF=-423.5032438\S2=0.7545

1\S2-1=0.\S2A=0.750016\RMSD=0.000e+00\RMSF=1.146e-05\Dipole=0.8355532,

1.7821861,-0.1624532\Quadrupole=11.039693,9.141867,-20.18156,-6.859687

8,-1.5780724,-0.8924916\PG=C01 [X(C8H16N2)]\\@

Sum of electronic and thermal Free Energies= -423.312410 Hartrees

TS1

1\1\GINC-SPARTAN-RC030\FTS\UM062X\6-
31+G(d)\C8H16N2(1+,2)\UWILLE\12-Oc

t-2017\0\\#p M062X/6-31+G* nosymm scf=(qc,direct) opt=(ts,noeigentest,

calcfc,z-matrix,maxcycle=500) freq=noraman\\geom&freq\\1,2\C,-5.004888

0014,2.4568308571,-1.6519859693\C,-5.9317973811,3.3995852662,-1.981577

1609\C,-6.0093647385,3.1024331077,0.1972638769\N,-5.0636749225,2.28810

69624,-0.2823956391\H,-4.3141230961,1.9049864876,-2.2695706618\H,-6.20

01442492,3.8248300319,-2.9372395206\H,-6.28803964,3.1932181035,1.23744

89242\N,-6.5470139043,3.788098204,-0.8146562836\C,-4.3323880576,1.3102

933487,0.4940694331\H,-4.3630687074,1.5951138908,1.5458784838\H,-5.058

173772,0.1991553143,0.4065413332\C,-7.6027757484,4.7983762382,-0.70260

04048\H,-7.2209897735,5.7591313586,-1.0498681307\H,-8.4592638952,4.491

2256276,-1.3038138264\H,-7.9011433068,4.879187139,0.3423382196\C,-2.96

40784001,0.9763719778,-0.0406196208\H,-2.4666185525,0.3065916665,0.664

9135637\H,-3.0180475546,0.4521226255,-1.0007868401\H,-2.3391157041,1.8

694878827,-0.1602638429\C,-4.782144387,-2.0553953591,0.7015724444\H,-5

.2616104321,-3.0398462025,0.6276362827\H,-4.4925175639,-1.915338788,1.

7477207729\H,-3.8748808349,-2.0924282952,0.0908862048\C,-5.7254848444,

-0.9755206994,0.2363306446\H,-6.6185009978,-0.8307409165,0.8481438449\

H,-5.9529165343,-0.971706827,-0.8325491167\\Version=AM64L-G09RevB.01\H

F=-423.4785846\S2=0.759175\S2-
1=0.\S2A=0.750055\RMSD=0.000e+00\RMSF=5.

169e-06\Dipole=-0.7250543,1.5191936,-0.1474297\Quadrupole=68.5621902,-

18.7207683,-49.841422,-63.3513858,9.2683383,-7.6163998\PG=C01 [X(C8H16

N2)]\\@

n_{imag} = -1421.6520 cm^{-1}

Sum of electronic and thermal Free Energies= -423.292263 Hartrees

Product association complex I

1\1\GINC-SPARTAN-RC088\FOpt\UM062X\6-
31+G(d)\C8H16N2(1+,2)\UWILLE\08-S

ep-2017\0\\#p M062X/6-31+G* nosymm scf=(qc,direct) opt=(calcfc,z-matri

x,maxcycle=500) freq=noraman\\geom&freq\\1,2\C,-2.4943420941,0.6896749

37,0.1934694912\C,-1.1546415725,0.8645597883,0.0407197176\C,-2.0790770

812,2.8637347942,0.1221501458\N,-3.0676306243,1.955277147,0.2442288739

\H,-3.0839329049,-0.2111971382,0.2670500187\H,-0.3571658344,0.14071296

27,-0.0426595765\H,-2.2130545079,3.935715339,0.1257330814\N,-0.9176536

853,2.2203793375,-0.0020661873\C,-4.4227607202,2.2396627593,0.39667105

36\H,-4.6760317921,3.2906540874,0.4049228349\C,0.3975379885,2.85006470

69,-0.1535072432\H,1.0245849361,2.5818186087,0.6975922434\H,0.85262439

9,2.5078604164,-1.0836916375\H,0.2668312532,3.9312363323,-0.1867753382

\C,-5.4017977539,1.1370452566,0.5285412949\H,-6.4023046449,1.552259665

8,0.653078041\H,-5.4148100103,0.4908717361,-0.3604010888\H,-5.18972443

88,0.5029759876,1.4006532126\C,-1.9761460162,-2.6598683823,0.278176790

3\H,-1.3696978854,-3.5693347572,0.2670513823\H,-1.6217477551,-2.047707

9002,1.1166497902\H,-1.7737673463,-2.1275363396,-0.6595381581\C,-3.459

4466999,-2.9993529521,0.4197013986\H,-4.095989673,-2.1045642187,0.4302

300684\H,-3.7997050738,-3.6254024965,-0.409361029\H,-3.6516684622,-3.5

413806772,1.3493898208\\Version=AM64L-G09RevB.01\HF=-423.50623\S2=0.76

07\S2-1=0.\S2A=0.750072\RMSD=0.000e+00\RMSF=3.106e-06\Dipole=0.6537837

,2.0783795,-0.1268396\Quadrupole=14.9445798,6.7755244,-21.7201042,-11.

5645485,-3.5213845,0.3547615\PG=C01 [X(C8H16N2)]\\@

Sum of electronic and thermal Free Energies= -423. 315781 Hartrees

TS2

1\1\GINC-SPARTAN-RC070\FTS\UM062X\6-
31+G(d)\C8H16N2(1+,2)\UWILLE\21-Se

p-2017\0\\#p M062X/6-31+G* nosymm scf=(qc,direct) opt=(ts,noeigentest,

calcfc,z-matrix,maxcycle=500) freq=noraman\\geom&freq\\1,2\C,-2.197842

9869,1.6817150825,0.0979506167\C,-1.5855837266,1.9644968474,-1.0857233

043\C,-3.6569772594,2.6998293924,-1.1934089819\N,-3.4870527171,2.15525

79496,0.0092752423\H,-1.8276691534,1.1950693982,0.9881690326\H,-0.5785
171902,1.777232453,-1.4276118488\H,-4.5722408231,3.1440821751,-1.55912
47714\N,-2.5162710192,2.6002987449,-1.877726345\C,-4.5413292024,1.9798
403305,1.0344735146\H,-4.1387550681,2.3811738957,1.9710981856\H,-5.377
1255564,2.6153470751,0.7319044864\C,-2.2818084645,3.0948073863,-3.2380
034325\H,-1.5152054432,3.8703012867,-3.2125545636\H,-1.9623694635,2.26
54297867,-3.8698838285\H,-3.2117728401,3.5104710763,-3.6248198038\C,-4
.953250989,0.5328242197,1.1300556058\H,-5.1561018886,0.1346229033,-0.1
73968795\H,-4.1835770792,-0.1450875281,1.5029193591\H,-5.9129675059,0.
3836735465,1.6235826301\C,-5.912035766,-1.6363224854,-1.3621701141\H,-
6.0554129073,-2.046527984,-2.3686935079\H,-6.8901111455,-1.6166413709,
-0.8727443442\H,-5.2686794036,-2.3302116441,-0.8128156834\C,-5.3030448
625,-0.2544073382,-1.4214631256\H,-5.9462623885,0.5083405953,-1.871355
0296\H,-4.2871911503,-0.219682795,-1.8300571922\\Version=AM64L-G09RevB
.01\HF=-423.471584\S2=0.758797\S2-1=0.\S2A=0.750042\RMSD=0.000e+00\RMS
F=1.880e-06\Dipole=0.8872096,1.333733,-0.3943012\Quadrupole=20.3973531
,-7.8484806,-12.5488725,-22.8474555,7.8576849,-12.2785399\PG=C01 [X(C8
H16N2)]\\@

n_{imag} = -1459.0602 cm^{-1}

Sum of electronic and thermal Free Energies= -423.283181 Hartrees

Product association complex II

1\1\GINC-SPARTAN-RC008\FOpt\UM062X\6-
31+G(d)\C8H16N2(1+,2)\UWILLE\13-S

ep-2017\0\\#p M062X/6-31+G* nosymm scf=(qc,direct) opt=(calcfc,z-matri

x,maxcycle=500) freq=noraman\\geom&freq\\1,2\C,-2.2697247872,0.6797912

881,-0.0299625971\C,-0.9436815959,0.9881041116,-0.0251823307\C,-2.0802

641894,2.8733677247,0.0160770502\N,-2.958962817,1.8716084663,-0.004195

609\H,-2.779422783,-0.2727593139,-0.0410620557\H,-0.0690235584,0.35473

15733,-0.0362107955\H,-2.3245109418,3.926257726,0.0385669502\N,-0.8484

755637,2.3631026826,0.0042475459\C,0.4011582016,3.1299975913,0.0307481

077\H,0.9600074562,2.8760410958,0.9321234781\H,0.9861406671,2.89113903

04,-0.8579859965\H,0.1605445559,4.192669617,0.0356225599\C,-5.08150843

78,1.0726021161,0.923130598\H,-6.0115317078,0.5889845126,0.6569273942\

H,-4.758747186,1.0591091353,1.9576879775\C,-2.2448326276,-2.8055992673

,0.1526058166\H,-1.850031778,-3.8248271188,0.1301396009\H,-1.704673829

7,-2.2693445583,0.9420509031\H,-1.9981844721,-2.3481817751,-0.81327957

92\C,-3.7518201302,-2.8143631369,0.4086985987\H,-4.1768520145,-1.80221

2955,0.4579026582\H,-4.2822763475,-3.3511717823,-0.3823509275\H,-3.984

1764884,-3.3037873116,1.3584315157\C,-4.4360351209,2.0018131694,-0.041

9692542\H,-4.7584011417,1.8065008193,-1.0681904877\H,-4.6518898727,3.0

551198995,0.1822468636\\Version=AM64L-G09RevB.01\HF=-423.4953566\S2=0.

754886\S2-1=0.\S2A=0.750018\RMSD=0.000e+00\RMSF=7.756e-06\Dipole=0.694

7762,2.2228966,-0.1649188\Quadrupole=13.2772869,7.2545751,-20.531862,-

10.896913,-0.9397405,-0.0072279\PG=C01 [X(C8H16N2)]\\@

Sum of electronic and thermal Free Energies= -423.306166 Hartrees

TS3

1\1\GINC-SPARTAN-RC046\FTS\UM062X\6-31+G(d)\C8H16N2(1+,2)\UWILLE\11-Oct-2017\0\\#p M062X/6-31+G* nosymm scf=(qc,direct) opt=(ts,noeigentest, calcfc,z-matrix,maxcycle=500) freq=noraman\\geom&freq\\1,2\C,-2.824683541,1.3213961889,-1.8490693398\C,-2.9793219634,1.8866658262,-3.0783876699\C,-4.6475320649,2.5580175652,-1.8097669594\N,-3.8737723795,1.7600802714,-1.0647507632\H,-2.0697860764,0.6534547369,-1.4624407205\H,-2.3781351048,1.8110231328,-3.9723378372\H,-5.5486355443,3.0497972879,-1.4715003313\N,-4.1231831595,2.6500636834,-3.0336068364\C,-4.1565772728,1.3211177918,0.2701113519\H,-4.8210037866,2.005193936,0.7926210066\H,-4.8385170064,0.1445119079,0.1492599209\C,-4.6435836199,3.4841222691,-4.1340816829\H,-4.6568510341,2.8563217194,-5.0281248976\H,-5.6777105244,3.7279798729,-3.8809491923\C,-4.3259429897,-2.0644680478,0.0090815962\H,-4.7435563824,-3.0693322761,-0.1295374887\H,-3.8155432978,-2.0574420021,0.9769346362\H,-3.5812681273,-1.9148292815,-0.7797551028\C,-5.4213164039,-1.0291476292,-0.0491169473\H,-6.1509695202,-1.0713778041,0.7617695474\H,-5.9005458268,-0.905686324,-1.0236388198\C,-3.8025017085,4.7370827391,-4.331350854\H,-2.7700888085,4.487609031,-4.591042913\H,-4.2230115476,5.3275932355,-5.1491260207\H,-3.7981383584,5.3533173341,-3.42

83278665\H,-3.2460287418,1.0829196896,0.8147153605\\Version=AM64L-G09R

evB.01\HF=-423.4763943\S2=0.759221\S2-1=0.\S2A=0.750057\RMSD=0.000e+00

\RMSF=4.735e-06\Dipole=-0.0691271,0.7332157,-0.3196596\Quadrupole=26.0

412909,-14.9696028,-11.0716881,-32.091098,28.3827922,-24.2582268\PG=C0

1 [X(C8H16N2)]\\@

n_{imag} = -1432.7183 cm^{-1}

Sum of electronic and thermal Free Energies= -423.288887 Hartrees

Product association complex III

1\1\GINC-SPARTAN-RC128\FOpt\UM062X\6-
31+G(d)\C8H16N2(1+,2)\UWILLE\09-S

ep-2017\0\\#p M062X/6-31+G* nosymm scf=(qc,direct) opt=(calcfc,z-matri

x,maxcycle=500) freq=noraman\\geom&freq\\1,2\C,-2.5425115507,0.6234597

242,-0.1016897504\C,-1.2018435719,0.8326118603,-0.0407331644\C,-2.2128

712321,2.8026547697,-0.117228802\N,-3.1513961257,1.8601278755,-0.15073

17705\H,-3.1092758322,-0.2963082864,-0.1182113842\H,-0.3741188965,0.14

09428032,0.0051336307\H,-2.3825006151,3.8695727227,-0.1418647142\N,-1.

0038375635,2.2089332062,-0.0505732443\C,0.2204496858,2.8561472454,-0.0

018090856\H,1.1095125208,2.2472596531,0.0365712812\H,0.2305095504,3.93

47657798,-0.0186500528\C,-1.9292100027,-2.7162957262,0.1191905364\H,-1

.2900592719,-3.6025235855,0.1541001859\H,-1.6708595191,-2.0987225596,0

.9881880902\H,-1.6667915707,-2.169123522,-0.7949193092\C,-3.405319839,

-3.1118103758,0.1330021283\H,-4.0741068094,-2.2414252653,0.1080528338\

H,-3.654114434,-3.7341592161,-0.730499705\H,-3.6510123805,-3.678237026

1,1.0350207331\C,-4.6092401498,2.0924884498,-0.1971367219\H,-4.9906548

187,1.5481170761,-1.0647118354\H,-4.7491432698,3.1601141804,-0.3799921

48\C,-5.2823974732,1.6503456711,1.0940369085\H,-6.3535536296,1.8557850

362,1.0269657252\H,-5.1571147582,0.5773797289,1.2644653784\H,-4.879719

4429,2.1929957807,1.9533912487\\Version=AM64L-G09RevB.01\HF=-423.49948

57\S2=0.760392\S2-1=0.\S2A=0.750066\RMSD=0.000e+00\RMSF=4.736e-06\Dipo

le=0.4929484,2.0393996,-0.1864352\Quadrupole=16.3373076,6.0177571,-22.

3550647,-13.9656622,-0.3016899,-0.4299979\PG=C01 [X(C8H16N2)]\\@

Sum of electronic and thermal Free Energies= -423.310556 Hartrees

Reactant association complex [MeSH – Et•]

1\1\GINC-SPARTAN-RC015\FOpt\UM062X\6-31+G(d)\C3H9S1(2)\UWILLE\13-Oct-2

017\0\\#p M062X/6-31+G* nosymm scf=(qc,direct) opt=(calcfc,z-matrix,ma

xcycle=500) freq=noraman\\geom&freq\\0,2\H,-4.1410104931,0.6216848133,

-0.7139544411\C,-4.6986051419,-1.92057974,0.4273511609\H,-4.9982169199

,-2.9046537342,0.8210091595\H,-4.3262800883,-1.3400543209,1.2794435868

\H,-3.8590115302,-2.0906648397,-0.2537490326\C,-5.8320257519,-1.234962

3916,-0.257267573\H,-6.6217992242,-0.7693428481,0.3219535528\H,-6.0330

465274,-1.4172217144,-1.3068817645\S,-3.6233055384,1.6812614152,-0.065

5986368\C,-4.9845843152,1.8536388552,1.1311181376\H,-5.936399265,2.027

4431656,0.6266206406\H,-5.0610341842,0.9783613419,1.7796797123\H,-4.75

01454337,2.7238688295,1.7471071358\\Version=AM64L-G09RevB.01\HF=-517.7

392191\S2=0.755033\S2-1=0.\S2A=0.75002\RMSD=0.000e+00\RMSF=1.947e-05\D

ipole=-0.6033488,-0.4337154,0.274071\Quadrupole=5.7853949,-3.7942223,-

1.9911726,1.6350213,-3.0096703,2.2130131\PG=C01 [X(C3H9S1)]\\@

Sum of electronic and thermal Free Energies= -517.665886 Hartrees

TS4

1\1\GINC-SPARTAN-RC099\FTS\UM062X\6-31+G(d)\C3H9S1(2)\UWILLE\27-Oct-20

17\0\\#p M062X/6-31+G* nosymm guess=check opt=(ts,noeigentest,calcfc,z

-matrix,maxcycle=500) freq=noraman\\geom&freq\\0,2\H,-4.6482102586,0.1

337435799,0.7709576406\C,-6.291962239,-0.7513163226,-0.767577046\H,-6.

9145250691,-1.573081872,-1.1515522304\H,-5.7095048057,-0.3648058254,-1

.6099177058\H,-6.9669971507,0.0402971336,-0.4287904899\C,-5.4058489621

,-1.2241567732,0.3424637497\H,-4.5415711562,-1.8360941007,0.0915769819

\H,-5.8586203544,-1.4445693585,1.3069645465\S,-3.9169391345,1.37358764

32,0.9245395738\C,-2.7699671322,1.0208731884,-0.4451365503\H,-3.298659

512,0.9244178373,-1.3962520921\H,-2.0838770195,1.8676996859,-0.5179648

085\H,-2.1845179856,0.1193179117,-0.252077417\\Version=AM64L-G09RevB.0

1\HF=-517.7332511\S2=0.759369\S2-1=0.\S2A=0.75005\RMSD=7.383e-09\RMSF=

1.047e-05\Dipole=-0.1175208,-0.7495663,-0.6280257\Quadrupole=3.6389121

,-1.9796651,-1.6592469,7.4622212,3.6295766,-1.7608356\PG=C01 [X(C3H9S1

)]\\@

n_{imag} = -948.9048 cm^{-1}

Sum of electronic and thermal Free Energies= -517.659386 Hartrees

Product association complex IV

1\1\GINC-SPARTAN-RC030\FOpt\UM062X\6-31+G(d)\C3H9S1(2)\UWILLE\13-Oct-2

017\0\\#p M062X/6-31+G* nosymm scf=(qc,direct) opt=(calcfc,z-matrix,ma

xcycle=500) freq=noraman\\geom&freq\\0,2\H,-5.5861436954,-0.0335336857

,-0.7792166944\C,-4.5058020159,-1.4349289344,0.4928716632\H,-4.6342432

101,-2.436237527,0.9161412875\H,-4.3171324859,-0.7508935111,1.32800398

95\H,-3.6069565906,-1.4496198236,-0.1323502877\C,-5.7337847145,-1.0133

955007,-0.3125793022\H,-6.6253405736,-0.958233767,0.3210570543\H,-5.94

1968073,-1.7288971628,-1.1141839413\S,-3.2717639416,1.7794258744,-0.03

61357094\C,-4.5169500326,2.1463528485,1.2135162557\H,-5.473663753,1.67

69379801,0.9684590967\H,-4.1921641773,1.8497997772,2.2126038984\H,-4.6

670078511,3.2330574217,1.2069760308\\Version=AM64L-G09RevB.01\HF=-517.

770637\S2=0.752985\S2-1=0.\S2A=0.750006\RMSD=0.000e+00\RMSF=1.475e-05\

Dipole=-0.4766006,0.1305705,0.433342\Quadrupole=3.172771,-0.5863687,-2

.5864022,-2.5527872,-4.3564752,1.9991037\PG=C01 [X(C3H9S1)]\\@

Sum of electronic and thermal Free Energies= -517.690993 Hartrees

Appendix 2

The linear form of the Eyring equation is given below:

$$\ln\frac{k}{T} = \frac{-\Delta H^{\neq}}{RT} + \ln\frac{k_B}{h} + \frac{\Delta S^{\neq}}{R}$$

Where:

k = reaction rate constant

T = absolute temperature

$\Delta H^{\ddagger}$ = enthalpy of activation

R= gas constant

k_B = Boltzman constant

h = Plank's constant

$\Delta S^{\ddagger}$ = entropy of activation

$$\ln\frac{k_C}{T} = \frac{-\Delta H_C^{\neq}}{RT} + \ln\frac{k_B}{h} + \frac{\Delta S_C^{\neq}}{R}$$

$$\ln\frac{k_H}{T} = \frac{-\Delta H_H^{\neq}}{RT} + \ln\frac{k_B}{h} + \frac{\Delta S_H^{\neq}}{R}$$

Dividing equation ln (k_C/T) by ln (k_H/T) gives:

$$\ln\frac{k_C}{k_H} = \left(\frac{-\Delta H_C^{\neq}}{RT} + \ln\frac{k_B}{h} + \frac{\Delta S_C^{\neq}}{R}\right) - \left(\frac{-\Delta H_H^{\neq}}{RT} + \ln\frac{k_B}{h} + \frac{\Delta S_H^{\neq}}{R}\right)$$

$$\ln\frac{k_C}{k_H} = \left(\frac{-\Delta H_C^{\neq}}{RT} + \frac{\Delta S_C^{\neq}}{R}\right) - \left(\frac{-\Delta H_H^{\neq}}{RT} + \frac{\Delta S_H^{\neq}}{R}\right)$$

$$\ln\frac{k_C}{k_H}=\left(\frac{-\Delta H_C^{\neq}}{RT}-\frac{-\Delta H_H^{\neq}}{RT}\right)+\left(\frac{\Delta S_C^{\neq}}{R}-\frac{\Delta S_H^{\neq}}{R}\right)$$

$$\ln\frac{k_C}{k_H}=\left(\frac{-\left(\Delta H_C^{\neq}-\Delta H_H^{\neq}\right)}{R}\right)\times\frac{1}{T}+\left(\frac{\Delta S_C^{\neq}-\Delta S_H^{\neq}}{R}\right)$$

Appendix 3

Table A.1. The GC peak areas (PA) of the products of the competition kinetic experiments for the 5-*exo* cyclisation of the 6,6-diphenyl-5-hexenyl radical (**25b**) at 24 ± 1 °C.

Solvent	**[*t*-BuSH] (M)**	**PA (26b-H)**	**PA (44)**	**PA (25b-H)**
t-BuPh	0.100	2867330	2674300	138823
	0.120	3788477	2538475	216097
	0.120	5653038	2455739	195174
	0.140	4718140	2978416	271575
	0.140	5471898	2865417	304542
	0.175	16178424	4557394	917135
	0.175	9592936	5215127	602909
	0.180	9896774	4042508	815987
	0.180	8809258	3630102	538065
	0.210	21084787	6183409	1629529
	0.210	16545300	4865300	1292191
	0.245	21676509	6542836	1788876
	0.245	25027606	5710096	1692795
	0.280	29463079	7779273	2203263
	0.280	21506556	6394309	1917846
	0.315	30192527	7617108	2860633
	0.315	26969828	7207530	2730314
[EMIm][NTf_2][a]	0.100	2697476	1383330	146678
	0.100	2205236	1630036	143187
	0.140	4668090	2867969	308302
	0.140	3809167	1890222	258857
	0.160	6217781	2641407	471852
	0.160	5819032	2431535	420228
	0.180	7413460	3018454	574868
	0.180	6516695	2770697	584870
	0.200	10252244	3449326	755683
	0.200	8621955	3206400	763641

[a]After extraction with *t*-BuPh.

Table A.2. The GC peak areas (PA) of the products of the competition kinetic experiments for the 5-*exo* cyclisation of the 5-hexenyl radical (**25a**) at 24 ± 1 °C.

Solvent	[*t*-BuSH] (M)	PA (26a-H)	PA (25a-H)
t-BuPh	0.200	2181607	8232498
	0.200	1949249	7501251
	0.100	1652037	3891495
	0.100	1720667	3568789
	0.050	1082606	1288891
	0.050	1127100	1256155
	0.040	936273	972208
	0.040	932843	1087603
	0.030	619619	537741
	0.030	617134	633463
	0.015	108405	57063
	0.015	119444	62019
	0.200	658765	4267934
	0.200	709539	4768640
	0.120	527232	2305708
	0.120	528571	2302210
	0.120	1255560	4646330
	0.120	1546834	6601933
	0.080	464900	1394156
	0.080	422285	1318469
	0.080	1284968	3510013
	0.080	1305275	4240249
	0.050	246815	523805
	0.050	303071	720989
	0.050	904869	1820880
	0.050	1111133	2065856
	0.045	320551	622624
	0.045	324630	593473
	0.045	789176	1218156
	0.045	896234	1846877
	0.040	277971	489047
	0.040	282916	505124
	0.040	797271	1512540
	0.040	899715	1272116
	0.035	234959	373797
	0.035	13444	19854
[EMIm][NTf_2][a]	0.200	658765	4267934
	0.200	709539	4768640
	0.120	527232	2305708
	0.120	528571	2302210
	0.120	1255560	4646330
	0.120	1546834	6601933
	0.080	464900	1394156
	0.080	422285	1318469

0.080	1284968	3510013
0.080	1305275	4240249
0.050	246815	523805
0.050	303071	720989
0.050	904869	1820880
0.050	1111133	2065856
0.045	320551	622624
0.045	324630	593473
0.045	789176	1218156
0.045	896234	1846877
0.040	277971	489047
0.040	282916	505124
0.040	797271	1512540
0.040	899715	1272116
0.035	234959	373797
0.035	13444	19854

[a]After extraction with *t*-BuPh.

Table A.3. The GC peak areas (PA) of the products of the competition kinetic experiments for the 5-*exo* cyclisation of the 5-hexenyl radical **25a** at different temperatures.[a],[b]

Solvent	**T/^{o}C**	**PA (26a-H)**	**PA (25b-H)**
[EMIm][NTf_2]	23	1644363	4931183
		1430361	4243334
	35	2463706	5534610
		2689731	5952246
		2493869	6045848
	40	1487399	2624447
		1101196	2184955
		1272098	2234433
	50	1752593	2958459
		1894963	3227176
		1661790	2651263
	60	1737166	2502029
		1615546	2343803
		1380378	1596527
	70	1820565	2175743
		1919109	2236602
		2106345	1792376

[a] [*t*-BuSH] = 0.1 M. [b]After extraction with *t*-BuPh.

Table A.4. The GC peak areas (PA) of the products of the competition kinetic experiments for the 5-*exo* cyclisation of the 5-hexenyl radical **25c** at 24 ± 1 °C.

Solvent	[*t*-BuSH] (M)	PA (26c-H)	PA (25c-H)
t-BuPh	0.20	17376349	1138224
	0.20	18465690	1234845
	0.20	17427237	1161424
	0.16	12044680	629619
	0.16	14342216	723686
	0.16	13647953	718415
	0.14	11739984	512875
	0.14	11992576	544566
	0.14	12612813	604422
	0.12	10314274	357355
	0.12	10914290	384378
	0.12	10472364	372962
	0.08	7173548	131776
	0.08	6213255	122442
	0.08	7055116	147387
[EMIm][NTf_2][a]	0.20	7297025	870077
	0.20	8051753	1027732
	0.20	7514317	918366
	0.18	5336233	588756
	0.18	7087165	675313
	0.18	3128120	286273
	0.16	7166390	737283
	0.16	5032328	464845
	0.16	3817809	348348
	0.14	4712709	384539
	0.14	4005898	332831
	0.14	4109512	337303
	0.12	5905294	427965
	0.12	3755855	268719
	0.12	2614139	158726

[a]After extraction with *t*-BuPh.

Table A.5. The GC peak areas (PA) of the products of the competition kinetic experiments for the 5-*exo* cyclisation of the 5-hexenyl radical **25c** at different temperature.[a]

Solvent	T/°C	PA (26c-H)	PA (25c-H)
t-BuPh	35	13926382	559217
		14265479	491989
		13303933	462448
	45	13105208	421751
		12865150	406296
		13140473	424296
	55	9653706	246804

		9433441	221358
		9448381	225445
	65	11348062	260149
		12372328	291469
		11858680	283787
	75	12187774	256514
		12197398	238893
		12049374	241660
[EMIm][NTf_2][b]	25	5078440	193661
		5361283	203020
		4047226	82533
	35	2472917	85518
		3015528	103734
		3056982	92006
	45	2824179	80243
		2350001	52071
		2172088	50156
	55	4772478	96737
		4701170	84760
		5085493	59804
	65	3427879	41829
		3531066	25318
		3203586	52327

[a] [*t*-BuSH] = 0.12 M. [b]After extraction with ethyl acetate and diethyl ether.

Table A.6. The GC peak areas (PA) of the products of the competition kinetic experiments for the 5-*exo* cyclisation of the 5-hexenyl radical **25d** at 24 ± 1 °C.

Solvent	**[*t*-BuSH] (M)**	**[26d-H]**	**[25d-H]**
t-BuPh	0.80	57708559	801011259
	0.80	58234026	798354275
	0.80	56459741	808857715
	0.72	46783620	734458430
	0.72	50967457	728716510
	0.72	45068708	735045930
	0.64	39645459	661215375
	0.64	39311746	654923685
	0.64	36806606	649855838
	0.56	30195123	581192951
	0.56	30407406	578776537
	0.56	30000549	614037587
	0.48	20654718	505319297
	0.48	20121217	497828219
	0.48	18780683	493889588
	0.40	14815639	420403123
	0.40	13642774	419662463
	0.40	13838278	416610547
[EMIm][NTf_2]	0.80	19050680	455118512

	0.80	23325854	489778986
	0.80	21353638	488112744
	0.72	19262051	437098695
	0.72	17707479	411034351
	0.72	17486259	420026538
	0.64	13364520	430392033
	0.64	14215517	379345915
	0.64	15986716	396230005
	0.56	13008441	377961710
	0.56	12883275	356869561
	0.56	9889042	356709648
	0.48	8913395	328511195
	0.48	7814492	298211406
	0.48	7260645	290381119
	0.40	6554147	284167320
	0.40	5958002	281379069
	0.40	3588734	222634446

[a]After extraction with ethyl acetate and diethyl ether.

Table A.7. The GC peak areas (PA) of the products of the competition kinetic experiments for the 5-*exo* cyclisation of the 1-methyl-5-hexenyl radical (**63a**) at 24 ± 1 °C.

Solvent	**[*t*-BuSH] (M)**	**PA (63a-H)**	**PA (*trans*-64a-H)**	**PA [*cis*-64a-H]**
t-BuPh	0.20	90144	3087	11484
	0.20	89750	2922	11411
	0.20	86812	3036	11909
	0.18	78936	3012	11399
	0.18	83212	2966	11803
	0.18	80899	3040	11743
	0.16	71634	3026	11690
	0.16	71168	2890	11326
	0.16	68204	2966	11466
	0.14	59524	2873	11115
	0.14	57408	2869	11197
	0.14	54137	2647	10170
	0.12	45720	2886	10816
	0.12	44686	2652	10444
	0.12	42683	2430	9417
	0.10	34742	2437	9353
	0.10	37465	2561	9815
	0.10	33115	2373	9082
[EMIm][NTf_2][a]	0.20	60993	1052	4281
	0.20	61253	1093	4614
	0.20	65097	1289	5238
	0.18	57892	1118	4592
	0.18	55770	1009	4238
	0.18	54019	1118	4539
	0.16	49934	986	4162

0.16	48859	1025	4275
0.16	49876	1103	4559
0.14	55247	1309	5404
0.14	43336	1035	4254
0.14	43416	1112	4562
0.12	36223	994	4113
0.12	34094	869	3572
0.12	32279	854	3507
0.10	29058	932	3803
0.10	29324	893	3740
0.10	24917	834	3453

[a]After extraction with *t*-BuPh.

Table A.8. The GC peak areas (PA) of the products of the competition kinetic experiments for the 5-*exo* cyclisation of the 1-methyl-5-hexenyl radical (**63a**) at different temperatures.[a]

Solvent	T/^{o}C	PA (63a-H)	PA (*trans*-64a-H)	PA (*cis*-64a-H)
t-BuPh	25	90144	3087	11484
		89750	2922	11411
		86812	3036	11909
	40	125708	4795	18244
		129483	4678	17518
		127194	4918	18548
	45	127845	4671	17362
		126554	5091	18714
		125750	5069	18949
	55	105261	4216	15537
		104010	4165	15434
		104304	4408	16362
	60	107896	3941	14813
		112771	4756	17360
		105493	4663	17253
	65	125528	5421	19896
		120669	5902	21190
		121637	5875	21210
[EMIm][NTf_2][b]	4	15706	294	1589
		13708	280	1436
		9087	210	1199
	25	32847	1022	4093
		29719	988	4041
		29394	897	3721
	45	18234	898	3163
		19917	1676	6155
	65	18825	2543	8157
		12835	1995	6221
		20852	2734	8668
	85	15659	3026	8719
		14448	3073	8711

	14956	3326	9413
95	22583	8099	22311
	20967	6931	19094
	25273	7817	21548
115	12321	5757	14817
	11378	5573	14637
	12912	6062	15526

[a] [*t*-BuSH] = 0.1 M. [b]After extraction with *t*-BuPh.

Table A.9. The GC peak areas (PA) of the products of the competition kinetic experiments for the 5-*exo* cyclisation of the 1-ethyl-5-hexenyl radical (**63b**) at 24 ± 1 °C.

Solvent	**[*t*-BuSH] (M)**	**PA (63b-H)**	**PA (*trans*-64b-H)**	**PA (*cis*-64b-H)**
t-BuPh	0.20	60039	2892	8239
	0.20	59290	2915	8326
	0.20	61422	2937	8511
	0.18	51360	2811	8048
	0.18	49144	2684	7727
	0.18	50766	2656	7625
	0.14	35008	2481	7262
	0.14	32791	2495	7278
	0.14	35569	2395	7040
	0.12	27082	2209	6614
	0.12	28693	2381	6952
	0.12	28255	2144	6458
	0.10	21209	1913	5790
	0.10	22477	2116	6278
	0.10	21545	1906	5629
[EMIm][NTf_2][a]	0.20	49723	1459	3818
	0.20	43197	1241	3301
	0.20	50236	1486	3813
	0.18	48383	1587	4092
	0.18	36425	1186	3096
	0.18	51073	1613	4235
	0.16	41094	1393	3669
	0.16	39340	1329	3559
	0.16	34298	1126	2933
	0.12	32170	1384	3834
	0.12	28961	1230	3405
	0.12	30686	1234	3486
	0.10	27372	1299	3642
	0.10	22320	1029	2880
	0.10	23761	1152	3198

[a]After extraction with *t*-BuPh.

Table A.10. The GC peak areas (PA) of the products of the competition kinetic experiments for the 5-*exo* cyclisation of the 1-ethyl-5-hexenyl radical (**63b**) at different temperatures.[a]

Solvent	T/°C	PA (63b-H)	PA (*trans*-64b-H)	PA (*cis*-64b-H)
t-BuPh	25	60039	2892	8239
		59290	2915	8326
		61422	2937	8511
	40	42986	2321	6457
		37556	2042	5714
		56966	3057	8529
	50	73887	4014	11142
		44080	2403	6644
		47047	2575	7257
	60	51997	4102	10873
		32804	2992	7933
		34434	2767	7479
	70	29674	3140	8158
		30426	2930	7676
		36377	3657	9490
[EMIm][NTf_2][b]	25	27372	1299	3642
		22320	1029	2880
		23761	1152	3198
	40	14883	1324	3535
		19070	1168	3084
		15927	924	2405
	50	12157	931	2455
		12511	1131	2778
		12167	1007	2460
	60	9451	1305	3235
		19501	1928	4886
		12579	1355	3281
	70	11920	1553	3773
		11469	1710	4052
		10912	1762	4229

[a] [*t*-BuSH] = 0.1 M. [b]After extraction with *t*-BuPh.

Table A.11. The GC peak areas (PA) of the products of the competition kinetic experiments for the 5-*exo* cyclisation of the 1-isopropyl-5-hexenyl radical (**63c**) at 24 ± 1 °C.

Solvent	[*t*-BuSH] (M)	PA (63c-H)	PA (*trans*-64c-H)	PA (*cis*-64c-H)
t-BuPh	0.20	76120	3707	10401
	0.20	78718	3685	10354
	0.20	78109	3584	10230
	0.18	65851	3843	10668
	0.18	66496	3689	10444
	0.18	68406	3838	10826
	0.16	57878	3531	10271
	0.16	53742	3410	10035

	0.16	57424	3482	10277
	0.14	47554	3325	9681
	0.14	46713	3294	9605
	0.14	46257	3401	9571
	0.12	39826	3209	9601
	0.12	39280	3413	9674
	0.12	38400	3171	9066
	0.10	31930	3100	9031
	0.10	28774	2943	8393
	0.10	29392	2844	8208
[EMIm][NTf_2][a]	0.20	51787	1488	4191
	0.20	51784	1454	4069
	0.20	63448	1732	5010
	0.18	44516	1301	3802
	0.18	53340	1610	4434
	0.18	58792	1813	5036
	0.16	50957	1694	4730
	0.16	45050	1467	4162
	0.16	46794	1542	4365
	0.14	39470	1395	4061
	0.14	40541	1420	4121
	0.14	37549	1314	4033
	0.12	30896	1315	3780
	0.12	34869	1550	4388
	0.12	32650	1372	4003
	0.10	25726	1379	3702
	0.10	25701	1333	3707
	0.10	26492	1351	3825

[a]After extraction with *t*-BuPh.

Table A.12. The GC peak areas (PA) of the products of the competition kinetic experiments for the 5-*exo* cyclisation of the 1-isopropyl-5-hexenyl radical (**63c**) at different temperatures.[a]

Solvent	**T/^{o}C**	**PA (63c-H)**	**PA (*trans*-64c-H)**	**PA (*cis*-64c-H)**
t-BuPh	25	76120	3707	10401
		78718	3685	10354
		78109	3584	10230
	35	77203	4797	13349
		77893	4278	11972
		77439	4397	12104
	40	77750	4667	12795
		77972	4603	12920
		80951	4875	13518
	50	77784	5046	13916
		76659	5263	14104
	55	72106	5298	14229
		71424	5386	14252
		66963	5458	14278

[EMIm][NTf_2][b]	25	25726	1379	3702
		25701	1333	3707
		26492	1351	3825
	35	26182	1976	5460
		26061	2102	5657
		23426	2821	7527
	40	21649	2347	6274
		14134	4005	10642
		20520	1865	5045
	45	27022	3040	7845
		23462	2355	6254
		25307	2512	6378
	58	24783	3963	9919
		24717	3505	8788
		25722	3660	9236
	70	25995	3738	9302
		21774	2742	6024
		19691	2610	5798

[a] [*t*-BuSH] = 0.1 M. [b]After extraction with *t*-BuPh.

Table A.13. The GC peak areas (PA) of the products of the competition kinetic experiments for the 5-*exo* cyclisation of the 1-*t*-butyl-5-hexenyl radical (**63d**) at 24 ± 1 °C.

Solvent	**[*t*-BuSH] (M)**	**PA (63c-H)**	**PA (*trans*-64c-H)**	**PA (*cis*-64c-H)**
n-hexane	0.20	75364	2748	4582
	0.20	73278	3186	5076
	0.20	64807	2994	4659
	0.18	63844	2791	4379
	0.18	64874	3085	4860
	0.18	59350	3039	4884
	0.16	54561	2489	3943
	0.16	49988	2573	4047
	0.16	53526	2976	4674
	0.14	100462	5213	8151
	0.14	37893	2270	3623
	0.14	12819	571	851
	0.12	38882	2466	3960
	0.12	29258	1956	3002
	0.12	35555	2554	4063
	0.10	25788	1782	2768
	0.10	27544	1884	2885
	0.10	29568	2434	3856
[EMIm][NTf_2][a]	0.20	60168	1290	2185
	0.20	63466	1249	2139
	0.20	67123	1337	2289
	0.18	58203	1232	2162
	0.18	59835	1270	2178
	0.18	56217	1232	2134

0.16	48962	1101	1892
0.16	51619	1232	2156
0.16	48735	1154	1978
0.14	53298	1391	2438
0.14	49036	1295	2175
0.14	49231	1358	2312
0.12	33823	1076	1728
0.12	37697	1124	1904
0.12	36444	1095	1825
0.10	27392	892	1465
0.10	27716	963	1635
0.10	31328	1168	1944

[a]After extraction with *t*-BuPh.

Table A.14. The GC peak areas (PA) of the products of the competition kinetic experiments for the 5-*exo* cyclisation of the 1-*t*-butyl-5-hexenyl radical (**63d**) at different temperatures.[a]

Solvent	**T/^{o}C**	**PA (63d-H)**	**PA (*trans*-64d-H)**	**PA (*cis*-64d-H)**
n-Hexane	25	75364	2748	4582
		73278	3186	5076
		64807	2994	4659
	35	79864	4620	7069
		74909	3973	6197
		69505	3844	5972
	45	69156	5758	8388
		59166	4530	6554
		56959	4879	7205
	55	66873	7436	10384
		58715	5761	8158
		62610	6212	8707
	75	83012	9621	13282
		93076	9356	13026
		82595	8788	12115
[EMIm][NTf_2][b]	25	27392	892	1465
		27716	963	1635
		31328	1168	1944
	40	39365	1991	3180
		42384	2255	3588
		34585	1551	2479
	50	23415	2017	3000
		30915	2250	3424
		30796	2174	3294
	60	31690	2507	3843
		33803	2888	4372
		27542	2477	3736
	70	34634	4501	6373
		29135	3864	5358

		29940	3696	5240
	80	29976	4563	6422
		24422	3446	4796
		29359	4677	6489

[a] [*t*-BuSH] = 0.1 M. [a]After extraction with *n*-hexane.

Table A.15. The GC peak areas (PA) of the products of the competition experiments for the intramolecular homolytic substitution of the radical **78** at different temperatures.[a],[b]

Solvent	**T/°C**	**PA (78-H)**	**PA (79)**
[EMIm][NTf_2]	24	284	20513
		256	22855
		290	21859
	59	741	30218
		747	25952
		754	26744
	81	1083	18495
		1321	31346
		1124	24800
	10	2753	24104
		2171	27974
		2201	23003

[a] [*t*-BuSH] = 0.1 M. [b]After extraction with diethyl ether and ethyl acetate.

Table A.16. The GC peak areas (PA) of the products of the competition kinetic experiments for the 5-*exo* cyclisation of the alkoxyl radical **82b** at different temperatures.[a]

Solvent	**T/°C**	**PA (82b-H)**	**PA (*trans*-83b-H)**	**PA (*cis*-83b-H)**
t-BuPh	24	5824	15747	53481
		6396	17653	60156
		6295	16606	56507
	35	6707	19263	64919
		6446	19561	65377
		5903	18252	60826
	40	6442	18948	63938
		6408	18803	63336
		6500	18412	61755
	45	6241	19418	63831
		6005	18288	60464
		5553	18479	60884
	50	5257	16624	54281
		5595	18065	59085
[EMIm][NTf_2][b]	24	6644	14145	43473
		6192	14069	43273
		6481	13715	42090
	35	5681	12699	38123
		5138	11749	35251

40	5762	12325	36625
	4877	12011	35788
	5152	11859	35303
45	5697	13830	40559
	4832	11488	33637
50	4626	11058	32117
	4625	11320	33128
70	4730	12728	35114
	4985	12240	33544
	5356	11733	32192

[a] [*t*-BuSH] = 0.05 M. [b]After extraction with diethyl ether and ethyl acetate.

Table A.17. The GC peak areas (PA) of the products of the competition experiments for intermolecular addition of radical **90** to MA at 24 ± 1 °C.[a]

Solvent	**[MA] (M)**	**PA (90-H)**	**PA (91a-H)**	**PA (92a-H)**
Benzene	0.20	541722103	22804216	11447160
	0.20	528901856	22853713	11388432
	0.40	445327311	27417194	17847127
	0.40	507920759	30334520	20246708
	0.40	479676262	29511579	36232899
	0.50	448112299	28765168	20680055
	0.50	478632794	31331735	23514041
	0.60	428920436	29651242	35930012
	0.60	424113741	30396086	72598005
	0.60	437062709	31633162	25178266
	0.66	432645614	31615872	74090037
	0.66	455807737	33085779	25568096
	0.66	443831754	31585218	26107869
[EMIm][NTf_2][b]	0.20	109767117	6686330	3906689
	0.20	150700364	8181650	4422004
	0.20	173182076	9202884	4712910
	0.30	114219968	7684767	5584865
	0.30	181774873	11398647	6978213
	0.30	172566957	11190802	6620589
	0.40	107448131	7942714	6115277
	0.40	161420488	11136188	7808248
	0.40	181924093	11860803	8297451
	0.50	164766565	11213104	8669653
	0.50	167828059	11804481	8525727
	0.50	181924093	11860803	8297451
	0.60	160389817	11571836	9677966
	0.60	193459666	13898633	10604866
	0.60	208749055	14891093	11023299
	0.66	126056395	10252976	7823915
	0.66	120248873	9121180	7734717
	0.66	155642464	11600919	9705064

[a] [*t*-BuSH] = 0.1 M. [b]After extraction with diethyl ether and ethyl acetate.

Table A.18. The GC peak areas (PA) of the products of the competition experiments for the intermolecular addition of radical **90** to MA at different temperatures in [EMIm][NTf_2].[a],[b]

T/°C	[MA] (M)	PA (90-H)	PA (91a-H)	PA (92a-H)
23	0.4	445327311	27417194	17847127
	0.4	507920759	30334520	20246708
	0.4	479676262	29511579	36232899
33	0.4	845051236	50742957	26198965
	0.4	850030561	48920643	23423766
45	0.4	467554594	29036125	15858810
	0.4	475244068	30064248	16760401
	0.4	461020376	28660836	16030238
53	0.4	422783158	27455721	15645020
	0.4	521839212	31728252	17221281
	0.4	476695293	30075051	17089672
60	0.4	387378450	31877785	20605956
	0.4	409221309	33424188	20238418
	0.4	392516040	32165861	26201600
65C	0.4	476817307	36837340	25615255
	0.4	452555276	33985553	22641662
	0.4	486192583	32764277	21710104

[a] [*t*-BuSH] = 0.1 M. [b]After extraction with diethyl ether and ethyl acetate.

Table A.19. The GC peak areas (PA) of the products of the competition experiments for intermolecular addition of radical **90** to MA at 24 ± 1 °C.

Solvent	[*t*-BuSH] (M)	[MMA] (M)	PA (90-H)	PA (91b-H)	PA (92b-H)
Benzene	0.1	0.1	437430096	14072097	12832612
	0.1	0.1	447622527	13572290	11206894
	0.1	0.1	467417885	14167540	11211092
	0.1	0.15	404120513	18068538	22274146
	0.1	0.15	429278852	16518836	18210470
	0.1	0.15	436895091	16568201	18830980
	0.1	0.2	397117713	18885486	24837877
	0.1	0.2	399875654	18274361	24743245
	0.1	0.2	417021277	18226013	24889451
	0.1	0.25	401557595	19190197	29496023
	0.1	0.25	393227427	19199532	30204609
	0.1	0.25	440228039	21932953	31644197
	0.1	0.3	390640540	19526791	31434826
	0.1	0.3	413440877	21617901	35647808
	0.1	0.3	381860545	19724206	34342275
	0.1	0.33	376200461	19873898	35484760
	0.1	0.33	387854924	20945032	36662322
	0.1	0.33	427142322	23531734	40026836
[EMIm][NTf_2][a]	0.1	0.1	196557634	5650021	6107231
	0.1	0.1	144540592	4103175	4788831
	0.1	0.1	230145458	5122424	6090247

0.1	0.15	176752724	5872873	8226706
0.1	0.15	184592977	5378533	7216118
0.1	0.15	201647732	4502529	8148092
0.1	0.2	165137469	5753494	9140276
0.1	0.2	153944269	4782435	7110685
0.1	0.2	198453579	5179008	7747013
0.1	0.25	135044491	4977312	7303463
0.1	0.25	148663520	4745190	7368783
0.1	0.25	198453579	5179008	7747013
0.1	0.3	133096316	5034576	8053839
0.1	0.3	182136724	5536831	8338778
0.1	0.3	201356993	5449050	8672168
0.1	0.33	143272210	5255146	7735396
0.1	0.33	187919175	5722486	8933327
0.1	0.33	164439492	4716359	7738808

[a]After extraction with diethyl ether and ethyl acetate.

Table A.20. The GC peak areas (PA) of the products of the competition experiments for the intermolecular addition of radical **90** to MA at different temperatures.[a],[b]

Solvent	**T/^{0}C**	**[*t*-BuSH] (M)**	**[MMA] (M)**	**PA (90-H)**	**PA (91b-H)**	**PA (92b-H)**
Benzene	23	0.1	0.2	397117713	18885486	24837877
		0.1	0.2	399875654	18274361	24743245
		0.1	0.2	417021277	18226013	24889451
	44	0.1	0.2	208345916	9179508	11555019
		0.1	0.2	247992797	12049733	15171554
		0.1	0.2	267469204	13638003	17352543
	55	0.1	0.2	245877544	12156448	14815082
		0.1	0.2	268409437	14800609	17590970
		0.1	0.2	283061772	14632977	17332788
	65	0.1	0.2	367929454	19744337	19662282
		0.1	0.2	365024223	19350754	21782743
		0.1	0.2	383872245	20894777	24160610
		0.1	0.2	297172294	17714253	19453711
	75	0.1	0.2	310652773	17579541	21158148
		0.1	0.2	344427316	20013536	23110562
[EMIm][NTf_2]	23	0.1	0.2	165137469	5753494	9140276
		0.1	0.2	153944269	4782435	7110685
		0.1	0.2	198453579	5179008	7747013
	44	0.1	0.2	54332743	2603266	3842159
		0.1	0.2	56686762	3007959	4627422
		0.1	0.2	65787080	3139224	4739500
	55	0.1	0.2	87346796	4955866	6569154
		0.1	0.2	87906145	5601458	7186611
		0.1	0.2	94762556	5635596	7203768
	65	0.1	0.2	101094018	6341758	9152072
		0.1	0.2	92172401	6212834	8794596
		0.1	0.2	102437180	6810056	9254304
	75	0.1	0.2	152135722	11205358	14470634

	0.1	0.2	128592598	9055767	12566573
	0.1	0.2	241251506	10890698	12540236

[a] [*t*-BuSH] = 0.1 M. [b]After extraction with diethyl ether and ethyl acetate.

Table A.21. The GC peak areas (PA) of the products of the competition kinetic experiments for the 5-*exo* cyclisation of the 5-hexenyl radical (**25a**) at 24 ± 1 °C to explore the recyclability of [EMIm][NTf_2].

Run	PA (25a-H)	PA (26a-H)	PA 1-Heptene	[25a-H]	[26a-H]	[1-Heptene]
Run 1	22608	4087	43025	0.0056520	0.00102175	0.0086050
	24038	4269	42093	0.0060095	0.00106725	0.0084186
	21634	3884	40280	0.0054085	0.00097100	0.0080560
Run 2	21623	4037	41503	0.0054058	0.00100925	0.0083006
	22040	4833	41603	0.0055100	0.00120825	0.0083206
	22011	4274	42695	0.0055028	0.0010685	0.0085390
Run 3	21335	5027	42710	0.0053338	0.00125675	0.0085420
	19918	4317	43813	0.0049795	0.00107925	0.0087626
	20569	4432	41750	0.0051423	0.00110800	0.0083500